EXHALED BREATH MICROANALYSIS IN VETERINARY MEDICINE

Cathy Wyse

December 2001

Department of Veterinary Clinical Studies

University of Glasgow Veterinary School

ABSTRACT

Breath microanalysis is an investigative method that is of considerable potential for non-invasive monitoring of health status, and early detection of disease in veterinary medicine. The aim of this thesis was to investigate the potential use of breath analysis for assessment of gastrointestinal transit and *in vivo* lipid peroxidation in animals.

Initial studies in this thesis describe the use of the ^{13}C-octanoic acid breath test (^{13}C-OBT) and the ^{13}C-lactose-ureide (^{13}C-LUBT) for assessment of gastric emptying and oro-caecal transit time in the dog. The results revealed that collection of exhaled breath could be performed quickly, easily, and with minimal disturbance of the animal. The data produced could be fitted by simple mathematical models derived for analysis of gastric emptying breath tests, and reproducibility was comparable to previous reports of this test in humans. Furthermore, the parameters of the ^{13}C-OBT were significantly altered by increased test meal energy density, a condition known to delay the rate of gastric emptying. In this study, the recovery of $^{2}H_2O$ in saliva did not occur simultaneously with the recovery of $^{13}CO_2$ in breath following ingestion of ^{2}H and ^{13}C-octanoic acid in a dog. This finding indicates that the post-gastric processing of ^{13}C-octanoic acid imposes a delay on the recovery of breath $^{13}CO_2$, and confirms that the ^{13}C-OBT does not provide a real-time measurement of gastric emptying in the dog. The results of these studies have shown that the ^{13}C-OBT and the ^{13}C-LUBT are potentially useful methods for assessment of gut transit in dog, although further validation is necessary.

Lipid peroxidation is increasingly associated with many pathological processes, and the breath pentane test has been described as a non-invasive method for *in vivo* assessment of lipid peroxidation in humans. In order to assess the application of the breath pentane test in animals, a system for cryogenic concentration of exhaled breath samples, and analysis by gas chromatography (GC) was developed. Good specificity for discrimination of ethane and pentane from other breath hydrocarbons was demonstrated. The assay was sensitive to 0.5ppb and 5ppb pentane and ethane, respectively. Inter and intra-assay variation were comparable to previous studies. The test was sensitive enough to detect pentane in the exhaled breath of horses. Intra-subject variability in pentane exhalation in a group of 5 horses was lower than previously reported in man.

The "electronic nose" is a method of analysis of gas samples that could potentially be applied for measurement of breath pentane. In these studies an array of composite polymer sensors, sample presentation system and data analysis protocol was integrated to form an "electronic nose" system. Composite polymer sensors were constructed by depositing a layer of a polymer solution with suspended carbon black particles on the surface of inter-digitated gold electrodes. Initial work demonstrated that these sensors were sensitive to alterations in temperature and humidity and that their baseline resistance was dependant on the percentage carbon black particles suspended in the polymer layer. Further work demonstrated that whilst the electronic nose was capable of discriminating between specific compounds, the specificity of this instrument was not sufficient to permit application for analysis of breath hydrocarbons. However, the unique chemical "fingerprint" measurement provided by the electronic nose could in the future be used to address problems in veterinary clinical investigation that cannot be contended using current analytical methods.

The results of these studies suggest that the microanalysis of exhaled breath is a simple and potentially useful investigative method in veterinary medicine and is worthy of further investigation.

Authors Declaration

The work in this thesis was performed solely by the author except where the assistance of others is acknowledged.

Cathy Wyse

December 2001

ACKNOWLEDGMENTS

I am grateful to my supervisors Professor Jon Cooper and Dr Philippa Yam for arranging funding for this project and for their help and advice throughout. I am indebted to Dr Tom Preston of SUERC for help with the stable isotope breath tests and with gas-chromatography analysis, and for general advice and help with the design of all of these studies. This project would never have been completed without the continued help of Professor Sandy Love, and I am very grateful for his advice on the design of these experiments and for proof-reading the thesis. I am grateful to Christine Slater of the Department of Child Health, for help and advice on the analysis of saliva samples. I am also grateful to Dr Andrew Glidle for his help with the fabrication of sensors and of the electronic nose system. I would like to thank Dr Douglas Morrison who synthesised the ^{13}C-lactose-ureide used in Chapter Three, and also helped with the analysis of some of the breath samples. I would like to thank Dr Chris Mills for designing and fabricating the syringe pump system used in the electronic nose studies, and for proof-reading parts of the text. I am grateful to Paul O'Gorman and Jason Donnelly of SUERC for their help with analysis of breath samples and construction of the gas-chromatography apparatus. I would like to thank Bill Monaghan and Mary Robertson for their help with aspects of sensor fabrication and in obtaining chemicals and equipment. I am also grateful to the many owners who volunteered their dogs for use in these studies. I would like to acknowledge the Engineering and Physical Sciences Research Council, Petsavers and the Department of Veterinary Clinical Studies for generous funding of these studies.

LIST OF CONTENTS

CHAPTER 3 - PRELIMINARY STUDIES ON STABLE ISOTOPE BREATH TESTS FOR ASSESSMENT OF GASTROINTESTINAL TRANSIT IN THE DOG

LIST OF FIGURES

LIST OF TABLES

CHAPTER 1 - INTRODUCTION

This thesis describes the application of advances in the analysis of exhaled breath for the assessment of two diverse clinical measurements in veterinary medicine, the assessment of gastrointestinal transit and the *in vivo* assessment of lipid peroxidation. This first chapter will review the physiology of gastrointestinal transit and lipid peroxidation and the current methods available for their assessment in animals.

1.1 GASTROINTESTINAL TRANSIT IN THE DOG

1.1.1 Gastrointestinal Motility

The relationship between gastrointestinal motility and transit is poorly understood, largely due to the technical difficulties of concurrent measurement of gastrointestinal motility and transit. The integrated study of motility and transit is necessary in order to understand the physiological mechanisms controlling the passage of ingesta through the gastrointestinal tract. The myogenic properties of the gastrointestinal smooth muscle cell are the fundamental basis of gut motility, and provide an electrical framework through which stimuli modify gut transit. Physiological, pharmacological and pathological alterations in gastric emptying and intestinal transit are mediated through the interplay of a hierarchy of control mechanisms (Figure 1.1).

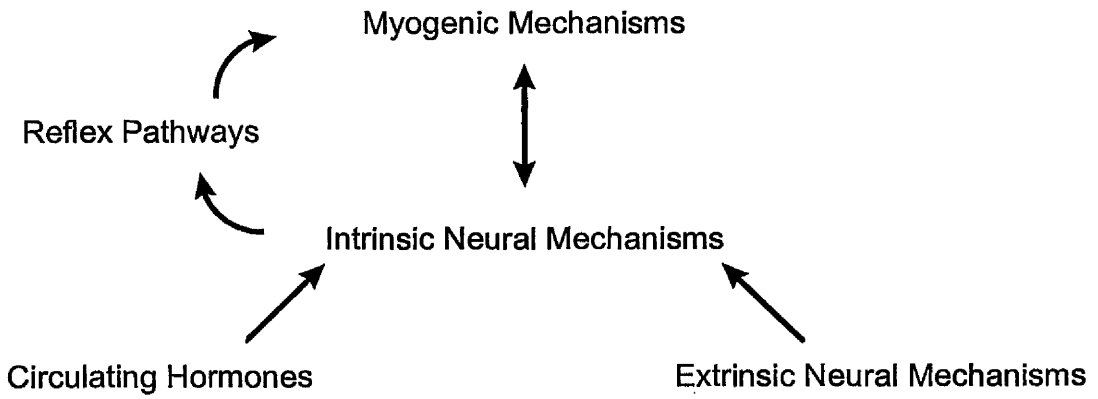

Figure 1.1 Mechanisms controlling gastrointestinal motility

Myogenic Mechanisms

The canine gastrointestinal myocyte is characterised by an omnipresent, cyclically recurring membrane depolarization from the cell resting potential, known as the slow wave, pacesetter potential or basal electrical rhythm (Kelly *et al.,* 1969). The slow wave is responsible for the basic rhythmicity of the gastric myocyte, and recent experimental evidence confirmed that the slow wave originates in specialised pace-making cells located in the intestinal musculature, the interstitial cells of Cajal (Thomsen *et al.,* 1998). Studies using electromyography have demonstrated a proximal to distal gradient in the resting potential of the smooth muscle cells of the canine stomach, from -48mV in the fundus to -75mV in the pylorus (Kelly *et al.,* 1969) Figure 1.2. This intrinsic gradient in electrical activity is responsible for regional variation in slow wave configuration, and for functional differentiation of the stomach. Ion channels responsible for the generation of the slow wave are present in all gastric myocytes, but are inactivated by the more positive resting potential of the fundus, so that the fundus does not display any spontaneous membrane depolarizations (Szurszewski, 1987). The resting potential of the canine fundus is close to the

mechanical threshold of approximately -52mV (Morgan *et al.*, 1981), resulting in prolonged depolarization and tonic contraction.

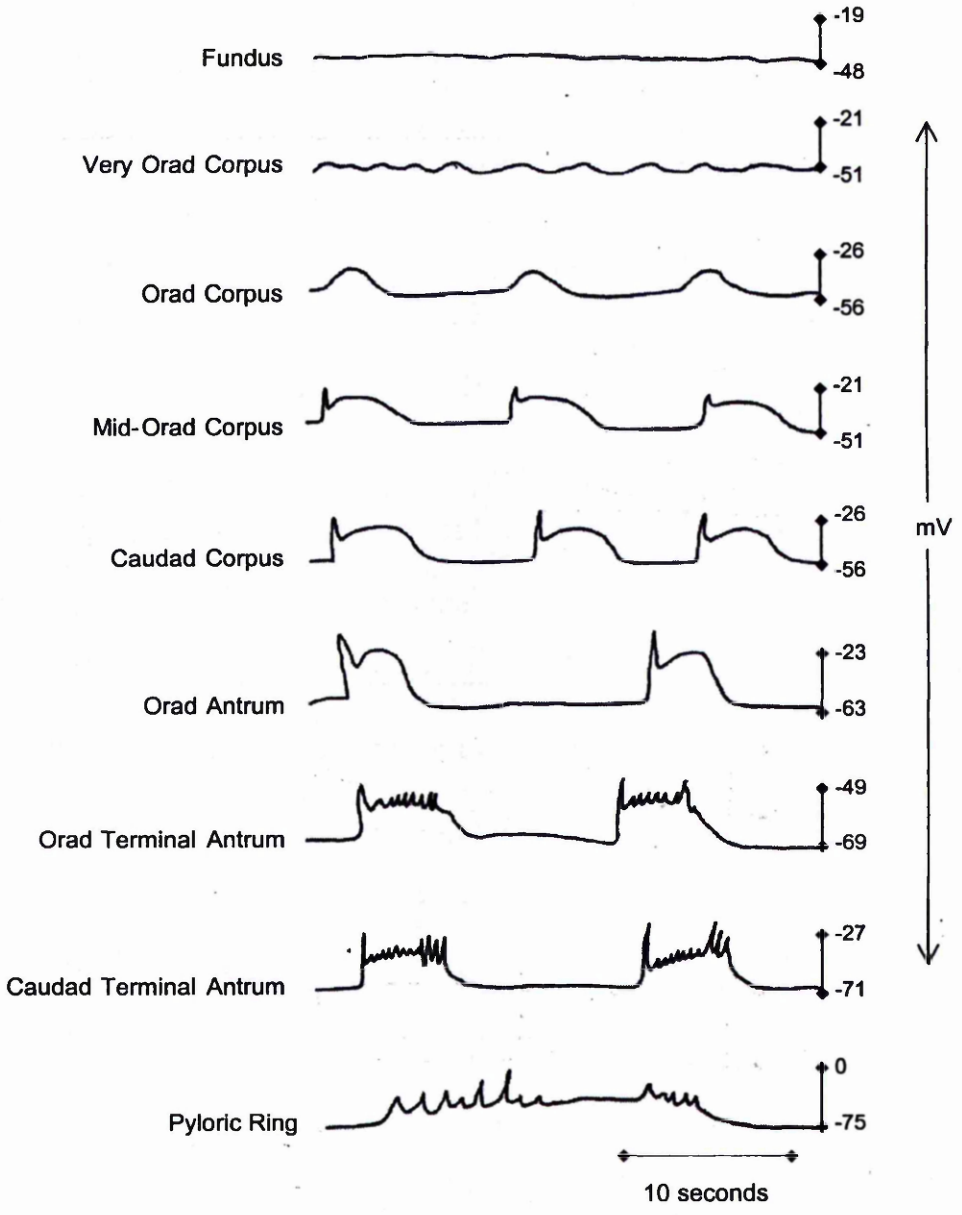

Figure 1.2 Intracellular resting potential and spontaneous action potentials recorded in different regions of the canine stomach (Redrawn from Szurswewski, 1987).

Inhibitory stimuli cause membrane hyperpolarization and decreased tone, while excitatory stimuli cause depolarization and increased tone (Szurszewski, 1987). Slow waves are propagated aborally and circumferentially towards the pylorus from an area

on the greater curvature called the gastric pacemaker, at a rate of 5.5 cycles/minute in the dog (Weber and Kohatsu, 1970; Kelly *et al.,* 1969).

The pacemaking region of the small intestine has been identified in the duodenum, and the intrinsic frequency of the slow wave decreases distally ranging from 14 - 18 waves.min^{-1} in the duodenum to 10 - 12 waves.min^{-1} in the ileum (Szurszewski, 1969). This decreasing frequency generates a proximal to distal pressure gradient, facilitating aborad transit of chyme (Basilisco and Phillips, 1993). Slow wave propagation occurs at a faster rate along the circular axis, than the longitudinal axis, allowing each depolarisation complex to be organised into a coordinated ring of excitability (Szurszewski, 1987).

The gastrointestinal slow wave is triphasic and consists of an upstroke potential, a plateau potential and a repolarization phase. (Mayer, 1994) (Figure 1.3). The upstroke potential is associated with a short initial muscle contraction, P1, and the plateau potential with a longer contraction, P2 (Szurszewski, 1987; Bauer and Sanders, 1985). Action potentials trigger contractions only when they occur during a plateau phase and in this way the slow wave sets the pace at which contraction occurs, but does not itself initiate the contraction (Bauer and Sanders, 1985). Inhibitory (vasoactive intestinal peptide, noradrenalin) and excitatory stimuli (pentagastrin, cholecystokinin and acetylcholine) affect the force and duration of phasic contraction by alteration of the amplitude and duration of the plateau potential (Morgan *et al.,* 1978; Ozaki *et al.,* 1993). The biphasic contractile activity of the antrum has important implications for solid-liquid discrimination in the stomach, as P1 causes pyloric contraction before the arrival of P2, resulting in retropulsion of solid particles and facilitating trituration (Kelly *et al.,* 1969). The proximal to distal gradient in resting potential is responsible for a

progressive acceleration in slow wave propagation as each complex migrates distally towards the pylorus, facilitating the mechanical breakdown of solid food (Mayer, 1994).

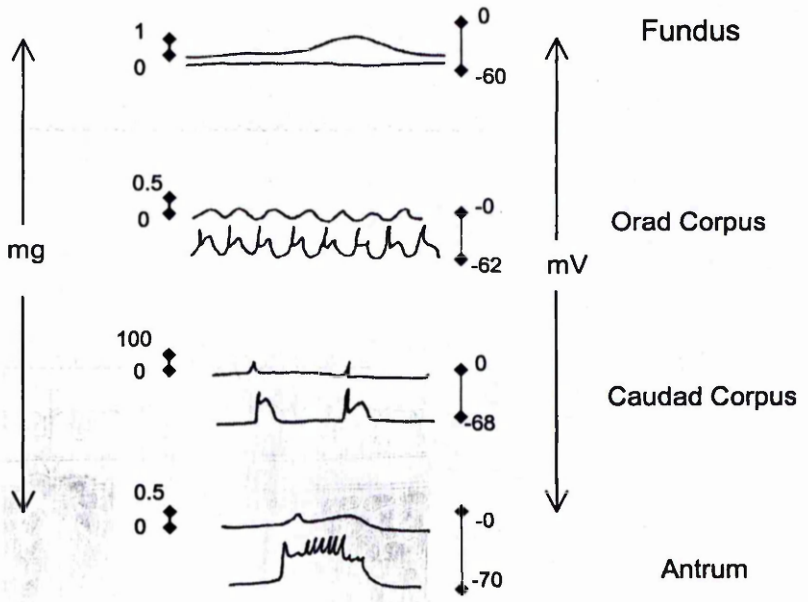

Figure 1.3 Simultaneously recorded mechanical and intracellular electrical activity recorded from different regions of the canine stomach. Top tracing shows mechanical activity and bottom tracing electrical activity (Redrawn from Szurszewski, 1987).

Intrinsic Neural Mechanisms

The ability of the gut to maintain coordinated propulsive motility following extrinsic denervation suggested the presence of local nervous regulatory mechanisms (Bayliss and Starling, 1900a; Bayliss and Starling, 1900b). This finding, along with the large number of neurons present in the gut and not of extrinsic origin, led to the recognition of the enteric nervous system (ENS) as a distinct division of the autonomic nervous system (Langley and Anderson, 1895). The ENS is capable of integrative function independent of the cephalic brain (Wood, 1994). There are two major ganglionated plexuses of the ENS: the submucosal (Meissner) plexus is located in the submucosa; and the myenteric (Auerbach) plexus between the longitudinal and circular muscle layers (Conklin, 1992) Figure 1.4.

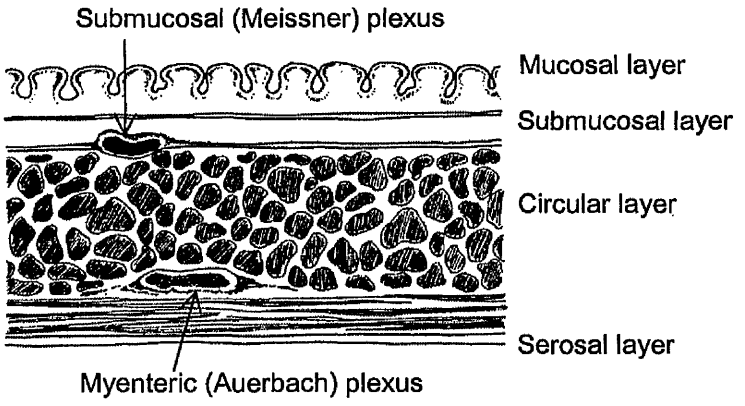

Figure 1.4 Transverse section of the canine ileum, showing intramural plexuses and tissue layers

The enteric neurons can be classified functionally and morphologically according to the combination of neuroactive substances they contain. However, each enteric neuron can contain more than one neurotransmitter and more than one neurotransmitter can be released in response to stimulation. Experimental evidence using appropriate antagonists has shown that acetylcholine is the primary excitatory neurotransmitter, but some residual transmission is blocked by antagonists of tachykinin (Holzer *et al.*, 1986). The major inhibitory neurotransmitter of the ENS is thought to be nitric oxide, NO (Bult *et al.*, 1990; Allescher *et al.*, 1992; Orihata and Sarna, 1996), with vasoactive intestinal peptide (VIP) also contributing to transmission (Allescher and Daniel, 1994). The intersitial cells of Cajal are believed to play a modulatory role on the inhibitory and excitatory effects of the ENS on the gastrointestinal smooth muscle (Kunze and Furness, 1999).

Intrinsic primary afferent neurons (IPANs) project into the mucosa where they are sensitive to luminal stimuli. Their cell bodies are located in the myenteric plexus and IPANs are connected to efferent cells by interneurons in the plexuses to form intrinsic neural reflex arcs that allow autonomous response to chemical and mechanical stimuli,

temperature and pain. This reflex pathway is replicated in overlapping networks contained in most regions of the gastrointestinal tract, and constitutes the basic neural circuitry of the ENS.

Extrinsic Neural Mechanisms

Parasympathetic innervation to the gut is supplied mainly by the vagal and pelvic nerves. Parasympathetic pre-ganglionated fibres synapse mainly at the myenteric plexus, and vagal innervation of a restricted number of critical neurons (command hypothesis) in the myenteric plexus accounts for the potent modulatory effect of vagal input on the gut (Gerston *et al.*, 1994).

Sympathetic innervation to the gut is supplied by nerves that run between the spinal cord and the pre-vertebral ganglia and between these ganglia and the gut. Few fibres directly innervate smooth muscle cells and most terminate in contact with neuronal cell bodies of intra-mural plexuses (Davenport, 1982).

Gastrointestinal Peptides

Gut hormones are produced by the enterochromaffin cells of the gut mucosa and exert their hormonal or paracrine effects on other cells of the gastrointestinal tract. Some gut peptides (VIP, enkephalins) were originally thought to be hormones released by endocrine cells of the gut, however immunocytochemical techniques have identified these as neuroendocrine agents released exclusively by nerves of the gut (Walsh, 1994). More than 100 different physiologically active peptides are produced in the digestive system, which makes the gut the largest endocrine organ in the body, both in terms of number of hormones produced and number of endocrine cells. There are hundreds of

published studies on the effects of physiologically active peptides on gastrointestinal motility (Appendix 3). However, the effects of hormones on gastrointestinal motility are complex and remain poorly understood. Many hormones affect gut motility when administered systemically at pharmacological doses, and these cannot be considered to play a physiological role in regulating gut motility. The phase of the interdigestive migrating motor complex (MMC) during which an exogenous hormone is administered, or the nature of the test meal ingested may significantly alter the effect of an administered hormone. A useful method for investigation of gut hormones involves the administration of antagonists while monitoring specific phases of motility. Finally, although many gut hormones have been shown to affect gut motility, this finding does not confirm that they have a role in altering the gut transit time. The actions of some gut hormones, paracrine and neurocrine peptides on gastric and small intestinal motility are outlined in Appendix 3.

1.1.2 Gastrointestinal Motor Patterns

Distinct patterns of activity characterise the motility of the canine gut during the interdigestive and the fed state. The interdigestive state is associated with a cyclic recurring complex of motor activity, the migrating motor complex (MMC) that migrates periodically from the stomach to the distal small intestine, every 105 -134 minutes in the fasted dog (Code and Marlett, 1975). In the small intestine the MMC begins in the duodenum and migrates caudally (Sarna, 1985). The MMC is characterised by a band of intense contractile activity (Phase III) that is followed by a period of relative quiescence (Phase I) and then a period of irregular activity, Phase II (Szurszewski, 1969). Phase II may be followed by a brief period of intermittent contractile activity, Phase IV (Sarna, 1985). Phase III is associated with sudden onset of bursts of action potentials with every slow wave, Phase II with persistent but irregular action potential

activity and Phase I by a relative absence of action potential activity (Code and Marlett, 1975). The interdigestive MMC is interrupted by feeding for about 8 hours in the dog and replaced by a pattern of persistent phasic contractile activity that mixes and propels the gut contents (Bueno *et al.,* 1981; Kunze and Furness, 1999). Studies of interdigestive motor patterns of the small intestine of the dog demonstrated two further motor patterns, slowly propagating bursts of rhythmic activity and prolonged high amplitude contractions. These patterns appeared to be unique to the distal small intestine, ileum and colon (Quigley, 1984). The interdigestive pattern of motility is thought to be generated through the ENS, since the MMC persists following vagotomy, removal of sympathetic ganglia and total extrinsic denervation, but is abolished by tetrodotoxin (Kunze and Furness, 1999). The MMC also continues to cycle in the extrinsically denervated segment of small intestine (Aeberhard *et al.,* 1980). However, central pathways have at least a modulatory role in the initiation of the interdigestive MMC since intracerebroventricular administration of somatostatin and cholecystokinin alters the frequency of the MMC (Bueno and Ferre, 1982) as does mental stress (Gue *et al.,* 1988; 1989). Hormones were strongly implicated in the initiation of the IDMMC as motilin, PP and somatostatin all cycle with the MMC and can initiate Phase III of the MMC when administered exogenously (Hall *et al.,* 1983; Bueno *et al.,* 1986; Mochiki *et al.,* 1996). However it is now believed that the cyclic activity of gut hormones occurs as a consequence of the MMC motor activity, rather than initiating the pattern. If circulating gut hormones were responsible for initiation of the MMC, then motor activity should occur simultaneously in all regions of the gut, which is not the case (Bueno *et al.,* 1981). Neither does exogenous administration of hormones initiate MMC in all regions (Bueno *et al.,* 1981). Furthermore, peak motilin levels occur immediately after Phase III, suggesting that peripheral motilin levels may increase as a consequence of the MMC, rather than initiating the pattern (Keane *et al.,*

1980). Cyclic entrainment of the gut peptides by the MMC may serve to co-ordinate the motor and secretory events in the gut (Sarna, 1985).

The mechanism for disruption of the interdigestive MMC by food is not clearly understood. Interruption of the MMC by a meal is not affected by vagotomy or splanchnectomy or mesenteric ganglionectomy (Sarna, 1985), suggesting that either intrinsic neural excitation or hormonal mechanisms are important. Candidate hormones include gastrin, cholecystokinin (CCK), insulin, pancreatic polypeptide (PP) and secretin, all of which are released following a meal and can disrupt the MMC when administered exogenously (Bueno *et al.,* 1982; Lee *et al.,* 1980; Mukhopadhyay *et al.,* 1975; Eeckhout *et al.,* 1978; Thomas *et al.,* 1980). The fact that feeding disrupts the MMC in Thiry-Vella loops[1] of isolated intestine even when the food does not come into contact with them is further evidence to suggest that a systemic hormonal mechanism may be important (Thor *et al.,* 1987). However other mechanisms must have a role since exogenous administration of hormones can only reproduce the fed pattern in the proximal small intestine (Thor *et al.,* 1987) and total parenteral nutrition of the dog did not interrupt the MMC (Weisbrodt, 1976).

Pancreatic polypeptide levels cycle with the MMC, peaking at Phase II, (Hall *et al.,* 1983). Pancreatic polypeptide is unlikely to play a physiological role in the interruption of the MMC since patterns of intestinal motility in the dog were unaffected by exogenous administration at doses equivalent to endogenous PP levels, or by complete removal of PP from the circulation using a highly specific antibody (Bueno *et al.,* 1982; Thor *et al.,* 1987).

---

[1] Loops of intestine that remain within the peritoneal cavity but are attached to the rest of the gut only through the mesenteric vessels.

Somatostatin administration inhibited and disrupted the MMC (Bueno *et al.,* 1982) and although plasma somatostatin exhibited cyclic variation with antral motility, it was not thought to play an important role in modulation of the MMC (Bueno *et al.,* 1986). Gastrin administered at doses that stimulate acid production, abolished the MMC in the stomach of the dog, and produced dose-related increases in frequency of antral slow waves and incidence of action potential activity (Strunz *et al.,* 1979). Peptide YY (PYY) transiently inhibited MMC in the canine stomach (Suzuki *et al.,* 1983). Physiological doses of cholecystokinin inhibited the interdigestive MMC in the stomach and duodenum of the dog (Schlang and Kelly, 1981), but CCK-antagonism failed to restore the MMC pattern in the postprandial dog (Thor *et al.,* 1988), suggesting that factors other than CCK must have a role the interruption of the MMC in the dog. Separate phases of the MMC may be controlled by different mechanisms since Phase II was inhibited by vagal blockade in the dog, but Phase III activity was unaffected (Hall *et al.,* 1982).

1.1.3 Gastric Emptying

In the dog, as in man, liquid-phase emptying follows an exponential pattern (Meyer, *et al.,* 1979; Iwanga *et al.,* 1998) while solid meals empty in a slower, more linear pattern (Meyer *et al.,* 1979) following a lag phase that is representative of the process of trituration[2] (Theodorakis, 1980; Meyer *et al.,* 1985; Hornof *et al.,*1989). The gastric emptying of liquids and solids are controlled by different mechanisms, and the concurrent ingestion of liquids does not affect the rate of gastric emptying of the solid phase in the dog (Meyer *et al.,* 1979). Fundic contractions are responsible for the maintenance of the pressure gradient between stomach and duodenum that facilitates

---

[2] Mechanical breakdown and mixing of food in the stomach

gastric emptying of liquids and experimental denervation of the fundus caused accelerated gastric emptying of liquids in the dog (Wilbur and Kelly, 1973). Gastric discharge of solids into the duodenum is not a continuous process, instead occurring as a series of intermittent pulses (Malbert and Ruckebusch, 1989; 1991).

The proximal stomach acts as an expansile and contractile reservoir for the storage of food (Read and Houghton, 1989). Two reflexes mediate this function. Deglutition is accompanied by a vago-vagal reflex relaxation of the fundus called "receptive relaxation", while gastric distension incites a second fundic reflex relaxation called "accommodative relaxation" (Cannon and Leib, 1910). Vagal denervation of the proximal stomach in the dog caused increased intra-gastric pressure, due to failure of the receptive relaxation reflex (Wilbur and Kelly, 1973). Accommodative reflex relaxation of the stomach occurs in response to gastric distension, when gastric smooth muscle lengthens to accommodate increases in gastric volume (Mayer, 1994). This reflex can be initiated in the isolated stomach in cats (Schulze-Delrieu and Shirazi, 1987), and a vago-vagal reflex is thought to have only a modulatory role (Mayer, 1994). Together, the receptive and accommodative reflexes facilitate the function of the stomach as a storage organ. A slow increase in fundic tone allows material to pass to the antrum and prevents reflux into the proximal stomach during antral contractions (Read and Houghton, 1989). Studies in the dog have demonstrated that this recovery in fundic tone occurs concurrently with the gastric emptying of the liquid phase (Azpiroz and Malagelada, 1994), suggesting that proximal gastric tone is an important modulator of the emptying of liquids. Experimental denervation of the proximal stomach in the dog accelerated the gastric emptying of liquids, again confirming an important role for fundic tonic contraction in modulating liquid-phase gastric emptying (Wilbur and Kelly, 1973). However, the gastric emptying of liquids is not exclusively controlled by the

proximal stomach, and outlet resistance from the antro-pyloro region and the duodenum are also thought to play a role (Weisbrodt *et al.,* 1969; Miller *et al.,* 1981a).

Triturition (refers to the mechanical breakdown and mixing of food to a semi-liquid chyme) is achieved via the repeated to-fro movement of ingesta in the antrum. Antral contraction is composed of circular rings of muscular contraction (peristalsis) that increase in amplitude and velocity as they travel distally towards the pylorus (Minami and McCallum, 1984). As the wave of contraction approaches the distal antrum, the pylorus and proximal antrum close and particles too large to pass through the pylorus (>2mm) are propelled back into the body of the stomach. This action of contractile retropulsion reduces digestible food particles to a size suitable for gastric emptying, in the range of 0.1-0.5mm in the dog (Hinder and Kelly, 1977; Meyer, 1979; Becker and Kelly, 1983; Hinder and van Garde, 1983) and facilitates the stomach's role as a mill for the trituration of solid food. Because antral contractions are responsible for this action, the distal stomach is thought to control the rate of emptying of solids from the stomach. In man and in the dog, the trituration function of the distal stomach is represented by a period of decreased gastric emptying known as the lag phase. The lag phase follows ingestion of a meal and its rate and characteristic is dependant on the composition of the meal (Nusynowitz and Benedetto, 1994). This phase is followed by linear emptying of the stomach and together, these two patterns of gastric emptying depict a model of the gastric digestion of solids (Nusynowitz and Benedetto, 1994).

Indigestible solids that are resistant to trituration, are retained in the stomach and empty during the phase III contractile activity of the MMC (Minami and McCallum, 1984). The rate and pattern of emptying of indigestible solids when ingested in the interdigestive state is dependent on the phase of the MMC at the time of administration (Gruber *et al.,* 1987). When administered with solid food, indigestible solids (<2mm)

are retained in the stomach until the digestible solids have emptied, and the interdigestive motor pattern is recovered (Hinder and Kelly, 1977).

1.1.4 Small Intestinal Transit

In contrast to the stomach, solids and liquids traverse the small intestine simultaneously (Hammer *et al.,* 1998), since the ingesta leaving the stomach has been milled and mixed to a semi-liquid chyme. Following gastric emptying chyme is spread rapidly through the small intestine; nutrient-rich chyme will delay further gastric emptying and decrease small intestinal transit time by acting on the duodenal and ileal chemoreceptors (Husebye, 1999). There are essentially two types of small intestinal contraction that occur in the post-prandial period, propulsive and segmenting contractions (Basilisco and Phillips, 1993). Electric activity is propagated through the smooth muscle cells of the intestine, forming an interconnecting syncytium that facilitates propagation of activity along the intestine and orad to aborad propulsion of chyme (Szurszewski, 1998). Segmenting or stationary contractions occur when contraction is not co-ordinated with adjacent musculature, causing mixing rather than propulsion of chyme (Schemann and Ehrlein, 1986b). Both propulsive and segmenting contractions serve to optimise small intestinal absorption and further digestion of food. Propulsive contractions spread chyme over a greater gut surface area, and segmenting contractions maximise contact time between chyme and mucosa by decreasing gut transit (Husebye, 1999). The propulsive contractions are largely responsible for gut transit, and it is the length of their aboral propagation, rather than their frequency that determines rate of flow (Schemann and Ehrlein, 1986b). Segmenting contractions can be further separated into individual stationary contractions, stationary clusters of contractions and migrating clusters of contractions, all of which serve to reduce transit rate and increase luminal mixing (Schemann and Ehrlein, 1986b). Ingestion of food reduces the length of spread of

propulsive contractions and increases the frequency of stationary and migrating clusters of contractions in the jejunum of the dog (Schemann and Ehrlein, 1986b). Prolonged propagated pressure waves are distinct propulsive contractions confined to the distal ileum (Kruis *et al.*, 1985) and the fact that infusion of short chain fatty acids into the ileum induced propagated pressure waves, illustrates their function to clear caecal reflux (Fich *et al.*, 1989).

1.1.5 Factors Affecting Gastrointestinal Motility

Meal Effects

The physicochemical properties of the ingested meal are some of the most important factors determining the rate of gastric emptying. The rate of gastric emptying can be specified in terms of a constant rate of nutrient delivery to the duodenum in man (Brener *et al.*, 1983; Hunt *et al.*, 1985), and in the dog (Weisbrodt *et al.*, 1969; Miller *et al.*, 1981b; Hinder and van Garde, 1983; Leib *et al.*,1986) and this effect is mediated by the action of products of digestion on chemoreceptors in the small intestine (Minami and McCallum, 1984). Isocaloric meals of all three nutrients, carbohydrates, protein and fat exert a similar inhibitory effect on the rate of gastric emptying (Hunt and Stubbs, 1975; Calbet and MacLean, 1997). The degree of inhibition is related to the length of small intestine exposed to the nutrient, rather than simply the nutrient concentration (Lin *et al.*, 1989), as the recruitment of increasing numbers of receptors results in a greater inhibition of gastric emptying (Stanghellini *et al.*, 1994). In addition, the presence of glucose in the distal small intestine produces a more potent inhibition of the rate of gastric emptying than in the proximal small intestine of the dog (Lin *et al.*, 1992). The mechanisms by which the intestinal chemoreceptors respond to changes in the nutrient density of the post-prandial chyme may involve sensitivity to osmotic

effects (Barker *et al.,* 1974) or the binding of calcium on the luminal border of the enterocyte, by the products of digestion of triglycerides (Hunt, 1983). Cholecystokinin is also thought to be involved in the mediation of the response of the rate of gastric emptying to the post-prandial chemoreceptor, since the administration of CCK antagonists diminished nutrient-mediated inhibition of gastric emptying (Stanghellini *et al.,* 1994). The gastric motor response to intestinal chemoreceptors may also be mediated by the central nervous system, since the responses of the gut to the presence of food can be inhibited by truncal vagotomy (Sarna, 1985). Furthermore, ablation of vagal primary sensory afferents by capsaicin abolished the inhibition of gastric emptying induced by fat, in the rat (Holzer *et al.,* 1994). Excitation of the intestinal chemoreceptors inhibits the pumping action of the antrum and increases the motor activity of the proximal part of the duodenum, so increasing resistance to gastric emptying (Weisbrodt *et al.,* 1969).

The rate and pattern of jejunal and ileal transit is affected by the nutrient density of the chyme delivered from the stomach (Spiller *et al.,* 1984; Siegle and Ehrlein, 1988). Enteral infusion of a nutrient solution decreased jejuneal motility in the dog (Siegle and Ehrlein, 1988; Schmid and Ehrlein, 1993), and in man (Spiller *et al.,* 1984) by decreasing the length of contractions and increasing the incidence of stationary contractions (Siegle and Ehrlein, 1988; Schmid and Ehrlein, 1993). This effect appeared to be determined in part by the absorptive capacity of the gut, and a hypertonic nutrient solution had a more potent effect on motility than hypertonic saline (Schmid and Ehrlein, 1993). Infusion of isotonic fat and protein solutions into the ileum decreased the rate of small intestinal transit, while infusion of fat into the jejunum had no effect in the dog (Read *et al.,* 1984), and accelerated intestinal transit in man (Hammer *et al.,* 1998). Ileal feedback inhibition of intestinal transit, sometimes known

reduce further delivery of nutrients from the stomach and proximal small intestine, thus allowing for optimal absorption and digestion of nutrients (Read *et al.,* 1984). The control of intestinal motor patterns in response to the presence of nutrients in the gut is thought to mediated by hormonal effects and intrinsic neural reflexes (Siegle and Ehrlein, 1988), and similar to gastric emptying may be subject to local regulation by osmo- and chemo-receptors sensitive to amino acids and glucose (Barker *et al.,* 1974) or specific calcium binding affinities (Hunt, 1983; Schemann and Ehrlein, 1986a). Increasing the volume of solid and liquid test meals of constant caloric content resulted in an increased rate of gastric emptying, an effect mediated by the action of distension on the mechanoreceptors in the gastric musculature (Moore *et al.,* 1984; Hunt *et al.,* 1985). The rate of gastric emptying of non-nutrient meals is directly proportional to the volume present in the stomach (Hunt *et al.,* 1985). The emptying of complex nutrient meals is mainly controlled by feedback from chemoreceptors sensitive to increased nutrient concentration in the duodenum, and in these conditions the regulatory effect of the intestinal receptors is thought to override the effects of increased intra-gastric volume (Miller *et al.,* 1981b).

The rate of gastrointestinal transit is sensitive to the osmolarity of the ingested meal, an effect mediated by duodenal osmoreceptors (Barker *et al.,* 1974). However, the regulation of the rate of gastric emptying is mainly a function of the nutrient density of the meal; osmolarity becomes of physiological significance only at high tonicity levels (Calbet and Maclean, 1997). Small intestinal transit is similarly sensitive to the osmolarity of the chyme delivered from the stomach. Enteric perfusion of hypertonic saline decreased jejunal motility in the dog, but this inhibitory effect was not as great as that produced by hypertonic glucose, suggesting that intestinal motility is more sensitive to nutrient concentration than osmolarity (Schmid and Ehrlein, 1993).

Particle size is an important determinant of the rate of gastric emptying (Read and Houghton, 1989), large particles leave the stomach at a slower rate than smaller particles. The greater inertia of large particles tends to divert them to the lateral sides of the flow of food being propelled towards the pylorus (Read and Houghton, 1989). These slower moving particles are pushed back into the antrum by the strong retropulsive forces that accompany pyloric contraction. As the antral contraction moves distally, the pylorus partially closes, allowing only small particles to enter the duodenum and further decreasing the rate of gastric emptying of large particles. In the dog, larger particles are subjected to shearing forces by the stomach walls until they are reduced to particle sizes of less than 2mm and then allowed to pass through the pylorus (Meyer *et al.,* 1979). Ingesta that cannot be broken down to a particle size less than 2mm, is retained in the stomach and emptied during the phase III of the MMC (Meyer *et al.,* 1979).

Stress

Studies in both humans and animals have demonstrated a predominant inhibitory effect of experimental stressors (e.g. restraint, acoustic stress, pain) on gastrointestinal function (Stanghellini *et al.,* 1983; Musial and Enck, 1993). Stress is thought to affect gastrointestinal motility by interfering with neural pathways from the central nervous system, or by hormonal mediation (Gue *et al.,* 1988). Acoustic stress (1 hour music stress) caused a transient inhibition of gastric emptying and delayed the recovery of the MMC in dogs, and increased gastrin and pancreatic polypeptide levels (Gue *et al.,* 1988). These hormonal changes may have been involved in the mediation of the gastrointestinal effects of stress, or simply a direct effect of stress. A further study demonstrated that a kappa-opioid agonist (dynorphin) attenuated the inhibitory effect of stress on gastric motility in the dog, indicating that these effects may be mediated by

central pathways (Gue *et al.,* 1988). The similarity between the effects of systemic administration of corticotropin releasing factor (CRF) and acoustic stress on gastric motility in the dog suggests that CRF may play a role in stress-induced alteration of gastrointestinal motility (Gue *et al.,* 1988). In contrast to the effects of acoustic stress, restraint stress caused increased intestinal motility in dogs during fasting and after feeding (Muelas *et al.,* 1993). Differences in the effects of stress on gastrointestinal motility may reflect the different stress models adopted, which may affect motility by different central pathways or hormonal mechanisms.

For many years it was believed that stressful life events were involved in the pathogenesis of gastroduodenal ulceration, by affecting gastric motility and secretion, but the evidence to support this association remains anecdotal, despite extensive research. However it is possible that alterations in gastric emptying induced by stress could affect duodenal clearance of biliary/pancreatic secretions, causing increased duodeno-gastric reflux, and ulcer formation (Soll, 1997). Although alterations in gastric function induced by stress may interact with other factors to potentiate ulcerogenesis, it is no longer believed that stress has a primary role in the pathogenesis of gastroduodenal ulceration (Soll, 1997).

Exercise

There are conflicting reports of the effect of exercise on gastrointestinal motility; maximal exercise is associated with delayed gastric emptying (Brown *et al.,* 1994), but exercise at intensities of less than 70% of maximal oxygen consumption have no consistent effect on gastrointestinal motility (Mudambo *et al.,* 1997). Sub-maximal exercise was associated with increased duodenal motor activity and delayed gastric

emptying of a liquid meal in dogs (Kondo *et al.*, 1994). Many factors could be involved in alterations in gastrointestinal motility induced by exercise, in the dog. Endogenous opioids are released during exercise in the dog (Radosevich *et al.*, 1989), and have also been associated with central control of gastric motility in the dog (Lopez *et al.*, 1991). Increased sympathetic tone with associated release of catecholamines could also affect gastrointestinal motility during exercise (Brown *et al.*, 1994).

1.1.6 Methods for Assessment of Gastric Emptying, Small Intestinal and Oro-Caecal Transit Time

In 1898, WB Cannon took the first x-rays of liquid barium passing through the stomach of a cat. Over one hundred years later, many sophisticated methods are available for assessment of gastrointestinal transit, but the method described all those years ago, of radiographic imaging of barium is still widely used. A review of the methods available for assessment of gastric emptying and oro-caecal transit time in the dog, is given below.

1.1.6.1 Diagnostic Imaging

Radiology

Radiography and fluoroscopy can be used to monitor the gastrointestinal transit of radiopaque solids and liquids but although the time of onset and completion of gastric emptying can be estimated, only limited information is provided on the rate and pattern of gastric emptying. Many radiopaque test meals are available for radiographic assessment of GI motility, including:

- Liquid barium
- Barium mixed with food

- Radiopaque indigestible solids

Radiography is a widely used method for assessment of gastric emptying of liquids, despite the fact that delayed gastric emptying is rarely detectable in the liquid phase (Parkman *et al.,* 1995). In one canine study, gastric transit of liquid barium was normal in five cases of pyloric hypertrophy, despite subsequent demonstration of gross delays in gastric emptying using radioscintigraphy (Hornof *et al.,* 1989). Intestinal transit has been assessed in the dog using fluoroscopy by introducing liquid barium into the small intestine through an ileal catheter (Siegle and Ehrlein, 1988) or a jejunal catheter (Schemann and Ehrlein, 1986a;1986b). Attempts to assess solid-phase gastric emptying in dogs by mixing liquid barium with solid food produced data with wide variation between individuals, and between different studies, making generation of reference ranges difficult (Burns and Fox, 1986; Miyabayashi and Morgan, 1984). This method is difficult to apply in the clinical setting, because of the necessity for sequential imaging over a long time period (Hornof *et al.,* 1989). Furthermore, there is some evidence that barium may separate from the test meal and empty with the liquid phase (Miyabayashi and Morgan, 1984).

Indigestible radiopaque solids have been used as markers of solid-phase gastric emptying in dogs (Wilbur and Kelly, 1973; Meyer *et al.,* 1985; Hall *et al.,* 1992; Guilford *et al.,* 1997). The type of marker used in these studies were sections of radiopaque tubing (Hall *et al.,* 1992) teflon, polyamide and polypropylene spheres (Wilbur and Kelly 1973; Gruber *et al.,* 1987) and barium impregnated polyethylene spheres (Guilford *et al.,* 1997), BIPS, Arnolds Veterinary Products Ltd., Shrewsbury, UK. BIPS are radiopaque markers that have been designed specifically for investigation of gastric emptying in dogs and cats; a 1.5mm sphere is designed to mimic

solid-phase gastric emptying and a 5mm sphere designed to accumulate orad to an obstructing lesion (Lamb, 1999).

Gastric emptying of indigestible solids is dependent on particle size, and larger spheres (>2mm) are retropelled into the proximal stomach and empty from the stomach with the interdigestive motor pattern (Wilbur and Kelly, 1973). Studies in dogs have demonstrated that smaller markers (1.5 – 2mm, diameter) may empty with solid food but this occurs subject to extensive variation between and within individual dogs (Meyer *et al.,* 1985; Lester *et al.,* 1999). Accordingly, the gastric emptying of small BIPS (1.5mm diameter) did not correlate with the emptying of a radio-labelled solid meal in cats (Goggin *et al.,* 1999) or dogs (Lester *et al.,* 1999), and the gastric half emptying times are longer for BIPS than for canned food in dogs and cats (Meyer *et al.* 1985; Lamb, 1999). Conversely, one study indicated that the gastric emptying of both large (5mm) and small (1.5mm) BIPS was significantly correlated with the gastric emptying of concurrently ingested food (Guilford *et al.,* 1997). It is surprising that the gastric emptying of both large and small markers correlated with the emptying of food in this study, nevertheless these results may indicate that the gastric emptying of BIPS is sufficiently sensitive for clinical application. However, the gastric transit of indigestible radiopaque markers cannot be taken to represent the gastric transit of solid food since these markers are resistant to trituration, and consequently cannot provide a physiological representation of the sieving and triturative functions that characterise solid-phase gastric emptying.

Oro-caecal and small intestinal transit time has also been assessed in the dog using radiographic techniques (Ehrlein *et al.,* 1987; Guilford *et al.,* 1997). Superimposition of radiopaque markers and difficulty in identifying regions of the gastrointestinal tract may

lead to errors in the use of contrast radiology for assessment of intestinal transit. Nevertheless, a recent study demonstrated a good correlation between the radiographic location of radiopaque markers in the dog, and their actual location determined after death (Guilford *et al.*, 1997).

Radioscintigraphy

The evaluation of gastrointestinal motility by scintigraphic imaging following ingestion of a radionuclide-labelled meal, was first described in 1966 (Griffith *et al.*, 1966) and is now considered to be the gold standard method for investigation of gastrointestinal transit (Parkman *et al.*, 1995). Two radiopharmaceuticals that emit gamma radiation at different energies (eg ^{99}Tc and ^{111}In) can be used to preferentially label the solid and liquid phases of gastric emptying allowing the mechanisms and rates of each emptying phase to be monitored simultaneously (Parkman *et al.*, 1995). Radioscintigraphy can also be used to simultaneously assess gastric emptying and small intestinal transit time (Iwanga *et al.*, 1998).

There are some inherent sources of error associated with the measurement of gastrointestinal transit using scintigraphy, and correction factors have been derived to compensate for inaccuracies associated with the technique. Correction factors may be necessary to allow for radioactive decay of the isotope over the duration of the test. Furthermore, anterior movement of the marker in the stomach may cause self-attentuation of the radionuclide, and the lag phase of gastric emptying may be overestimated because the marker has moved anteriorly to lie closer to the camera (Christian *et al.*, 1983). Other errors are due to self-attentuation caused by the spreading of food in the stomach leading to initial counts greater than 100%, and overlap of activity in the small intestine over the area of interest in the stomach.

Gastric emptying and intestinal transit time have been extensively evaluated in dogs by monitoring the transit of a radioisotope labelled test meal by external scintigraphy (Malagelada *et al.,* 1980; Caride *et al.,* 1984; Burrows *et al.,* 1985; Theodorakis, 1980; van der Brom and Happe, 1985; Hornof *et al.,* 1989; Hammer *et al.,* 1998; Iwanga *et al.,* 1998). Scintigraphy is limited in its application by the requirement for access to specialist equipment, and the radiation hazard of the radionuclide tracer. Positioning of the dog in front of the gamma camera has also presented a problem in some canine radioscintigraphy studies, involving considerable struggling (Hornof *et al.,* 1989) or requiring sedation (van den Brom and Happe, 1985) or restraint in a Pavlov sling (Theodorakis, 1980; Lawaetz *et al.,* 1981), all of which could potentially affect the rate of gastrointestinal transit.

Ultrasonography

The development of techniques of high resolution, real-time ultrasonography has facilitated the application of this method for the assessment of gastrointestinal transit. A close correlation between the rate of both liquid and solid-phase gastric emptying measured by ultrasonography and by scintigraphy was demonstrated (Bolondi *et al.,* 1985; Benini *et al.,* 1999). Ultrasonography is used to quantitatively assess gastric emptying by measuring the flow volume through a defined area of interest, and also allows clear visualisation of antral contraction. However, the rate of gastric emptying measured using ultrasonography is based on the observed change in antral volume, and this may not represent a true measurement of gastric emptying, particularly if antral contents are retropelled into the fundus (Ahluwalia and Thompson, 1993). The use of ultrasonography for assessment of motility of regions of the gut other than the stomach has not yet been described. The main disadvantage of ultrasonography for assessment of gastrointestinal transit is that it is reliant on the skill of the operator making this a

subjective method for assessment of gut transit. Although the variability of the results using this method will always be reliant on the expertise of the operator, studies have shown that the variance between operators is not significantly large (Irvine *et al.,* 1993). Gastric and small intestinal contractions can be visualised using ultrasonography in dogs, and delayed gastric emptying may be indicated by the presence of fluid in the stomach 18 hours after feeding (Lamb, 1999). The use of ultrasonography as a method for quantitatively assessing canine gastric emptying warrants further investigation.

Magnetic Resonance Imaging

Magnetic resonance imaging (MRI) can be used to provide a three dimensional image of the stomach and allows gastric emptying and gastric motility to be assessed simultaneously and non-invasively (Schwizer *et al.,* 1994). A significant advantage of MRI over other methods is that gastric morphology can be visualised at the same time as gastric motility is evaluated, allowing the effect of gastric structural disorders on motility to be investigated (Maughan and Leiper, 1996). Magnetic resonance imaging was originally described as a method to assess liquid-phase gastric emptying (Schwizer *et al.,* 1994), but a solid-phase marker has recently been described (Feinle *et al.,* 1999), and should facilitate further application of this method. Magnetic resonance imaging requires expensive equipment that is not yet widely available in veterinary medicine and the use of MRI for assessment of gastrointestinal transit in dogs has not yet been described.

1.1.6.2 Tracer Studies

Tracer studies involve the serial aspiration of samples of gastrointestinal contents (through an oro-gastric tube or a fistula or catheter inserted in the gut wall) following ingestion of a known concentration of a non-absorbable marker substance. The rate of

gastrointestinal transit is proportional to the decrease in concentration of the marker. Tracer studies usually involve insertion of intra-luminal gastrointestinal catheters during laparotomy and there are many reports describing the use of this method for assessment of gastrointestinal transit in experimental dogs (Muller-Lissner *et al.,* 1982; Becker and Kelly, 1983; Gruber *et al.,* 1987; Gue *et al.,*1989; Haba and Sarna, 1993). Two catheters are used to assess small intestinal transit time, the test meal is inserted through the first catheter and its rate of passage through the intestine monitored by sampling through the second more distally placed catheter (Lin *et al.,* 1989). Markers used in these studies include indigestible solids, dye solutions, or a freeze-dried or radio-labelled meal.

Indigestible solids, such as lengths of plastic tubing or spheres, can be administered by oro-gastric intubation or in food, and their subsequent passage through the gastrointestinal tract monitored by sampling through a gastro-intestinal catheter or at necropsy. Dye dilution techniques are used to assess liquid-phase transit and involve the oral administration of a known concentration of a non-absorbable indicator substance (such as polyethylene glycol, phenol red, indocyanine green or chromium oxide) and assume that a homogenous suspension is formed with the gut secretion. Serial samples are taken through an oro-gastric tube or gastric or intestinal catheter and the changes in concentration of the marker are used to calculate the rate of gastric emptying or intestinal transit. Intestinal tracer studies have provided valuable information on the physiology of gastrointestinal transit, and there are several decades of literature supporting these techniques. However the invasive nature of intestinal tracer studies confines their use to the research laboratory.

1.1.6.3 Electrical Resistance

Impedance Epigastrography

Impedance epigastrography involves monitoring the fluctuation in an alternating current applied across the epigastric region. An alternating current is applied across the epigastric region using a pair of standard ECG electrodes, and a second pair of electrodes is used to monitor the change in potential difference (Spyrou and Castillo, 1993). The ingestion of a meal causes increased electrical resistance across the stomach, followed by an exponential decrease in impedance, and these changes are an indirect representative of gastric emptying (Sutton *et al.,* 1985). This technique has correlated well with liquid-phase gastric emptying rates measured using scintigraphy (Magnall *et al.,* 1988). Impedance epigastrography has been confined to the measurement of the gastric emptying of liquids and a solid-phase marker for use with this method has not yet been described. The technique is very sensitive to artefact induced by even slight body movement during the test (Spyrou and Castillo, 1993). There are no reports available on the use of this technique in the dog.

Applied Potential Tomography

Applied potential tomography (APT) is based on the same principle as impedence epigastrography, but a multi-electrode array is used to enclose the upper abdomen. An alternating current is passed through the abdomen and the potential difference between all combinations of the other 14 electrodes is measured. Successive neighbouring electrodes are used to input the current until all possible configurations have been used. The resulting array of data is used to construct grey-scale plots that represent the conductivity distribution of a cross-sectional image of the stomach (Spyrou and Castillo, 1993). Applied potential tomography is a more accurate method for measuring the rate of gastric emptying than impedance epigastrography, and can be used to

monitor the gastric emptying of a solid meal, provided that the meal is of either higher or lower conductivity than the body tissue. The use of this technique in the dog has not yet been described.

1.1.6.4 Plasma Tracers

Acetominophen Absorption Test

The acetominophen or paracetamol absorption test is a method for assessing the rate of gastric emptying of the liquid phase (Heading *et al.,* 1973). Plasma drug concentrations are measured in serial blood samples following ingestion of acetominophen in solution, and the rate of gastric emptying is related to the appearance of acetominophen in the blood (Heading *et al.,* 1973). Acetaminophen is poorly absorbed in the stomach, rapidly absorbed from the duodenum, and serum acetaminophen can be correlated with the rate of gastric emptying measured using scintigraphy (Clements *et al.,* 1978). Serum acetaminophen can be measured easily by chromatography (Spiller, 1993), and the absorption test protocol is relatively simple. However, this method of measuring gastric emptying is invasive and unsuitable for measuring the gastric emptying of the solid phase. Acetominophen may be subject to limited absorption in the stomach, that could result in substantial variation in the results (Heading *et al.,* 1973). Nevertheless, the acetominophen absorption test was used successfully to assess the effect of test meals on liquid-phase gastric emptying in dogs (Mizuta *et al.,* 1990).

Sulphapyridine Absorption Test

The sulphapyridine absorption test is used to assess oro-caecal transit time. The test is based on the liberation of sulphapyridine from microbial degradation of sulphasalazine in the colon (Spiller, 1993). Plasma sulphapyridine is monitored following oral administration of sulphasalazine, and the first detection of sulphapyridine is taken to

represent the oro-caecal transit time (Spiller, 1993). The test correlated well with oro-caecal transit times measured in dogs using the hydrogen breath test (Papasouliotis *et al.,* 1995). The test was used in one study to assess the effects of a test meal on the small intestinal transit time of the dog (Mizuta *et al.,* 1990). The sulphapyridine absorption test is subject to all the disadvantages associated with the use of the hydrogen breath test for assessment of oro-caecal transit time, with the added disadvantage of requiring intravenous catheterization.

1.1.6.5 Breath Tracers

Breath tracer studies of gastrointestinal transit involve detection of a gas or isotope either produced in response to the ingestion of a meal, or administration of a labelled substrate. The substrate or meal is rapidly digested and absorbed at the site of interest, by enzymatic degradation, or microbial digestion, and the rate of appearance of the gas or isotope in breath is a direct reflection of the gastrointestinal transit of the substrate.

Hydrogen Breath Test (H_2BT)

The H_2BT can be used as a method for assessment of oro-caecal transit time, and this test is based on the microbial digestion of a carbohydrate substrate in the colon (Bond and Levitt, 1975). Microbial fermentation of poorly absorbable carbohydrate (such as lactulose) in the anaerobic colonic environment results in the production of methane, hydrogen and short chain fatty acids. Hydrogen is highly diffusable, and appears in the breath 4 – 5 minutes following arrival of the substrate in the colon (Bond and Levitt, 1975; Spiller, 1993). The H_2BT has received some clinical and experimental application in man (Caride *et al.,* 1984) in the dog (Papasouliotis *et al.,* 1995), cat (Muir *et al.,* 1991), and in the horse (Murphy *et al.,*1998), but the usefulness of this test is limited by its dependence on the integrity of the colonic flora. Furthermore, up to 25%

of normal human subjects produce methane rather than hydrogen precluding the use of the H_2BT in these individuals (Spiller, 1993). Conflicting H_2 signals may also be derived from carbohydrate eaten before the commencement of the test, rather than from the test substrate. The non-absorbable carbohydrate substrate (lactulose) is hyper-osmolar causing secretion of water into the small intestine, increased luminal volume and consequently increasing intestinal transit (Spiller, 1993). It is a major drawback of the H_2BT that the substrate (lactulose) actually affects the parameter to be measured (intestinal transit).

Stable Isotope Breath Tests (SIBT)

The evolution of quick and accurate methods for the detection of stable isotopes permitted the application of stable isotope breath tests (SIBTs) for assessment of gastrointestinal transit (Preston *et al.*, 1988). The first SIBTs to be described for measuring the rate of gastric emptying were the ^{13}C-acetate breath test (Mossi *et al.*, 1994) and the ^{13}C-bicarbonate breath test (Bjorkman *et al.*,1991). Despite promising initial results, the ^{13}C-bicarbonate gastric emptying breath test could not be correlated with a simultaneous scintigraphic study, and hence does not appear to be a suitable substrate for use in assessment of gastric emptying (Bjorkman *et al.*, 1991). The ^{13}C-acetate liquid phase gastric emptying breath test has been correlated with scintigraphic (Braden *et al.*, 1995) and dye dilution methods (Mossi *et al.*, 1994) and has been applied for assessment of liquid phase gastric emptying in pharmacological and exercise physiology studies (Duan *et al.*, 1995; Leese *et al.*, 1995; Mudambo *et al.*, 1997). A ^{13}C-glycine breath test can also be used for assessment of liquid-phase gastric emptying and this test showed good correlation with the rate of gastric emptying measured using ultrasonography, despite a wide inter-subject variation (Benamouzig, 1999).

Solid-phase gastric emptying is a far more sensitive indicator of delayed gastric emptying than the liquid-phase (Parkman *et al.,* 1995), so a breath test for solid-phase gastric emptying is of particular interest for clinical application and pharmacological research. The ^{13}C-octanoic acid breath test (^{13}C-OBT) was developed as a marker of the solid phase of gastric emptying, and this test has now been correlated with scintigraphy in numerous studies (Ghoos *et al.,* 1993; Delbende *et al.,* 2000) and recently with ultrasonography (Capello *et al.,* 2000). Unlike ^{13}C-acetate, ^{13}C-octanoic acid enters the bicarbonate (HCO_3^-) pool following hepatic oxidation, causing a slight delay before the produced $^{13}CO_2$ is represented by an increased ^{13}C enrichment in the exhaled breath (Pallikarakis *et al.,* 1991). This delay precludes direct comparison of the gastric emptying coefficients obtained using the ^{13}C-OBT with quantitative methods such as radioscintigraphy, unless a correction factor is used. The ^{13}C-OBT has been applied for assessment of gastric emptying in pharmacological (Choi *et al.,* 1998b; Symonds *et al.,* 2000) and in clinical studies (Samson *et al.,* 2001; Ziegler *et al.,* 1996). The ^{13}C-acetate breath test has also been proposed as a potential probe of solid-phase gastric emptying (Meier-Augenstein *et al.,* 1999), but recent studies have shown poor correlation between this test and scintigraphy (Bromer *et al.,* 2001). ^{13}C-*Spirulina* is a novel substrate that has recently been validated for use in gastric emptying breath tests (Viramontes *et al.,* 2001; Ebert *et al.,* 2001). *Spirulina* is an edible algae that is cultured in $^{13}CO_2$ to produce a 99% ^{13}C-enriched substrate that is thought to be more representative of the food matrix than octanoic acid (Lee *et al.,* 2000a). Incorporation of the ^{13}C-substrate into pre-packed muffin meals and simplification of the test protocol has now established the ^{13}C-breath test as an investigative method that can be applied at the "point-of-care" (Lee *et al.,* 2000b; Bromer and Parkman 2001; Chey *et al.,* 2001). However, the clinical application of this test is limited by poor understanding of the effects of physiological and pathological abnormalities on the performance of the test.

^{13}C-glycosyl-ureide breath tests have been developed for assessment of oro-caecal transit time (Heine *et al,*.1995). These tests are similar to the hydrogen breath test as they are based on the microbial fermentation of a non-absorbable carbohydrate in colon, and are dependent on normal colonic microflora. However unlike the hydrogen breath test, the substrate does not affect the rate of intestinal transit and there can be no interfering signal produced by fermentation of dietary fibre (Wutzke *et al.,* 1997).

The SIBTs have many distinct advantages over other methods for assessment of gastrointestinal transit. The non-radioactive and non-invasive nature of these tests means that they can be performed in all subject groups, away from the analytical centre and in addition, serial tests in one individual are possible. The test meals used in these studies are identical to normal food and the protocol produces minimal disturbance of the subject. One or more substrates can be combined to allow concurrent assessment of different phases of gut transit. A combination of the ^{13}C-glycine and ^{14}C-octanoic acid breath test allowed solid and liquid phase gastric emptying to be assessed simultaneously (Maes, 1994a). This combined test involved using a radioisotope, but it is also possible to combine two stable isotope labels and mathematically deconvolute the resultant curve to allow separate interpretation of each test. This method was applied to a combined ^{13}C-octanoic acid and ^{13}C-lactose-ureide breath test, allowing gastric emptying, oro-caecal and small intestinal transit time to be assessed simultaneously (Geypens *et al.,* 1999c). The application of the SIBT is currently limited by the requirement for expensive and technically complex methods for measurement of the carbon isotope ratio. While these tests have been validated for application in healthy subjects, there have been relatively few studies investigating the effect of disease on the kinetics of tracer absorption and excretion. Further research is necessary to determine the metabolic fate of the tracers, and validate the tests for use in

all subjects. Simplification of the test protocol may facilitate future clinical application of these tests, meanwhile they remain accurate and non-invasive methods for experimental assessment of gastrointestinal transit.

1.2 OXIDATIVE STRESS AND CELL MEMBRANE LIPID PEROXIDATION

Oxidative stress is increasingly recognised as an important mechanism in many physiological processes including aging (Kapahi *et al.,* 1999), toxicity (Riely *et al.,* 1974) and disease (Babbs, 1992). Oxidative stress refers to an imbalance between the rate of free radical production and the ability of antioxidant mechanisms to protect cells against oxidation by free radicals. Free radicals are defined as "...any chemical species capable of independent existence and containing one or more unpaired electrons" and a superscript dot ($^{\bullet}$) is used to indicate the location of the unpaired electron (Gutteridge, 1995).

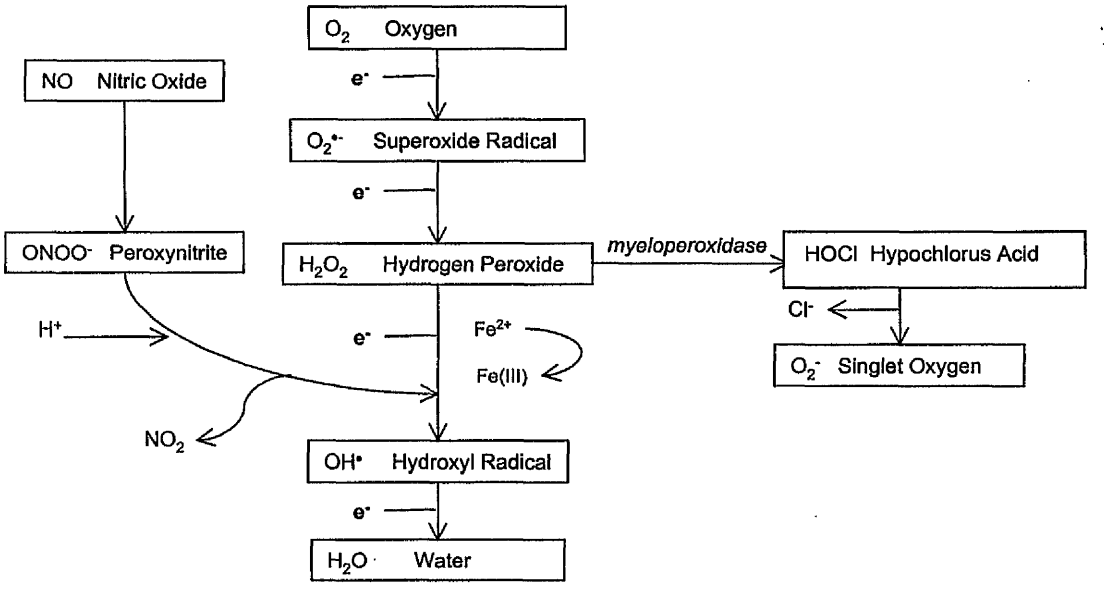

Figure 1.5 Generation of free radicals during aerobic respiration

Oxidative stress causes tissue injury by damaging cellular macromolecules, and has been associated with a number of diseases, such as chronic inflammatory diseases (Grisham and Granger, 1988) and cancer (Hietanen *et al.*, 1994). Oxidative stress increases during disease, but is not itself a pathogenic process, occurring during aerobic respiration as the chemical and heat energy essential for life is generated by reduction of molecular oxygen to water (Figure 1.5).

1.2.1 Free Radicals and Reactive Oxygen Species

Some free radicals and reactive oxygen species that are important in mediating damage to cellular macromolcules are reviewed below:

Superoxide Radical ($O_2^{\bullet-}$)

A superoxide radical is generated following transfer of one electron to oxygen (Figure 1.5). In aqueous solution superoxide radical undergoes spontaneous dismutation to form hydrogen peroxide and oxygen, a reaction catalysed by the enzyme $Cu^{2+}Zn^{2+}$-superoxide dismutase:

$$2O_2^{\bullet-} + 2H^+ \xrightarrow{Cu^{2+}Zn^{2}superoxidedismutase} H_2O_2 + O_2 \qquad \text{(Eq. 1.1)}$$

The superoxide radical is not very damaging to cellular components in itself, but it can react with other free radicals to facilitate tissue damage (Aikens and Dix, 1991).

Hydrogen Peroxide (H_2O_2)

Hydrogen peroxide is quickly decomposed to water and oxygen by enzymes such as catalase and glutathione peroxidase. Hydrogen peroxide is a weak oxidising and

reducing agent, but in the presence of transition metal ions, or exposure to ultraviolet light, H_2O_2 may decompose to generate hydroxyl radicals (Gutteridge and Halliwell, 1990).

Hydroxyl Radical ($^{\bullet}OH$)

The hydroxyl radical is generated by high energy ionisation of water, as may occur during ultrasonication of aqueous solutions and by homolytic fission of the O-O bond in H_2O_2 :

$$H_2O \rightarrow {}^{\bullet}OH + H^{+} + e^{-} \rightarrow H_2O_2 \qquad \text{(Eq. 1.2)}$$

$$^{\bullet}OH + H^{+} + e^{-} \rightarrow H_2O_2 \qquad \text{(Eq. 1.3)}$$

$$H_2O_2 \xrightarrow{\text{uv-light}} 2\,{}^{\bullet}OH \qquad \text{(Eq. 1.4)}$$

The hydroxyl radical can also be generated by reductive cleavage of the bonds between the oxygen atoms in H_2O_2 (Babbs, 1992), a reaction catalysed by transition metals called the Fenton reaction:

$$Fe^{2+} + H_2O_2 \rightarrow Fe^{3+} + OH^{-} + {}^{\bullet}OH \qquad \text{(Eq. 1.5)}$$

$$Fe^{3+} + H_2O_2 \rightarrow Fe^{2+} + HO_2 + H^{+} \qquad \text{(Eq. 1.6)}$$

The hydroxyl radical is the most aggressive radical known, and reacts immediately with any biomolecules in the vicinity of its formation. This reaction involves abstraction of a hydrogen atom and generates a less reactive free radical:

$$^{\bullet}OH + R\text{-}H \rightarrow H_2O + R^{\bullet} \qquad \text{(Eq. 1.7)}$$

e.g. $^{\bullet}OH$ + alcohol $\rightarrow$ H_2O + hydroethyl radical (Eq. 1.8)

Singlet Oxygen

Singlet oxygen (O_2^-) is an electronically excited form of molecular oxygen, generated during photosensitization reactions. Photosensitized molecules such as methylene blue, riboflavin and bilirubin are capable of absorbing light at certain wavelengths, causing them to become electronically excited. Singlet oxygen is generated when the excitation energy of the photosensitised molecule is transferred to molecular oxygen, while the photosensitised molecule returns to its ground state energy. Singlet oxygen reacts with biomolecules by direct chemical reaction or by transferring activation energy, a mechanism called quenching (Kohno *et al.*, 1995). Singlet oxygen can react directly with carbon-carbon bonds to generate peroxides, and this process is important in lipid peroxidation (Section 1.2.3).

Nitric Oxide ($NO^\bullet$) and Nitrogen Dioxide ($NO_2^\bullet$) Radicals

Nitric oxide is synthesised *in vivo* from the amino acid L-arginine, a reaction catalysed by the enzyme nitric oxide synthase, NOS (Kroncke *et al.*,1997):

$$\text{L-arginine} \xrightarrow{\text{NOS}} NO^\bullet + \text{L-citrulline} \qquad \text{(Eq. 1.9)}$$

Nitric oxide is not very reactive with cellular macromolecules, but readily reacts with superoxide radicals to form peroxynitrite, $ONOO^-$ (Kroncke *et al.*, 1997):

$$NO^\bullet + O_2^{\bullet-} \rightarrow ONOO^- \qquad \text{(Eq. 1.10)}$$

Peroxynitrite is itself damaging to cells, and can also decompose at acid pH to release nitrogen dioxide and hydroxyl radical, a reaction that does not require transition metal catalysis:

$$OONO^- + H^+ \rightarrow {}^\bullet OH + NO_2 \qquad \text{(Eq. 1.11)}$$

Nitrogen dioxide is a free radical that is capable of initiating lipid peroxidation by hydrogen abstraction from fatty acid side chains. Nitric oxide can also decompose in

the presence of oxygen and water to yield potent n-nitrosating agents (Grisham and Yamada, 1992):

$$2NO^{\bullet} + O_2 \rightarrow 2NO_2^{\bullet} \quad \text{(Eq. 1.12)}$$

$$2NO_2^{\bullet} \leftrightarrow N_2O_4 \xrightarrow{H_2O} NO_2^- + NO_3^- \quad \text{(Eq. 1.13)}$$

$$NO_2^- + N_2O_4 \xrightarrow{H_2O} NO^{\bullet} + 2NO_3^- \quad \text{(Eq. 1.14)}$$

$$NO^{\bullet} + NO_2^{\bullet} \leftrightarrow N_2O_3 \xrightarrow{H_2O} 2NO_2^- \quad \text{(Eq. 1.15)}$$

Nitrogen dioxide ($NO_2^{\bullet}$) dinitrogen trioxide (N_2O_3) and dinitrogen tetroxide (N_2O_4) can promote the nitrosation of primary and secondary amines to cause formation of carcinogenic nitrosamines.

Hypochlorous Acid

Hypochlorous acid is formed in the phagocyte cytoplasm from hydrogen peroxide and chlorine ions, a reaction catalysed by myeloperoxidase (Babbs, 1992):

$$H_2O_2 + Cl^- \xrightarrow{myeloperoxidase} HOCl + H_2O \quad \text{(Eq. 1.16)}$$

Hypochlorous acid is a strong oxidant, and may also generate hydroxyl radicals by reactions occurring both dependently and independently of transition metal catalysis:

$$HOCl + O_2^{\bullet -} \longrightarrow {}^{\bullet}OH + HCl^- + O_2 \quad \text{(Eq. 1.17)}$$

$$HOCl + Fe^{2+} \longrightarrow {}^{\bullet}OH + HCl^- + Fe^{3+} \quad \text{(Eq. 1.18)}$$

1.2.2 Sources of Free Radicals

Enzymatic Sources

Several enzymes have been identified that generate free radicals *in vivo* as a result of their catalytic activity. Xanthine oxidase was the first enzyme to be shown to produce superoxide radical *in vivo* (Granger *et al.*, 1981), and is used experimentally as a source

of superoxide radical. Xanthine oxidase catalyses the oxidation of hypoxanthine to uric acid, while reducing oxygen to hydrogen peroxide and superoxide radical (McCord and Fridovich, 1968). Under normal conditions, xanthine oxidase produces no free radicals and serves as a NAD^+ dependent dehydrogenase. However, when oxygen is limited (e.g. during ischaemia), the energy balance of the cell is altered, ATP is converted to AMP which is catabolised to hypoxanthine (Figure 1.6). Upon reperfusion, xanthine dehydrogenase is converted to xanthine oxidase and oxygen is reduced to superoxide radical (Granger *et al.*, 1981). Reperfusion of the ischaemic feline ileum was accompanied by increased production of superoxide radical, and increased capillary permeability (Granger *et al.*, 1981). Administration of the enzyme superoxide dismutase, greatly attenuated the increased capillary permeability that accompanied reperfusion, suggesting that this effect was mediated by the superoxide radical (Granger *et al.*, 1981).

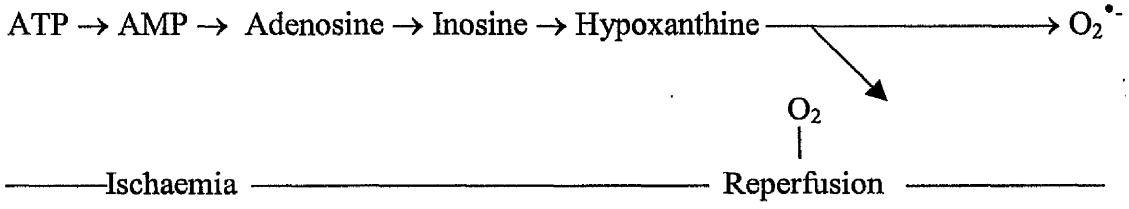

Figure 1.6 Production of superoxide during ischaemia

Other enzymes that can catalyse the reduction of molecular oxygen by less than four electrons include NADPH oxidase and aldehyde oxidase (Grisham and Granger, 1988):

$$NADPH + O_2 \xrightarrow{NADPH\ oxidase} NADP^+ + O_2^{\bullet-} \qquad \text{(Eq. 1.19)}$$

$$R\text{-}CHO + O_2 \xrightarrow{aldehyde\ oxidase} RCOOH + O_2^{\bullet-} \qquad \text{(Eq. 1.20)}$$

Subcellular Organelles

The electron transport chain within the mitochondria and endoplasmic reticulum are the most important sites for free radical production in the aerobic cell. Superoxide is generated during the process of electron transport, when an electron is passed to oxygen instead of to the next electron carrier, and it is thought that between 1 - 3 % of oxygen reduced in the mitochondria is released as superoxide radical (Halliwell and Gutteridge, 1999). The process of electron transfer is arranged to facilitate electron movement along each component of the chain, rather than to oxygen. Superoxide production is greatest when mitochondrial enzyme complexes are reduced, i.e., when the rate of reduction of oxygen to water is limited by low oxygen concentrations (Freeman and Crapo, 1982). Conditions such as these might occur during tissue ischaemia resulting in an accumulation of enzyme co-factors and facilitating mitochrondrial production of superoxide (Freeman and Crapo, 1982).

Inflammatory Cells

Resting neutrophils and macrophages are dependent on anaerobic mechanisms for the majority of their respiratory activity, however both cells exhibit a surge in oxygen consumption during phagocytosis (Babior *et al.*, 1973). This increased oxygen uptake is not affected by inhibitors of mitochondrial electron transport and is thought to occur due to activation of an enzyme complex at the cell membrane, causing oxidation of NADPH, reduction of oxygen and generation of superoxide (Babior *et al.*, 1976).

$$NADPH + 2O_2 \longrightarrow NADP^+ + H^+ + 2O_2^{\bullet-} \qquad \text{(Eq. 1.21)}$$

During phagocytosis, the antigenic particle is engulfed, and enclosed in a phagocytic vacuole, where it is exposed to high concentrations of superoxide. Within the vacuole, superoxide may undergo dismutation to produce the more reactive hydrogen peroxide

(Babior *et al.*, 1973). Hydrogen peroxide may destroy particles within the vacuole directly, or be converted to the highly reactive hydroxyl radical before destroying the antigen.

Auto-Oxidation

Several molecules including glyceraldahyde, catecholamines and flavins are capable of auto-oxidising in the presence of oxygen to generate superoxide radicals (Freeman and Crapo, 1982).

Haem Proteins

Iron in the haem ring of haemoglobin is generally in the Fe^{2+} state, but delocalisation of the electron results in an intermediate compound, where iron is in the Fe^{3+} state and bound to superoxide radical (Balagopalakrishna *et al.*, 1996):

$$\text{Haem-Fe}^{2+}\text{-O}_2 \leftrightarrow \text{Haem–Fe}^{3+}\,\text{O}_2^{\bullet-} \qquad \text{(Eq. 1.22)}$$

The haem-Fe^{3+} compound is called methaemoglobin and is unable to bind oxygen. Oxidation of this compound releases superoxide, and it is estimated that 3% of human haemogloblin undergoes such oxidation each day (Halliwell and Gutteridge, 1999).

1.2.3 Chemistry of Lipid Peroxidation

Lipid peroxidation can be defined as the oxidative deterioration of polyunsaturated lipids (Tappel and Zalkin, 1959) and is an important mechanism of cell toxicity implicated in many disease states. Lipid peroxidation causes damage *in vivo*, by affecting the integrity of the cell membrane, inactivating membrane bound enzymes and

receptors and increasing membrane permeability. If the lysosome membrane is affected by lipid peroxidation, hydrolytic enzymes may be released. Lipid peroxidation can also cause damage to cell membrane proteins by affecting the fluidity of the lipid layer in which they are suspended (Halliwell and Gutteridge, 1999). Lipid peroxidation is a self-propagating chain reaction that occurs in three phases, initiation, propagation and termination. (Figure 1.7).

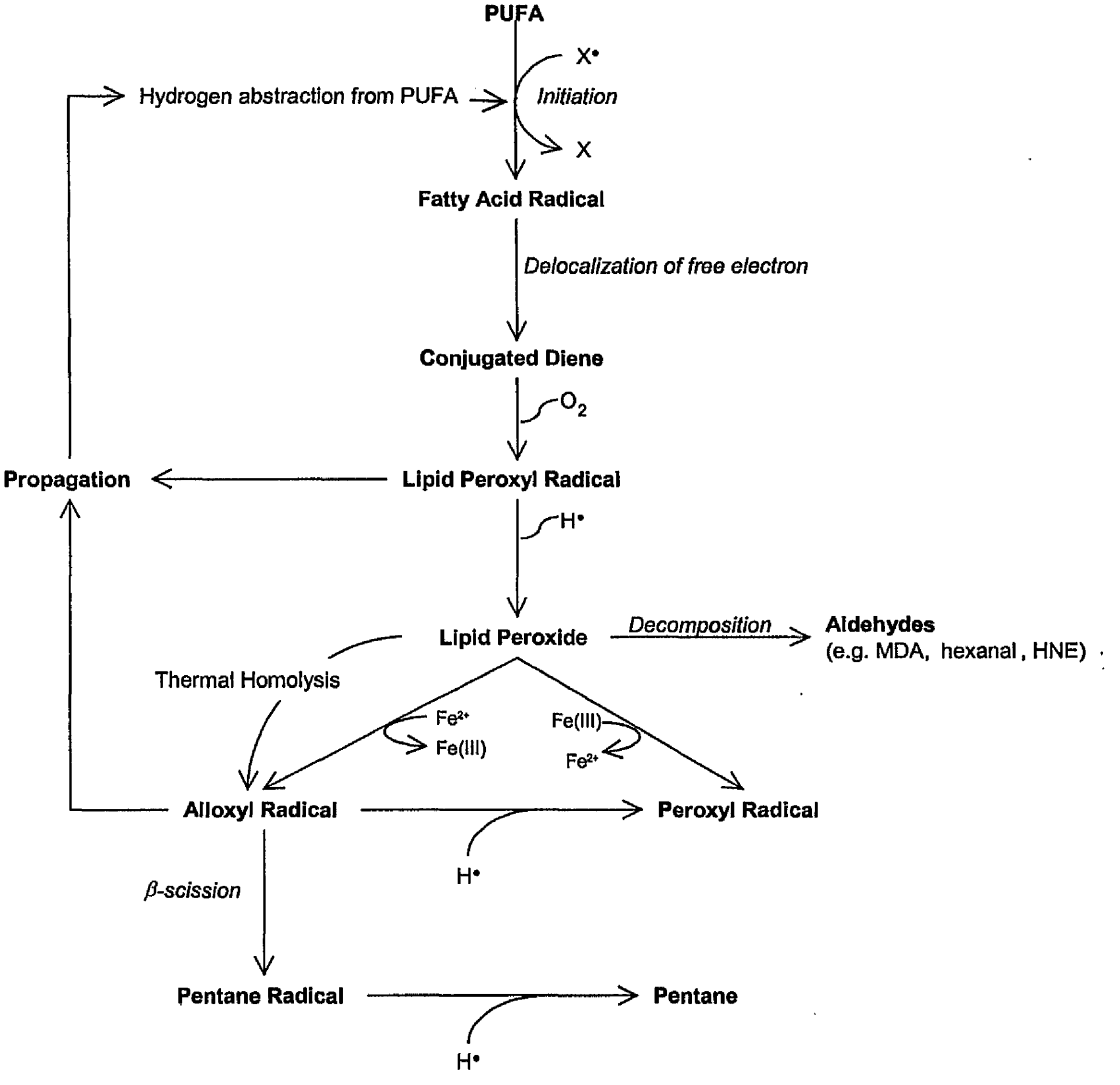

Cobalt(II), Cu^{2+} and Cu^{+} can also promote lipid decomposition

Figure 1.7 An overall view of the process of lipid peroxidation

Lipid peroxidation is initiated by abstraction of a hydrogen atom ($H^{\bullet}$) from a methylene group ($-CH_2-$) of a fatty acid side chain (Aikens and Dix, 1991). Polyunsaturated fatty acids are particularly sensitive to lipid peroxidation, since the presence of a double bond weakens the C-H bonds on the carbon atom adjacent to the double bond, predisposing it to hydrogen abstraction (Wagner *et al.*, 1994). Molecules with sufficient reactivity to initiate lipid peroxidation include hydroxyl radical ($^{\bullet}OH$), the protonated form of superoxide ($HO_2^{\bullet}$), alloxyl radical ($RO^{\bullet}$) and peroxyl radical ($ROO^{\bullet}$).

e.g. $^{\bullet}OH + -CH_2- \longrightarrow -^{\bullet}CH_2- + H_2O$ (Eq. 1.23)

Abstraction of a hydrogen atom from a methylene group gives rise to a carbon centred radical ($-^{\bullet}CH_2-$), which undergoes molecular stabilisation to form a conjugated diene, and in the presence of oxygen becomes a peroxyl radical:

$R^{\bullet} + O_2 \longrightarrow ROO^{\bullet}$ (Eq. 1.24)

Peroxyl radicals can abstract hydrogen atoms from other fatty acids to generate a lipid hydroperoxides (ROOH) and a carbon radical:

$ROO^{\bullet} + -CH_2- \longrightarrow ROOH + -^{\bullet}CH_2-$ (Eq. 1.25)

The carbonyl group formed can react with oxygen to form a peroxyl radical, which can then abstract hydrogen atom from a methylene group, thus propagating the chain reaction of lipid peroxidation. Lipid peroxides (ROOH) are stable at physiological temperatures, but metal complexes can react with lipid peroxides to give alloxyl and peroxyl radicals:

e.g. $ROOH + Fe^{2+} \longrightarrow Fe^{3+} + RO^{\bullet} + OH^-$ (Eq. 1.26)

Reactions of Fe^{3+} and ROOH are slower than Fe^{2+}, and this explains why the rate of lipid peroxidation increases in the presence of a reducing agent, e.g. ascorbate (Davies and Slater, 1987). However, it is unlikely that transition metal ions actually initiate

lipid peroxidation, but simply propagate a pre-existing process by catalysing the decomposition of pre-formed lipid peroxide (Davies and Slater, 1987).

The alloxyl radicals generated during lipid peroxide decomposition are further degraded into a variety of compounds including aldehydes, alkanes and isoprostanes. Alloxyl radicals derived from peroxidation of linoleic acid can degrade by β-scission to a pentane radical and an aldehyde. The pentane radical can abstract a hydrogen atom from a fatty acid chain to form pentane:

$$RO^{\bullet} \xrightarrow{\beta\text{-scission}} \text{pentane radical} \xrightarrow{H^{\bullet}\ abstraction} \text{pentane} \qquad \text{(Eq. 1.27)}$$

Ethene and ethane are produced in similar reactions from linolenic acid (Rieley *et al.*, 1974). An aldehyde, malondialdehyde (MDA) is formed during peroxidation of polyunsaturated fatty acids (PUFAs) with two or more double bonds. MDA is rapidly metabolised *in vivo*, accounting for the very low concentrations of MDA identified in human plasma (Gutteridge and Quinlan, 1983). 4-Hydroxy-2-*trans*-nonenal (HNE) is formed during peroxidation of 6-carbon PUFAs. HNE is cytotoxic, but rapidly reacts with proteins when formed *in vivo* (Segall *et al.*, 1985). Isoprostanes are compounds formed during peroxidation of arachidonic acid, that are structurally similar to prostaglandin $F_{2\alpha}$ (hence they are referred to as F_2-isoprostanes). The F_2-isoprostanes are rapidly excreted and metabolised *in vivo*, and the majority of plasma F_2-isoprostanes are esterified to phospholipids (Morrow *et al.*, 1990). Termination is the final stage of lipid peroxidation and can occur when two radicals annihilate each other:

$$\text{e.g.} \quad LO_2^{\bullet} + LO_2^{\bullet} \longrightarrow LOOL + O_2 \qquad \text{(Eq. 1.28)}$$

Termination is also mediated by the presence of an anti-oxidant (e.g. α-tocopherol) which provides a source of easily-abstracted hydrogen atoms, to direct free radical generation away from the cell membrane:

$LO_2^{\bullet} + \alpha\text{-TocH} \longrightarrow \alpha\text{-Toc}^{\bullet} + LO_2H$ (Eq. 1.29)

The α-tocopherol radical can also contribute to termination of lipid peroxidation by reacting with a second peroxyl radical:

$\alpha\text{-Toc}^{\bullet} + LO_2^{\bullet} \longrightarrow \alpha\text{-TocOOH}$ (Eq. 1.30)

1.2.4 Measurement of Lipid Peroxidation

Lipid peroxidation is a complex process that accompanies many types of cell insult including trauma, infection, toxicity and ischaemia (Riely *et al.,* 1974; Grisham and Granger, 1988; Hietanen *et al.,* 1994). Detection and quantification of lipid peroxidation is an important means of assessing the role of this process in disease and evaluating the efficacy of anti-oxidant mechanisms. There are three main approaches to investigation of lipid peroxidation:

1 Quantification of loss of substrate

2 Measurement of primary peroxidation products, e.g. lipid hydroperoxides

3 Measurement of secondary peroxidation products, e.g. decomposition products of lipid hydroperoxides.

The composition of the end products of lipid peroxidation is dependent on the concentration of transition metal ions and on the fatty acid composition of the substrate. Investigation of lipid peroxidation should involve analysis at more than one stage of the process, since no one test can be an index of overall lipid peroxidation. Detection of lipid peroxidation *in vivo* is particularly problematic, since biological material is susceptible to lipid peroxidation during the assay. The three main approaches to investigation of lipid peroxidation are discussed below.

1.2.4.1 Quantification of Loss of Substrates

The process of lipid peroxidation involves the depletion of membrane lipid polyunsaturated fatty acids side chains; hence, by monitoring the concentration of specific fatty acids, lipid peroxidation may be quantified. This method requires *in vitro* hydrolysis of cell membrane lipids, followed by separation and quantification of fatty acids by gas-chromatography (GC) gas-chromatography mass spectrometry (GC-MS) or high pressure liquid chromatography (HPLC) (Piretti *et al.*, 1987). Oxygen is also a substrate for lipid peroxidation and the rate of oxygen uptake by carbon centred radicals and peroxide decomposition can be used as an index of lipid peroxidation. This method requires *in vitro* separation of membrane lipids and oxygen uptake is detected using an oxygen electrode.

1.2.4.2 Measurement of Primary Peroxidation Products

Assessment of the primary products of lipid peroxidation (lipid peroxides), is an attractive method for assessment of lipid peroxidation, since it allows assessment of the early stages of the process, without relying on the degradation products (eg hydrocarbon gases, MDA).

Iodometric Assay

One of the oldest methods for assessment of lipid peroxides is the iodometric hydroperoxide assay. This test is based on the oxidation of iodide (I^-) by peroxides to generate the chromophore I^{3-} in the presence of excess iodide:

$$ROOH + H^+ + I^- \rightarrow ROH + H_20 + I^{3-} \quad \text{(Eq. 1.31)}$$

$$I^{3-} \leftrightarrow I_2 + I^- \quad \text{(Eq. 1.32)}$$

Molecular oxygen can compete with lipid peroxides for oxidation of iodide, so reaction conditions must be strictly anaerobic (Thomas *et al.*, 1989). The appearance of the

triiodide chromophore is detected spectrophotometrically at 360nm (Jessup *et al.*, 1994). The iodometric assay is a sensitive method for detection of lipid peroxides, but its application is limited by the requirement for strictly anaerobic test conditions.

Ferrous Oxidation Xylenol-Orange (FOX) Test

The ferrous oxidation xylenol orange (FOX) test is another sensitive and simple method for detection of lipid peroxides, but unlike the iodometric assay, is not sensitive to oxygen concentration. This test is based on the oxidation of Fe^{2+} to Fe^{3+} by lipid peroxides, a reaction that can be measured colourimetrically using the indicator xylenol-orange. Xylenol-orange binds ferric ions to produce a blue complex that can be detected spectrophotometrically at 560nm (Nourooz-Zadeh *et al.*, 1994). The FOX test cannot be easily applied for detection of lipid peroxides in plasma since ferric ions present in plasma may react with xylenol-orange to produce a colour change that is not related to the presence of lipid peroxides (Nourooz-Zadeh *et al.*, 1994). Triphennylphosphine oxide (TPP) is a compound that can specifically reduce lipid peroxides and addition of TPP can allow non-lipid peroxide mediated colour changes to be detected (Nourooz-Zadeh, 1999).

Glutathione Peroxidase

This enzyme has a Se centre, is fat soluble and is thought to protect the cell from peroxidation. Glutathione peroxidase reacts with peroxides to oxidise reduced glutathione, GSH, to oxidised glutathione, GSSG (Allen *et al.*, 1990). Addition of glutathione reductase and NADPH reduces GSSG back to GSH, resulting in consumption of NADPH. Since NADPH uptake in this reaction can be stoichiometrically related to the original peroxide concentration, quantification of NADPH can be used as an index of lipid peroxidation. Similarily, GSSG can also be

quantified using HPLC (Halliwell and Gutteridge, 1999). This test requires that peroxides are cleaved from membrane lipids using phospholipase, but is not sensitive to oxygen.

Cyclooxygenase Test

Trace quantities of lipid hydroperoxides can stimulate cyclooxygenase (COX) activity and this mechanism can be used to assess the presence of peroxides (Marshall *et al.*, 1985). The COX test is particularly interesting since it relates the concentration of lipid peroxides to one of their potential actions *in vivo*, i.e. eicosanoid synthesis. The test can detect very low concentrations of lipid peroxides, since it is based on the very sensitive requirement of COX for lipid peroxide (Marshall *et al.*, 1985). Cyclooxygenase activity is quantified as oxygen uptake, measured using an oxygen electrode (Marshall *et al.*, 1985).

Haem Proteins

Lipid peroxides react with haem and haem proteins to produce reactive intermediates that produce light when reacted with luminol (Pastorino *et al*, 1999). Detection of light emission using a luminometer allows the concentration of peroxides present in the sample to be measured. The sample must be separated using HPLC before the reaction to avoid the scavenging of reactive species formed during the test, by antioxidant present in the sample.

Gas Chromatography Mass Spectrometry (GC-MS)

Lipid peroxides can be quantified using GC-MS (Frank *et al.*, 1989). This technique involves reduction of hydroperoxides to hydroxy compounds, separation by gas chromatography and identification and quantification by mass spectrometry.

1.2.4.3 Measurement of Secondary Lipid Peroxidation Products

Secondary lipid peroxidation products are compounds formed following degradation of lipid peroxides. Their formation is therefore dependent on the rate of peroxide decomposition, a process that is itself dependent on temperature and the presence of transition metal ions.

Diene Conjugation

The process of peroxidation of polyunsaturated fatty acids involves formation of structures with two double bonds joined by a single bond, called conjugated dienes (Gutteridge and Quinlan, 1983). These compounds absorb light in the ultraviolet region at 230 - 235nm, and measurement of conjugated diene concentrations in isolated lipoproteins and pure lipids can be used to assess lipid peroxidation (Corongiu and Banni, 1994). Conjugated dienes are not a good indicator of lipid peroxidation in biological samples, since many substances absorb light between 230 - 235nm, such as haem proteins and purines (Halliwell and Gutteridge, 1999). Lipids can be extracted from biological samples using organic solvents, or conjugated dienes can be separated using high performance liquid chromatography, enabling application of this test in biological samples. Human samples require separation of conjugated dienes by high performance liquid chromatography or gas chromatography-mass spectrometry due to the presence of octadeca-9,11-dienoic acid, which absorbs light at similar wavelengths to conjugated dienes. The origin of this compound is unknown, but it is thought to be absorbed from food or to arise from bacterial metabolism, and it is not an indicator of lipid peroxidation (Halliwell and Gutteridge, 1999). The sensitivity of the conjugated diene test can be increased by second derivative spectroscopy, since changes in the second derivative spectrum are clearer than simple wavelength-absorbance spectrum (Corongiu and Banni, 1994).

Hydrocarbon Gases

Hydrocarbon gases such as pentane and ethane are produced by β-scission of alloxyl radicals (Riely *et al.*, 1974). These gases can be detected in exhaled air using gas chromatography, and this is a useful method for detection of lipid peroxidation *in vivo* (Aghdassi and Allard, 2000). Background levels of pentane and ethane are relatively high and variable, and a washout period of breathing hydrocarbon-free air may be necessary. A particular disadvantage of pentane assessment is that it is subject to some metabolism in the body (Allerheiligen *et al.*, 1987), while methodological problems have limited the application of ethane as a marker of lipid peroxidation.

Luminescence

During the process of lipid peroxidation, excited carbonyls and singlet oxygen may emit light by Russell's mechanism (Nakano *et al.*, 1994). Quantification of luminescence using a photon counter is a simple method for detection of lipid peroxidation in isolated cells or membrane fractions (Halliwell and Gutteridge, 1999). Assessment of lipid peroxidation using luminescence has correlated well with other techniques (Nakano *et al.*, 1994). The appearance of luminescence in phospholipids extracted from rat-liver microsomes, was dose-dependently suppressed by the anti-oxidant, α-tocopherol (Nakano *et al.*, 1994), indicating that oxidative processes were responsible for the emission of light.

Fluorescence

The decomposition of lipid peroxides to aldehydes such as MDA and HNE may involve the generation of fluorescent products via complex chemistry, that can be detected using fluorescence spectrophotometry (Shimasaki, 1994; Cominacini *et al.*, 1991).

Parinaric Acid

Parinaric acid is a fluorescent polyunsaturated fatty acid that is very sensitive to lipid peroxidation. This compound can be incorporated into lipids, and lipid peroxidation monitored by loss of the characteristic fluorescence of parinaric acid (Kuypers *et al.*, 1987). This method can be used for continuous monitoring of lipid peroxidation, and parinaric acid can be easily incorporated into the lipid fraction of cell membranes, microsomes, lipoproteins and liposomes (Halliwell and Gutteridge, 1999). However, the oxidative damage to parinaric acid is not a direct parallel of the peroxidative breakdown of naturally occurring polyunsaturated fatty acids, since parinaric acid is more sensitive to lipid peroxidation.

Thiobarbituric Acid Test

The thiobarbituric acid (TBA) test is probably the most widely used measure of lipid peroxidation, mostly due to its simplicity, despite its inaccuracy and non-specificity. The test is based on the development of a pink chromagen when one molecule of MDA reacts with 2 molecules of TBA to form a TBA_2-MDA adduct. The pink chromagen was definitively identified as a TBA_2-MDA adduct using nuclear magnetic resonance (Nair *et al.*, 1986). The TBA test is carried out by heating the sample with TBA in acid conditions, and measuring the appearance of the pink chromagen by absorbance at 532nm or fluorescence at 553nm (Chirico, 1994). Most of the MDA-TBA adduct is generated by decomposition of lipid peroxides during the test process (Halliwell and Gutteridge, 1999) and the rate of decomposition is affected by metal ion concentration, temperature and pH of the reaction, making standardisation difficult (Gutteridge and Quinlan, 1983). Furthermore, decomposition of lipid peroxides during the TBA test may generate peroxyl radicals ($RO_2^{\bullet}$) that induce further lipid peroxidation, effectively amplifying the lipid peroxidation process already present in the test material (Gutteridge

and Halliwell, 1990). Application of the TBA test in biological samples is problematic since substances such as bile pigments and amino acids may absorb light at 553nm, and separation of the TBA_2-MDA adduct by high performance liquid chromatography is necessary (Chirico, 1994; Largilliere and Melancon, 1988). This test remains a useful method for assessment of lipid peroxidation in controlled *in vitro* systems, such as the oxidation of lipids in cell membrane extracts and liposomes.

Isoprostanes

Free radical catalysed metabolism of arachidonic acid results in production of four unique families of prostaglandin-F_2 like compounds called F_2-isoprostanes (Morrow *et al.*, 1990). The F_2-isoprostanes are produced primarily via a cyclooxygenase independent pathway, since high doses of cyclooxygenase inhibitors did not inhibit their generation (Morrow *et al.*, 1990). Induction of oxidative stress by administration of carbon tetrachloride or diaquat increased F_2-isoprostane production in rats, while infusion of the F_2-isoprostane, 8-epi-prostaglandin-$F_{2\alpha}$ caused decreased renal blood flow and increased renal glomular filtration rates (Morrow *et al.*, 1990). These findings suggested that the F_2-isoprostanes may be used to assess lipid peroxidation *in vivo*, and may themselves be involved in the pathophysiological process of oxidative stress (Morrow *et al.*, 1990). F_2-isoprostanes can be detected in biological fluids by extraction of phospholipids, alkaline hydrolysis to release F_2-isoprostanes, and separation and quantification by gas chromatography and mass spectrometry (Morrow and Roberts, 1999). F_2-isoprostanes can be detected in most physiological tissues including plasma, urine, CSF, lymph and synovial fluid, enabling detection of products of lipid peroxidation at site of release (Morrow and Roberts, 1999). One disadvantage of the F_2-isoprostane detection is that F_2-isoprostanes may be generated during the test if the sample contains arachadonyl containing lipids, however addition of anti-oxidants or free

radical scavenging agents can prevent this (Morrow and Roberts, 1999). The measurement of F_2-isoprostanes is a sensitive and precise method for assessment of lipid peroxidation *in vivo*, however the test currently requires expensive and time consuming separation techniques to separate the F_2-isoprostanes from prostaglandins, other isoprostanes and their metabolites (Mori *et al.*, 1999). F_2-isoprostane-specific immunoassays are now available and may prove to be a simple and accurate method for *in vivo* quantification of lipid peroxidation.

In conclusion, the assessment of lipid peroxidation is problematic, and there is currently no standard method for detection of this process *in vivo*. Oxidative stress is increasingly recognised as an important indicator of health status in both human and veterinary medicine and antioxidant drugs, lifestyles and foods are likely to be a important part of the preventative medicine of the future. The formulation of a simple and non-invasive method for assessment of lipid peroxidation in the living animal would represent a major conquest in the race to understand the complex process of oxidative stress and its implications for health and disease.

1.3 STUDY AIMS

The overall aim of these studies was to investigate the application of exhaled breath analysis as a method for clinical investigation in veterinary medicine, specifically:

1. Investigate the feasibility of application of the ^{13}C-octanoic acid and the ^{13}C-lactose-ureide breath test for assessment of gastric emptying and oro-caecal transit time in the dog.
2. Perform further validation of the ^{13}C-octanoic acid breath test for assessment of gastric emptying in the dog, by investigating the processes involved in metabolism of the substrate.

3. Validate a method for assessment of breath pentane and ethane in animals, thus permitting application of the breath hydrocarbon test in veterinary medicine.
4. Construct a sensitive micro-sensor array, gas flow system and data analysis system ("electronic nose") that allows analysis of gases that occur in exhaled breath, and investigate the potential application of this instrument for detection of breath hydrocarbons.

The application of the ^{13}C-octanoic acid breath test for assessment of gastric emptying and the ^{13}C-lactose-ureide breath test for assessment of oro-caecal transit time in the dog is described in Chapter Three. The application of the hydrocarbon breath test for assessment of *in vivo* lipid peroxidation was investigated using a gas-chromatography system (Chapter Four), and using a novel "electronic nose" assay (Chapter Five). Finally, an overall discussion of the potential application of breath analysis for clinical investigation in veterinary medicine is given in Chapter Six. An outline of the structure of this thesis is given in Figure 1.8.

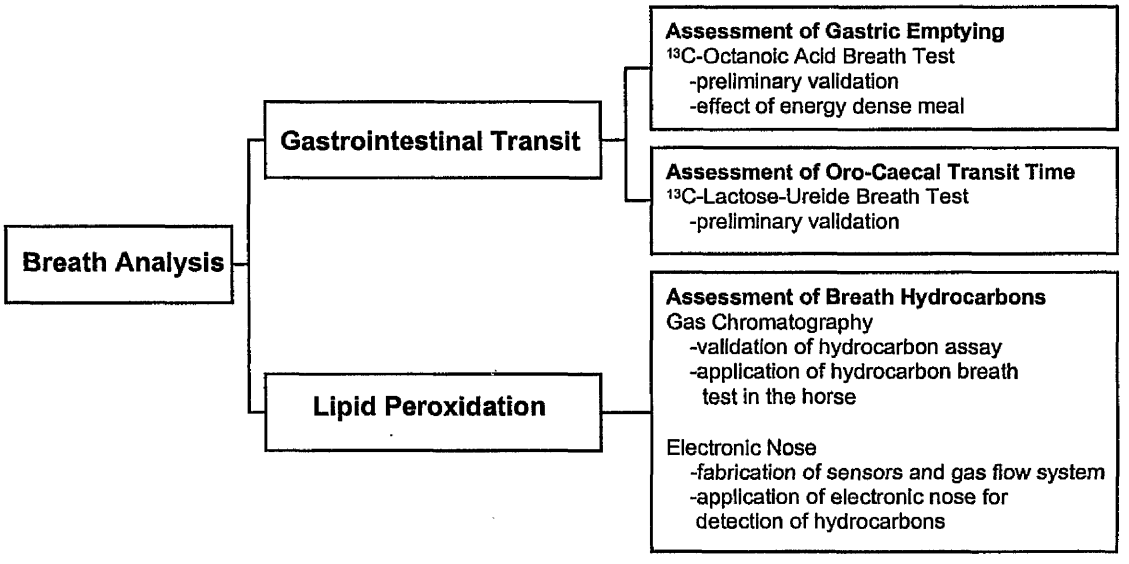

Figure 1.8 A schematic diagram illustrating the structure of this thesis.

CHAPTER 2 MATERIALS AND METHODS

2.1 INTRODUCTION

This Chapter outlines the general materials and methods used to carry out the experiments described in Chapters 3-5.

2.2 ANIMALS

Twenty seven clinically healthy dogs (Dog Nos. 1-27) and 5 horses (Horses Nos. 1-5), were available for use in these studies. Before commencement of the studies, all animals were accustomed to the breath collection procedure. Dog Nos. 1-6 were housed in individual kennels and were fed a canine maintenance dry ration (Selected Protein, Catfish and Rice, Pedigree Petfoods) when not involved in a study. Dog Nos. 7 - 27 were housed in an individual kennel for the duration of each test only. Full details of all the animals are given in Appendix 4. These studies were approved by the Animal Ethics and Welfare Committee of the University of Glasgow.

2.3 BREATH COLLECTION TECHNIQUES

Breath samples were collected using a plastic mask, connected to a one-way valve (Disposable non-rebreathing valve, Quintron) attached to a reservoir bag (disposable 250ml mini-collection bag, Quintron or 1 litre Tedlar bag, SKC Ltd., Figure 2.1. The mask was fitted around the muzzle and the animal was allowed to breathe normally until the reservoir bag filled with exhaled air. In the stable isotope studies (Chapter Three), expiratory breath samples were taken in duplicate in 20ml syringes (Plastipak, Becton Dickinson) by aspiration through a three-way tap (Rocket of London) attached to the reservoir bag. The syringes were sealed with a second three-way tap and samples were immediately transferred into collection tubes (Exetainer, Labco Systems) by

attaching the syringe to a 19G 2 inch needle (Becton-Dickinson), depositing the sample into the tube, and replacing the tube lid.

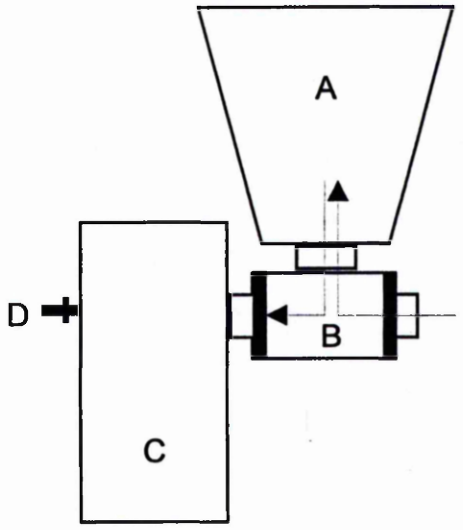

A Face mask

B One-way valve

C Breath collection bag

D Sample collection port

Figure 2.1 The apparatus used to collect exhaled breath in these studies

2.4 TEST MEALS

The standard test meal used in the stable isotope studies consisted of 1 slice of wholemeal bread (36g, 980kJ/100g), 200ml skimmed milk (146kJ/100ml) and 5g margarine (2593kJ/100g); total energy provided by the meal was estimated as 775kJ. The octanoic acid substrate was added to an egg yolk, and then baked in a microwave oven to increase retention of the substrate in the solid-phase (Maes, 1994a). Either ^{13}C-octanoic acid, (Octanoic acid-1-^{13}C (minimum 99% atom % ^{13}C), Isotec Inc.) or octanoic acid (Caprylic acid (n-octanoic acid) Sigma Chemicals), were used in studies as in the relevant sections.

2.5 STABLE ISOTOPE (^{13}C) BREATH TEST STUDY DESIGN

Following an overnight fast (12 hours) the dogs were allowed 15-20 minutes of exercise at walk. They were then returned to their kennels, and following a 30 minute adjustment period, a baseline breath sample was taken in duplicate (t = -30mins) and after a further 30 minutes the dogs ingested the test meal. Breath samples were collected in duplicate immediately before (t = 0mins) ingestion of the test meal, and then every 15 minutes for 4 hours, and every 30 minutes for another 2 hours. Dog Nos. 7-27 were allowed a short walk 4 hours after ingestion of the test meal, but Dog Nos. 1 - 6 remained at rest in their kennels throughout the sampling period. To ensure complete washout of the tracer, at least 1 week was allowed between tests for each dog, where a labelled substrate was ingested (Schoeller *et al.,* 1977). Animals had access to water at all times during the test, but access to food was denied until the end of the sampling period. Carbon dioxide production was taken to be 0.194 litres per square metre of body surface area per minute (Mauderly, 1974). Body surface area was calculated using a formula derived for use in dogs, body surface area (m^2) = 10.1 x body weight (g) $^{2/3}$/10,000 (Thomas, 1911).

2.6 ^{13}C MEASUREMENT

^{13}C-enrichment in breath was measured with reference to a 3% CO_2 (balance N_2) gas standard that had been independently calibrated against an international standard. ^{13}C-enrichment is expressed in units of ppm excess ^{13}C, having subtracted the average ^{13}C-abundance of the pre-dose (baseline) breath samples. All samples were analysed within 4 weeks of collection by continuous flow isotope ratio mass spectrometry (CF-IRMS) (ABCA, Europa Scientific). Following separation of gas components by gas chromatography, the CO_2 sample was introduced into the isotope ratio mass spectrometer. The sample was ionised and the ion beams passed through a magnetic

field (Figure 2.2). The radius of curvature of the path is proportional to the mass and velocity such that:

$$r^2 = \frac{B^2 2Vm}{e}$$

where m = ion mass.g^{-1}

B = magnetic field strength.$tesla^{-1}$

V = accelerating voltage.V^{-1}

r = radius of curvature.m^{-2}

e = charge on ion.$coulombs^{-1}$

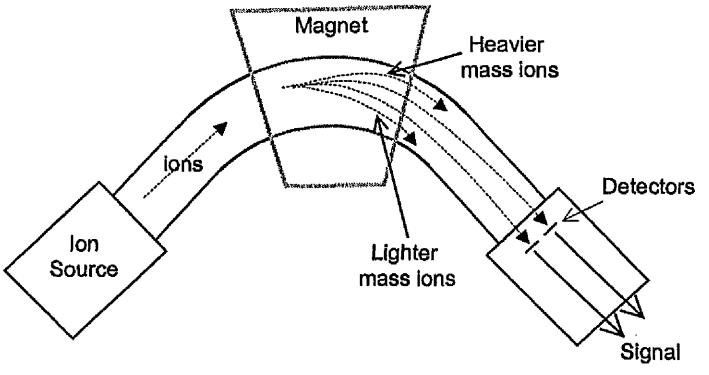

Figure 2.2 A schematic diagram of an isotope ratio mass spectrometer illustrating the separation of ions based on their path through a magnetic field. This radius of this path is proportional to the mass of the ion.

In this way, ions were separated by their mass to charge ratio. The separated ion beams were detected on Faraday collectors at mass 44, 45 and 46. The ^{13}C-abundance of the normal diet ingested by the dogs, and the components of the test meal were also analysed by CF-IRMS, in combustion mode (Preston and McMillan, 1988).

2.7 BREATH ^{13}C DATA ANALYSIS

2.7.1 Calculation of Atom Percent Excess (APE)

Atom percent ^{13}C (AP) refers to the expression of delta units (see below) in absolute terms by comparison with the known ^{13}C:^{12}C ratio of the PDB standards. Data output from the IRMS is in the form of delta (δ) units, where the ^{13}C:^{12}C of the samples are expressed relative to the ^{13}C:^{12}C of the 3% CO_2/N_2 standards.

$$\delta(per\ mil) = \frac{R(sample)}{[R(Reference) - 1]} \times 1000 \qquad \text{McKinney } et\ al.,\ 1950 \qquad \text{(Eq. 2.1)}$$

where $R = {}^{13}C/{}^{12}C$

By international convention delta units are expressed relative to the "PDB" standard, a limestone fossil of *Belemnitella americana* from the Cretaceous Pee Dee Formation in South Carolina. Results are expressed as $\delta^{13}C_{PDB}$, and the PDB standard has a $\delta^{13}C$ value of 0% and an absolute ^{13}C:^{12}C ratio of 0.0112372. The sign of the $\delta^{13}C$ value for any sample indicates whether it has a lower ratio of ^{13}C:^{12}C than the PDB standard (a negative value indicates a lower ratio).

Atom percent ^{13}C (AP) refers to the expression of delta units in absolute terms by comparison with the known ^{13}C:^{12}C ratio of the PDB standards.

$$Atom\ Percent\ [{}^{13}C] = \frac{0.0112372 \times \left(\frac{\delta}{1000}\right) + 1}{\left[0.0112372 \times \left(\frac{\delta}{1000}\right) + 1\right] + 1} \qquad \text{(Eq. 2.2)}$$

Atomic percent excess (APE) refers to the recovered ^{13}C-enrichment above baseline and is calculated by:

$$Atom\ Percent\ Excess\ (APE) = \frac{^{13}C(t) - {}^{13}C(0)}{100} \qquad \text{(Eq. 2.3)}$$

where $^{13}C(0)$ = AP ^{13}C at time = 0, ie before administration of ^{13}C dose

2.7.2 Percentage Dose Recovered (PDR)

The results of the ^{13}C breath studies were expressed either as a percentage of the total administered ^{13}C dose recovered in breath (percentage dose recovered, PDR), or as breath ^{13}C (ppm) (APE).

$$Percentage\ Dose\ Recovered\ (PDR) = \frac{mmol\ excess\ {}^{13}C(Recovered)}{mmol\ excess\ {}^{13}C\ (Administered)} \times VCO_2$$

$$mmol\ excess\ {}^{13}C(Recovered) = \frac{^{13}C(t) - {}^{13}C(0)}{100} \times VCO_2 \qquad \text{(Eq. 2.4)}$$

$$mmol\ excess\ {}^{13}C(Administered) = \frac{\%\,{}^{13}C(Substrate) - {}^{13}C(Base) \times Dose(mmol)}{100}$$

(Eq. 2.5)

2.7.3 Data Modelling

The formula described for fitting gastric emptying breath test data in man was used to model the data in these canine studies. This equation is derived from the χ^2 statistical distribution and took the form:

$y = at^b e^{-ct}$ Ghoos *et al.*, 1993 (Eq. 2.6)

where y = measured values of PDR

a, b and c are regression constants

t = time in hours

The formula describes a single peak curve where a is a scaling factor, t^b describes the ascending part of the curve and e^{-ct} describes the exponential decay of the ^{13}C signal The Solver function of an Excel software package was used to predict values for a, b and c by non-linear regression.

2.7.4 Calculation of Gastric Emptying Parameters

Three variables were calculated using the plotted ^{13}C-enrichment curve, the gastric emptying coefficient (GEC), the time to peak breath ^{13}C-enrichment (t(max)), and the half dose recovery time (t½). The GEC was defined as a global index of the rate of gastric emptying, calculated as the natural log of a, ln a (Maes, 1994a). The half dose recovery time (t½) is the time when the area under the fitted cumulative $^{13}CO_2$ excretion curve equals half of the ^{13}C dose recovered in breath. The t½ was calculated using the Excel function Gammainv (0.5;b + 1;1/c). t(max), was the time of peak recovery of breath calculated as b/c (Ghoos *et al.,* 1993; Maes, 1994a).

2.8 GAS CHROMATOGRAPHIC DETECTION OF PENTANE AND ETHANE

2.8.1 Materials

Helium, hydrogen, argon and nitrogen gas were supplied by BOC Gases. Glassware was supplied by Young Scientific. Magnesium perchlorate, soda lime and glass wool were supplied by Sigma-Aldrich. Tedlar gas sampling bags (volume, 1litre) were obtained from SKC Gas products. The adsorbent material used in these studies was the porous polymer 2,6-diphenyl-p-phenylene oxide (Tenax GC 60/80 mesh, Sigma-

Aldrich). Gas tight syringes and needles (Hamiliton Microlitre Syringe, Varian, UK) were used to transfer gases. All fittings and tubing were stainless steel and gas tight and supplied by Glasgow Valve and Fitting Company.

2.8.2 Apparatus

Gas Chromatography

Pentane and ethane were analysed using a AI model 93 gas chromatograph (Burke Electronics, UK) with a 15m × 0.53mm Chrompack fused silica Plot capillary column (Varian,UK), or a 15m × 0.53mm PoroplotQ column. The carrier gas was high purity helium maintained at a column flow rate of 7mls/min. The samples were detected using a flame ionization detector maintained at a constant temperature of 250°C. Following injection of a sample, the oven temperature remained at an initial 40°C for 1.5 minutes, and then increased to 180°C at a rate of 15°C/min, and then returned to 40°C. Analysis of each sample took approximately 18 minutes. Output from the flame ionization detector was directed to a computer equipped with GC analysis software (JCL600 Chromatography Data Systems).

Cryogenic Concentration System

A cryogenic focusing system was developed based on the method described by Arterbery *et al.,* (1994), that enabled concentration of alkanes to levels that could be detected by the flame ionization detector. A stainless steel U-loop (outer diameter 1/8", length 6") packed with 2,6-diphenyl-p-oxide (Tenax) was connected to two 4-port gas tight valves, 4-port switching valves, 1/16" fittings, Valco Instruments (Figure 2.3), using stainless steel 1/16" to 1/8" reducing union fittings (Swagelok, Glasgow Valve and Fitting Company). The valve system was connected to the GC-column and to a glass sampling chamber (Young Scientific Glassware). The sampling chamber

contained soda-lime and magnesium perchlorate to remove H_2O and CO_2 from the gas samples, and was connected by gas-tight taps to the gas-sample bag or to an Ar cylinder, and to the valve system (Figure 2.3). The loop was opened by moving the valve system to the "sample" position, allowing gas to be transferred from the sampling chamber to the loop (Figure 2.4). During cryogenic concentration, the loop was immersed in an ethanol-liquid nitrogen slush bath (-117°C) for 5minutes. The gas sampling bag was attached to the sampling port (Figure 2.3) and 150ml of gas sample was withdrawn into the 500ml gas-tight syringe. The valve connecting the sampling chamber and the gas-sampling bag was then closed, and the valve connecting the sampling chamber with the stainless steel loop was opened, allowing the 150ml sample to be injected (Figure 2.3). The loop was then isolated by moving the valve system to the "isolate" position (Figure 2.4); the liquid nitrogen slush bath was then removed and the loop was heated for two minutes on a heating block maintained at 160°C. The valve system was then moved to the "inject" position, allowing the trapped gas sample to enter the GC-column. The system was flushed for two minutes following each sample with a stream of Ar delivered through the sampling chamber, delivered at 16ml.min^{-1}. Blanks, comprising high purity nitrogen were run routinely during each experiment. Further details of the preparation of gas samples are given in Chapter 4.

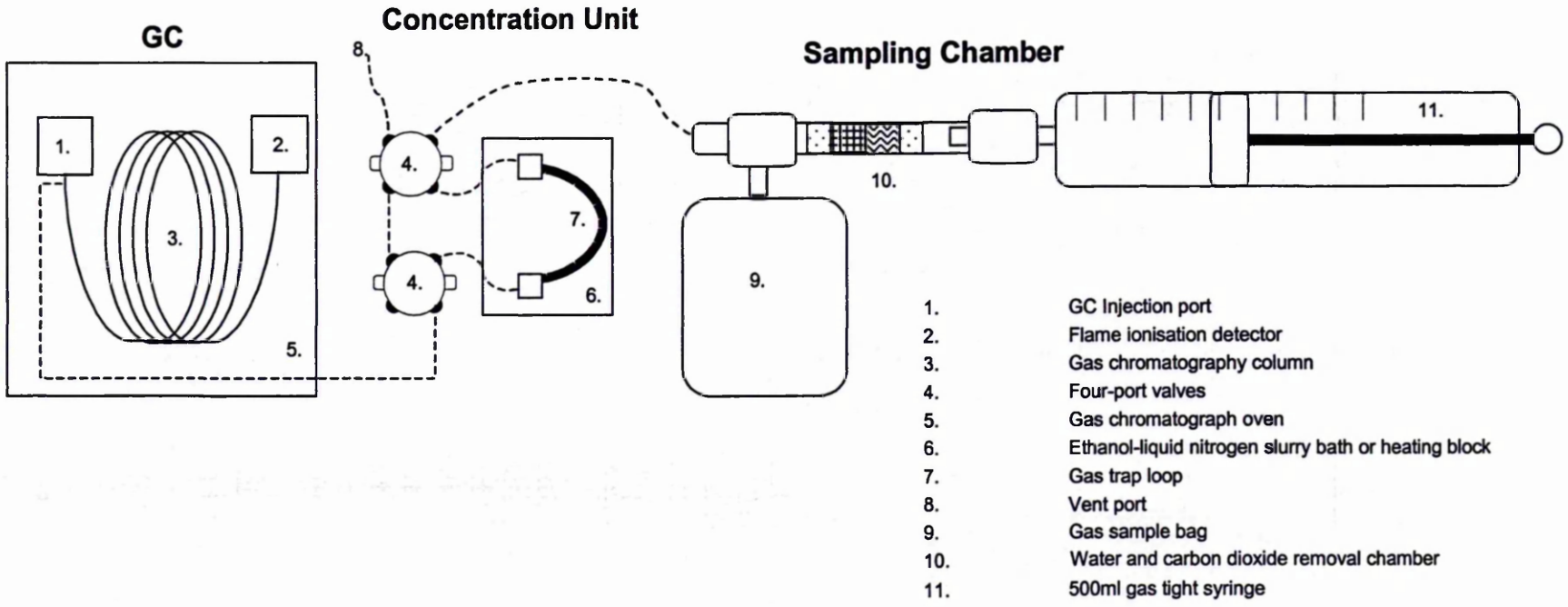

Figure 2.3 The cryogenic concentration system used to concentrate breath samples in this study.

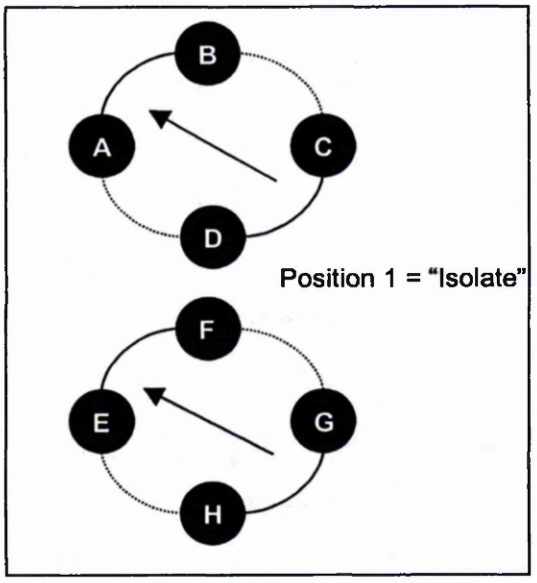

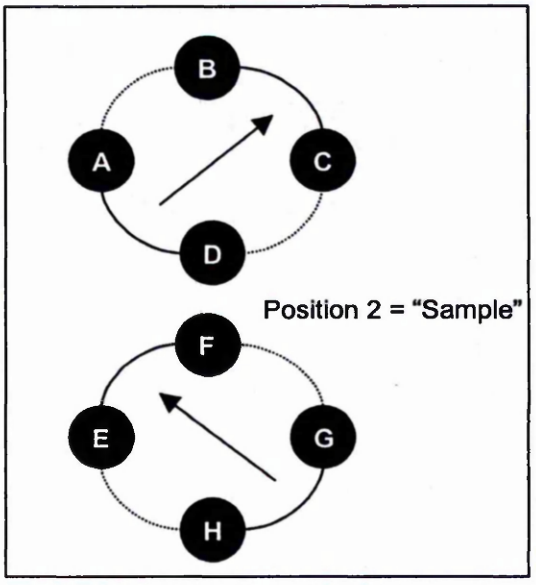

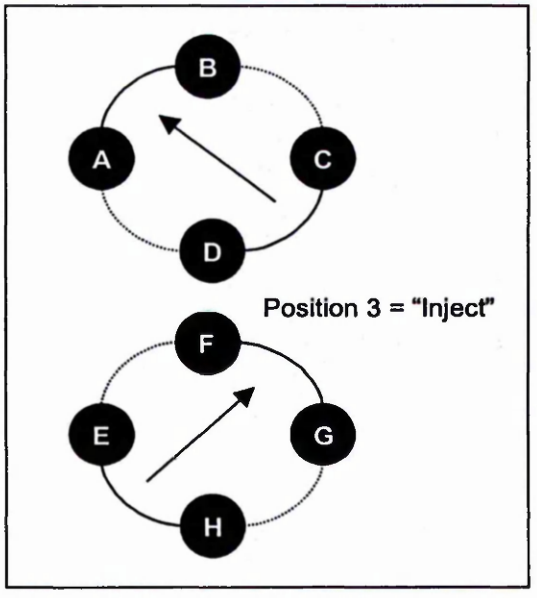

Figure 2.4 The operation of the combination of two 4-way valves in this study. These diagrams illustrate the operation of the four-port valves shown in Figure 2.1. The connections between valves are shown below.

Port A - GC Column
Port B - Injector
Port C - Port F
Port D - Gas sampling loop
Port E - Gas sampling loop
Port F - Port C
Port G - Sample input
Port H - Vent

Position 1 allowed isolation of the gas sampling loop from the GC column, for desorption of the trapped gases.

Position 2 allowed the gas sample to be drawn through the loop during cryogenic concentration, and also allowed flushing of the loop.

Position 3 brought the gas sampling loop in line with the GC column allowing injection of the trapped sample.

2.9 ELECTRONIC NOSE INSTRUMENTATION

2.9.1 Reagents

Methanol, acetone, Opticlear, toluene, chloroform, ethanol, tetrahydrofuran (Sigma-Aldrich, UK) and chlorobenzene (Analar, UK) were used as supplied. Photoresist S1818 and Microposit developer were supplied by Shipley Ltd., UK. The polymers used in this study were poly(vinylpyrrolidone), poly(styrene), poly(4-vinylphenol), poly(ethylene oxide), poly(methyl methacrylate), poly(vinyl acetate), poly(vinyl pyridine), poly(ethylene-*co*-methylacrylate), poly(caprolactone), poly(ethylene glycol), poly(sulfone), poly(ethylene-*block*-polyethylene glycol), poly(2-vinyl pyridine-*co*-styrene), poly(vinyl methylketone), poly(vinyl chloride-*co*-vinyl acetate), poly(ethylene-*co*-vinyl acetate), poly(acrylonitrile-*co*-butadiene-*co*-styrene toluene) and poly(isobutylene); these were obtained from Sigma-Aldrich and used as supplied. The carbon black, Black Pearls 2000 (BP2000) was supplied by Cabot Company. The solvents used in this study were chloroform, tetrahydrofuran, tolulene and ethanol depending on the solubility of the individual polymer; these were obtained from Sigma-Aldrich and used as supplied.

2.9.2 Fabrication of Interdigitated Microelectrodes

Interdigitated microelectrodes were fabricated using the technique of photolithography and lift-off (Figure 2.5). Microscope glass slides were cleaned by 5 minutes ultrasound in a citrus-oil based cleaning solvent (Opticlear), followed by 5 minutes ultrasound in acetone, then methanol and finally 3 minutes wash in reverse-osmosis (RO) water. A layer of photoresist S1818 was deposited onto the slide by spinning at 4000rpm for 30

seconds, giving a coating thickness of 1.8μm. The coated slides were baked at 90°C for 15 minutes, immersed in chlorobenzene for 15 minutes and then baked at 90°C for a further 15 minutes. The resist-coated slides were brought into close contact with a chrome or acetate mask (originally fabricated using photolithography) using a mask aligner, and then exposed to UV light for 10 seconds, and developed for 90 seconds using Microposit developer.

Gold deposition was carried out using a thin film deposition system until the thickness of deposited metal reached 800nm. The thickness of the deposited metal was controlled using a quartz crystal microbalance. The slides were then immersed in acetone for up to 12 hours (lift-off), to remove residual gold and reveal the patterned microelectrode.

The surface profile of the deposited electrodes was examined using a Dektak surface profiling system (Dektak 3ST, Sloan Technology).

Step 1 - Slide Cleaning

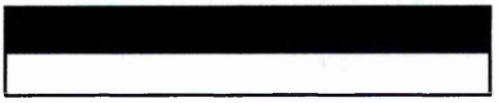

Step 2 - Resist Deposition

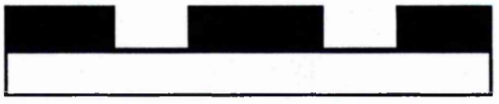

Step 3 - Pattern Exposure & Development

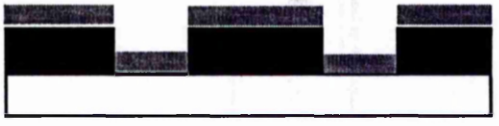

Step 4 - Gold Deposition

Step 5 - "Lift Off" in Acetone

Figure 2.5 Steps involved in fabrication of electrodes using the techniques of photolithography and lift-off

Two types of inter-digitating electrodes were fabricated in these studies, and these are illustrated in Figure 2.6. Electrode 1 measured 3mm × 4.5mm and had an inter-digital gap measuring 40μm. Electrode 2 measured 1mm × 4mm and was designed to facilitate surface mounting with an inter-digital gap measuring 80 or 40μm. A detail of the 800nm deposited metal layer is shown in the scanning electron micrograph in Figure 2.7.

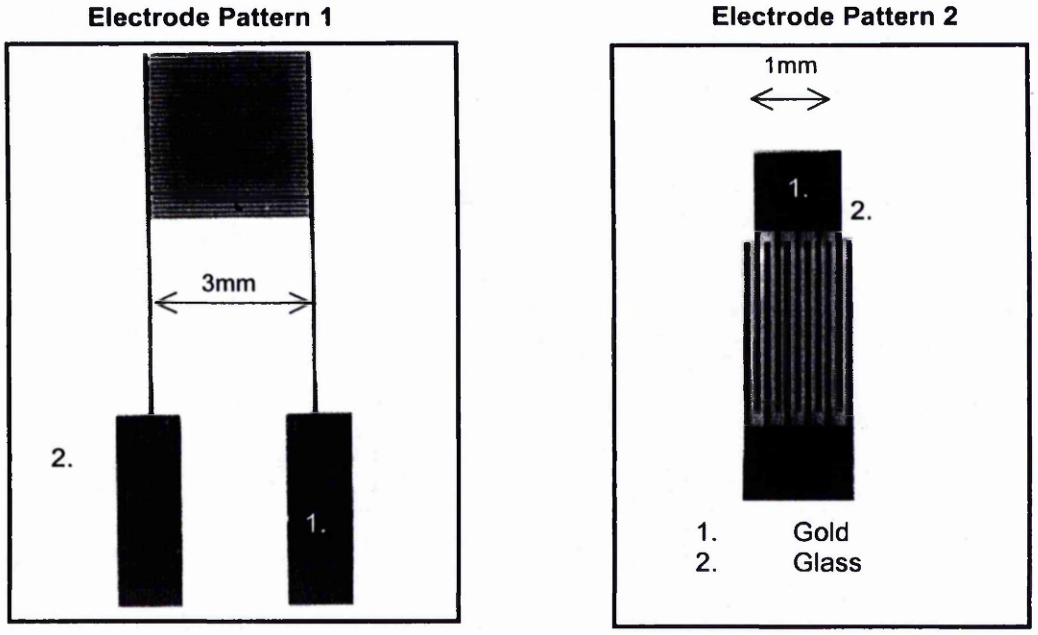

Figure 2.6 A plan view of the interdigitated electrodes used in these studies Electrode pattern 1 had an interdigital gap of 40μm. Electrode 2 had an inter-digital gap of 80μm and was designed to facilitate surface mounting. The numbers 1 and 2 indicate the deposited gold layer and the glass substrate, respectively.

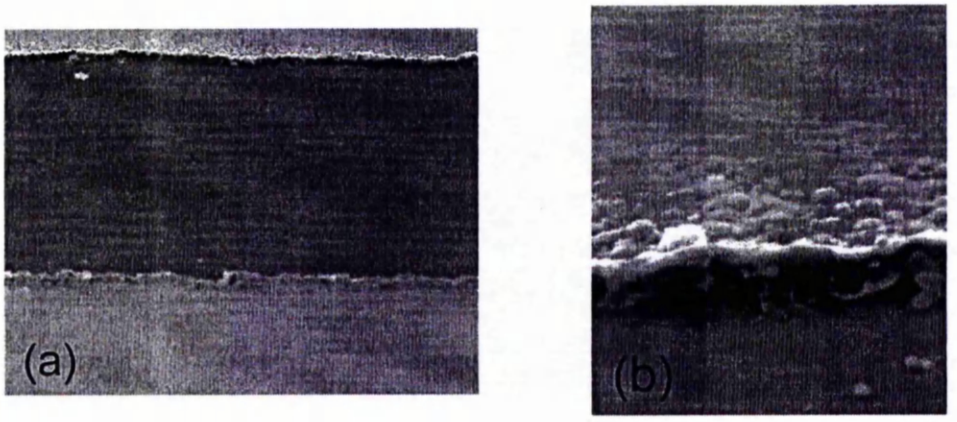

Figure 2.7 Scanning electron micrograph of the deposited metal layer (800nm) on glass substrate. Figure 2.7(a) shows detail of metal digit on glass magnified × 1700. Figure 2.7(b) shows details of metal digit on glass magnified × 10,000.

Deposition of Composite Polymer Films

The composite polymer films were made from a solution of polymer in which the carbon black particles were suspended, as previously described (Severin *et al.,* 2000). The insulating polymer (160mg) was dissolved in an appropriate solvent (20ml), and carbon black (40mg) was then suspended in the solution. This composition produced a solution of 80% polymer and 20% carbon black, by weight of solids. The solvent was tetrahydrofuran, chloroform, dichloromethane, ethanol or toluene, depending on the solubility of the polymer (Table 2.1).

Table 2.1 The polymers and solvents used to create composite polymer solutions for deposition on electrode surfaces in these studies.

	Polymer	**Abbreviation**	**Solvent**
1	Poly(methyl methacrylate)	PMMA	Toluene
2	Poly(vinyl chloride-*co*-vinyl acetate)	PVVA	Chloroform
3	Poly(caprolactone)	PCL	Dichloromethane
4	Poly(vinyl pyrrolidone)	PVPr	Chloroform
5	Poly(isobutylene)	PIB	Toluene
6	Poly(styrene)	PS	Toluene
7	Poly(ethylene-*co*-vinyl acetate)	PEVA	Toluene
8	Poly(ethylene-*co*-methylacrylate)	PEMA	Toluene
9	Poly(sulfone)	PSF	Tetrahydrofuran
10	Poly(acrylonitrile-*co*-butadiene-*co*-styrene toluene)	PABS	Toluene
11	Poly(ethylene-*block*-polyethylene glycol)	PEGPEG	Toluene
12	Poly(ethylene glycol)	PEG	Tetrahydrofuran
13	Poly(vinyl methylketone)	PVPK	Toluene
14	Poly(4-vinylphenol)	P4VP	Tetrahydrofuran
15	Poly(vinyl acetate)	PVA	Tetrahydrofuran
16	Poly(2-vinylpyridine-*co*-styrene)	P2VPS	Ethanol

Following addition of the carbon black, the solution was sonicated for at least 45 minutes to ensure homogenous distribution of the carbon black particles. The solution was spin coated onto the gold microelectrodes at speeds of approximately 300rpm, and

multiple coats were applied until the sensor resistance value was in the region of 100 – 1000Ω. The sensors were dried at room temperature for 12 – 24 hours. This process produced a polymer layer with suspended fine carbon black particles that allowed charge to pass across the digit of the electrode.

2.9.3 Resistance Measurement

The DC electrical resistance across each composite polymer sensor was measured using digital multimeters.

2.10 STATISTICAL ANALYSES

All statistical analysis was carried out using Microsoft Excel for Windows 95, Version 7.0a or Minitab Version13. Further details of the statistical methods used to analyse data are given in the relevant sections. Where duplicate samples were taken, analysis of test results utilised the mean of duplicate measurements taken at each time point. Results were expressed as the mean $\pm$ error and values of $p \leq 0.05$ were considered significant.

CHAPTER 3 - PRELIMINARY STUDIES ON STABLE ISOTOPE BREATH TESTS FOR ASSESSMENT OF GASTROINTESTINAL TRANSIT IN THE DOG

3.1 PRELIMINARY INVESTIGATIONS OF THE ^{13}C-OCTANOIC ACID BREATH TEST FOR ASSESSMENT OF GASTRIC EMPTYING IN THE DOG

3.1.1 Study Aims

The specific objectives of these studies were to:

1. Assess basal $^{13}CO_2$ excretion in the dog at rest and following a test meal;
2. Estimate the dose of ^{13}C-octanoic acid necessary to provide an adequate ^{13}C-signal in breath;
3. Assess the repeatability of the ^{13}C-octanoic acid breath test parameters in healthy dogs;
4. Assess the relationship between body size and the parameters of the ^{13}C-OBT.

3.1.2 Introduction

The ^{13}C-octanoic acid breath test (^{13}C-OBT) has been validated for assessment of solid-phase gastric emptying in man (Ghoos *et al.*, 1993; Ziegler *et al.*, 1996; Delbende *et al.*, 2000; Perri *et al.*, 1998) and in the horse (Sutton *et al.*, 1999). The test has also been applied in the cat (Peachey *et al.*, 2000) and the mouse (Symonds *et al.*, 2000). The ^{13}C-OBT involves monitoring ^{13}C recovery in exhaled breath following ingestion of a test meal with a ^{13}C-labelled substrate, ^{13}C-octanoic acid. Octanoic acid is a medium chain fatty acid that is rapidly and completely absorbed in the duodenum, carried to the

liver via the venous portal system and oxidised completely and rapidly to produce carbon dioxide, which enters the bicarbonate pool, before being excreted in breath (Schwabe *et al.,* 1964). Since gastric emptying is the rate-limiting step in the digestion and metabolism of octanoic acid, the excretion of $^{13}CO_2$ in breath reflects the rate and pattern of gastric emptying (Ghoos *et al.,* 1993). Entry of the carbon label into the bicarbonate pool imposes an inevitable delay prior to recovery of isotope in breath; studies in man have derived a correction factor to allow for this delay, but no such data are available for animals. Octanoic acid was shown *in vitro* to remain tightly bound to the solid phase of gastric emptying (Maes, 1994a) and octanoic acid absorption from the intestine is not limited by simultaneous carbohydrate ingestion or intravenous fatty acid infusion (Schwabe *et al.,* 1964).

Studies using radioscintigraphy and intestinal fistulation have provided valuable data on canine solid-phase gastric emptying under experimental conditions, but the significance of disordered solid-phase gastric emptying in canine gastric disease remains poorly understood, due to the absence of a simple and non-invasive test. The aim of this present study was to investigate the feasibility of applying the ^{13}C-octanoic acid breath test for monitoring the gastric emptying of a solid test meal in the dog, and to develop a suitable breath sampling method, test protocol, test meal and substrate dose to enable future validation and application of the test in canine medicine and research.

3.1.3 Materials and Methods

Animals

27 healthy dogs (Dog Nos. 1-27) were used in these studies. They were aged between 0.7 - 12 years and weighed between 5 - 38kg. Full details of these animals are given in Appendix 4.

Test Meal

The test meal is described in Chapter 2, and either 100mg unlabelled octanoic acid or 50 or 100mg ^{13}C-octanoic acid was included as the carbon substrate.

Study Design

Breath tests were carried out as described in Chapter Two. To assess basal $^{13}CO_2$ excretion in the fasted dog, three dogs (Dog Nos. 1, 2 & 3) did not ingest a test meal, but remained fasting for the duration of the test period. To assess the effect of the test meal three dogs (Dog Nos. 1, 2 & 3) ingested a test meal with 100mg unlabelled octanoic acid. To assess the effect of ^{13}C-octanoic acid dose on breath ^{13}C, three dogs (Dog Nos. 1, 2 & 3) ingested a test meal labelled with 50 mg ^{13}C-octanoic acid and three dogs (Dog Nos. 4, 5 & 6) ingested a test meal labelled with 100mg ^{13}C-octanoic acid. To assess the repeatability of the ^{13}C-OBT within healthy dogs (intra-subject variability), four dogs (Dog Nos. 1, 2, 3, & 4) ingested a 50mg dose of ^{13}C-OA on six separate occasions. To assess the repeatability of the ^{13}C-OBT between healthy dogs (inter-subject variability) and to assess the relationship between body size and the parameters of the ^{13}C-OBT, 27 dogs ingested a 50mg dose of ^{13}C-OA on one occasion.

Table 3.1: Study Design

Test Description		Test Meal	Substrate	Dogs*	Replicates#
Controls	Basal ^{13}C-excretion	None	None	3	1
	Unlabelled meal	Standard	100mg OA	3	1
Effect of Substrate Dose	Labelled ^{13}C meal	Standard	50mg ^{13}C-OA	3	1
	Labelled ^{13}C meal	Standard	100mg ^{13}C-OA	3	1
Reproducibility Study	Labelled ^{13}C meal	Standard	50mg ^{13}C-OA	4	6
	Labelled ^{13}C meal	Standard	50mg ^{13}C-OA	27	1

* Number of dogs included in test
\# Number of times test was repeated in each dog
OA Octanoic acid
Standard test meal 1 slice bread, 1 egg yolk, 5g margarine and 200ml milk

Data Analysis

Data modelling and calculation of breath test parameters were carried out as described in Chapter Two. Intra and inter- subject coefficients of variation were calculated to enable comparison with previous studies of gastric emptying in dogs using other methods.

$$\text{Coefficient of Variation (CV)}\% = \left(\frac{\text{standard deviation}}{\text{mean}}\right) \times 100 \qquad \text{(Eq. 3.1)}$$

The relationship between body size and $t_{½}$ and $t_{(max)}$ was examined by calculating a correlation coefficient (r). Body size was expressed as body surface area calculated as:

$$\textit{Body Surface Area}\left(m^2\right) = \frac{\textit{weight}(g)^{2/3}\,(10.1)}{10^4} \qquad \text{Thomas, 1911 (Eq. 3.2)}$$

3.1.4 Results

The test meal was ingested in less than 2 minutes by all animals. The pattern of $^{13}CO_2$ excretion remained constant and low over the 6 hour sampling period following both the fasted test and the ingestion of the test meal and 100mg unlabelled octanoic acid. Mean ^{13}C-excretion in breath over the 6 hour sampling period in three dogs was 10845.77 ± 2.07 ppm in the fasted study (Figure 3.1), and 10839.66 ± 2.02 ppm following ingestion of the test meal and unlabelled octanoic acid (Figure 3.1).

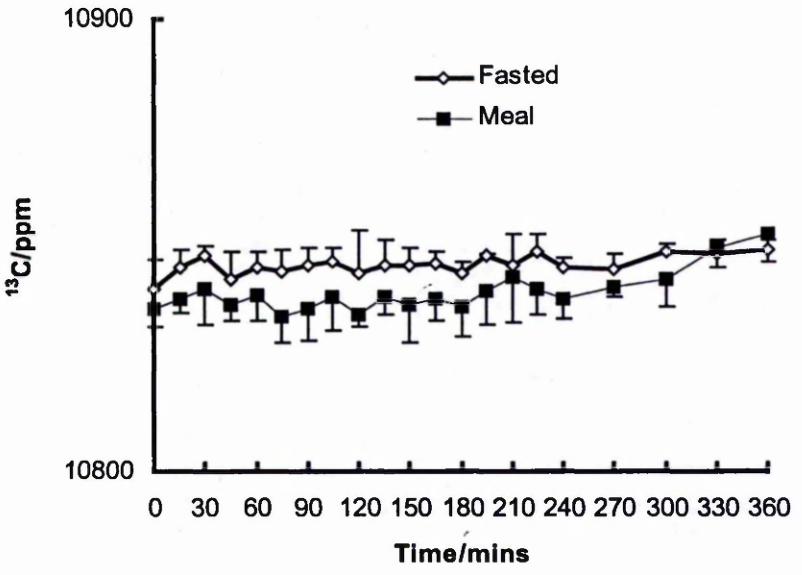

Figure 3.1 Basal breath ^{13}C-excretion (mean ± sd) following a 12 hour fast and following an unlabelled test meal in three dogs.

Ingestion of test meals and labelled substrate (^{13}C-octanoic acid), was associated in all cases with significant increases above baseline levels of $^{13}CO_2$ excretion, and these increases were proportional to the dose of ^{13}C-octanoic acid administered (Figure 3.2). The ^{13}C contribution from the test meal is also shown in Figure 3.2, data from Figure 3.1, above.

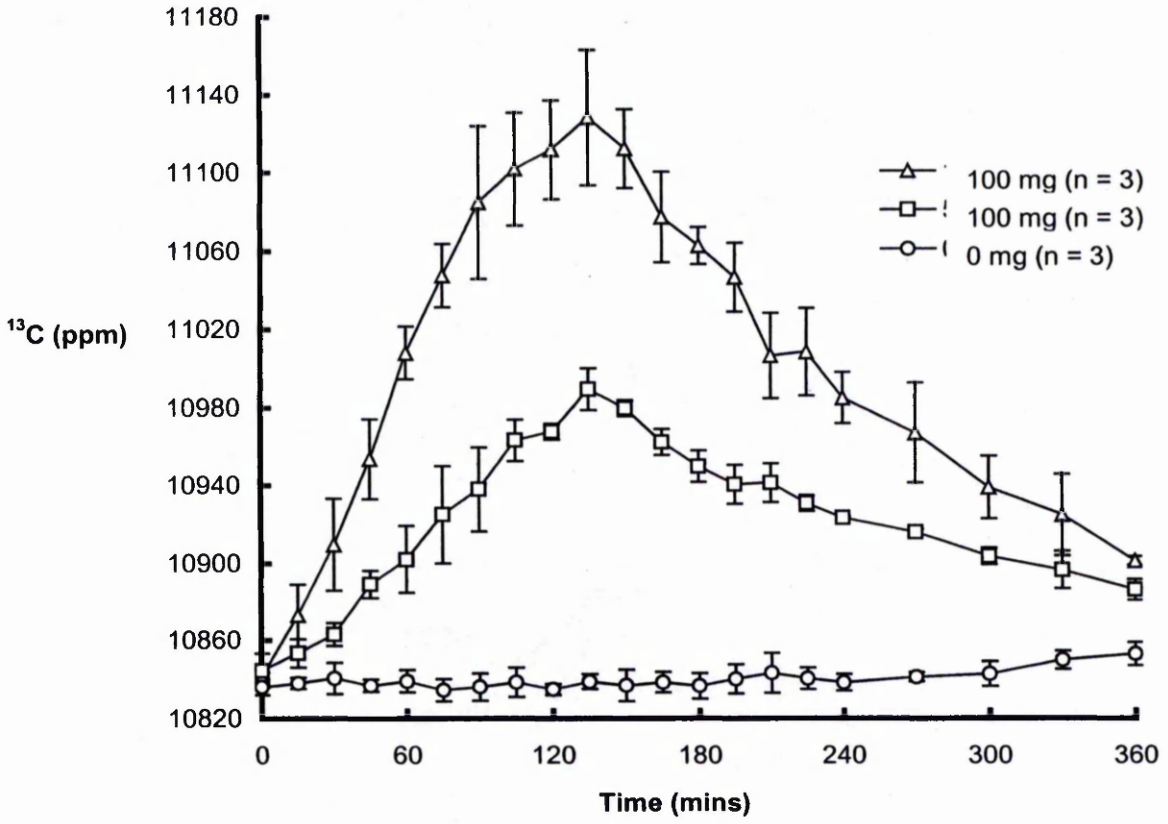

Figure 3.2 Effect of dose ^{13}C-OA on ^{13}C-excretion in breath in 6 healthy dogs.

The formula $y = at^b e^{-ct}$, derived to describe gastric emptying breath test data in man (Ghoos *et al.,* 1993) was used to fit the data from the dogs in this study (Figure 3.3). The data from Dog No. 12 could not be fitted by the model, probably due to low CO_2 pressure in the breath samples collected from this animal, and these data were not included in the analysis. Mean values of GEC, $t_{(max)}$ and $t_{½}$ for all animals are shown in Table 3.2. Intra-subject coefficients of variation were calculated by analysing the data obtained when the test was repeated on 6 separate occasions in 4 dogs (Table 3.3). The variation between dogs, or inter-subject variation is shown in Table 3.4.

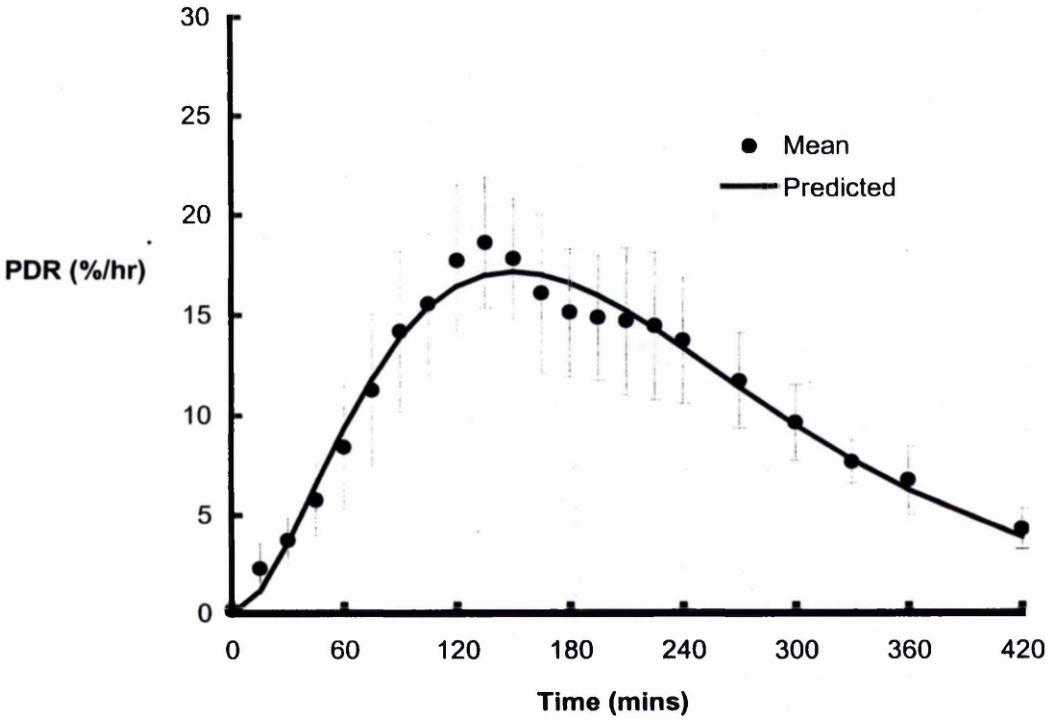

Figure 3.3 The predicted gastric emptying curve and breath ^{13}C-excretion data when the breath test protocol was repeated in 4 dogs on 3 separate occasions.

Table 3.2 Breath test parameters for ^{13}C-OBT repeated in 4 dogs 6 times

	GEC	$t_{½}.hour^{-1}$	$t_{(max)}.hour^{-1}$
Mean	2.91	3.43	2.68
sd	0.47	0.50	0.44

Table 3.3 Intra-subject coefficients of variation (sd/mean × 100%) for ^{13}C-OBT repeated on six occasions in four individuals.

Dog No.	GEC	$t_{½}.hour^{-1}$	$t_{(max)}.hour^{-1}$
1	17%	15%	16%
2	17%	8%	11%
3	16%	19%	21%
4	15%	15%	16%
Mean	16%	14%	16%

Table 3.4 Breath test parameters for ^{13}C-OBT repeated once in 27 dogs.

	GEC	$t_{(max)}$.hour^{-1}	$t_{½}$.hour^{-1}
Mean	2.67	2.68	3.41
sd	0.97	0.66	0.90
CV.%$^{-1}$	36%	25%	26%

The relationship between the breath test indices and body size was not statistically significant (r = 0.12 and 0.10 for $t_{(max)}$ and $t_{½}$, respectively). In approximately 33% of all breath tests carried out in this study, the recovery of ^{13}C described two or more distinct peaks (Figure 3.4).

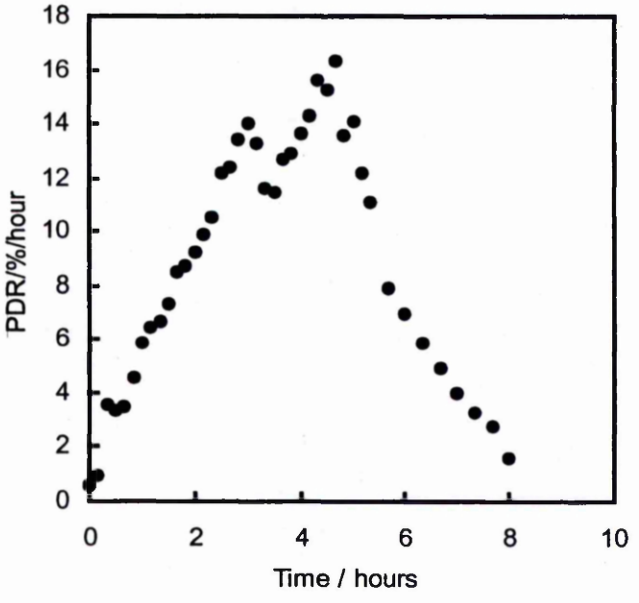

Figure 3.4: Measured ^{13}C-recovery values during ^{13}C-OBT in Dog No. 3, illustrating typical phasic pattern of ^{13}C-recovery.

3.1.5 Discussion

The results of this study suggest that the ^{13}C-OBT is a reproducible and simple method for the assessment of solid-phase gastric emptying in the dog. Breath tests monitoring breath ^{13}C-excretion following ingestion of a ^{13}C-labelled substrate are increasingly used for clinical diagnosis and research in human gastroenterology (Swart and van der Berg, 1998). The use of investigative breath tests in the dog has been previously reported, including the hydrogen breath test for measuring oro-caecal transit time (Papasouliotis *et al.*, 1995) and the ^{13}C-urea breath test for assessing the presence of *Helicobacter spp.* in the stomach (Cornetta *et al.*, 1998). In the present study breath samples were collected using a face mask attached to a reservoir bag by a unidirectional valve, thus ensuring that only exhaled air could enter the reservoir bag, and be collected through the sampling port. The reliability of this method was demonstrated by the good correlation in ^{13}C levels between replicate samples (Appendix 5). The breath sampling procedure could be completed in each animal in less than two minutes and was extremely well-tolerated by all animals in this study. However, the CO_2 pressure in many of the breath samples taken in this study was low (approximately 1%), and the breath collection method in dogs requires further optimisation.

^{13}C has a natural abundance of 1.1% of the total carbon, so that all ^{13}C breath tests are carried out against a background level of the naturally occurring isotope (Schoeller *et al.*, 1977). For this reason it was necessary to establish basal levels of $^{13}CO_2$ excretion before attempting to enrich breath ^{13}C, by administration of an exogenous source. In this study, basal $^{13}CO_2$ was monitored in three dogs over six hours, and levels were low and remained stable throughout this period. This finding confirmed the potential for enrichment of breath ^{13}C in the dog, for the purposes of the ^{13}C-OBT and for other ^{13}C-labelled breath tests.

The metabolism of a test meal produces a shift in background ^{13}C-abundance that is a reflection of the enrichment above or below natural abundance of the carbon contained in the meal (Schoeller *et al.,* 1980). In order to ensure that ingestion of the test meal did not affect basal ^{13}C excretion in this study, three dogs were fed a test meal with 100mg of unlabelled ^{13}C-octanoic acid, and their levels of ^{13}C excretion monitored over six hours. There was no significant alteration in the level or pattern of basal ^{13}C-excretion following administration of the test meal, indicating its suitability as a carrier for administration of the solid-phase marker, octanoic acid. The ^{13}C-octanoic acid substrate, has been previously shown to remain bound to the solid-phase of a test meal identical to that used in the present study, in several *in vitro* (Maes, 1994a) and *in vivo* studies in man (Ghoos *et al.,* 1993; Perri *et al.,* 1998; Choi *et al.,* 1998a).

On administration of the test meal with the labelled substrate, a significant and dose-related increase in ^{13}C-excretion was detected in all dogs. The mathematical model derived to describe data obtained using the ^{13}C-OBT in man was used to fit the data in this canine study, and the pattern of recovery of the isotope in breath was comparable to that described in man. Reproducibility within subjects (intra-subject variation), was assessed by repeating the test in four dogs on six occasions, under identical conditions of meal timing and composition. Mean intra-subject coefficients of variation in the dogs in this study for GEC (16%) and $t_{½}$ (14%) were comparable to those reported using the ^{13}C-OBT in man, 11% for GEC and 27% for $t_{½}$ (Ghoos *et al.,* 1993). The intra-subject coefficients of variation illustrate the normal day-to-day variance that could be expected for repeated breath tests in healthy dogs. The coefficients of variation in this study reflect relatively high intra-subject variation, but significant variation in gastric emptying rates between and within individuals has been previously reported in the dog (Hinder and Kelly, 1977) and in man (Brophy *et al.,* 1986). Inter-subject variation was

assessed by performing the test on 27 dogs, and this study revealed the values of the breath test parameters that might be expected in any healthy individual. Inter-subject variation was greater than intra-subject variation in this study, but was comparable to a previous report of gastric emptying in the dog using radioscintigraphy (Iwanaga *et al.*, 1998). The inherent variability in the rate of gastric emptying was illustrated by the relatively high inter- and intra-subject variation among the animals in this study, and could confound the discrimination of alterations in gastric emptying rate produced by drugs or disease.

In many cases the pattern of ^{13}C-recovery in this study followed a phasic or multi-peak pattern. This pattern was also reported when the ^{13}C-OBT was applied in ponies (Wyse *et al.*, 2001) in man (Meier-Augenstein *et al.*,2001) and in the mouse (Symonds *et al.*, 2000), and using radioscintigraphy in the dog and in man (Lawaetz *et al.*, 1981; Becker and Kelly, 1983). The observation of phasic patterns in different species and using different methods to assess gastric emptying suggests that this pattern may reflect a physiological event that occurs during solid-phase gastric emptying. Duodeno-gastric reflux is a common occurrence during gastric emptying in healthy dogs (Sonnenberg *et al.*, 1982), and could cause intermittent patterns of $^{13}CO_2$ recovery during the ^{13}C-OBT. It is also possible that recurrence of the MMC would produce a phasic pattern of gastric emptying, and indeed, phasic patterns in plasma drug kinetics following oral administration in the liquid phase, can be attributed to cyclic gastric motility patterns (Oberle and Amidon, 1987). However, variability in gastric emptying induced by the motility patterns of the interdigestive state were unlikely to be responsible for variability in the pattern of emptying of digestible food in this study, since the MMC is interrupted by feeding until gastric emptying has been completed and after several hours of fasting (Code and Marlett, 1975). Phasic patterns of solid-phase gastric emptying

could have important implications for our understanding of gastric physiology and for modelling and analysis of gastric emptying data for clinical and research purposes.

No significant relationship between the breath test parameters ($t_{½}$ and $t_{(max)}$) and body size could be detected in the dogs in this study. In contrast, previous studies have demonstrated an inverse linear relationship between the rate of gastric emptying and body size in man (Lavigne *et al.*, 1978; Brogna *et al.*, 1998) and in the dog (Allan *et al.*, 1996). Factors other than body size such as stress, sex and age could affect the rate of gastric emptying and may thus have masked a relationship between body size and the breath test parameters in this study.

The ^{13}C-OBT offers several distinct advantages over the other methods for assessing solid-phase gastric emptying in the dog. All non-invasive methods currently available for assessment of gastric emptying require that the dog is either sedated or restrained, both of which could affect the rate of gastric emptying (Zontine, 1973; Gue *et al.*, 1989). The ^{13}C-OBT is completely non-invasive and breath samples can be taken with minimal disturbance of the animals. Radioscintigraphy is the gold-standard method for assessment of gastric emptying (Parkman *et al.*, 1995) but requires access to a nuclear medicine facility and experienced personnel for several hours, as well as necessitating exposure of the animal and personnel to ionising radiation. Radiation regulations require that dogs are housed in isolation kennels for 48 hours after radioscintigraphy. In contrast, the ^{13}C-OBT requires no specialist equipment or expertise, and can be performed in the field, since $^{13}CO_2$ can be stored in sealed breath sample tubes for up to 60 days (Schoeller *et al.*, 1977), and samples can be posted to the laboratory for analysis. Analysis of the breath test data can be completely automated and provides data describing the rate and pattern of gastric emptying that is non-subjective and

quantitative. The test meal in the ^{13}C-OBT is similar to food normally ingested by the animal, and any food could potentially be used, providing a generous tracer dose is given. Neither the octanoic acid substrate nor the ^{13}C label pose any risk to health.

The results of these studies have indicated that the ^{13}C-OBT may be a simple, reproducible and safe method for the assessment of gastric emptying of solids in the dog. Further validation, including correlation of the test with reference methods for assessing gastric emptying is now justified.

3.2 THE EFFECT OF MEAL COMPOSITION ON THE RATE OF GASTRIC EMPTYING IN THE DOG

3.2.1 Study Aim

The objective of this study was to assess the effect of altering test meal composition on the parameters of the ^{13}C-octanoic acid breath test.

3.2.2 Introduction

Gastric emptying of nutrient meals is a complex and highly regulated process directed towards delivering ingesta to the small intestine at a rate that matches absorptive capacity (Hunt and Stubbs, 1975). Isocaloric amounts of all three nutrients (protein, carbohydrate and fat) exert similar regulatory effects on gastric emptying, mediated through the action of glucose on small intestinal osmoreceptors (Barker *et al.*, 1974) or binding of Ca^{2+} in the epithelium by products of triglyceride digestion (Hunt, 1983). The magnitude of the induced delay in gastric emptying is related to the progressive

recruitment of inhibitory sensors along the length of the small intestine. The spread of nutrient along the gut depends on the rate of absorption along successive centimetres of gut (Lin *et al.*, 1989; 1992). Efflux of nutrient ($kcal.min^{-1}$) is closely matched to small intestinal absorptive capacity, and several studies have demonstrated a close relationship between the rate of gastric emptying of glucose ($kcal.min^{-1}$) and the rate at which glucose is infused into the small intestine ($min.kcal^{-1}$) (McHugh and Moran, 1979; Brener *et al.*, 1983). Regulation of the rate of gastric emptying of nutrients in this way is consistent with the reservoir function of the stomach, and optimises the digestion and absorption of food.

The gastric emptying of dietary lipids is complex, and intra- and extra-cellular fats are probably expelled in separate phases (Edelbroek *et al.*, 1992). Extra-cellular fats such as oil empty after the liquid phase and at a similar rate to the solid phase of gastric emptying. Intra-cellular fats empty with the solid phase (Meyer *et al.*, 1986b). Regulation of the gastric emptying of lipids is mediated by the actions of lipolytic products on small intestinal receptors, since the rate of gastric emptying of fats reverted to volume-dependence (ie non-nutrient meals) when pancreatic lipase was eliminated from the duodenum in dogs and a similar effect was evident following administration of a specific lipase inhibitor (Meyer *et al.*, 1994). However, exclusion of pancreatic lipase did not completely attenuate the effects of oil ingestion indicating that gastric lipase may also be involved in mediating fat-induced delays in gastric emptying (Meyer *et al.*, 1994). It is probable that delayed gastric emptying of fat is mediated at least in part by a vago-vagal reflex, since functional ablation of the vagal sensory pathway from the gastrointestinal tract abolished the gastric response to intestinal fat perfusion (Holzer *et al.*, 1994). Increased meal energy density is known to induce delayed gastric emptying in the dog, and the ability of the octanoic acid breath to detect such a delay would be a

good indicator of the potential usefulness of this test for detecting disordered gastric emptying induced by disease.

3.2.3 Materials and Methods

Animals

Four dogs were used in this study, dog numbers 1, 2, 3 and 4, see Appendix 4.

Test Meals

Two test meals were used in this study a high energy density meal (approximately 1423kJ), Meal 1, and a low energy density meal (approximately 775kJ), Meal 2. Meal 1 was identical to the standard meal used in the preliminary studies (Section 3.1), and Meal 2 was made up of the standard energy density meal with 25g margarine added. 175mls skimmed milk was used in the high energy density meal and 200mls in the standard meal, in order that the volumes of both meals remained constant. All test meals were labelled with 50 mg ^{13}C-octanoic acid.

Study Design

Each dog (n = 4) ingested each meal on 3 separate occasions and in random order (Appendix 6). Due to the repeatability of ^{13}C-concentration between replicate breath samples (Appendix 5), single breath samples were taken at each time point. Breath samples were collected immediately before (t = 0 min) ingestion of the test meal, and then every 10 minutes for 6 hours, and every 20 minutes for another 2 hours. Statistical analyses for significance was carried out using a two factor ANOVA, with repeated measures, with factors being individual dogs, and test meal.

3.2.4 Results

There was a significant difference between the breath test parameters following the high energy density meal compared to the standard meal. The GEC was significantly decreased following the high energy density meal ($p < 0.01$), while $t_{½}$ and $t_{(max)}$ were significantly increased ($p < 0.01$ and 0.05, respectively). The mean effect of the high energy density meal compared to the standard meal is shown in Table 3.5.

Dog No.	GEC			$t_{½}$.hour^{-1}			$t_{(max)}$.hour^{-1}		
	Meal			Meal			Meal		
	1	2	Difference	1	2	Difference	1	2	Difference
1	2.52	2.28	0.24	3.63	3.78	-0.47	2.99	3.02	-0.03
2	2.60	2.19	0.41	3.58	4.20	-0.62	2.87	3.34	-0.46
3	2.85	2.17	0.69	3.46	4.00	-0.54	2.72	3.37	-0.65
4	2.82	2.18	0.64	3.66	4.11	-0.46	2.76	3.29	-0.54
Mean	2.70	2.21	0.49	3.58	4.02	-0.44	2.83	3.26	-0.42
SE			0.10			0.10			0.14

Table 3.5: The effect of test meal composition on the parameters of the ^{13}C octanoic acid breath test in the dog. Meal 1 was a standard energy density meal, while meal 2 was a fat-enriched meal. The mean and standard error of the indices used to describe the rate of gastric emptying are shown following ingestion of each meal on 3 occasions in 4 dogs. The gastric emptying indices are, the gastric emptying coefficient (GEC), half dose recovery time ($t_{½}$.hours^{-1}) and time of maximal breath ^{13}C-enrichment ($t_{½}$.hours^{-1}).

3.2.5 Discussion

In this study an oil-enriched test meal was used to induce delayed gastric emptying in dogs and assess the ability of the ^{13}C-octanoic acid breath test to detect alterations in gastric emptying in dogs. The ^{13}C-tracer remained labelling the solid phase of gastric

emptying. Previous investigators have demonstrated that ^{13}C-octanoic acid remained bound to the solid-phase using test meals where the energy density had been similarly increased using margarine (Robertson and Mahers, 2000; Maes, 1994a). The function of the increased amount of margarine in the test meal was to increase the energy density of the meal and induce a delay in solid-phase gastric emptying which was assessed using the ^{13}C-octanoic acid breath test.

Several mechanisms have been suggested to account for the retention of oil in the stomach, including formation of a stable emulsion or layering of oil in the ingesta. However, intra-gastric retention of oil has been demonstrated in the absence of layering (Jian *et al.*, 1982). Formation of an oil-emulsion is unlikely in the acid environment of the stomach (Cortot *et al.*, 1981), and Meyer *et al.*, (1986b) demonstrated that only a small amount of extra-cellular fat emptied from the canine stomach as an emulsion. Retrograde movement of oils into the proximal stomach has been demonstrated during gastric emptying, and this could account for their retention (Houghton *et al.*, 1990). Such movement of oil may function to disperse the oil droplets into spherules of suitable diameter for gastric emptying (Meyer *et al.*, 1986b). Furthermore, gastric lipase is secreted in the fundic mucosa, and proximal migration of oils could enhance gastric lipolysis (Edelbroek *et al.*, 1992).

Oil-enriched test meals have been used as experimental models of delayed gastric emptying, assessed using the ^{13}C-OBT (Mansi, *et al.*, 1998), and the ^{13}C-OBT has been used to assess delayed gastric emptying induced by changes in meal composition in man (Maes, 1994a; Peracchi *et al.*, 2000). The ability of the ^{13}C-OBT to detect delayed gastric emptying was assessed in this study by repeating the test protocol in dogs following random ingestion of test meals of different composition. Ingestion of the

high energy density meal was associated with significant alterations in rate and pattern of recovery of ^{13}C in breath, with increased values of $t_{½}$ and $t_{(max)}$ and decreased values of GEC. This finding is an indication of the sensitivity of the ^{13}C-OBT in detecting delayed gastric emptying in dogs, and confirms the potential use of this test for investigation of altered gastric emptying that may be associated with disease or drugs.

3.3 A COMPARISON OF THE RATE OF RECOVERY OF $^{13}CO_2$ IN EXHALED BREATH WITH THE RATE OF RECOVERY OF ^{2}H IN BODY WATER FOLLOWING INGESTION OF $^{2}H/^{13}C$-OCTANOIC ACID IN A DOG

3.3.1 Study Aim

The specific objective of this study was to assess the contribution of bicarbonate kinetics to the delay in appearance in $^{13}CO_2$ in breath during the ^{13}C-OBT in the dog, by comparing recovery of ^{13}C in breath with ^{2}H in saliva following simultaneous ingestion of ^{2}H and ^{13}C-octanoic acid.

3.3.2 Introduction

The ^{13}C-octanoic acid breath test has the disadvantage of not providing a real time measure of gastric emptying, since the post-gastric processing of octanoic acid requires oxidation and distribution through the bicarbonate pool, conferring an inevitable delay before the ^{13}C signal is detected in breath. In man, correlation of the ^{13}C-octanoic acid breath test and scintigraphy allowed this delay to be quantified and an appropriate correction factor derived (Ghoos *et al.,* 1993). Recent studies investigating the contribution of post-gastric processing of octanoic acid have utilised ^{2}H-octanoic acid and concurrent scintigraphy and have shown that there is no difference between the

gastric emptying of the radioisotope and appearance of ^{2}H in the body water pool. These studies led to the conclusion that ^{2}H-octanoic acid can be used for validation of the ^{13}C-octanoic acid breath test, when scintigraphy is unavailable (Bluck *et al.*, 1998;1999; Jackson *et al.*, 2001). Following gastric emptying, ^{2}H enters the body water pool and can be detected instantaneously, while the ^{13}C undergoes a delay before detection in breath CO_2 due to metabolism and entry into the bicarbonate pool. Simultaneous assessment of ^{2}H and ^{13}C excretion rate would allow this delay to be estimated, and the contribution of bicarbonate kinetics to the timing of ^{13}C-recovery during the ^{13}C-OBT in the dog to be assessed.

3.3.3 Materials and Methods

Animal

One healthy female dog was used in this study (Dog No. 19). Her weight was 25kg and further details are given in Appendix 4.

Test Meal

The test meal used in this study consisted of 200g tinned dog food (Select Chicken and Rice, Selected Protein, Pedigree Petfoods). The octanoic acid substrate was added to 3 egg yolks, baked and finally mixed thoroughly with the dog food. The energy density of the meal was estimated as 1500kJ. Either ^{13}C-octanoic acid, (Octanoic acid-1-^{13}C (minimum 99% atom % ^{13}C), Isotec Inc.), ^{2}H-octanoic acid (Octanoic-d_{15} acid (minimum 98% atom % ^{2}H), Cambridge Isotope Laboratories) or octanoic acid (Caprylic acid (n-octanoic acid) Sigma-Aldrich), were used in studies as described below.

Breath and Saliva Collection

Breath samples were collected as described in Chapter Two. Saliva samples were collected by allowing the dog to chew a sponge-covered ball. After 5 minutes the cover was removed from the ball and placed into a sample tube, inside of which was a small funnel allowing the saliva to drain into the distal end of the tube (Figure 3.5). The tubes were centrifuged at 4000g for 20 minutes so that the saliva collected beneath the funnel. Saliva samples were immediately stored at -20°C and analysed within 4 weeks.

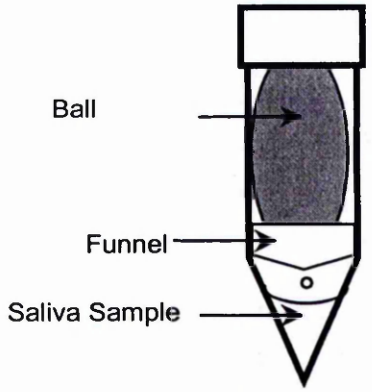

Figure 3.5: The apparatus used for centrifuging saliva samples.

Study Design

The dog ingested a test meal with either 850mg n-octanoic acid (one occasion) or 100mg ^{13}C-octanoic acid and 750mg ^{2}H-octanoic acid (two occasions). Breath and saliva samples were collected at 30 minutes and immediately before ingestion of the test meal, and then every 15 minutes for 4 hours, and every 30 minutes for a further 2 hours. A further saliva sample was collected 24 hours after ingestion of the meal. At least two weeks was allowed between tests where an isotope was administered.

^{13}C-analysis and ^{2}H-analysis

^{13}C-analysis was carried out as described in Chapter Two. ^{2}H-enrichment in saliva was also analysed by continuous flow isotope ratio mass spectrometry; abundance ratio of

mass 2 and 3 were measured. Before analysis, the saliva samples were equilibrated with hydrogen gas (5% in He), so the isotopic information of the saliva is transferred into the gas phase (Scrimgeour *et al,* 1993). Hydrogen gas was added to an evacuated sample tube (Exetainer) into which a 400µl aliquot of saliva had been added. Equilibration of hydrogen gas with the water was carried out a platinum-on-alumina catalyst (Aldrich) physically isolated from the saliva sample in a glass vial. The samples were kept at room temperature for a 3 day equilibration period, after which the ratio of ^{2}H:^{1}H was determined by isotope ratio mass spectrometry, as described in Chapter 2. Reference water samples of 0 (tap water) and 75 ppm excess ^{2}H were used as standards. The enrichment of deuterium (ppm excess) was calculated with reference to the standard water after correction for the contribution of H_3^+ to the ^{2}H:^{1}H ratio (Prosser and Scrimgeour, 1995). The ^{2}H-elimination constant in dogs was taken from values quoted by Speakman *et al.,* (2001) for dogs of similar weight and taken to remain stable at 6.6 X 10^{-5}.min^{-1}. Although minor this value was used to correct measured 2H-enrichment for elimination from body water. Recovery of ^{2}H in body water was expressed in parts per million excess and plotted against time.

Data Analysis

All data analyses were performed using Microsoft Excel 97. Results of ^{13}C-analysis were expressed as either % dose administered recovered per hour, PDR (Chapter 2), or ppm ^{13}C-enrichment, while results of ^{2}H-analysis were expressed as ppm ^{2}H-excess.

^{2}H-recovery expressed in ppm, and ^{13}C-recovery expressed in PDR/hour were modelled using the equation described by Siegel *et al.,* (1988) and modified by Maes (1994a):

$$y = m\left(1-e^{-kt}\right)^{\beta} \qquad \text{(Eq. 3.4)}$$

where y is the percentage of cumulative $^{13}C/^{2}H$ excretion in breath, t is time in hours and m, k and β are constants where m represents the total cumulative $^{13}C/^{2}H$-recovery when time is infinite. The Solver function of a Microsoft Excel computer programme was used to predict values for m, k and β by non linear regression analysis, and allowed the calculation of two indices, the half dose recovery time ($t_{½}$) and the time of maximal $^{2}H/^{13}C$ recovery (t_{lag}). $t_{½}$ was defined as the area under the fitted cumulative recovery curve when half of the administered dose is excreted, when time is infinite, and calculated mathematically using the formula:

$$t_{½} = \left(\frac{-1}{k}\right) \times \ln\left(1-2^{\frac{-1}{\beta}}\right)$$ Ghoos *et al.*, 1993, (Eq. 3.5)

t_{lag} was defined as the time at the point of inflexion of the fitted cumulative recovery curve, and calculated mathematically using the formula:

$$t_{max} = \frac{(\ln\beta)}{k}$$ Ghoos *et al.*, 1993, (Eq. 3.6)

3.3.4 Results

The novel method of saliva collection described in this study was well-tolerated by the dog, and saliva volumes of approximately 500µl were collected at most time points. The test meal containing 850mg octanoic acid was palatable and ingested within 2 minutes on each occasion. The ratio of $^{2}H:^{1}H$ remained stable and low over six hours following ingestion of a test meal and 850mg unlabelled octanoic acid (mean ^{2}H-enrichment, 1.6±1.4 ppm excess). A significant increase in ^{2}H was detected in the saliva following ingestion of the test meal (Figure 3.6). The cumulative ^{13}C-excretion curve and the ^{2}H-excretion curve following ingestion of $^{2}H/^{13}C$-octanoic acid on two separate occasions in the dog in this study are shown in Figure 3.6. The gastric

emptying coefficients $t_{½}$ and t_{lag} were calculated from the breath ^{13}C-excretion curve and the ^{2}H-excretion curve, and are shown in Table 3.6. Recovery of ^{2}H in saliva was quicker than recovery of ^{13}C in breath as determined by the difference in the gastric emptying indices for each isotope; 1.33 and 1.59 hours for $t_{½}$ and t_{lag} respectively (Table 3.6).

Table 3.6 The mean gastric emptying coefficients calculated following ingestion of ^{13}C-and ^{2}H-octanoic acid BT on two separate occasions in the dog in this study.

Test	$t_{½}$ / hour	t_{lag} / hour
^{13}C-breath test	5.12	3.43
^{2}H-saliva test	3.79	1.84
Difference	1.33	1.59

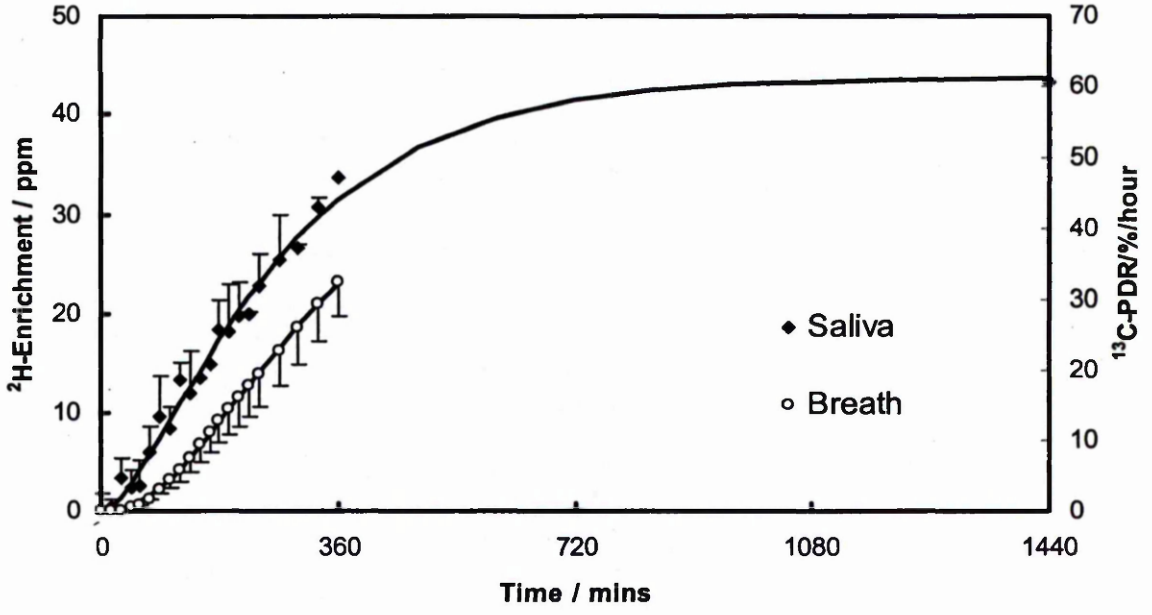

Figure 3.6 A comparison of mean ^{13}C and ^{2}H-recovery following ingestion of $^{2}H/^{13}C$-octanoic acid on two separate occasions by the dog in this study. The points show the measured data and the curves are the values predicted by the model.

3.3.5 Discussion

The ^{13}C-OBT is an indirect method for assessment of gastric emptying and the accuracy of this method is reliant on rapid and reproducible metabolism of octanoic acid following entry into the duodenum. Post-gastric processing of octanoic acid is thought

to be consistent between and within individuals (Drewe *et al.*, 1998), but produces a delay between the recovery of isotope in breath and absorption of octanoic acid in the duodenum. This delay precludes direct comparison of the ^{13}C-OBT with radioscintigraphy or other real-time methods for assessing gastric emptying, unless appropriate correction factors are employed. In human studies, correlation with radioscintigraphy has enabled a correction factor to be derived, that allows direct comparison of breath test data with other methods for assessment of gastric emptying (Ghoos *et al.*, 1993).

The gastric emptying of deuterated (^2H_2O)-octanoic acid was shown to be almost identical to the "gold standard" method of radioscintigraphy (Bluck *et al.*, 1998). The ^{2}H label is a stable isotope of hydrogen, but unlike $^{13}CO_2$, ^{2}H does not enter the bicarbonate pool, and D_2O can be detected in the body water almost immediately following oxidation of octanoate (Bluck *et al.*, 1999). D_2O is an ideal tracer for *in vivo* studies as it is non-toxic, has a similar distribution volume to water and accumulates in plasma and saliva according to its rate of entry into the body water (Davis *et al.*, 1987). Routine use of ^{2}H-octanoic acid for assessment of gastric emptying is limited by the higher purchase and analytical costs of this isotope. The higher cost of ^{2}H-octanoic acid is partly due to the large dose required to label the body water pool compared with that of ^{13}C-octanoic acid required to label the bicarbonate pool.

In the present study, D_2O was detected in the saliva of a dog over 6 hours following simultaneous ingestion of ^{13}C/^{2}H-octanoic acid, in order to estimate the contribution of post-gastric processing of octanoic acid on the rate of ^{13}C-recovery in breath. A novel method for saliva collection in the dog was developed that allowed serial samples of relatively large volumes (500µl) to be collected non-invasively over a long time period.

Previous workers have attempted to collect saliva in dogs by swabbing the mouth (Vincent and Michell, 1992) chemical stimulation of salivation (Beerda *et al.,* 1996) or fistulation of the salivary glands (Pagani *et al.,* 1988). These latter methods were too invasive for the purposes of this present study, while swabbing the mouth could not reliably be used to collect serial samples of sufficient volume over the 6 hour test period.

The ratio of ^{2}H:H remained stable over a six hour period following ingestion of a test meal and unlabelled octanoic acid, indicating the suitability of the test meal as a carrier for administration of ^{2}H-octanoic acid. The rate of gastric emptying (as assessed using the ^{13}C-OBT) was slower in the dog in this study, than in earlier studies in the dog (Section 3.1). A more energy-dense meal was ingested, due to the large dose (850mg) of unpalatable octanoic acid administered, and the increased meal energy density could have mediated a slower rate of gastric emptying (Section 3.2). The times of maximal ^{2}H and ^{13}C excretion were not coincident in this study indicating that as has been previously reported in man (Ghoos *et al.,* 1993), the post-gastric metabolism of octanoic acid imposes a delay on ^{13}C-recovery in breath. Comparison of the t_{lag} and $t_{½}$ for ^{2}H in saliva and ^{13}C in breath in this study allowed the length of this delay in the dog to be estimated. The difference between $t_{½}$ for ^{2}H and ^{13}C-recovery in this study was 1.33 hours; this value is similar to reported differences between $t_{½}$ of 1.1 hours when the ^{13}C-OBT was compared with radioscintigraphy in man (Ghoos *et al.,* 1993) and 1.77 hours when the ^{13}C-OBT and ^{2}H-octanoate saliva test were compared in man (Bluck *et al.,* 1998). This finding confirms that, as is the case in man and the horse, the post-gastric processing of octanoic acid imposes a delay on the recovery of ^{13}C in breath in the dog and signifies that the ^{13}C-OBT does not yield real-time information about the rate of gastric emptying in the dog. The results of this study suggest that t_{lag} - 1.33 hours may

be a suitable correction factor for the ^{13}C-OBT in the dog. Further studies to validate the ^{13}C-OBT for clinical application should include correlation against radioscintigraphy, and investigation of the effect of physiological abnormalities on the absorption and metabolism of octanoic acid.

3.4 THE ^{13}C-LACTOSE-UREIDE BREATH TEST AND THE HYDROGEN BREATH TEST FOR ASSESSMENT OF ORO-CAECAL TRANSIT TIME IN THE DOG

3.4.1 Study Aim

The specific objective of this study was to investigate the feasibility of applying the ^{13}C-LUBT for assessment of oro-caecal transit time in the dog, compared with the H_2BT.

3.4.2 Introduction

Oro-caecal transit time (OCTT) is an important indicator of small intestinal function and a simple test of OCTT would be a useful tool in the investigation of gastrointestinal disease. Current methods for assessment of OCTT rely on either detection of a signal produced when a marker is metabolised by colonic microflora, or imaging of the passage of a radio-labelled or radio-opaque substrate into the caecum. The assessment of OCTT in the dog using imaging methods such as radiography (Bruce *et al.*, 1999) and radioscintigraphy (Iwanga *et al.*, 1998; Farrugia *et al.*, 1998) carry the same problems as the use of these methods in assessing gastric emptying (Section 3.1). Nevertheless these methods are commonly applied for assessment of gastrointestinal transit and radioscintigraphy is considered to be the "gold standard" method for assessment of OCTT.

Radioscintigraphy can be used to simultaneously evaluate gastric emptying, small intestinal transit time and OCTT by combining two isotopes in the test meal (Iwanaga *et al.*, 1998). This "dual-isotope" method has been used to examine the effect of motility-modifying drugs on regional gastrointestinal transit in the dog (Chiba *et al.*, 2000). Intestinal fistulation has provided useful information on OCTT in the dog but is too invasive for routine use (Williams *et al.*, 1984). Oro-caecal transit time can be investigated by HPLC or spectrophotometric detection of sulphapyridine in plasma or saliva following ingestion of sulphasalazine. Sulphasalazine is cleaved to sulphapyridine by colonic microbial activity but is resistant to enzymatic digestion in the proximal intestine (Spiller, 1993). Cleavage of sulphasalazine did not occur when this compound was instilled directly into the small intestine, but increases in sulphapyridine were detected following instillation into the caecum (Mizuta *et al.*, 1990) indicating the specificity of this method for assessment of OCTT. The sulphapyridine test can be combined with the acetaminophen test to simultaneously investigate gastric emptying and OCTT in the dog (Mizuta *et al.*, 1990).

The hydrogen breath test (H_2BT) is a useful non-invasive method for assessment of OCTT in the dog (Papasouliotis *et al.*, 1995). This test is based on the production of hydrogen gas during fermentation of indigestible carbohydrates in the hind-gut. Hydrogen can easily pass through the colonic mucosa into the blood where it is subject to no further metabolism, but passes through the pulmonary alveoli to be excreted in breath (Bond and Levitt, 1975). Lactulose is generally used as a source of indigestible carbohydrate in this test, although this substance has a dose-dependent accelerating effect on gastrointestinal transit (Wutzke *et al.*, 1997; Miller *et al.*, 1997) and the use of lactulose as a substrate in the H_2BT probably affects discrimination between pathological and normal transit. Large intestinal fermentation of solid food containing

unabsorbable carbohydrate also produced significant increases in breath hydrogen in man (Read *et al,* 1985) and in the dog (Pouteau *et al.,* 1998). The significant rise in breath H_2 after a carbohydrate-rich meal was shown to be closely correlated with the passage of a radioactive marker into the caecum, suggesting that solid food can be used to indicate OCTT in the H_2BT (Read *et al.,* 1985). Detection of OCTT using lactulose as a substrate in the H_2BT has been shown in several studies to be correlated with the reference method of scintigraphy in man (Sciarreta *et al.,* 1994; Miller *et al.,* 1997) with intestinal transit of an indigestible marker in man, (polyethylene glycol) (Bond and Levit, 1975) and with the sulphapyridine test in the dog (Papasouliotis *et al.,* 1995). Some healthy human subjects fail to produce breath hydrogen, possibly due to scavenging of hydrogen by colonic microflora (Bond and Levitt, 1975), and this, combined with the prokinetic effects of lactulose limit the clinical application of the test.

The lactose-[^{13}C]-ureide breath test (^{13}C-LUBT) was recently described as a non-invasive method for assessment of OCTT in man (Heine *et al.,* 1995). Lactose-ureide is the condensation product of lactose and urea, and the molecular bond between lactose and urea in this compound is resistant to small intestinal enzymatic cleavage, but can be split by colonic flora (Merry *et al.,* 1982). Studies on human intestinal biopsy specimens have shown that a small intestinal enzyme (β-galactosidase) degraded lactose-ureide to glucose-ureide (Ruemelle *et al.,* 1997). Glucose-ureide is thought to be exclusively degraded in the large intestine by an unknown enzyme (glucoseureidehydrolase) synthesised by *Clostridium innocuum* (Mohr *et al.,* 1999). Cleavage of glucose-^{13}C-ureide yields ^{13}C-urea, which is further degraded by bacterial ureases to produce $^{13}CO_2$ and NH_3 (Heine *et al.,* 1995). Recovery of ^{13}C-glucose-ureide in urine following ingestion of ^{13}C-lactose-ureide indicates that the disaccharide bond is

ureide bond to brush border enzymes (Wutzke *et al.*, 1997; Morrison *et al.*, 1999). Furthermore, pre-treatment with oral antibiotics abolished the breath ^{13}C-signal following ingestion of ^{13}C-lactose-ureide, indicating the specificity of this compound to bacterial degradation (Heine *et al.*, 1995). The colonic bacterium (*C. innocuum*) responsible for the degradation of glucose-ureide is thought to be present in all adults, children and babies over 8 months (Mohr *et al.*, 1999); this organism is not present in babies under 6 months precluding the application of the ^{13}C-LUBT in these subjects (van den Driessche *et al.*, 2000). The ^{13}C-LUBT has shown good correlation with the reference method of radioscintigraphy (Geypens *et al.*, 1999a) and has shown good sensitivity in detecting pharmacological modification of OCTT with propantheline and octreotide (Geypens *et al.*, 1999b), and pathological alterations in OCTT in children (van den Driessche *et al.*, 1999). The ^{13}C-LUBT was also used to demonstrate the prokinetic effect of lactulose on OCTT (Geypens *et al.*, 1998c). The ^{13}C-LUBT has been combined with the ^{14}C-OBT to simultaneously assess gastric emptying and OCTT (Geypens *et al.*, 1998b;1998d) and this method was used to detect pharmacological modification of regional gastrointestinal transit in man following administration of erythromycin, propantheline and cisapride (Geypens *et al.*, 1998b;1999c). Mathematical deconvolution of the breath ^{13}C-excretion curve following a combined ^{13}C-OBT and ^{13}C-LUBT allowed a distinct pattern for gastric emptying and OCTT to be detected, facilitating application of this combined test in children (Geypens *et al.*, 1998e). This present study was designed to assess the feasibility of applying the ^{13}C-LUBT in the dog, and to compare the use of this test with a standard method for assessment of OCTT, the H_2BT.

3.4.3 Materials and Methods

Animals

Two dogs were used in this study, Dog Nos. 2 and 3.

Test Meal

The test meal consisted of 400g tinned dog food (Selected Protein, Hills), and 250mg ^{13}C-lactose-ureide was mixed into the food. ^{13}C-lactose-ureide was synthesised by acid-catalysed condensation of lactose with ^{13}C-urea. Grated raw potato (70g) was mixed into the meal in order to provide a source of indigestible fibre to induce intestinal fermentation and production of hydrogen gas.

Breath Collection

Breath samples were collected using the procedure and apparatus described in Chapter Two. Breath samples for hydrogen analysis were stored in 30ml syringes sealed with a three-way tap, before analysis within 1 hour.

Breath Analysis

Breath ^{13}C-excretion was analysed as described in Chapter Two. Breath hydrogen concentration was measured using a exhaled hydrogen monitor (GMI Exhaled Hydrogen Monitor, GMI Medical), which was calibrated against a standard hydrogen nitrogen gas mixture (GMI 1956, GMI Medical). The exhaled hydrogen monitor measures hydrogen by means of a sensitive electrochemical cell, with a stated accuracy of ± 2 ppm hydrogen, over a concentration range of 0 – 250ppm.

Study Design

In order to induce suitable colonic microbial activity the dogs ingested 2.5g lactose ureide in food (400g Selected Protein) 24 hours before ingestion of the test meal. The dogs ingested the test meal with 250mg ^{13}C-lactose-ureide at 9:00hours on the morning of the test, and a second meal of 400g Selected Protein only, was ingested during the test at 16:30hours. The breath test protocol was identical to that described in Chapter Two except breath samples were collected every 30 minutes for twelve hours.

Data Analysis

Data were expressed as the percentage of the administered ^{13}C dose recovered in breath, or ppm hydrogen recovered in a 20ml sample of exhaled air. Breath hydrogen data are presented as the value detected above baseline (ppmOB), where baseline levels of H_2 exhalation were estimated by calculating the mean of samples taken at the –30, 0 and 30 min time points. Oro-caecal transit time was defined as the point of detection of a significant and sustained (over >2 timepoints) rise in $^{13}CO_2$ or H_2 (Wutzke *et al.* 1997). The cumulative sum (CUSUM) procedure (Appendix 7) was used to detect the point at which a significant increase in $^{13}CO_2$ and H_2 occurred (Papasouliotis *et al.* 1995).

3.4.4 Results

The lactose-ureide and raw potato test meal was palatable and ingested by both dogs in less than two minutes. A significant increase above baseline in ^{13}C-excretion and in hydrogen excretion in exhaled breath was detected in both dogs following ingestion of the test meal, and ^{13}C and H_2 exhalation had returned to baseline levels 1440mins later. Oro-caecal transit times calculated using the CUSUM procedure, for the ^{13}C-LUBT and the BH_2T in both dogs are shown in Table 3.7.

Table 3.7: Oro-caecal transit time measured in two dogs using the breath hydrogen test and the ^{13}C-lactose-ureide breath test.

	Orocaecal Transit Time.mins^{-1}	
	Breath Hydrogen Test	^{13}C-Lactose Ureide Breath Test
Dog 2	150	480
Dog 3	150	450

Peaks in ^{13}C-exhalation did not coincide with peaks in hydrogen excretion in either of the dogs (Figure 3.8), and the OCTT measured using the H_2BT was significantly shorter than the OCTT measured using the ^{13}C-LUBT. The CUSUM procedure was successfully used to automate decision of the point of significant increase in breath $^{13}C/H_2$, and hence estimate OCTT. An example of a CUSUM-plot with illustrated OCTT, is given in Figure 3.7.

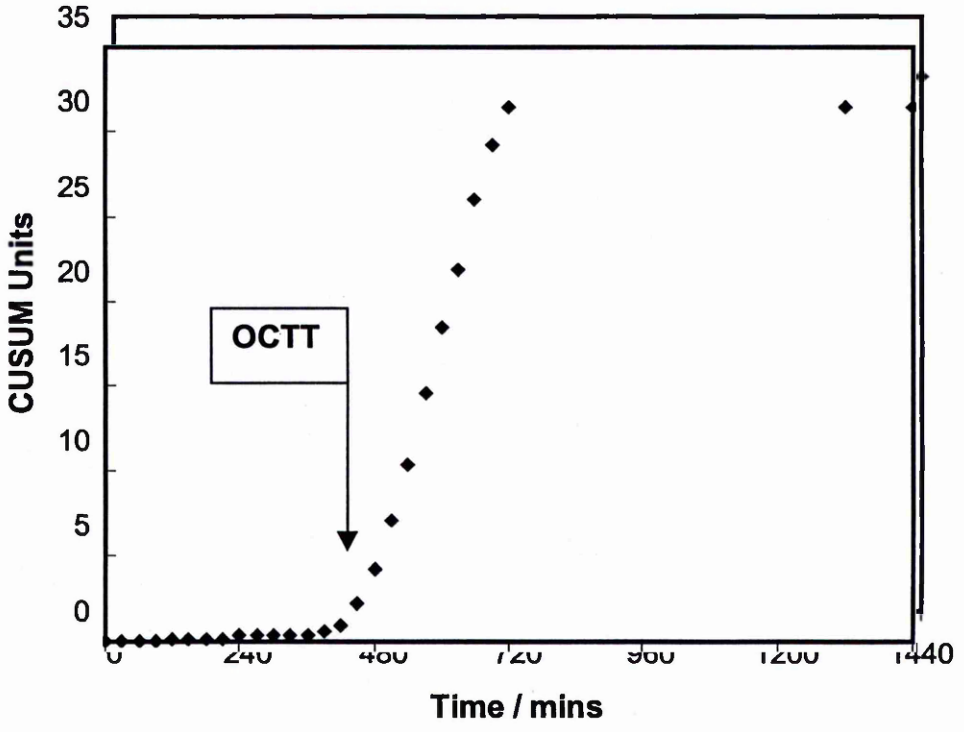

Figure 3.7: A sample CUSUM-plot illustrating detection of point of significant increase in $^{13}CO_2$ excretion, and oro-caecal transit time. Data shown are for the ^{13}C-LUBT performed in Dog No. 3; OCTT, as defined by the ^{13}C-LUBT, was 450mins.

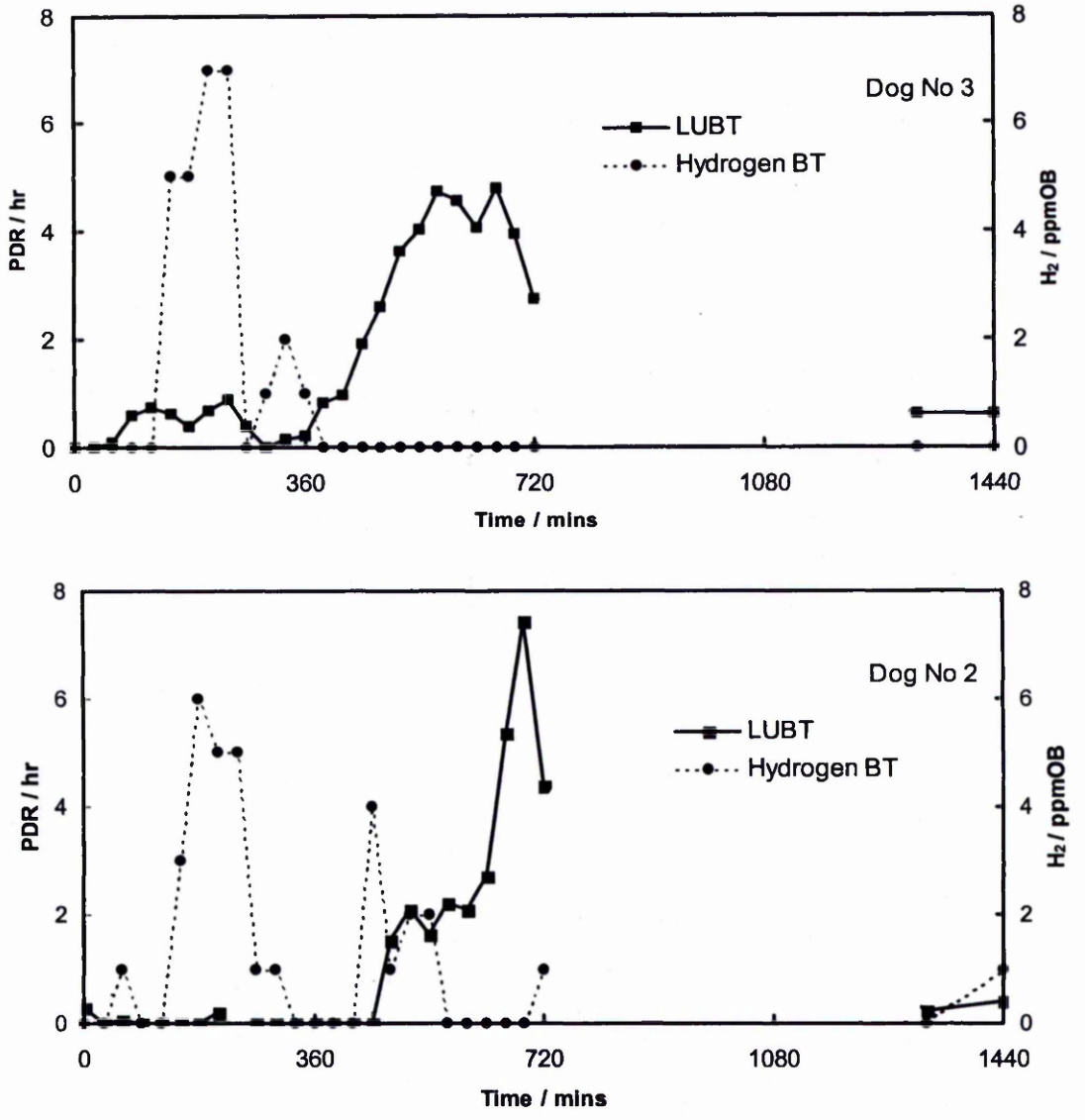

Figure 3.8: Mean ^{13}C-enrichment (^{13}C-LUBT) and H_2-concentration (H_2BT) in exhaled breath during the ^{13}C-lactose-ureide and breath hydrogen test in two dogs (Dog No. 3 above and Dog No. 2, below). Data are mean + standard deviation, PDR is the percentage of administered ^{13}C dose recovered in breath, and ppmOB is the parts per million hydrogen concentration measured over baseline values.

3.4.5 Discussion

This study has shown that ingestion of ^{13}C-LUBT in the dog produces a significant increase in the excretion of $^{13}CO_2$ in the exhaled breath. This finding suggests that the ^{13}C-LUBT may be a useful method for assessment of OCTT in the dog. Increases in breath H_2 following ingestion of a fibre rich meal were also detected in the dogs in this study, but these increases were not coincident with the observed increases in breath ^{13}C. A similar study compared OCTT assessed using the ^{13}C-LUBT with the H_2BT in man, and reported that OCTT was on average 1.18 hours later when assessed using the ^{13}C-LUBT compared with the lactulose H_2 breath test (Wutzke *et al.*, 1997). The accelerating effect of lactulose on intestinal transit was thought to be responsible for the discrepancy between the two tests (Wutzke *et al.*, 1997). However in the present study raw potato was used as a substrate, and while it is possible that this too provoked an increase in intestinal transit, this would be expect to also effect the OCTT of ^{13}C-lactose-ureide. The difference between peak H_2 and $^{13}CO_2$ in the dogs in this study could also be explained by small intestinal fermentation of food, producing an earlier peak in H_2. Zentek *et al.*, (1995) have reported that ileal degradation of amino acids in the dog produces large amounts of H_2 in breath.

The CUSUM procedure for analysis of ^{13}C-LUBT and H_2BT data described in this study allowed simple automated detection of the point at which a significant rise above baseline of breath $^{13}C/H_2$ occurred. This procedure should detect the point at which the first significant volume of substrate is presented to the caecal microflora, including the time taken for production and diffusion of gases to the lungs. Definition of OCTT as the point of detection of a significant increase above baseline levels of $H_2/^{13}$C exhalation minimises the variability imposed on the test by the rate of microbial metabolism of the substrate.

There is some evidence that large intestinal microbial activity is subject to considerable variation both between and within healthy individuals, and this variation could contribute to the variability of OCTT measured during the H_2BT and ^{13}C-LUBT. Instillation of lactose-^{13}C-ureide directly into the caecum produced a significant increase in breath $^{13}CO_2$ in 15-30 minutes in 5 human subjects; this delay reflects the bacterial degradation of the sugar-ureide bond and absorption and excretion of $^{13}CO_2$ (Geypens *et al.*, 2000). The time of maximal breath ^{13}C-excretion in these subjects varied from 90-225 minutes and total percentage recovery of isotope in breath varied from 4.8-16.6% (Geypens *et al.*, 2000). The variable recovery of isotope and the lengthy time of maximal ^{13}C-excretion in breath following caecal instillation of lactose-^{13}C-ureide suggest that the overall shape of the ^{13}C-excretion curve in the ^{13}C-LUBT depends on colonic microbial activity. Furthermore, recovery of ^{13}C in breath did not coincide with recovery of ^{15}N-urea in urine following ingestion of lactose-^{13}C-ureide and lactose-^{15}N-ureide, indicating that microbial digestion of urea imposed a delay on the appearance of the ^{13}C-signal in breath, that was not evident when urea was absorbed directly from the colon (Jackson *et al.*, 1999). This study suggested that the analysis of ^{15}N-urea in urine may be a more accurate indicator of OCTT following ingestion of lactose-ureide (Jackson *et al.*, 1999); however serial collection of urine samples would be more difficult to implement in the clinical setting. A significant increase in breath H_2 was detected 4-5 minutes after H_2 was instilled directly into the caecum, indicating the rapid diffusion of H_2 from the colon to the lungs (Bond and Levitt, 1975). Similarly, instillation of lactulose directly into the caecum was also associated with significant increases in H_2 exhalation in less than two minutes although values remained above baseline for a mean of 2.9 hours (Read *et al.*, 1985). These results suggest that the total production of H_2 and $^{13}CO_2$ during the H_2BT and ^{13}C-LUBT is dependent in

part on the activity of large intestinal microbes, and the point of significant increase in $H_2/^{13}C$ above baseline may be the best indicator of OCTT. The CUSUM procedure outlined in the present study allows simple and accurate detection of this point.

The advantages of the ^{13}C-LUBT over the other methods of assessment of OCTT are primarily that it is non-invasive and does not require exposure to radiation or access to specialised equipment. All adult animals are thought to harbour gut microbes capable of breaking down lactose-ureide (Mohr *et al.,* 1999); this is not the case for the H_2BT, as some healthy individual fail to produce H_2 in breath following ingestion of unabsorbable carbohydrate. The H_2 signal in breath may be confounded by fermentation of carbohydrates ingested before commencement of the test (Read *et al.,* 1985), but the ^{13}C-signal in ^{13}C-LUBT can only be derived from the metabolism of the test substrate. The ^{13}C-LUBT does require pre-treatment of the subject with lactose-ureide before the test to induce gut flora, and this procedure has been shown to produce higher breath ^{13}C-enrichment, due to induction of appropriate colonic microbial activity (Wutzke *et al.,* 1997). The ^{13}C-LUBT can potentially be combined with the ^{13}C-OBT allowing the simultaneous assessment of regional gastrointestinal transit, although the application of this test for investigation of pathological conditions requires further investigation.

It is of some significance, however, that the H_2BT, ^{13}C-LUBT and sulphapyridine tests for assessment of OCTT are all reliant on a healthy colonic microflora, and are therefore inherently unsuitable for application in subjects treated with antibiotics, or suffering from small intestinal bacterial overgrowth. Since bacterial contamination of the proximal intestine is frequently associated with small intestinal dysmotility (Nieuwenhuijs *et al.,* 1998) the validity of clinical tests of OCTT that rely on specific

colonic bacterial cleavage of test substrates is debatable. In human medicine, patients with gastrointestinal motility disorders often already suffer small intestinal bacterial contamination when symptoms of small intestinal dysmotility are sufficiently severe to require assessment of OCTT (Spiller, 1993). The ^{13}C-LUBT may be of most use for investigation of the effects of motility modifiying drugs on OCTT, and studies of the physiological functions of small intestinal motility in healthy subjects. The results of the present study are an indication of the potential application of the ^{13}C-LUBT for assessment of OCTT in the dog. However the small sample size used precludes any conclusions on the validity of this test; further study including correlation with the gold standard method of scintigraphy and investigation of the degradation of lactose-ureide in the dog, is necessary.

CHAPTER 4 VALIDATION OF A GAS CHROMATOGRAPHY METHOD FOR DETECTION OF EXHALED PENTANE AND ETHANE

4.1 ORIGINS OF EXHALED HYDROCARBONS

Biochemistry

Exhaled pentane and ethane were first associated with *in vivo* lipid peroxidation in 1973, (Riely *et al.,* 1974) and since then these markers have been widely applied as non-invasive indicators of oxidative stress in various pathological and physiological conditions (Aghdassi and Allard, 2000). The evolution of pentane and ethane in exhaled breath arises from the respective oxidation of ω–6 carbon fatty acids (linoleic or arachidonic acid) and ω-3 fatty acids (linolenic acid) (Donovan and Menzel 1978). Pentane and ethane are formed following decomposition of lipid peroxides, a process that is itself temperature dependant and sensitive to the availability of transition metal ions (Evans *et al.,* 1967). Therefore, the rate of production of pentane and ethane does not truly reflect the rate of lipid peroxidation, but rather the rate of decomposition of lipid peroxides, and may reflect an increased availability of transition metal ions rather than an increase in the overall rate of lipid peroxidation. The steps involved in the decomposition of lipid peroxides to yield alkanes are shown in Figure 4.1.

$LOOH + Fe^{2+} \rightarrow Fe^{3+} + OH^- + RO^{\bullet}$ —β-scission→ pentane radical —abstract $H^{\bullet}$ → pentane

——— (1) ——— (2) ——— (3) ———

Figure 4.1 The steps involved in the decomposition of lipid peroxides to yield alkanes. Firstly, lipid peroxides (LOOH) decompose in the presence of transition metal ions to yield the alloxyl radical, $RO^{\bullet}$ (1). Next, the fatty chain on the methyl side of the carbon chain bearing the alloxyl radical breaks down to yield a pentane or ethane radical (2.). Finally the pentane or ethane radical abstracts a hydrogen atom to form pentane or ethane (3).

In Vivo Metabolism of Ethane and Pentane

Following their formation, pentane and ethane have dissimilar pharmokinetics of elimination, and this has important implications for their use as markers of lipid peroxidation. The *in vivo* metabolism of both pentane and ethane was demonstrated unequivocally in the rat when 50 and 20% of an administered dose of ^{14}C-pentane and ^{14}C-ethane respectively, was recovered as $^{14}CO_2$ after 8 hours (Daugherty *et al.*, 1988). Further evidence for extensive metabolism of pentane was given by Springfield and Levitt (1994) who demonstrated that just 2.4% of pentane taken up by healthy rats was excreted in the breath, the remainder absorbed into the body tissue or metabolised. The hydrocarbons are metabolised to the corresponding alcohol by hepatic monooxygenases and the rate of metabolism increases with the molecular weight of the alkane (Frank *et al.*, 1980). Hepatic oxidation of pentane was demonstrated when a dramatic increase (85%) in exhaled pentane was detected after inhibition of cytochrome P450, signifying that metabolism of pentane could have considerable effects on the rate of pulmonary excretion (Allerheiligin *et al.*, 1987). Pentane is also metabolised in man, and levels of exhaled pentane in healthy subjects are often less than those in ambient air (Phillips *et al.*, 1994). Because both pentane and ethane are metabolised *in vivo*, their generation during cell membrane lipid peroxidation is superimposed on their rate of metabolic clearance (Frank *et al.*, 1980). Studies aiming to demonstrate that increases in exhaled hydrocarbons signify increased lipid peroxidation should theoretically quantify the rate of metabolic clearance of pentane and ethane. Otherwise, the possibility that alterations in hydrocarbon excretion may reflect decreased metabolic clearance of pentane and ethane rather than increased lipid peroxidation, cannot be excluded. The metabolic clearance of hydrocarbons *in vivo* is further complicated by the fact that differences in age, breed and sex were shown to significantly affect clearance of pentane and ethane from the atmosphere in experimental animals (Frank *et al.*, 1980).

Pentane is very soluble in body tissues, and the body fat represents a significant reservoir for pentane storage. Pentane had an elimination half-life of 3 hours in normal rats, but in congenitally obese rats the half-life of pentane was 8 hours (Springfield and Levitt, 1994). This finding suggests that the rate of exhalation of pentane may be a function of body composition, and that the fat stores could act as a reservoir from which pentane is released over long periods of time following exposure. Furthermore, an increased rate of pentane elimination might be induced by increased blood perfusion through adipose tissue, increased respiratory rates and alterations in blood lipids (Springfield and Levitt, 1994). Ethane is poorly soluble in body fat compared to pentane and mean solubility coefficients of 2.7 and 37 in rat fat were reported for ethane and pentane, respectively (Wade and Van Rij, 1985). The poor solubility of ethane in body fat combined with its slower rate of metabolic elimination suggest that ethane may be a more suitable marker of *in vivo* lipid peroxidation than pentane.

Whilst feeding and fasting are not thought to affect excretion of ethane and pentane (Risby *et al.*, 1999), variation in dietary ingestion of ω-3 and ω-6 fatty acids may play an important role in the relative concentration of exhaled hydrocarbons (Gelmont *et al.*, 1981; Pincemail *et al.*, 1987). The fatty acid content of the diet was shown to directly affect the composition of liver cell membrane phospholipids, which in turn affected the composition of the exhaled alkanes (Kivits *et al.*, 1981). Furthermore, pentane production in α-tocopherol-deficient rats was shown to be dependent on the linoleic acid content of the diet (Gelmont *et al.*, 1981).

The possibility that exhaled ethane and pentane could arise from microbial fermentation or lipid digestion in the gastrointestinal tract must also be considered (Gelmont *et al.*,

1981; Hotz *et al.,* 1987; Jeejeebhoy, 1991). Exhaled pentane levels in rats were rapidly depleted following administration of antibiotics (Gelmont *et al.,* 1981), and *in vitro* studies have demonstrated that human colonic flora produce pentane during fermentation of corn oil (50% linoleic acid) (Hiele *et al.,* 1991).

Environmental Sources of Exhaled Hydrocarbons

Levels of hydrocarbons in ambient air were found to be relatively high and variable (141±50 and 17.2±7.3 pmol.litre^{-1}, mean±sd for pentane and ethane respectively), when compared to the small increases expected in hydrocarbon excretion in breath during lipid peroxidation (Knutson *et al.,* 1999), Table 4.1. In many studies, subjects were required to breathe hydrocarbon-free air (HCFA) prior to collection of breath samples (Aghdassi and Allard, 2000; Mohler et al., 1996; Knutson *et al.,* 1999; Seabra *et al.,* 1991; Pincemail *et al.,* 1987). This procedure will ensure that increases in pentane and ethane reflect endogenous production, rather than variations in levels of pentane and ethane in the environment. Breath pentane levels decreased rapidly following HCFA inhalation; an initial rapid fall was attributed to loss of pentane from the lungs and a slower decline reflected elimination of lipid soluble pentane from body fat (Springfield and Levitt, 1994). Total elimination of pentane stores would require very long periods of HCFA inhalation and the optimal period of HCFA inhalation prior to breath sampling is thought to be between 4-10 minutes (Hotz *et al.,*1987; Knutson and Viteri, 1996). Despite washout periods of HCFA inhalation, pentane stored in body fat may continue to cause increases in breath pentane excretion at rates greater than production of pentane during *in vivo* lipid peroxidation (Springfield and Levitt, 1994). A washout period of HCFA inhalation adds further complexity to the hydrocarbon breath test (HCBT) and would be a particular obstacle to the application of the test in the clinical setting. For this reason, and because commercially available sources of HCFA usually

contain hydrocarbons at picomolar level, some researchers have chosen not to include a HCFA washout period in the HCBT protocol (Phillips, 1997). Instead, simultaneous samples of exhaled air and ambient air are taken, so that ambient levels can be taken as a baseline upon which alterations in hydrocarbons in breath are measured. The advantage of this method is that the expense and technical difficulty of HCFA inhalation is avoided, but this method generates more samples for analysis and cannot guarantee that alterations in ambient hydrocarbon levels have not affected the test results.

Table 4.1 Previously reported values for exhaled hydrocarbons in healthy human subjects. Most studies described the use of GC-FID for assessment of breath hydrocarbons and most studies did not incorporate a HCFA washout period or demonstrate separation of pentane and ethane.

Reference	n	Method	HCFA Washout	Isoprene Separated	Pentane	Ethane
Mendis *et al.*, 1994	43	GC-FID	None	Yes	0.57 ± 0.30nmol/l	Not measured
Pincemail *et al.*, 1987	22	GC	Yes	No	5 – 140pmol/l	Not measured
Sedghi *et al.*, 1994	31	GC-FID	None	No	3.01 ± 0.4nmol/l	0.33 ± 0.06nmol/l
Sobotka *et al.*, 1993	26	GC-FID	None	No	3.6 ± 1.2nmol/l	Not measured
Massias *et al.*, 1993	10	GC-FID	None	No	3.61 ± 2.05nmol/l	4.83 ± 3.0nmol/l
Knutson, *et al.*, 1999	11	GC-FID	0-30mins	Yes	8.12 ± 1.51pmol/l	10.4 ± 3.97nmol/l
Seabra *et al.*, 1991	5	GC-FID	10mins	No	69.6 ± 54.3pmol/l	139 ± 154 pmol/l
Chao *et al.*, 1999	15	GC-FID	None	Yes	70 ± 80pmol/l	Not measured
Mohler III *et al.*, 1996	27	GC-PID	1 min	Yes	1.5 ± 1.2ppb	Not measured
Pelli *et al.*, 1999	10	GC-FID	None	Yes	0.19 ± 0.09 nmol/l	0.23 ± 0.05nmol/l

Further investigation of the source of endogenous hydrocarbons and the relative contribution of metabolic elimination and production of hydrocarbons (Figure 4.2) in diseased states is necessary before the HCBT can be advocated as an investigative clinical tool. The simplicity of the HCBT belies the complex and poorly understood kinetics of hydrocarbon production *in vivo*. However, despite these problems, the HCBT remains one of the most useful non-invasive methods for assessment of oxidative stress. The HCBT has not yet been applied in veterinary medicine and could

be a useful method for monitoring oxidative stress, particularly given the current interest in anti-oxidant therapies for animals. The overall aim of this chapter was to validate and apply a gas chromatography assay for measurement of alkanes in the exhaled breath of animals.

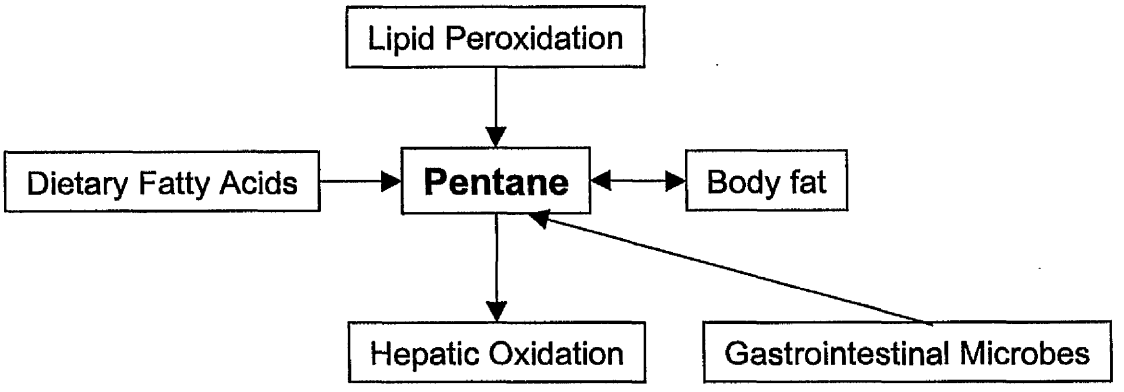

Figure 4.2 Production and elimination of pentane *in vivo*.

4.2 PRELIMINARY VALIDATION OF A GAS CHROMATOGRAPHY METHOD FOR ASSESSMENT OF EXHALED ALKANES

4.2.1 Study Aim

The aim of this study was to establish and validate a gas-chromatography assay suitable for measurement of levels of exhaled ethane and pentane.

4.2.2 Introduction

Analytical Methods used to Detect Exhaled Hydrocarbons

Exhaled hydrocarbons have been measured by gas-chromatography flame ionization detection (GC-FID), gas-chromatography mass spectrometry (GC-MS) and gas-

chromatography photoionization (GC-PID) (Table 4.1). Gas chromatography involves injection of a sample gas into a stream of carrier gas that is flowing through a narrow bore column, to a detector. The time taken for the sample to reach the detector is determined by its physical properties and by the length, nature and temperature of the column. The detector quantifies the separated gases in breath generally by flame ionization (FID), but photoionization detection (PID) has also been used to quantify gases in breath samples. During FID, the gas is ionised as it passes through a flame at the detector. This causes a current to flow between two electrodes next to the flame, and a detectable electric signal is generated. Photoionization involves ionization of the gas as it emerges from the GC column, by photons emitted from a UV lamp at the detector. The ionized molecules generate an electrical signal that is proportional to their concentration, and this is a more sensitive and rapid method of detection than FID (Mohler and Hathaway, 1999). PID can also potentially be a portable method for GC-analysis and the greater sensitivity of this method has facilitated analysis of exhaled hydrocarbons without necessitating a pre-concentration phase (Mohler *et al.,* 1996).

Concentration of Breath Samples

Because alkanes are present in breath at very low concentrations, detection by GC-FID requires concentration of the sample to levels of about 1ppm. In most cases concentration was achieved by adsorbing the sample onto a solid adsorbent column (Massias *et al.,* 1993), or freezing of the sample at low temperatures, cryogenic trapping (Kohlmuller and Kochen, 1993); the sample is desorbed from the trap by heating to temperatures of up to 300°C. Both adsorption and cryogenic concentration methods require that water is removed from the sample prior to concentration, and both methods involve an inevitable degree of loss of volatile organic compounds during the concentration process.

Interference from other Compounds in Breath

Isoprene (2 methyl-1,3-butadiene) is the significant light hydrocarbon excreted in human breath (Jones *et al.,* 1995), and this gas is present at higher concentrations than ethane or pentane although it is not associated with lipid peroxidation (Kohlmuller and Kochen, 1993). It is therefore of vital importance that the analytical technique used to detect hydrocarbons in exhaled breath is capable of separating pentane from isoprene, since these compounds have similar molecular weights and boiling points. An investigation in 1994 demonstrated that most GC columns do not separate isoprene and pentane (Springfield and Levitt, 1994). Most of the reported studies of the pentane breath test have failed to separate isoprene and pentane, despite the fact that isoprene is known to be the hydrocarbon present at the greatest concentration in exhaled breath. For this reason, much of the early work describing the assessment of lipid peroxidation using the pentane breath test requires re-examination.

Several other compounds have been identified that may interfere with GC-detection of pentane and ethane. Methane is present in exhaled breath at relatively high concentration in some individuals and is derived from microbial fermentation in the hind gut (McKay *et al.,* 1985). Good separation of the methane and ethane peak is necessary to ensure that the "tail" of the methane peak does not obliterate the ethane peak (Knutson *et al.,* 2000). Isopentane (2-methylbutane) has a similar molecular weight to pentane and is a common component of urban air. A recent study identified isopentane as another compound that may co-elute with pentane on some GC-columns (Mitsui *et al.,* 2000). Previous studies of the HCBT that did not confirm the identity of the pentane peak in breath using mass-spectrometry, may have unwittingly reported isopentane concentrations as well as, or in place of, pentane.

The HCBT is subject to a wide range of technical difficulties, and these along with the biochemical problems described in Section 4.1, account for a wide variation (up to 1000-fold) in the concentrations of exhaled hydrocarbons reported in the literature. The reliability of many clinical studies of *in vivo* lipid peroxidation using this method, particularly where no other measure of lipid peroxidation was used, is questionable. Most studies have failed to separate isoprene from pentane, failed to acknowledge that *in vivo* metabolism of pentane could affect results, failed to measure ambient pentane levels or provide a washout period of HCFA inhalation, and few authors have even commented on the wide disparity of their results with other studies. The relatively high concentration and variability of hydrocarbon levels in ambient air, combined with the very low concentrations in exhaled air and the technical difficulties of collecting, concentrating and measuring breath pentane and ethane have limited the application of the HCBT. However these difficulties must be rigorously addressed if the HCBT is to be a valid measure of *in vivo* cell membrane lipid peroxidation. The HCBT has considerable potential application for real-time monitoring of lipid peroxidation, as a diagnostic tool, a clinical indicator of homeostasis, and a method for health screening and monitoring of disease status away from the analytical centre. However meticulous attention to the precision and accuracy of methods for analysis of breath alkanes is necessary.

4.2.3 Materials and Methods

Reagents

Isoprene and isopentane were obtained from Sigma-Aldrich and used as supplied. Carbon dioxide (3% in N_2) was supplied by BOC gases. Ethylene was obtained by collecting headspace from the reaction (unimolecular dehydration) between

concentrated H_2SO_4 and ethanol (2µl) heated at 200°C for 1 hour (Vollhardt, 1987) according to the following equation:

$$H_2SO_4 + C_2H_5OH \rightarrow C_2H_4 + H_2O \qquad \text{(Eq. 4.1)}$$

A gas mixture containing 100ppm methane, ethane, butane, propane, pentane and hexane in nitrogen was obtained from Supelco (Scott Speciality Gases).

Gas Chromatography

The temperature conditions and the apparatus used for GC are described in full in Chapter Two.

Study Design

Samples (100µl) of a mixture of isoprene and pentane (195ppt) were analysed in order to assess the ability of the column to separate these compounds. Confirmation of the identity of the isoprene and pentane peaks was obtained using mass spectrometry. A mixture of ethylene, acetone, ethane, methane, propane, butane, hexane, isoprene, isopentane and pentane was analysed to confirm that there was good separation of the important volatile compounds that are present in exhaled air. In order to ensure that the CO_2 present in breath did not interfere with detection of the alkane peaks, 100µl 3% CO_2 gas was injected onto the GC column with 100µl 100ppm ethane.

Samples of ethane and pentane at known concentrations were prepared by injecting 500mls N_2 into a gas impermeable bag (Tedlar Gas Sampling Bags, SKC) and adding quantities of a standard 100ppm alkane standard mixture by injection through a teflon septum attached to the bag. Five concentrations were prepared, 50, 20, 5, 2 and 0.5ppb. Each concentration was measured in three separate assays. One litre of a 10ppb mixture

of pentane and ethane was prepared and measured five times to assess the repeatability of the assay.

Assay Validation

The assay was validated by evaluating the following parameters, as defined by the ICH guidelines for validation of analytical procedures[3].

Specificity is the ability to assess unequivocally the analyte in the presence of mixture components which may be expected to be present (e.g. CO_2, water, N_2). Specificity was evaluated by investigating separation of a mixture of volatile compounds present in breath by the GC method.

Linearity is the ability of an analytical procedure to obtain test results that are directly proportional to the concentration of analyte in the sample. The linearity of this method was investigating by analysing mixtures of ethane and pentane at 5 concentrations on 3 separate occasions. Linear regression analysis was used to investigate the significance of the relationship between detector response and analyte concentration. The assay detection limit is the lowest amount of analyte in a sample that can be detected. This value was established from the minimum level of detection in the linearity study.

---

[3] ICH Harmonised Tripartite Guideline "Validation of Analytical Procedures" recommended for adoption to the regulatory bodies of the European Union in 1994 by the ICH Steering Committee (International Conference on Harmonisation of Technical Requirements for Registration of Pharmaceuticals for Human Use)

Precision is defined as the closeness of agreement between a series of measurements obtained from multiple sampling of the same homogenous sample under the prescribed conditions. Precision is composed of repeatability (intra-assay variation), intermediate precision (inter-assay variation) and reproducibility (inter-laboratory variation). Inter-assay variation was expressed as the standard deviation and coefficient of variation obtained when 5 samples of known concentration were measured on three separate days. Intra-assay variation was expressed as the standard deviation and coefficient of variation obtained when a sample at similar concentration to exhaled air was measured five times. Repeatability or inter-assay variation was defined as precision under same conditions over short time period. Intermediate precision, or inter-assay variation was defined as assay precision under same conditions on different days.

4.2.4 Results

Specificity

Initial studies demonstrated that the GC column (PoraPlotQ, Chrompack, UK), did not separate pentane from isoprene. Pentane and isoprene showed similar retention times of 10.76, and 10.75 minutes, respectively. When a pentane and isoprene gas mixture was injected onto the column a single peak was eluted with a retention time of 10.63, and a peak area (325,870) that was roughly equivalent to the combined areas of the previous peaks for isoprene (146,750) and pentane (114,356). These measurements were repeated using a second GC column (SilicaPlot, Chrompack), and good separation of pentane and isoprene was then demonstrated (Figure 4.3), and this column was used in all further studies. Good separation was shown between the gases of interest pentane and ethane, and other gases that might be present in breath, namely isoprene, ethylene, hexane, butane, propane, isopentane and methane (Figure 4.3).

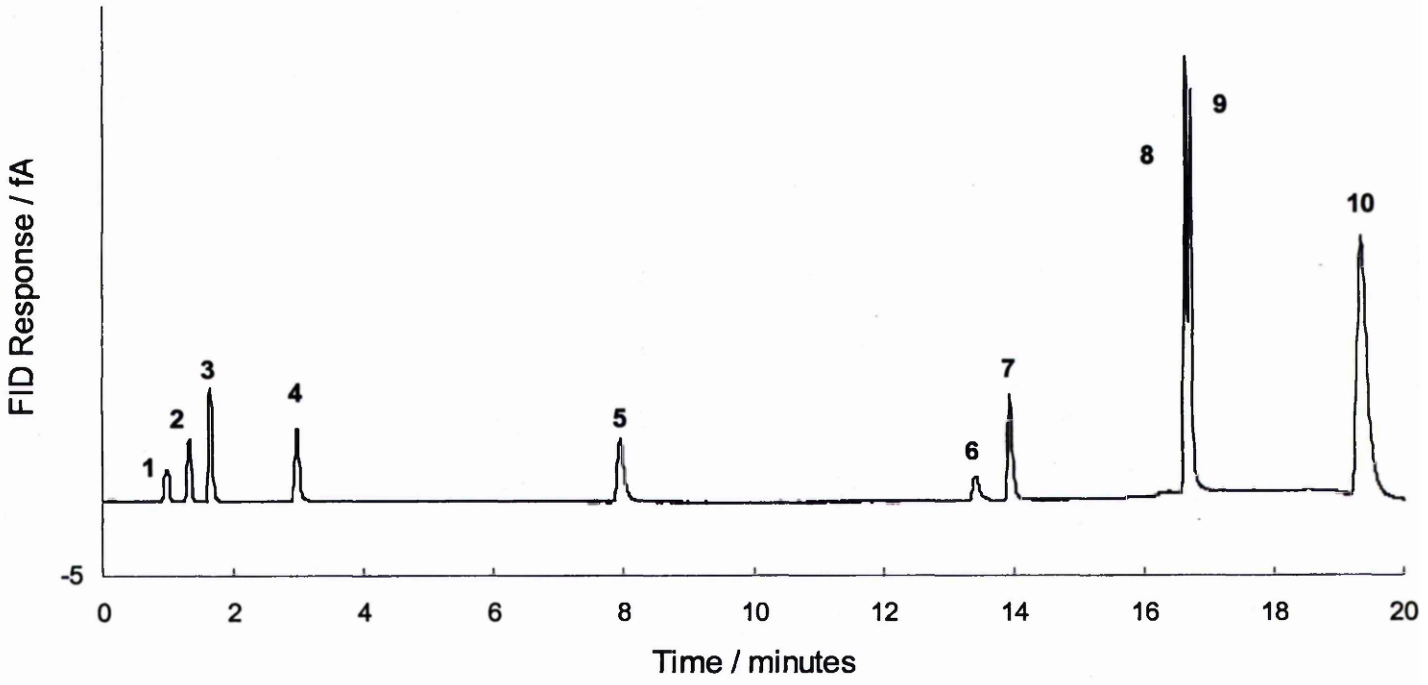

Figure 4.3 Gas chromatograph of standard gas mixture (all analytes at 100ppm) illustrating good separation between the compounds of interest in breath

1. methane	6. isopentane
2. ethane	7. pentane
3. ethylene	8. isoprene
4. propane	9. hexane
5. butane	10. heptane

It has been reported that CO_2 can interfere with detection of the ethane peak in breath (Knutson and Viteri, 1996). When ethane was injected onto the Silica-Plot column along with 3% CO_2, the resultant peak was narrowed (Figure 4.4), suggesting that CO_2 might indeed affect the ability to detect ethane. For this reason, a soda-lime trap was added to the concentration system, in order to remove CO_2 from exhaled breath samples.

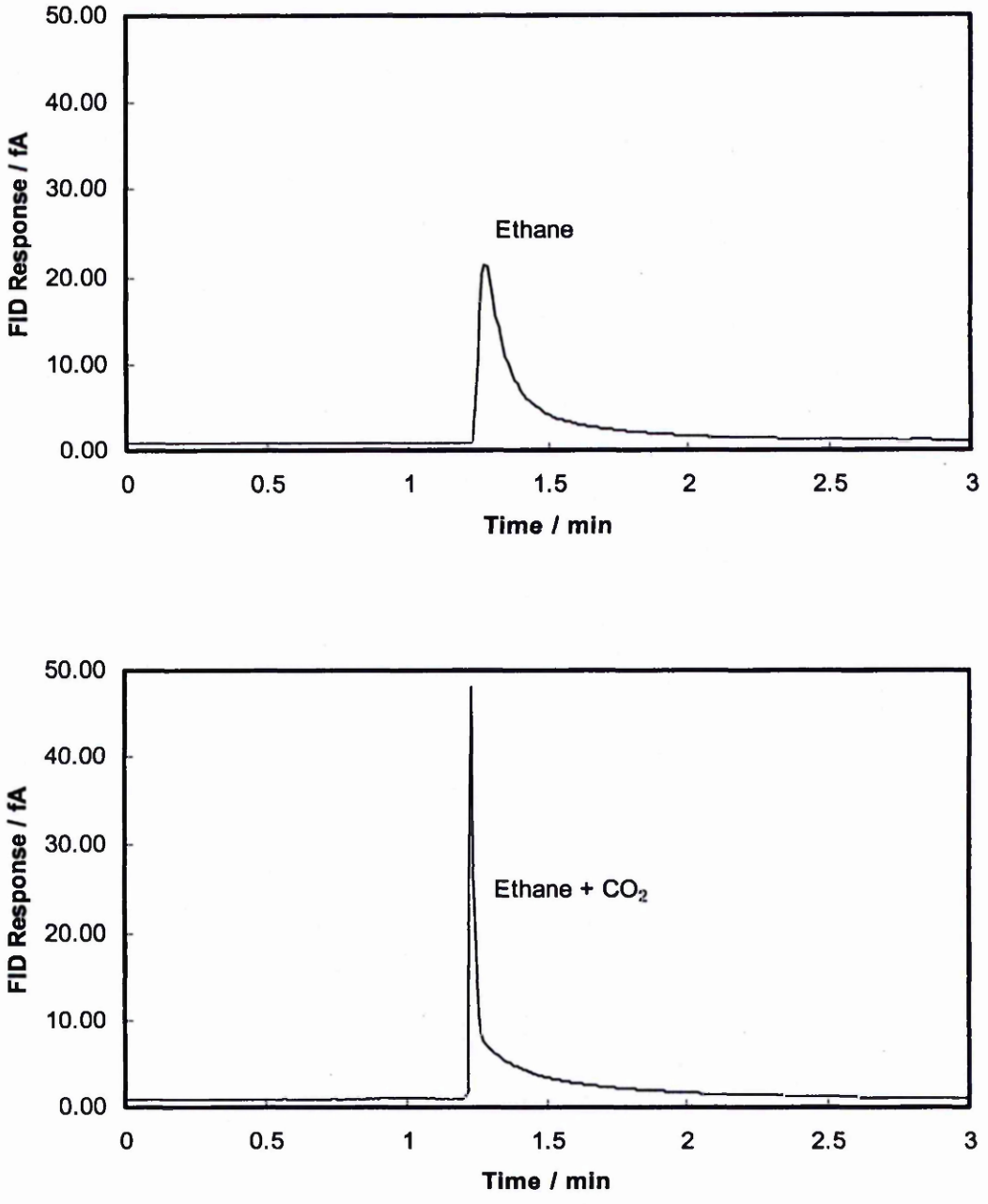

Figure 4.4 Effect of CO_2 on detection of ethane; the ethane peak was broader in the absence of CO_2

Precision and Limit of Detection

Analytical precision in measuring pentane and ethane are shown in Table 4.2. The limit of detection for pentane and ethane was 0.5ppb and 5ppb, respectively (Figure 4.5).

Table 4.2 Assay Precision

Analyte	Mean Intra Assay Variation (CV.%$^{-1}$, n=5)	Mean Inter Assay Variation (CV.%$^{-1}$, n=3)
Ethane	5.1%	11.4%
Pentane	1.2%	10.4%

Linearity and Detection Range

The calibration curves for pentane and ethane are shown in Figure 4.6; the detection range was 0.5 – 50ppb for pentane and 5 – 50ppb for ethane. Ethane could not reliably be detected at low concentrations during this assay due to the close proximity of the ethane peak to the artefact produced by the opening of the gas-sampling valve (Figure 4.5).

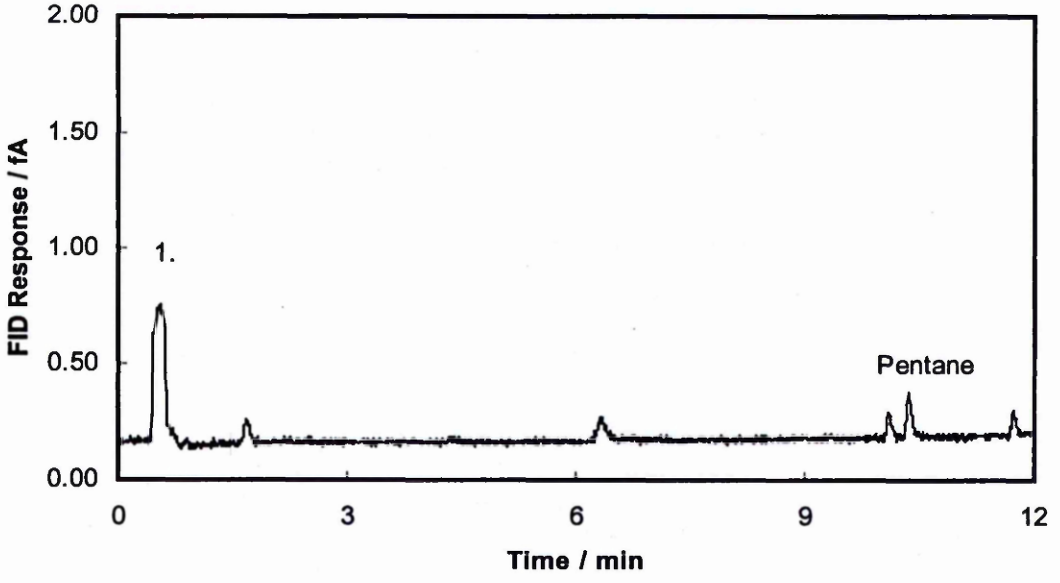

Figure 4.5 Gas chromatogram illustrating limit of detection of pentane. Peak 1 shows an artefact caused by opening of the gas sampling valve, which obscures the ethane peak.

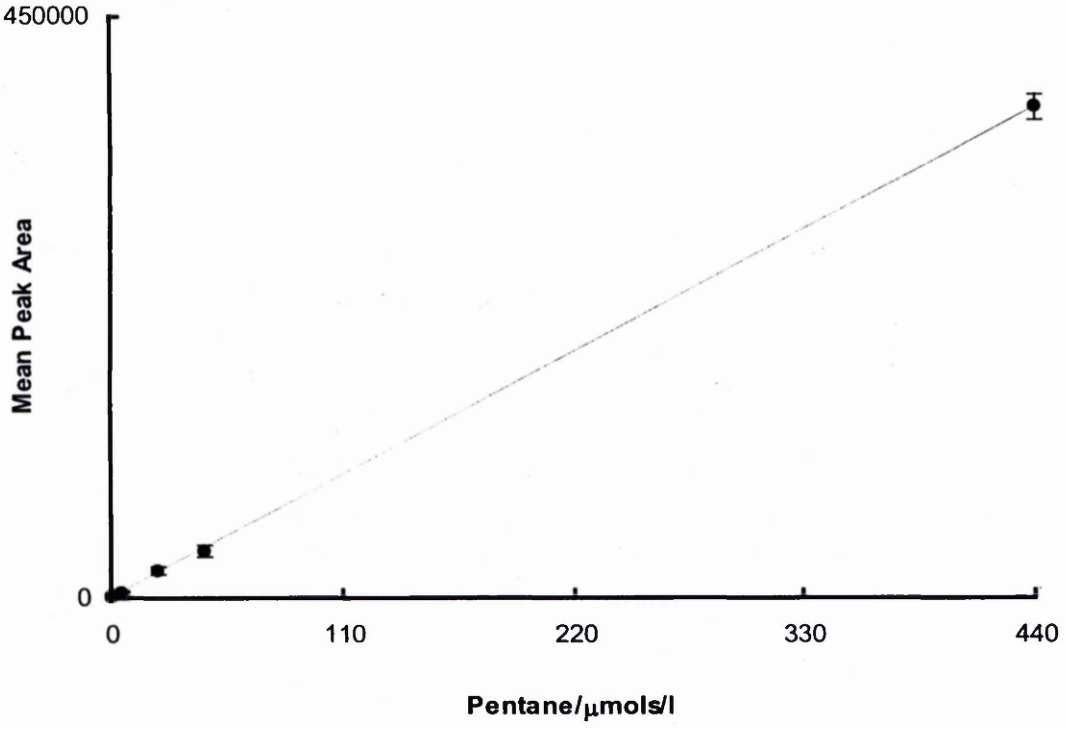

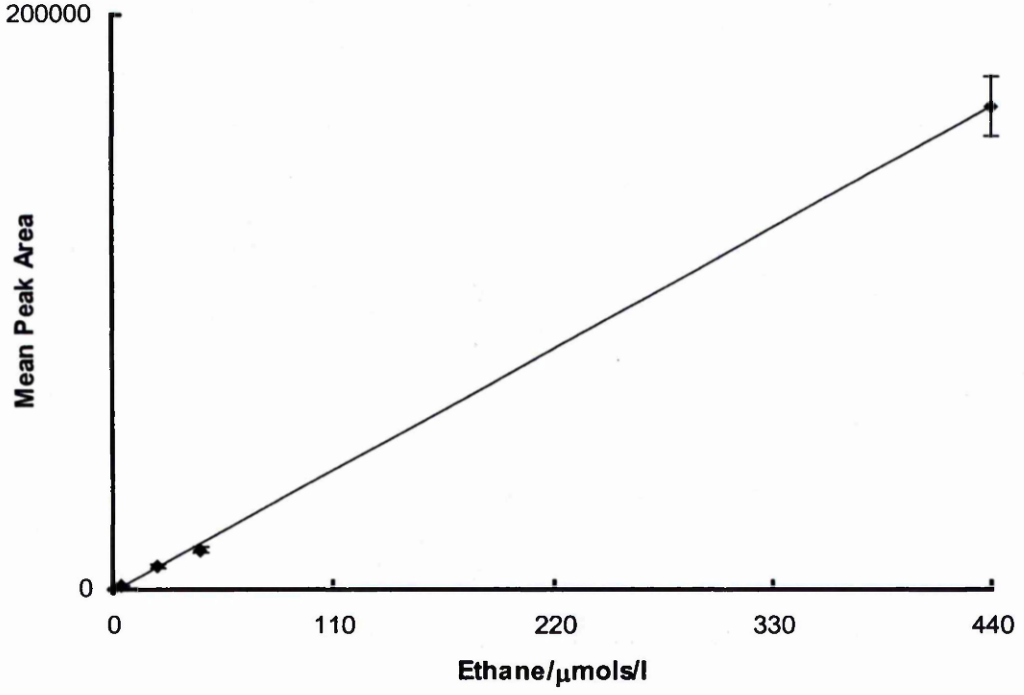

Figure 4.6 Calibration curve derived from measurement of 5 concentrations of ethane (below) and pentane (above) as part of three separate assays. Data are mean ± sd, and the line shows the fitted linear regression model; $r^2 = 0.996$ and 0.999 for ethane and pentane respectively.

4.2.5 Discussion

The HCBT is a potentially useful method for assessment of *in vivo* lipid peroxidation which occurs as a consequence of oxidative stress. While not a pathological process in itself oxidative stress is an indicator of health status and the HCBT could be used to assess the effects of pharmacological therapy or lifestyle changes on the pro-oxidant effects of disease.

The present study describes the preliminary validation of a GC method for measurement of exhaled hydrocarbons in animals. Analysis of exhaled hydrocarbons is subject to a range of physiological and technical difficulties as discussed in the previous sections, and the test requires meticulous validation. It has been reported that many GC columns fail to separate two important compounds in breath, pentane and isoprene (Springfield and Levitt, 1994). In this study it was demonstrated using GC-MS that pentane and isoprene co-elute on a Poraplot-Q column, but were separated on a SilicaPlot column. Good separation was also shown between other compounds present in breath such as ethylene, isopentane and methane, suggesting that this method would be adequately specific to permit detection of pentane and ethane in breath. The methane and ethane peaks were well separated at low elution temperatures of 40°C, while pentane eluted at temperatures around 150°C. A relatively wide temperature range (40°C – 180°C) was required to optimise the assay for concurrent measurement of pentane and ethane. The boiling point of pentane (36°C) required that assay components such as sample bottles, syringes and the gas sampling loops are heated to prevent condensation of pentane on vessel walls. In concurrence with previous studies (Phillips, 1997) it was found that CO_2 affected detection of ethane (Figure 4.5), and a soda-lime trap was added to the breath concentrating system to remove CO_2 from breath samples.

The very low levels of pentane and ethane in breath (10^{-9} mol.l^{-1}) require that samples are concentrated to the detection range of the assay, which in this case was in the region of 10^{-6} mol.l^{-1}. The cryogenic concentration system described in these studies was capable of removing pentane and ethane from a calibration hydrocarbon mixture at (5 – 50ppb), when an adsorbent material (Tenax) was packed into the gas-sampling loop and the loop frozen at –117°C. Cryogenic concentration at lower temperatures (-174°C) was found to be of limited use for removing hydrocarbons from breath, due to concurrent trapping of large amounts of nitrogen and oxygen at these temperatures. Previous studies have reported that condensed O_2 and N_2 could be vented into a gas-tight syringe following removal of the gas loop from the liquid nitrogen bath (Knutson *et al.*, 2000). This method was not adopted in the present study as it could result in loss of ethane. The use of an adsorbent trap cooled to temperatures of approximately -117°C facilitated concentration of hydrocarbons, while also permitting venting of oxygen and nitrogen. Previous studies have demonstrated that concentration of breath samples using an absorbent (Tenax) trap at a similar temperature allowed recovery of almost 100% pentane and ethane in exhaled breath samples (Risby *et al.*, 1999). The method described in the present studies allowed simple measurement of pentane at concentrations present in exhaled breath (ppb). However, ethane could not be reliably detected at low concentrations due to interference of an artefact caused by opening of the gas sampling valve, with the ethane peak. This artefact affected integration of the ethane peak and explains the higher inter and intra – assay coefficients of variation for ethane compared with pentane. This problem could be addressed by further reducing the initial temperature of the GC program (40°C). However, since this would cause unreasonable lengthening of the assay time (>60minutes), all further studies describe the measurement of pentane only.

It is generally agreed that ethane is a better marker of oxidative stress than pentane. Ethane is poorly soluble in body tissue (Springfield and Levitt, 1994) is metabolised at a slower rate than pentane (Allerheiligin *et al.,* 1987) and has not been shown to be produced during intestinal microbial fermentation. However, pentane is often measured in the HCBT since it is derived from ω-6 fatty acids, the most abundant fatty acids in cellular phospholipids. Ethane is probably a better physiological marker of oxidative stress but the volatile nature of this compound necessitates absorption at very low temperatures that limit this assay to the laboratory. In contrast, pentane can be absorbed at ambient temperatures, and this assay could more easily be applied outside of the laboratory.

This study has demonstrated that pentane and ethane could be detected using a GC assay with good assay specificity and linearity. Samples of pentane standard were detected with good assay precision but the measurement of ethane requires further optimisation. Further studies are now necessary to investigate the feasibility of using this method for analysis of breath hydrocarbons.

4.3 APPLICATION OF THE HYDROCARBON BREATH TEST FOR ASSESSMENT OF OXIDATIVE STRESS

4.3.1 Study Aim

The specific objectives of this study were to apply the GC assay developed in Section 4.2 for measurement of pentane in breath samples taken from animals and to assess inter and intra-subject variation in pentane exhalation in a small group of horses.

4.3.2 Introduction

Application and Validation of the HCBT for Assessment of in vivo Lipid Peroxidation

The principle advantage of the breath hydrocarbon test over the other methods for assessment of lipid peroxidation is that it is non-invasive, and in theory this method allows real time analysis of the rate of *in vivo* lipid peroxide decomposition. As with all markers for assessment of lipid peroxidation, breath alkanes cannot themselves reflect total body lipid peroxidation since the oxidation of the broad spectrum of fatty acids present in biological tissues yield different profiles of oxidation products (Halliwell and Gutteridge, 1999). For this reason the breath hydrocarbon test should ideally be applied in conjunction with other tests of lipid peroxidation, so that an overall index of the rate of lipid peroxidation is obtained.

Exhaled pentane and ethane can be derived from sources other than lipid peroxidation (Section 4.1) and the HCBT requires validation before increases in exhaled hydrocarbons can be attributed exclusively to increased lipid peroxidation. However validation of the hydrocarbon breath test is difficult, since there is no standard method for detection of lipid peroxidation in the living animal. The HCBT does not always correlate with other tests of lipid peroxidation such as measurement of 4-HNE, MDA or lipid peroxides (Chao *et al.,* 1999), but this is not surprising since these tests assess other stages in the process of lipid peroxidation. The hydrocarbon breath test has been indirectly established as an index of *in vivo* lipid peroxidation by the demonstration of increased breath pentane and ethane during experimentally induced lipid peroxidation, and the attenuation of these increases by anti-oxidants such as α-tocopherol. Rats deficient in vitamin-E excreted increased levels of breath pentane that were decreased following administration of vitamin-C or α-tocopherol (Gelmont *et al.,* 1981). Carbon tetrachloride (CCl_4) is a potent inducer of liver lipid peroxidation and was shown to

cause increased ethane excretion following intravenous administration in mice, and this increase was potentiated by administration of the pro-oxidant phenobarbital and surpressed by α-tocopherol (Riely *et al.,* 1974). Pretreatment of mice with anti-and pro-oxidative agents before administration of CCl_4 directly affected the subsequent rate of ethane evolution, suggesting that ethane excretion in breath was directly related to susceptibility to liver lipid peroxidation (Riely *et al.,* 1974). Similarly, induction of lipid peroxidation in rats by hypoxia was associated with increased ethane evolution, while dietary restriction, which is thought to decrease lipid peroxidation also decreased ethane exhalation in breath (Risby *et al.,* 1999).

Studies in man have shown that exercise and smoking induce lipid peroxidation, and increase hydrocarbon excretion in breath (Mohler *et al.,* 1996; Chao *et al.,* 1999). Supplementation with antioxidant vitamins surpressed the high pentane levels associated with smoking (Jeejeebhoy, 1991), and with heavy exercise (Chao *et al.,* 1999; Pincemail *et al.,* 1987). A randomized study of the effect of diet on *in vivo* lipid peroxidation demonstrated increased serum anti-oxidant capacity and reduced ethane exhalation during consumption of a fruit and vegetable diet, supporting the hypothesis that fruit and vegetable diets protect against lipid peroxidation (Miller *et al.,* 1998). The demonstration that induction of lipid peroxidation by exercise, pharmacological agents, and smoking was associated with increased breath alkane excretion, and that this increases was a function of oxidative status, and could be attenuated by anti-oxidants, is strong evidence that the hydrocarbon breath test is a useful indicator of *in vivo* lipid peroxidation.

Clinical Application of the HCBT

Exhaled pentane and ethane have been significantly associated with lipid peroxidation in numerous clinical studies (Table 4.3). Breath pentane was significantly increased in

human patients with liver disease (Hotz *et al.*, 1987), neonatal disease (Nycyk *et al.*, 1998) heart failure (Sobotka *et al.*, 1993) human immunodeficiency virus infection (Allard *et al.*, 1998) and schizophrenia (Phillips *et al.*, 1995). Lipid peroxidation is significantly associated with many chronic inflammatory diseases, and activation of phagocytes *in vitro* produced significant increases in head space pentane (Pitkanen *et al.*, 1989). In concurrence with this finding, there was a modest but statistically significant correlation between breath ethane levels and lipid peroxidation measured using chemiluminescence in patients with ulcerative colitis. However this association was not strong enough to permit diagnostic conclusions in individual patients (Sedghi *et al.*, 1994). Colitis induced experimentally in rats was associated with significant increases in breath pentane, but these increases were not apparent throughout the course of the disease (Ondrula *et al.*, 1993). In a similar study, breath ethane levels were significantly increased in colitic rats, but again this increase was not correlated with disease activity (Porter *et al.*, 1998). There was no overall correlation between breath pentane levels and intestinal inflammation in man, although this relationship was significant when selected groups of patients were compared (Kokoszka *et al.*, 1993). A recent Canadian study examined breath alkane output, plasma markers of lipid peroxidation and plasma antioxidant micro-nutrients in several clinical conditions associated with increased lipid peroxidation, including smoking, HIV infection, and inflammatory bowel disease. These conditions were associated with increased plasma lipid peroxidation markers and breath alkanes, and decreased plasma antioxidants (Allard *et al.*, 1998). Breath pentane levels were significantly associated with disease activity in rheumatoid arthritis (Humad *et al.*, 1988), but not in ulcerative colitis or Crohn's disease, although pentane and ethane excretion was significantly different between patients and controls (Pelli *et al.*, 1999).

Table 4.3 Previously reported values for HCBT in diseased subjects. Values are mean ± sd, unless otherwise indicated; *p* is the probability of no significant difference between hydrocarbon exhalation in healthy and diseased subjects.

Reference	**n**	**Disease**	**Pentane**			**Ethane**		
			Diseased	*Control*	*p*	*Diseased*	*Control*	*p*
Sobotka *et al.*, 1993	13	Heart failure	5.7 ± 2.1nmol/l	3.6 ± 1.2nmol/l	0.003	NM	NM	
Sedghi *et al.*, 1994	17	UC	3.4 ± 0.5nmol/l	3.01 ± 0.4nmol/l	NS	0.45 ± 0.04nmol/l	0.33 ± 0.06nmol/l	0.013
Allard *et al.*, 1998	49	HIV infection	9.05 ± 1.21 pmol/kg/min	6.06 ± 0.56 pmol/kg/min	< 0.05	28.1 ± 3.41 pmol/kg/min	11.42 ± 0.55 pmol/kg/min	< 0.05
Olopade *et al.*, 1997	12	Asthma	8.4 ± 2.9nmol/l	2.6 ± 0.2nmol/l	< 0.05	NM	NM	
Pelli *et al.*, 1999	10	UC	0.65 ± 0.51nmol/l	0.19 ± 0.09nmol/l	0.05	0.49 ± 0.29nmol/l	0.23 ± 0.05nmol/l	0.05
	10	CD	0.43 ± 0.29nmol/l		0.001	0.59 ± 0.28nmol/l		0.001
Toshniwal *et al.*,1992	16	MS	10.5 ± 4.2nmol/l	4.9 ± 1.1nmol/l	0.01	NM	NM	NM
Paredi *et al.*, 2000a	40	Asthma	NM	NM	NM	2.06 ± 0.3ppb (se)	0.88 ± 0.09ppb (se)	< 0.05
Paredi *et al.*, 2000b	23	CF	NM	NM	NM	1.99 ± 0.2ppb (se)	0.88 ± 0.09ppb (se)	< 0.05
Paredi *et al.*, 2000c	26	COPD	NM	NM	NM	2.77 ± 0.2ppb (se)	0.88 ± 0.09ppb (se)	< 0.01
Humad *et al.*, 1988	27	RA	79.5 ± 86.4 ppb	NM	NM	NM	NM	NM
Wendland *et al.*, 2001	74	CD	7.47 ± 0.98 pmol/kg/min(se)	4.97 ± 0.48 pmol/kg/min (se)	< 0.02	11.24 ± 1.17 pmol/kg/min(se)	5.46 ± 0.71 pmol/kg/min (se)	< 0.04
Hietanen *et al.*, 1994	40	Breast cancer	2.6 ± 2.8 ppb	0.6 ± 1.1ppb	< 0.01	5.7 ± 6.5 ppb	4.0 ± 7.0ppb	>0.05
Phillips *et al.*, 1995	88	Schizophrenia	11.3 ± 3.9pmol/l(se)	0	< 0.005	NM	NM	NM
Andreoni *et al.*, 1999	8	Cardiopulmonary bypass	NM	NM	NM	4.8 ± 1.7 $nmol/m^2/min$	3.0 ± 0.7 $nmol/m^2/min$	<0.002

CD	Crohn's disease	NM	Not measured
CF	Cystic fibrosis	NS	Not significant
COPD	Chronic obstructive pulmonary disease	MS	Multiple sclerosis
HIV	Human immunodeficiedcy virus	RA	Rheumatoid arthritis
UC	Ulcerative colitis	se	Standard error of the mean

Increases in exhaled pentane and ethane have been significantly associated with lipid peroxidation in numerous clinical studies (Table 4.3). In many of these studies it appeared that although alkane excretion was significantly greater in diseased subjects, these increases were not directly related to disease activity (Ondrula *et al.,* 1993; Porter *et al.,* 1998), suggesting that other factors, such as the oxidative status of the individual are important. Supplementation of patients with antioxidant vitamins often significantly reduced lipid peroxidation parameters, although there is little evidence that this was associated with an improved clinical outcome (Aghdassi and Allard, 2000). The HCBT would be a useful method for monitoring health by evaluation of oxidative stress status, and for investigation of alterations in lipid peroxidation caused by disease, and the efficacy of anti-oxidant agents in attenuating this process. The role of oxidative stress as an effect or a cause of disease is poorly understood, and the HCBT would be a valuable tool in the further investigation of the significance of oxidative stress in health and disease.

4.3.3 Methods

Animals

Three horses and two ponies were available for use in this study (Horse Nos 1-5). Full details of these animals are given in Appendix 4. They were maintained in loose-boxes and were bedded on either paper (Horse Nos. 1, 3 & 4) or straw bedding (Horse Nos. 2 & 5) and were fed dry hay (Horse Nos. 2, 3 & 5) or soaked hay (Horse Nos 1 & 4) . Review of veterinary clinical records indicated that Horse Nos. 1 and 4 had a history of recurrent airway obstruction (RAO) and Horse No. 5 had allergic dermatitis. Horse No. 2 had chronic lameness.

Breath Collection

Breath samples were collected using the apparatus described in Chapter Two. The horse was allowed to breathe through the breath collection mask for a few moments and then 1 litre breath samples were collected in Tedlar gas-sampling bags (SKC).

Gas Chromatography

The breath samples were analysed using the apparatus and procedure described in Chapter Two. All breath samples were analysed within 6 hours of collection.

Study Design

Breath samples were collected from each animal on two separate occasions (Day 1 and 2). Respiratory rate was recorded during the breath sampling procedure that typically lasted for 3 minutes. Samples of ambient air were collected in a gas-tight syringe and stored in Tedlar bags, at the same time that breath samples were collected from the horses. All animals remained at rest in their loose-boxes for 12 hours prior to breath collection. To assess the reproducibility of the pentane measurement within animals, a second breath sample was collected 15 minutes following collection of the first breath sample on Day 1, from Horse Nos. 1, 3 and 4.

Data Analysis

Pentane exhalation was expressed as ppb or nmol/litre pentane. ppb converted to pmol.litre^{-1} using the formula:

$$\text{pmol/litre} = \frac{\text{ppb}\,(10^{-9}/\text{l})}{[22.4\,(\text{l/mol})] \times [10^{-12}\,(\text{pmol/mol})]}$$ Arterbery *et al.*, 1994, (Eq. 4.2)

The coefficient of variation (CV) was calculated to assess the reproducibility of the breath pentane measurement:

$$\text{Coefficient of Variation (CV)} = \frac{\text{standard deviation}}{\text{mean}} \times 100 \qquad \text{(Eq. 4.3)}$$

A correlation coefficient was calculated to assess the reproducibility of the measurements in individual animals on different days.

4.3.4 Results

Pentane was detected in the breath of all animals, but ethane could not be detected in any of the horses, due to interference from the artefact produced by opening of the gas sampling valve. No pentane was detected in ambient air. Figure 4.7 shows a typical chromatogram of a horse breath sample. Addition of pentane standard to a breath sample produced an increase in area of the peak putatively identified as pentane.

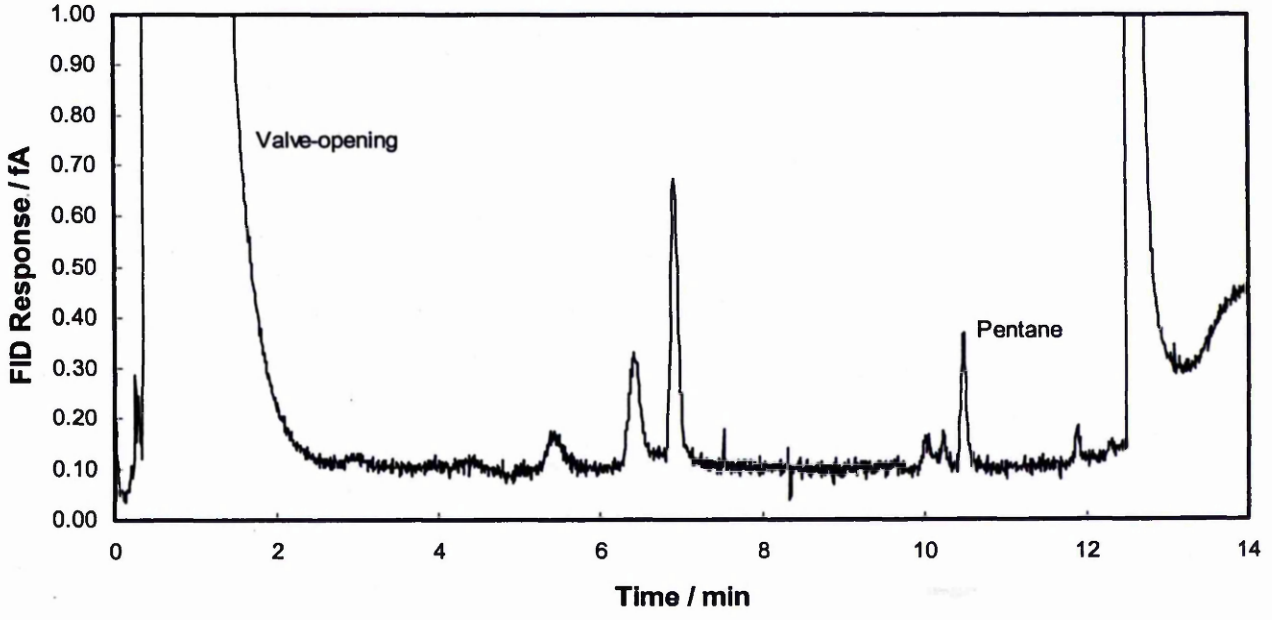

Figure 4.7 A typical chromatogram of a sample of horse breath sample (Horse No. 5, Day 2)

The breath sampling procedure, while not stressful for the horses, did produce changes in their ventilation rates and low respiratory rates were recorded in Horses 1, 2 & 3.

Table 4.4 Respiratory rates recorded during collection of breath samples from the horses in this study.

Horse No.	Respiratory Rate/Inspiration/min Day 1	Respiratory Rate/Inspiration/min Day 2
1	6	12
2	8	4
3	8	12
4	12	16
5	10	14

The values for pentane exhalation for the horses in this study are shown in Table 4.5 and 4.6, expressed in ppb and pmol.litre^{-1}. These tables illustrate the day-to-day variability in pentane exhalation in the horses in this study. Variation within a single day was assessed by measuring breath pentane in three horses twice on one day. The mean intra-subject coefficient of variation under these circumstances was 17%. The correlation coefficient for breath pentane measured in 5 horses on 2 occasions was 0.927 ($p < 0.01$).

Table 4.5 Pentane exhalation (ppb) in the five horses in this study

Horse No.	Day 1	Day 2	Mean	sd	CV.%$^{-1}$
1	3.33	1.99	2.66	0.95	36
2	1.21 (0.81)*	1.09	1.15	0.09	8
3	0.11 (0.14)*	0.50	0.30	0.28	91
4	0.48 (0.50)*	0.90	0.69	0.29	42
5	1.13	1.49	1.31	0.26	20

*Second breath sample taken after 15 minutes shown in brackets

Table 4.6 Pentane exhalation (pmol/l) in the five horses in this study

Horse No.	Day 1	Day 2	Mean	sd	CV.%$^{-1}$
1	136.47	81.38	108.93	38.95	36
2	49.58 (33.38)*	44.58	47.08	3.54	8
3	4.42 (5.94)*	20.50	12.46	11.37	91
4	19.82 (20.66)*	36.78	28.30	11.99	42
5	46.22	61.02	53.62	10.47	20

*Second breath sample taken after 15 minutes shown in brackets

4.3.5 Discussion

The GC assay developed in the previous section was an effective method for assessment of breath pentane, and this study is the first to describe the assessment of breath pentane in the horse. Breath samples for pentane analysis were easily collected from the animals, although the procedure did cause some horses to hypoventilate. This finding may be of some significance for application of the HCBT in animals, since the evolution of pentane is not homogenous over the expiratory period (Arterbery *et al.*,1994). Many human studies have attempted to standardise breath collection by sampling end expiratory air (Massias *et al.*, 1993) or by instructing subjects to breathe in time to a metronome (Arterbery *et al.*,1994). Manipulation of respiratory patterns is not easy in animals and further work is necessary to investigate the effect of breathing patterns on pentane exhalation in the horse.

Pentane was not detected in ambient air but was detected in the breath of all the horses in this study. The identity of the putative pentane peak in breath was confirmed by analysing a breath sample spiked with a standard pentane gas. Conclusive confirmation can only be obtained using GC-MS, but addition of the standard gas increased the area

of the pentane peak, suggesting that this peak is indeed pentane. Breath pentane measurements on a single day and on two separate days were relatively reproducible and intra-subject coefficients of variation for pentane exhalation were lower in the horses in this study than previously reported in man (Knutson *et al.*, 1999).
The values for exhaled pentane in the animals in this study were in the region (0.3 – 3ppb) previously reported for healthy humans. The small sample size (n=5) and the fact that just one healthy animal was available, precludes assessment of the clinical potential of the test. However, it may be of some significance that the healthy horse (Horse No. 4) had the lowest pentane levels, while one of the horses with RAO consistently showed the highest levels (Horse No. 2).

Recurrent airway obstruction in the horse is a progressive syndrome of the respiratory tract, characterised clinically by dyspnoea, nasal discharge, cough and exercise intolerance, and pathologically by inflammatory cell infiltration, loss of ciliated cells and goblet and smooth muscle cell hyperplasia (Ainsworth and Biller, 1999). RAO is generally thought to be a hypersensitivity reaction to environmental antigens, similar to human asthma. Previous studies have demonstrated increased pentane and ethane exhalation in human patients with asthma (Olopade *et al.*, 1997; Paredi *et al.*, 2000a) and the application of the HCBT for assessment of airway oxidative stress in the horse is worthy of further investigation.

There is already strong evidence to suggest that oxidative stress is involved in the pathogenesis of equine RAO (Art *et al.*, 1999). Acute episodes of RAO were associated with increased isoprostane levels in pulmonary epithelial lining fluid (Kirschvink *et al.*, 1999). Other indices of oxidative stress were also increased in the pulmonary epithelial lining fluid of horses suffering from acute RAO, compared with normal horses, and

these increases were directly related to the percentage of neutrophils in the bronchoalveolar fluid (Art *et al.,* 1999). Activation of phagocytic cells, such as neutrophils is associated with accelerated oxygen uptake, and increased production of superoxide radical, leading to oxidative stress and potentially to increased exhalation of pentane.

Assessment of lung function in the horse is difficult and generally reliant on invasive methods such as the collection of bronchoalveolar or tracheal fluid for cytological examination. The use of techniques such as nuclear scintigraphy and pulmonary function testing for investigation of equine respiratory function has been described, but expensive equipment is required and these methods are confined to specialist centres (Ainsworth and Biller, 1999). While collection of tracheobronchical fluid, scintigraphy, and pulmonary function testing are useful methods for diagnosis of disease, they are less suitable for routine monitoring of disease status. Equine RAO is a condition that is most efficiently treated by elimination of environmental allergens (Ainsworth and Biller, 1999). The ability to monitor the effect of environmental changes on airway inflammation, over short periods of time, would be a very valuable aid in the management of this condition.

The HCBT breath test and other non-invasive breath tests may have valuable applications for monitoring respiratory inflammation in equine veterinary medicine. This study demonstrated that exhaled breath samples can be easily collected from horses, without requiring particularly specialist equipment, and causing minimal disturbance to the animals. Pentane levels could be measured in the collected samples using gas chromatography, and pentane was detected in breath samples from all animals. Reproducibility of pentane measurements was good, both when animals were

sampled twice on one day and when samples taken on separate days were compared. The small sample size in this initial study precludes any conclusions about the predictive value of the test in the horse. However, high levels of pentane were measured reproducibly in one horse with RAO, and this finding indicates that the test is worthy of further investigation.

CHAPTER 5 CONSTRUCTION OF AN "ELECTRONIC NOSE" SYSTEM FOR ANALYSIS OF VOLATILE COMPOUNDS IN EXHALED BREATH

5.1 INTRODUCTION

The analysis of volatile compounds in breath is a potentially useful non-invasive method for investigation of disease and monitoring of health. Distinctive odours associated with disease processes have been recognised for many centuries, and the analysis of breath as a method of clinical investigation was made feasible in the 1970's with the advent of sensitive GC and GC-MS instruments. Many disease markers have now been identified in breath, but the validation and clinical application of these tests is currently precluded by the cost and complexity of the instruments necessary for breath analysis. Recent advances in electronic nose technology have potential application for detection of volatile organic compounds (VOC) in exhaled breath. This method of breath analysis would be cheaper and less complex than conventional methods such as GC-MS and GC, allowing the test to be performed quickly and simply, and by unskilled operators. A hand-held electronic nose that can be produced cheaply and that is simple to operate, could allow the transition of exhaled breath analysis from a complex research method, to a practical, non-invasive test for diagnoses and monitoring of health status. Such hand-held inexpensive electronic nose devices are already available for other applications, such as the CyranoScience e-nose, released in 2000 which is based on conducting polymer sensors and available for €5000.

The electronic nose is essentially an array of microsensors with a diverse and broadly tuned range of sensitivities, connected to a transducing element and a data analysis system. The integrated pattern of response of this array to an odourant can be used to identify compounds. This identification is base on prior "training" of the sensors for recognition of patterns of response that are distinct to specific odourants. The key

components of the electronic nose are the gas sensors that constitute the array. The basic principle of the gas sensor is that a test gas produces a physical or chemical change in a sensitive outer layer, and this change is converted to a quantifiable electrical signal by a transducer (Figure 5.1). The change in the sensitive-layer may be the production of ions, electrons, light or gases, or a change in mass or heat. The physical and chemical properties of the gas-sensitive layer determine the sensitivity and selectivity of the final device (Sethi, 1991).

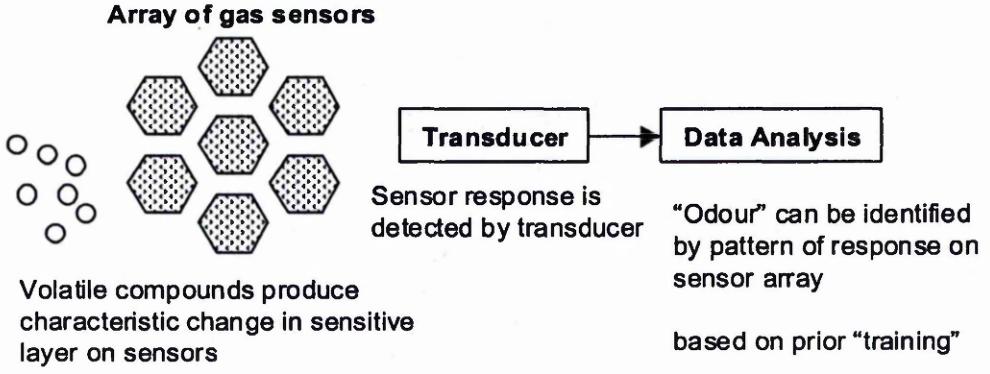

Figure 5.1 Principle of operation of the "electronic nose".

5.1.1 Electronic Nose Technology

Various technologies have been applied for fabrication of the gas sensors used in micro-sensor arrays and these can be classified according to the type of physical or chemical change that the sensor is sensitive to. The classification of sensors that are commonly used to construct microsensor arrays is shown in Figure 5.2.

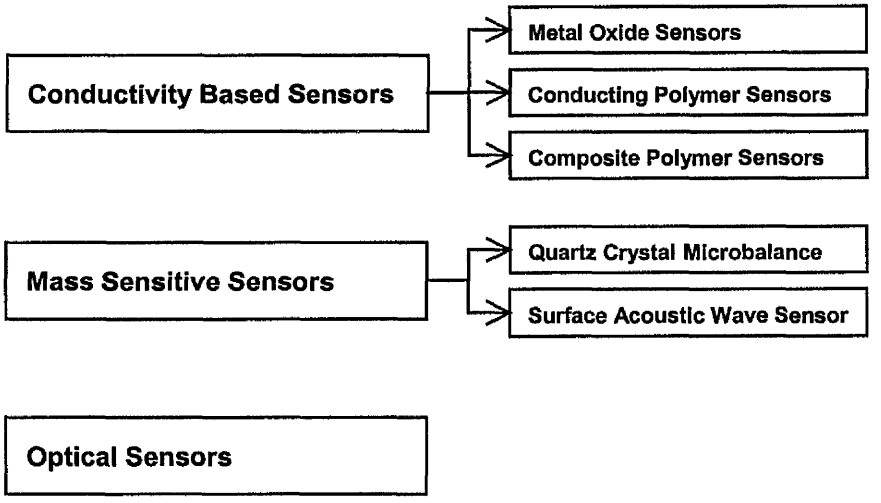

Figure 5.2: Sensors that are commonly used to construct microsensor arrays can be classified according to the physical or chemical change that the sensor is designed to detect.

Conductivity Based Sensors

Conductivity sensors are based on the detection of a change in the resistance of a metal or conducting polymer upon exposure to volatile organic compounds (Gardner, 2000). Metal oxide sensors respond to the change in resistivity in a layer of semi-conducting metal oxide deposited between two contacts. Metal oxide sensors are widely available and cheap, but are subject to drift and require operation at high temperatures.

Conducting polymer sensors are based on the principle that swelling of a conducting polymer layer following exposure to a VOC causes an alteration in the conductivity of an underlying electrode, and this alteration is proportional to the concentration of the VOC. Typically the conducting polymer sensor incorporates an interdigitated electrode with a conducting polymer electrochemically deposited between the digits. Conducting

polymers, such as poly(pyyrole) are electroconductive, in contrast to the insulating polymers used to fabricate composite polymer sensors. The advantage of the conducting polymer sensors is their high sensitivity (10 -100ppm), and unlike the metal oxide sensors, they can operate at ambient temperatures. However, electrochemical deposition of polymer is time-consuming and difficult to standardise. These sensors are also very sensitive to humidity, and often change in their relative responsiveness with the extent and frequency of analyte exposure.

Composite polymer sensors are composed of insulating polymers containing dispersed carbon particles. The ability of these polymers to conduct charge depends on the distance between the conducting carbon particles. Absorption of gas molecules into the polymer-carbon matrix causes swelling of the polymer and increases the distance between the carbon particles, thus increasing the resistance of the polymer (Lonergan *et al.,* 1996). Composite polymer sensors are cheap and easy to fabricate, and a wide range of polymers of different physical and chemical properties are available, allowing the specificity and sensitivity of the sensor to be manipulated.

Mass Sensitive Sensors

The piezoelectric sensors consist of the quartz crystal microbalance (QCM) and the surface acoustic wave (SAW) devices. These sensors are highly sensitive to mass changes on their surface. The QCM consists of a thin quartz crystal which resonates at a characteristic frequency when an oscillating electrical field is applied across the device. Changes in the resonating frequency are proportional to changes in the mass on the crystal surface (O'Sullivan and Guilbault, 1999). This property of the QCM allows it to function as a gas sensor. A thin polymer layer is applied at the surface of the crystal, and absorbance of gas molecules into this layer produces changes in the

resonant frequency of the crystal that are a function of the mass of the absorbed vapour (O'Sullivan and Guilbault, 1999). The QCM sensor is widely available, and a variety of polymer layers can be used to construct the gas sensor, allowing their function to be tailored to specific applications.

In the SAW sensor, an ac signal is used to generate an acoustic wave that passes over the surface of a piezoelectric substrate. When the wave reaches the output electrode, a phase shift in ac voltage is generated that is a function of the mass and absorption properties of a polymer deposited between the two electrodes. Absorbtion of analyte molecules produces changes in the mass at the crystal surface and a corresponding change in the relative shift in the frequency of the ac signal between the two electrodes (Sethi, 1991). The SAW sensors are very sensitive, and are capable of detecting mass changes at nanogram levels.

Optical Sensors

The optical sensor consists of an optical fibre coated with a chemically active fluorescent substance in a polymer matrix. An organic vapour causes the fluorescent emission spectrum of the polymer-dye matrix to be altered, and these alterations are detected by activating the sensor with a pulse of light from an external light source and monitoring the frequency of the light emitted. A wide range of fluorescent dyes are available for biological and immunological applications, and these can be utilised in the optical sensor. The optical sensor is sensitive, but complex instrument control systems are necessary and the life of the sensor is limited by photo-bleaching of the fluorescent dye.

Potential Clinical Application of the "Electronic Nose"

The sensitivity, speed and simplicity of operation of the electronic nose makes it an attractive tool for application in veterinary medicine. A prototype nose has already been applied in veterinary medicine for detection of oestrus in perineal swabs from cows (Lane and Wathes, 1998) and for detection of breath odours indicative of ketosis in the breath of cows (Elliott-Martin *et al.,* 1997). Several applications of the electronic nose in human breath analysis have been reported including a test for diabetes (Ping *et al.,* 1997) lung cancer (D'Amico, 2000), and for breath alcohol (Paulsson and Winquist, 1999). A prototype portable instrument using a SAW sensor electronic nose, and capable of on-line concentration and analysis of VOCs in breath has also been described (Groves and Zellers, 1996; Groves *et al.,* 1998). Previous studies have demonstrated that pentane could be detected using an electronic nose based on composite polymer resistive sensors, in pentane gas samples at similar concentrations to those presented for GC analysis in the hydrocarbon breath test (Doleman *et al.,* 1998). Detection of pentane and ethane using an electronic nose would greatly simplify the hydrocarbon breath test and facilitate further application of this test in the clinical setting. The broad spectrum of applications of the electronic nose in human medicine is illustrated in Table 5.1, and many of these applications could also be valuable in veterinary medicine. The novel non-specific nature of the electronic nose measurement may facilitate innovative approaches to problems in veterinary diagnostics that can not be adequately addressed using current technology.

Table 5.1 Applications of the electronic nose in medicine

Reference	Condition Detected	Analyte Matrix	Sensor Type
Gardner *et al.*, 1998	Class and growth of bacterial pathogens *Staphylococcus aureus* *Eschericha coli*	Bacterial culture headspace	6 × metal oxide semiconductor sensors
Hanson and Steinberger, 1997	Pulmonary infection	Exhaled breath	20 × conducting polymer sensors
Parry *et al.*, 1995	β-haemolytic streptococcal infection	Headspace of wound dressing	20 × conducting polymer sensors
Lane and Wathes, 1998	Oestrus in cows	Perineal swab headspace	12 × conducting polymer sensors
Thayler *et al.*, 2000	Differentiation of serum and cerebro-spinal fluid	Vapourised sample	32 × conducting polymer sensors
DiNatale *et al.*, 2000	Skin odour	Swab headspace	8 × quartz crystal microbalances
Aathithan *et al.*, 2001	Bacteriuria	Urine headspace	Conducting polymer sensors
DiNatale *et al.*, 1999	Haemoglobinuria	Urine headspace	Quartz crystal microbalances
Elliott-Martin *et al.*, 1997	Bovine ketosis	Exhaled breath	6 × metal oxide sensors
Ping *et al.*, 1997	Diabetes	Exhaled breath	Metal oxide sensors
Pavlou *et al.*, 2000	Classification of *Helicobacter pylori*	Growth media headspace	14 × conducting polymer sensors
D'Amico *et al.*, 2000	Lung cancer	Exhaled breath	8 × quartz crystal microbalances

5.2 STUDY OBJECTIVES

The overall aim of this chapter was to design and construct a composite polymer microsensor array, sample presentation system and data analysis protocol, that could potentially be developed for analysis of exhaled breath in veterinary medicine.

5.3 CONSTRUCTION OF COMPOSITE POLYMER SENSORS AND ANALYSIS OF SENSOR SENSITIVITY

5.3.1 Study Aim

The specific objective of this study was to construct a range of composite polymer sensors and investigate their sensitivity to changes in temperature, humidity and analyte concentration and to investigate the effect of carbon black loading on sensor resistivity.

5.3.2 Introduction

This section describes the fabrication of a composite polymer sensor, similar to sensors that have been previously used for construction of microsensor arrays in electronic noses (Doleman *et al.*, 1998; Swann *et al.*, 1998). The composite sensors were fabricated by coating electrodes with a layer of non-conducting polymer in which particles of conducting carbon are suspended (Figure 5.3). The carbon black particles allow charge to flow across the electrode digits, while the polymer layer produces a source of chemical diversity that can be manipulated for analysis of different types of analytes. Absorbtion of the analyte into the polymer-carbon black film causes swelling of the polymer which produces an increase in the resistance of the network of conducting regions provided by the carbon-black particles (Severin *et al.*, 2000), (Figure

5.3). Different test gases presented to the composite polymer sensor produce variable changes in the resistivity of the sensor depending on the ability of the analyte to be absorbed into the polymer layer. Absorbtion of gases into the polymer film produces a change in volume of as much as 150% of the original volume (Swann *et al.*, 1998), and this increase in volume is associated with an increase in the electrical resistance of the layer.

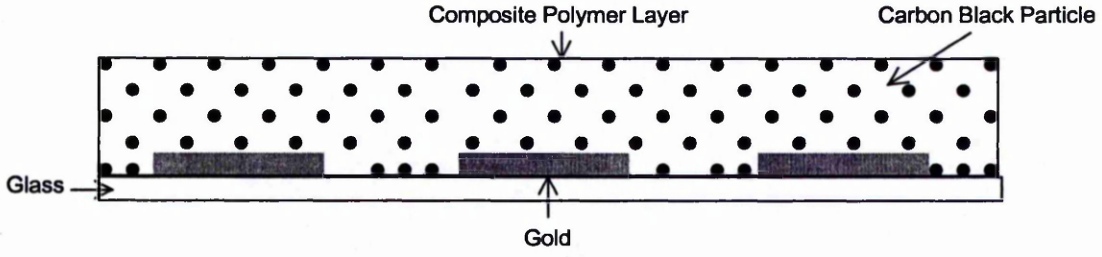

Figure 5.3 Schematic diagram of a transverse section through a composite polymer resistor sensor, illustrating the suspension of carbon black particles that allowed charge to pass across the digits of the electrodes.

5.3.3 Materials and Methods

Reagents

The specific polymers used in this study were poly(vinyl pyrrolidone), poly(styrene), poly(4-vinyl phenol), poly(caprolactone), poly(ethylene oxide), poly(methyl methacrylate), poly(vinyl acetate), poly(vinyl pyridine), poly(ethylene-*co*-vinyl-acetate), and poly(isobutylene); these were obtained from Sigma-Aldrich and used as supplied.

Fabrication of Sensors

Interdigitated gold microelectrodes were fabricated as described in Chapter Two. Electrode pattern 1 (Chapter Two) was used to construct the sensors in this study.

Deposition of Composite Polymer Films

The composite polymer films were made from a solution of polymer in which the carbon black particles were suspended (80% polymer and 20% carbon black, by weight of solids) as previously described (Severin *et al.,* 2000). Full details of the method used to cast the polymer layer are given in Chapter 2. The solution was spin coated (approximately 30 seconds at 100rpm) onto the gold microelectrodes, and multiple coats were applied until the sensor resistance value was in the region of 50 – 2000Ω. Two sensors were constructed using each of the nine polymers, and the mean values for the response of both sensors was reported.

Measurement of Resistance

Dc electrical resistance across each sensor was measured using a digital multi-meter.

Effect of Carbon Black Loading

To investigate the effect of carbon black loading on resistance, nine sensors were constructed using a solution of ethanol (20ml) and polyvinylpyrrolidine (160mg), with 20, 40, 60, 80, 100, 120, 140, 160 and 180 mg of carbon black in suspension, in order to produce sensors in which the carbon black percentage by weight of solids varied between 10 and 90%.

Temperature and Humidity Studies

A simple single-sensor chamber was constructed using a gas-tight bottle with attached gas tight PTFE valves and syringe port, Omnifit, (Figure 5.4). Leads were attached to the sensor through the lid of the sealed bottle, allowing sensor resistance to be monitored. A second gas tight bottle was used to form a water bubbler (Figure 5.4) and

was connected to the sensor chamber by plastic tubing (1/8" outer diameter, fluorinated ethylene propylene (FEP) tubing, Nalgene). The sensor was placed into the sensor chamber and baseline resistance was measured at room temperature and in air. Measurements were repeated while the sensor chamber was immersed in an ice bath, and in a warm water bath; the temperatures recorded under these conditions are given in the relevant results section. A 60-second adjustment period was allowed for sensor resistance to become stable under the altered test condition, before the resistance reading on the digital multimeter was recorded.

To investigate the effect of humidity, the sensor was placed inside the glass chamber, and a background flow of nitrogen was initiated until the resistance of the sensor became stable. Humidity was then increased using a water bubbler through which the nitrogen was passed before entering the sensor chamber (Figure 5.4).

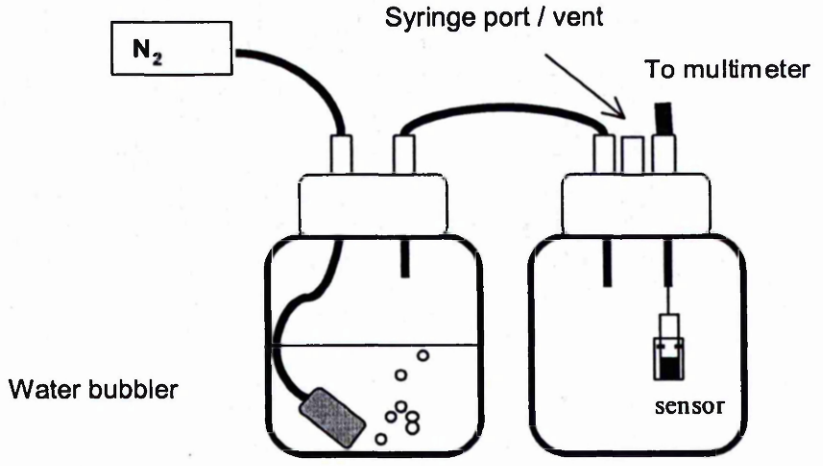

Figure 5.4 The apparatus used to examine the effect of temperature and humidity on sensor resistance. Water was added to the water bubbler chamber during the humidity study only.

Baseline Stability

The short term stability of the baseline of eight sensors (Table 5.2) was investigated by measuring resistance following a 6 minute nitrogen flush and a two minute equilibration period for 10 sequential samples.

Table 5.2 Baseline resistance of the 8 sensors used to investigate sensor stability.

Sensor	Polymer	Baseline Resistance.Ω^{-1}
1	Poly(methyl-methacrylate)	580
2	Poly(vinylchloride-co-vinyl-acetate)	900
3	Poly(caprolactone)	376
4	Poly(vinyl-pyrrolidone)	50.1
5	Poly(iso-butylene)	1139
6	Poly(styrene)	88.3
7	Poly(ethylene-co-vinyl-acetate)	4355
8	Poly(ethylene-co-methyl-acrylate)	2654

Linearity Study

Three sensors were found to be sensitive to methane (PMMA, PVP and PCL) and to investigate the linearity of the sensor response to increasing analyte concentrations, methane gas (natural gas) was presented to these sensors at increasing concentrations. The sensor chamber (volume = 132mls) was flushed with N_2 for 6 minutes before methane was added through the syringe port using a gas tight syringe. Increasing volumes of methane were added: 10, 20, 30, 40 and 50mls, resulting in methane concentrations of approximately 7, 15, 23, 30 and 39%. Resistance was recorded after two minutes of analyte exposure, and the system was flushed with N_2 for 6 minutes to allow recovery of baseline resistance before addition of the next methane sample.

5.3.4 Results and Discussion

The thickness of the polymer layer was characterised using a Dektak surface profile system. Figure 5.5 shows the results of a 2mm scan across two gold digits. Figure 5.6 shows the results of a scan across the gold digits and a layer of composite polymer. This was achieved by removing a layer of polymer at the bottom of the electrode, and scanning from top to bottom for 4mm.

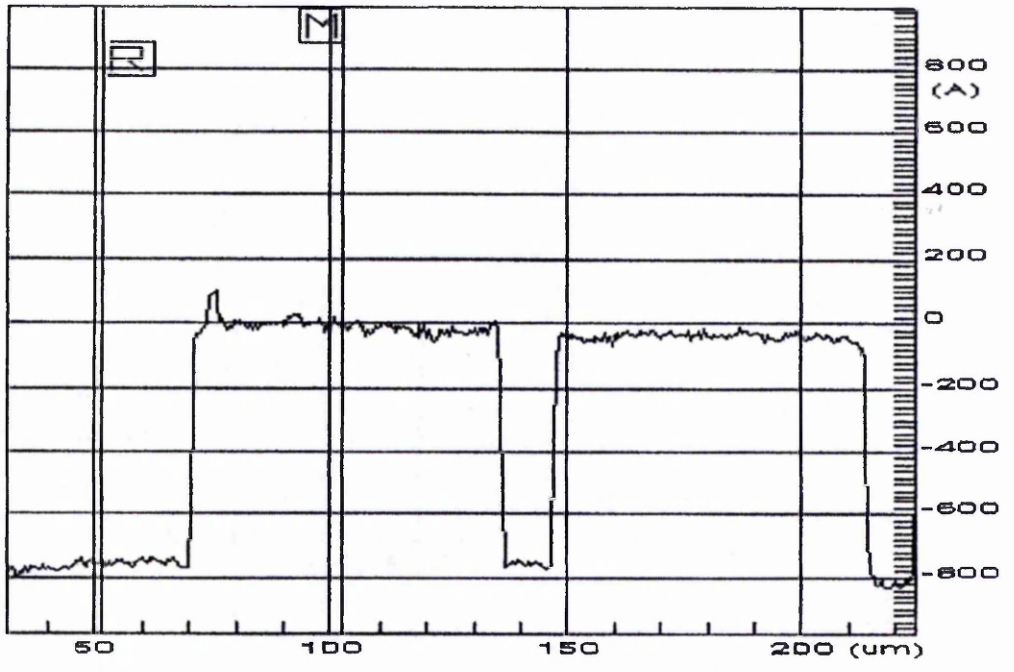

Figure 5.5 Plot of a 2mm scan along the surface of an interdigitated gold electrode, showing the gap between the digits (10μm) and the thickness of the deposited gold (80nm).

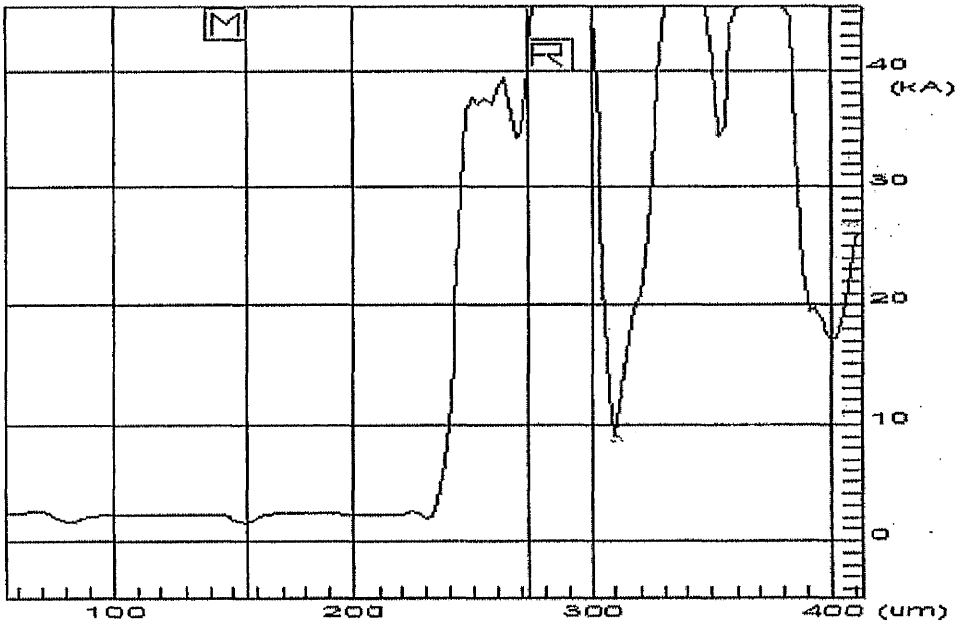

Figure 5.6 Plot of 4mm scan from bottom to top of a gold electrode with deposited polymer film; the first 200μm of the scan show the profile of the underlying gold electrodes, where a strip of polymer had been removed. The profile then shows the thicker and more uneven surface of the polymer film.

Carbon Black Dispersal

The dispersal of the carbon black particles was investigated by examining the underside of a composite polymer that was removed from a sensor. The imprint of the metal digits was visible and the imprint of the embedded finely dispersed carbon black particles could be seen under magnification (X 100) (Figure 5.7). The finely dispersed carbon black particles were also clearly visible when the coated electrodes were examined under X 100 magnification (Figure 5.8). These micrographs illustrate the fine network of conducting particles through which charge may pass, and upon which the conductivity of the polymer is dependent.

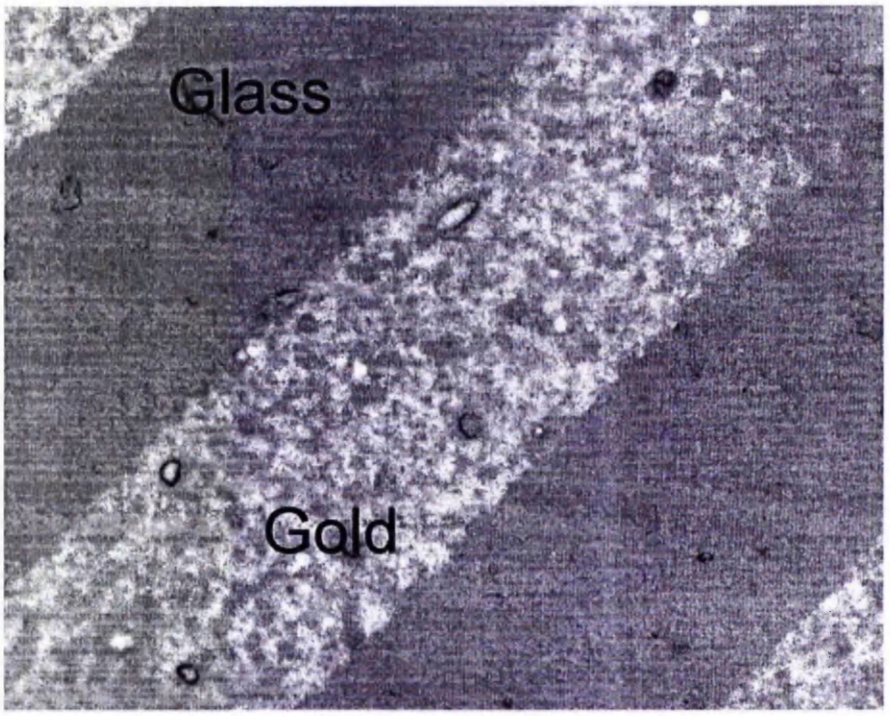

Figure 5.7 A composite polymer layer viewed from the underside, showing imprint of resistor digits and illustrating fine interdigital dispersal of carbon black particles. (Magnification × 100).

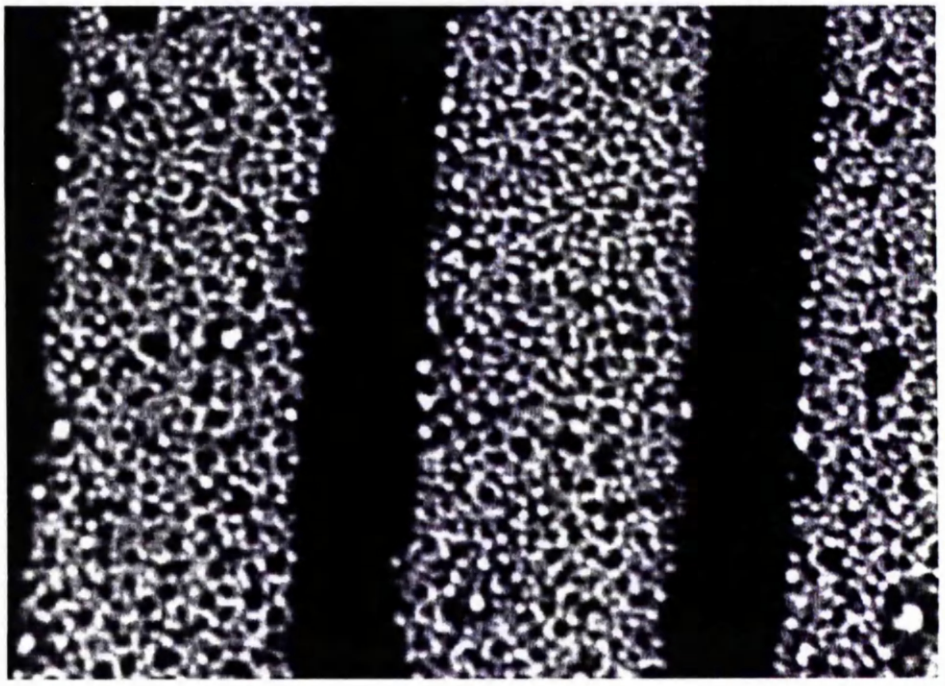

Figure 5.8 Micrograph illustrating fine dispersal of carbon black particles suspended in polymer matrix covering resistor digits (Magnification X 100).

Effect of Carbon Black Loading

The effect of the concentration of carbon black suspended in the polymer matrix, on the resistance of the electrodes was studied by comparing the baseline resistance of electrodes with increasing percentages of carbon black. Figure 5.9 illustrates the relationship between carbon black loading and decreasing electrode resistivity. This relationship, and indeed the increases in resistance following absorption of an analyte can be explained by percolation theory (Lonergan *et al.,* 1996)

The resistivity *(ρ)* of a composite polymer is predicted by the following formula:

$$\rho = \frac{(z-2)\rho_c\rho_m}{A+B+\left[(A+B)^2+2(z-2)\rho_c\rho_m\right]^{1/2}} \qquad \text{(Eq. 5.1)}$$

where $A = \rho_c\left[-1+(z/2)(1-(v_c/f))\right]$

$B = \rho_m\left[(zv_c/2f)-1\right]$

ρ_c = resistivity of carbon black particles

ρ_m = resistivity of insulating polymer

v_c = volume fraction of conductive filler

z = coordination number of conductive filler particles

f = total packing volume (Lonergan *et al.,* 1996)

This formula illustrates that the resistivity of the polymer is dependent on the volume of the conducting particles that make up the polymer-carbon black matrix. Thus a decrease in the volume fraction of carbon black (v_c) causes a corresponding increase in the resistivity of the polymer *(ρ)*, as was demonstrated in the present study (Figure 5.9).

If sufficient carbon black particles are present in the polymer matrix, an interconnected pathway of conducting particles is formed and the composite polymer becomes conductive, and the "percolation threshold" is reached (Lonergan *et al.*, 1996). Small increases in carbon black loading will initially cause large increases in the resistivity of the polymer (as illustrated in the initial part of Figure 5.9), but eventually further addition of carbon black will cause just small decreases in resistivity, as the polymer matrix becomes saturated with conducting particles. Sorption of an analyte into the polymer matrix produces increases in polymer resistivity by causing swelling and affecting the pathway of conducting particles. The magnitude of this effect will depend in part on the volume fraction of conducting polymer particles of the composite polymer. Thus, the sensitivity of the composite polymer to volume change, and swelling caused by analyte sorption, can be manipulated by altering the percentage loading of carbon black particles (Lonergan *et al.*, 1996). Composite polymers that are operating close to their percolution thresholds will have a high baseline resistance, and small volume changes will cause large increases in resistance (Lonergan *et al.*, 1996). This is concurrent with the behaviour of the sensors fabricated in the present study; sensors with a high baseline resistance tended to be very sensitive, although they were also very unstable. Sensors 4 and 7 (Table 5.3 and 5.4) had the highest baseline resistances and also displayed the highest response to temperature and humidity changes.

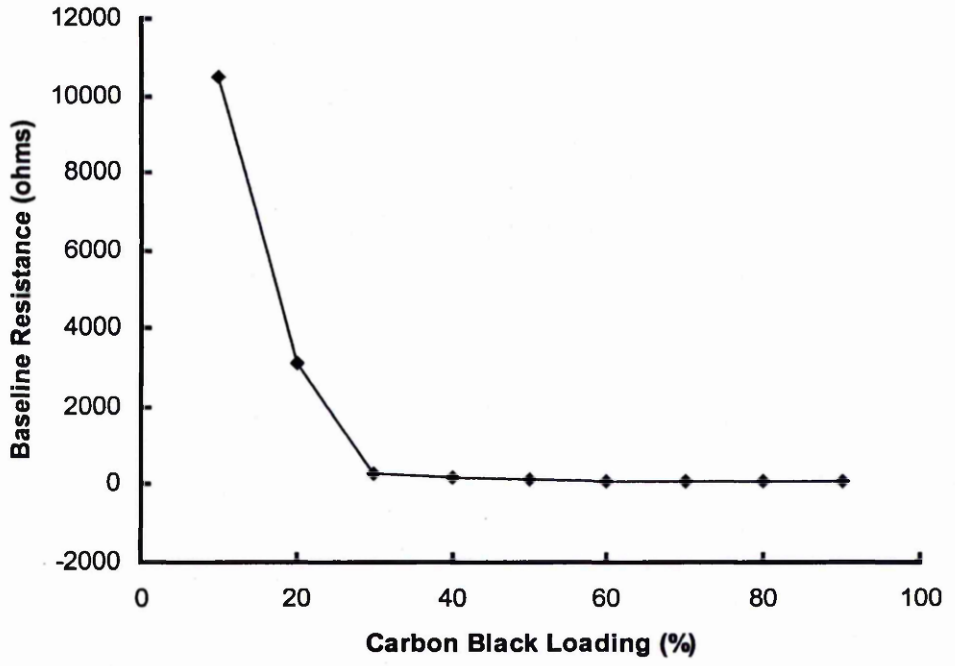

Figure 5.9 The relationship between carbon black concentration and electrode resistivity, in a composite polymer sensor.

Baseline Stability

The baseline resistance of the sensors was relatively stable; the mean coefficient of variation (sd/mean × 100) for baseline resistance over one hour in 8 sensors was 1.13%.

Effect of Temperature and Humidity on Baseline Resistance

All of the sensors displayed a change in resistance upon exposure to different conditions of temperature and humidity, and this change occurred quite rapidly, usually within 20-30seconds of exposure of the sensor to the test condition. The responses were expressed as the percent change in resistance (%ΔR) (Severin *et al.*, 2000) calculated by taking the maximum change in response value during the exposure period (ΔR_{max}) and expressing it as a percentage of the baseline resistance value at room temperature in air (R_b) (in the humidity experiments, baseline values were calculated in dry nitrogen gas).

$\%\Delta R = (\Delta R_{max}/R_b)\ 100$ Severin *et al.*, 1998 (Eq. 5.2)

The values of $\%\Delta R$, ΔR_{max}, and R_b for a batch of nine composite polymer sensors, and the effects of changes in temperature and humidity are shown in Table 5.3 and 5.4.

Table 5.3 Effect of temperature on baseline resistance of composite polymer sensors.

Sensor	$R_b.\Omega^{-1}$	Temperature = 14°C		
	[Air]	$R_{max}.\Omega^{-1}$	$\Delta R_{max}.\Omega^{-1}$	$\%\Delta R.\%^{-1}$
1	532.6	560.2	27.7	5.2
2	562.5	564.3	1.8	-0.3
3	163.8	166.0	1.1	1.3
4	1650.0	1747.5	97.5	5.1
5	691.3	702.8	11.5	1.6
6	159.4	156.6	-2.9	-2.7
7	980.6	858.9	-121.8	-17.1
8	280.0	284.7	2.4	1.7
9	397.6	409.0	5.7	2.9
Sensor	$R_b.\Omega^{-1}$	Temperature = 36°C		
	[Air]	$R_{max}.\Omega^{-1}$	$\Delta R_{max}.\Omega^{-1}$	$\%\Delta R.\%^{-1}$
1	532.6	473.3	-59.3	-11.1
2	562.5	554.2	-8.3	-2.2
3	163.8	160.8	-1.5	-1.8
4	1650.0	2002.5	352.5	15.3
5	691.3	702.1	10.8	2.9
6	159.4	155.9	-3.6	-2.8
7	980.6	1793.5	812.9	106.5
8	280.0	270.4	-4.8	-3.4
9	397.6	383.1	-7.3	-3.7

Sensor 1 - Poly(vinyl pyrrolidone)
Sensor 2 - Poly(styrene)
Sensor 3 - Poly(4-vinyl phenol)
Sensor 4 - Poly(ethylene oxide)
Sensor 5 - Poly(methyl methacrylate)
Sensor 6 - Poly(vinyl acetate)
Sensor 7 - Poly(vinyl pyridine)
Sensor 8 - Poly(ethylene-*co*-vinyl acetate)
Sensor 9 - Poly(isobutylene)

Table 5.4 The effect of humidity on composite polymer sensor baseline resistance

Sensor	$R_b.\Omega^{-1}$	N_2		
	[Air]	$R_{max}.\Omega^{-1}$	$\Delta R_{max}.\Omega^{-1}$	$\%\Delta R.\%^{-1}$
1	532.5	469.6	-62.9	-11.8
2	562.4	552.8	-9.6	-2.5
3	163.8	159.1	-2.3	-2.9
4	1650.0	1799.5	149.5	8.2
5	691.3	702.1	10.8	2.5
6	159.4	155.3	-4.0	-3.4
7	980.6	996.1	15.5	1.0
8	280.0	273.5	-3.2	-2.3
9	397.6	390.8	-3.4	-1.7

Sensor	R_b (Ω) (N_2)	Humidity ($N_2 + H_2O$)		
		$R_{max}.\Omega^{-1}$	$\Delta R_{max}.\Omega^{-1}$	$\%\Delta R.\%^{-1}$
1	469.6	557.4	87.8	18.7
2	552.9	560.1	7.2	2.2
3	159.1	164.2	2.6	3.2
4	1799.5	2411.0	611.5	25.2
5	702.1	711.3	9.2	1.5
6	155.4	157.2	1.9	1.2
7	996.1	3016.0	2019.9	268.1
8	273.5	278.2	2.4	1.7
9	390.8	391.0	0.1	0.1

Sensor 1 - Poly(vinyl pyrrolidone)
Sensor 2 - Poly(styrene)
Sensor 3 - Poly(4-vinyl phenol)
Sensor 4 - Poly(ethylene oxide)
Sensor 5 - Poly(methyl methacrylate)
Sensor 6 - Poly(vinyl acetate)
Sensor 7 - Poly(vinyl pyridine)
Sensor 8 - Poly(ethylene-*co*-vinylacetate)
Sensor 9 - Poly(isobutylene)

Alterations in baseline resistance were observed following changes in temperature in all sensors. However the greatest increases in sensor resistance were observed when water

vapour was presented to the sensors. This is in concurrence with previous reports and sensor sensitivity to humidity is one of the most significant problems in application of microsensor arrays for gas-detection (Paulsson and Winquist, 1999; Mielle, 2000). Various methods for standardization or adjustment for humidity have been suggested. Humidity sensors could be included in the electronic nose microsensor array so that electronic corrections for alterations in humidity could be made; however humidity sensors often have a slower response time, compared to gas-sensors (Mielle, 2000). Alternatively, samples can be passed through a desiccator, so that water vapour is removed before presentation to the sensor array. However, many desiccate materials remove volatile compounds as well as water. A Naphion® membrane has been applied for drying of gas samples prior to presentation to gas-sensors (McEntegart *et al.,* 2000) and this material is thought to remove water while minimizing loss of hydrophilic compounds. Sensor sensitivity to alterations in temperature and humidity increase the background noise of the gas-sensing device, and careful correction is necessary to optimize control of these variables.

Linearity of Sensor Response to Analyte Concentration

The linearity of the relationship between the response of sensor 1, 3 and 4 and increasing concentrations of methane is shown in Figure 5.10. The relationships appeared to be linear ($r^2 < 0.9$), although only very small changes in sensor resistance above baseline were recorded (0.1 – 2.5%). This finding is in concurrence with previous studies which reported that change in resistance ($\Delta R.R^{-1}$) should be a function of the concentration of the analyte that partitions into the polymer layer (Severin *et al.,* 2000). Each analyte will be absorbed into a specific polymer according to the characteristic gas-polymer partition coefficient of that polymer, but the magnitude of the

alteration in resistance so produced is a function of the analyte concentration (Severin *et al.*, 2000).

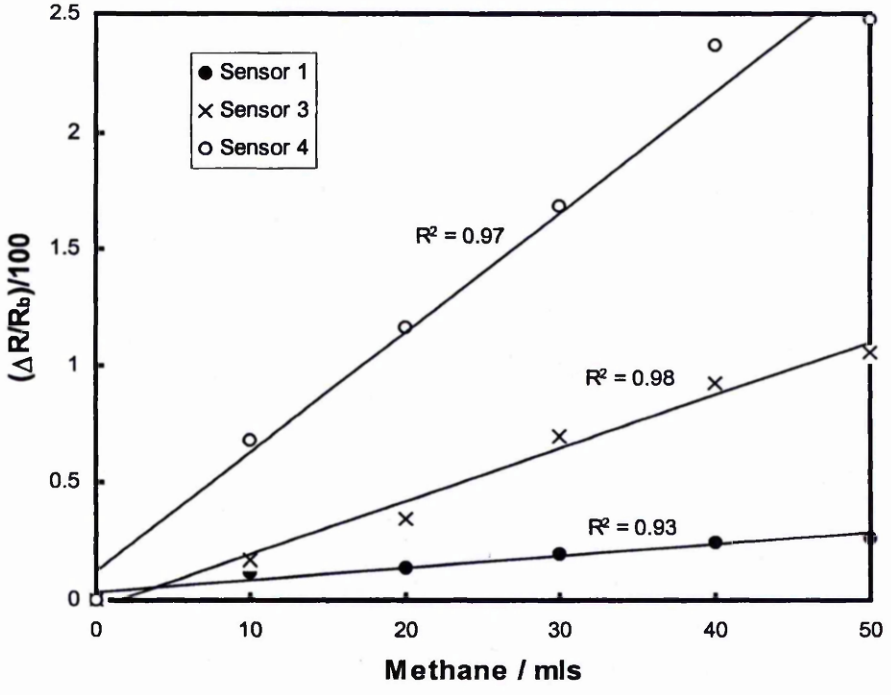

Figure 5.10 The relationship between sensor response and increasing concentrations of methane for Sensor 1 (PMMA), Sensor 3 (PCL) and Sensor 4 (PVP).

These studies have described the fabrication of a series of composite polymer sensors. The sensors were simple to produce and a fine dispersal of carbon black particles was evident within the polymer film. The sensors demonstrated a linear increase in resistivity in response to increasing concentration of analyte (methane). Some sensitivity to humidity and to alterations in ambient temperature was observed. These finding suggest that under controlled conditions, composite polymer sensors may be useful for the detection of compounds of interest that occur in the exhaled breath, and further investigation of the gas-sensing properties of these devices is warranted.

5.4 CONSTRUCTION OF A PROTOTYPE GAS SENSOR MICROARRAY AND FLOW SYSTEM FOR DETECTION OF VOLATILE COMPOUNDS IN EXHALED BREATH

5.4.1 Study Aims

The objectives of this study were to construct a microsensor array and gas flow system suitable for analysis of compounds present in exhaled breath and to investigate the specificity of this system in detecting standard gases present in breath. A second objective was to develop a protocol for mathematical simplification of the data obtained from the instrument.

5.4.2 Introduction

As outlined in the previous Chapter, the analysis of volatile organic compounds in exhaled breath holds considerable potential as a non-invasive clinical investigative tool, but technical difficulties currently preclude widespread application of this method.

The electronic nose has been successfully used to analyse breath, and several research groups world wide are currently involved in developing investigative breath tests using electronic nose technology (Pavlou and Turner 2000). Paulsson and Winquist, (1999) described the development of a gas sensor array for quantitative analysis of alcohol in breath. Measurements were carried out in parallel with GC analysis, and while the sensor array was able to quantify alcohol in breath, the performance of this assay was not acceptable for forensic application (Paulsson and Winquist, 1999). A gas sensor array that could discriminate patients with lung cancer from healthy volunteers based on samples of their exhaled breath has also been described (D'Amico *et al.*, 2000).

However no details of sensor performance or of the sensitivity and specificity of this method were available. Nevertheless there did appear to be some clustering of diseased samples on the data-plot, and this test is probably worthy of further investigation, particularly in light of some recent similar results found during GC-analysis of breath from patients with lung cancer (Phillips *et al.,* 1997). The electronic nose has also been applied for analysis of exhaled breath in veterinary medicine. Elliott-Martin *et al.,* (1997) described a breath test based on an array of conducting polymer sensors that could detect ketosis in cows with an 89% success rate compared with the standard method of serum β-hydroxybutanoate detection. Similarly, a gas-sensing breath test has been described for detection of diabetes in man that could be a useful non-invasive method for screening for this condition (Ping *et al.,* 1997). Finally, Hanson and Steinberger, (1997) presented some preliminary data describing the detection of pulmonary infection using an electronic nose to analyse exhaled air, and there did appear to be some discrimination between diseased and healthy subjects.

These studies suggest that electronic nose assays for analysis of exhaled breath are feasible and with careful validation, could find widespread application as screening tools in medicine, environmental health and forensic science. Problems that have been identified concerning application of the electronic nose in breath analysis include, sensor sensitivity to humidity, baseline drift, sensor drift and non-linear sensor behaviour (Paulsson *et al.,* 1999). Optimisation of the reliability and stability of the electronic nose assay, as well as careful analysis of assay specificity and accuracy will be required if the assay is to meet industry standards and become acceptable for routine application. This study describes the initial stages of the development of a prototype electronic nose assay for analysis of exhaled breath in veterinary medicine.

5.4.3 Materials and Methods

Reagents

The specific polymers used in this study were poly(methylmethacrylate) (PMMA), poly(vinyl chloride-*co*-vinyl acetate) (PVVA), poly(caprolactone) (PCL), poly(vinyl pyrrolidone) (PVPr), poly(isobutylene) (PIB), poly(styrene) (PS), poly(ethylene-*co*-vinyl acetate) (PEVA), poly(ethylene-*co*-methylacrylate) (PEMA), poly(sulfone) (PSF) poly(acrylonitrile-*co*-butadiene-*co*-styrenetoluene) (PABS), poly(ethylene-*block*-polyethylene glycol) (PEGPEG), poly(ethylene glycol) (PEG), poly(vinyl methyl ketone) (PVPK), poly(4-vinylphenol) (P4VP), poly(vinyl acetate) (PVA), poly(2-vinylpyridine-*co*-styrene) (P2VPS); these were obtained from Sigma-Aldrich and used as supplied. Pentane, isoprene, hexane, acetone, ethanol, hexanal, methanol, pentanol and isopropanol were all obtained from Sigma-Aldrich.

Fabrication of Sensors

Interdigitated gold microelectrodes were fabricated (electrode 2, Chapter 2), and composite polymer layers were deposited as described in Chapter Two.

Gas Flow System

A gas flow system was constructed so that the sample was continuously passed over the sensors. This system of dynamic headspace analysis is thought to be more efficient than analysis of a static headspace in electronic nose systems (Pavlou and Turner, 2000). The sensors were mounted on glass and enclosed in a glass chamber (approximate volume = 9cm^2). The sensor chamber was sealed using a gas-impermable polymer (0.7mm thick, Hexafluoro-propylene-vinylidene-fluoride copolymer, Viton®, Goodfellow Ltd) and plastic screws. Gas impermeable (FEP) and glass tubing connected the sensor chamber with a synchronised gas-tight syringe pump system

(Cole-Palmer) and a sample chamber (volume = 34cm^3) (Figure 5.11). Nitrogen was used to flush the chamber and syringes between samples.

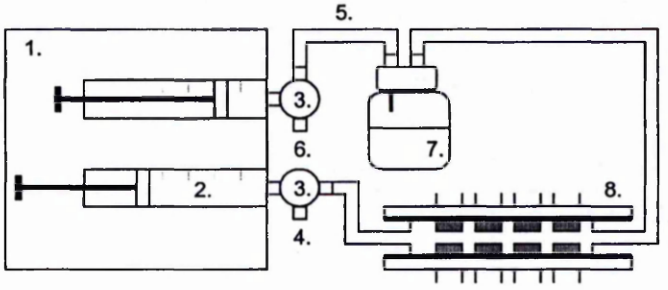

1. Syringe driving unit
2. Gas tight syringes
3. 3-way valve
4. Vent
5. Gas impermeable tubing
6. Nitrogen in
7. Sample chamber
8. Sensors mounted on glass board

Figure 5.11 The gas flow system and microsensor array used in these experiments.

Measurement of Resistance

The dc electrical resistance across each composite polymer sensor was measured using digital multimeters. These instruments were sensitive to changes in resistance of more than 1Ω in the range 200-2000Ω, and to changes of more than 0.1Ω in the resistance range 20-200Ω.

Study Design

The chamber was flushed with nitrogen for 6 minutes before baseline resistance of each electrode was measured at room temperature. The sample (100μl) was placed into the sample chamber and the headspace was flushed into the sensor chamber by the action of the syringe pumps. The sensors were allowed to reach equilibrium over 2 minutes after which resistance readings were recorded. A clean sample chamber was fitted and the system was flushed with nitrogen for 6 minutes. Nine analytes that are present in exhaled breath were used to assess the specificity of the electronic nose assay. The compounds used were acetone, ethanol, hexanal, hexane, isoprene, isopropanol, methanol, pentane and pentanol. Each analyte was presented to the sensors three times.

Data Processing: The resistance measurement of each sensor after analyte exposure was expressed as $\Delta R/R_b \times 100$, where R_b is the resistance measurement at baseline and ΔR is the differential resistance measurement after two minutes of exposure to the analyte (Lonergan *et al.,* 1996). The differential resistance measurement for each analyte on each of the 16 sensors were plotted on polar plots, and the reproducibility of the derived plots was assessed by plotting the standard deviation of three measurements for each analyte.

Statistical Pattern Recognition: Principal component analysis (PCA) is a method for expressing multivariate data in lower dimensions. PCA involves defining new variables (U_h) that maximise the variation in a p-dimensional scatter plot.
Consider a set of data obtained from some electronic nose sensors, where X is the sensor response, p is the number of sensors, y is the analyte identity, and n is the number of samples. y is defined as a linear combination of the sensor responses:

$$y_n = X_1 + X_2 + X_3 + X_4 + \ldots\ldots\ldots\ldots X_p \qquad \text{(Eq. 5.3)}$$

The first principal components of this data is the transformation U_1:

$$U_1 = b_{11}X_1 + b_{12}X_2 + b_{13}X_3 + \ldots\ldots\ldots\ldots b_{1p}X_p \qquad \text{(Eq. 5.4)}$$

U_1 is defined as the transformation of the p-dimensional data cluster onto a straight line on which there results the greatest variability (Flury and Riedwyl, 1988). The second component, U_2, is a projection onto a straight line that again maximises variation but is un-correlated, or orthogonal to U_1. This process continues to U_h, which is the linear projection which has maximum variance but remains un-correlated to sequence $U_1 \ldots U_h$.

Principal component analysis is a graphical method that aids data classification, and this method does not permit quantitative analysis of data.

The data for all sensors were normalised (global normalisation) over the entire array for a given analyte; this procedure ensures that the sensors were not simply responding to analyte concentration (Lonergan *et al.,* 1996).:

$$S_{ij} = \frac{\Delta R_{ij}}{\sum_{j} \Delta R_{ij}} \qquad \text{(Eq. 5.5)}$$

where ΔR_{ij} is the differential resistance change for sensor j after a 2 minutes exposure to analyte i, and $\sum_{j} \Delta R_{ij}$ is sum of the differential resistance changes for all sensors j, after a 2 minute exposure to analyte i. PCA analysis was performed using Minitab13, to classify the normalised values for each sensor's response to each analyte.

5.4.4 Results

Sixteen sensors of baseline resistance between 47.9 and 1812Ω were fabricated (Table 5.5). The thickness of the composite polymer layer was characterised using a Dektak surface profile system, and was typically 800nm.

Table 5.5 Details of the sixteen sensors fabricated in this study, showing range of baseline resistance readings.

Sensor	Polymer	Baseline Resistance.Ω^{-1}
1	Poly(methyl methacrylate)	590
2	Poly(vinylchloride-*co*-vinylacetate)	881
3	Poly(caprolactone)	385
4	Poly(vinyl pyrrolidone)	47.9
5	Poly(isobutylene)	1155
6	Poly(styrene)	90.0
7	Poly(ethylene-*co*-vinyl acetate)	1723
8	Poly(ethylene-*co*-methylacrylate)	1812
9	Poly(sulfone)	909
10	Poly(acrylonitrile-*co*-butadiene-*co*-styrenetoluene)	140.0
11	Poly(ethylene-*block*-polyethylene glycol)	220
12	Poly(ethylene glycol)	290
13	Poly(vinyl methylketone)	362
14	Poly(4-vinylphenol)	595
15	Poly(vinyl acetate)	207
16	Poly(2-vinylpyridine-*co*-styrene)	135.2

All of the sensors displayed a change in resistance upon exposure to different analytes, and this change occurred quite rapidly usually within 20-30 seconds of presentation of the test compound to the sensors. Many of the sensors failed to recover their original baseline resistance value following analyte exposure, showing considerable variation in baseline resistance over the course of an experiment. The differential response of sensor (n=16) resistance for each analyte was plotted on polar plots, revealing characteristic patterns for several compounds (Figure 5.12). The patterns of response were particularly similar for pentane, isoprene and hexane (Figure 5.12 (a) and (e)). The reproducibility of these measurements was illustrated by plotting the standard deviation for triplicate measurements of each analyte.

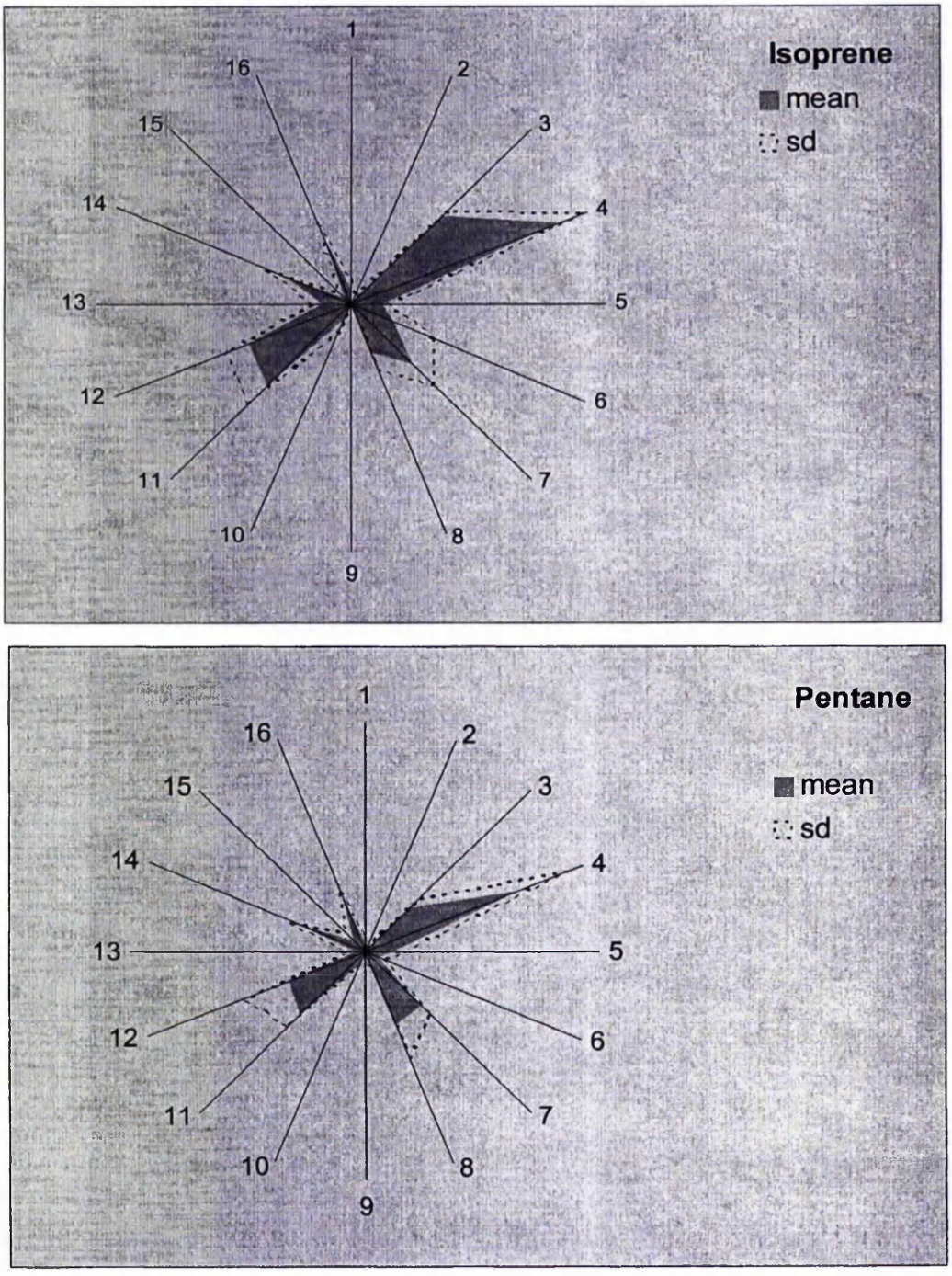

Figure 5.12 (a) Polar plots illustrating characteristic patterns of sensor response for different analytes. The response of each sensor is shown as the mean normalised differential resistance, when the analyte was presented to the sensor array three times. The dotted line is the standard deviation of sensor response of these three measurements.

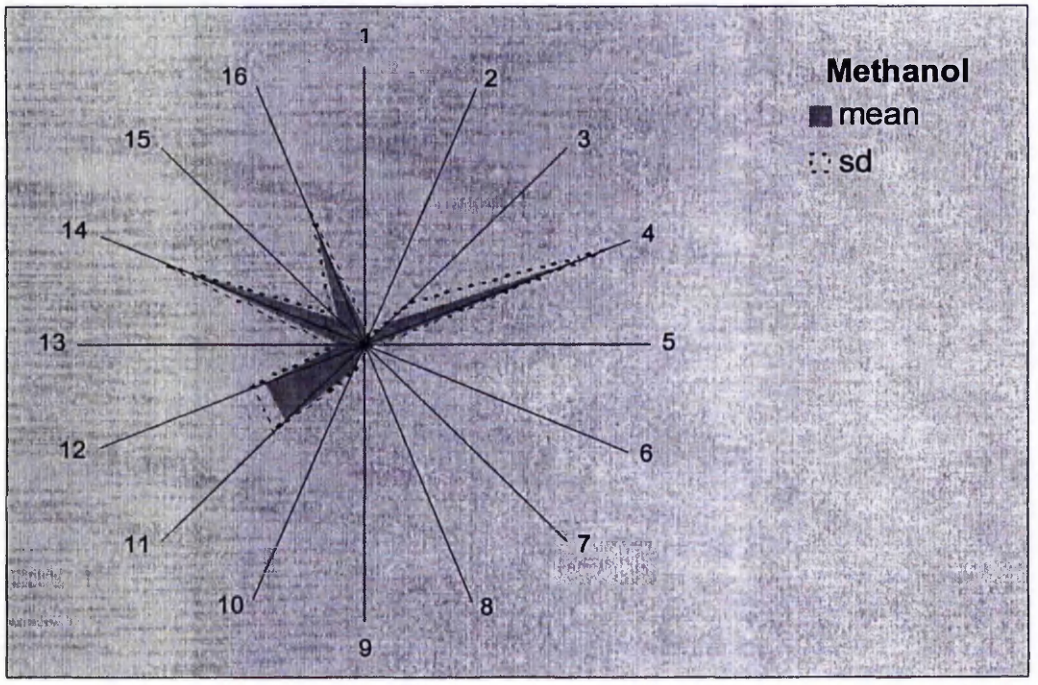

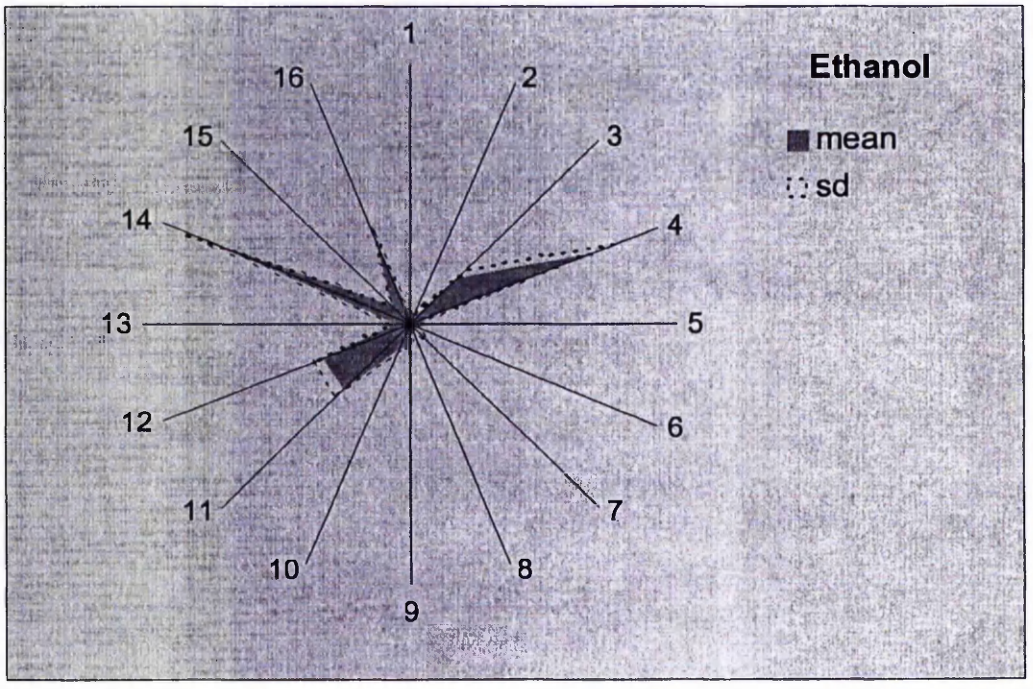

Figure 5.12 (b) Polar plots illustrating characteristic patterns of sensor response for different analytes. The response of each sensor is shown as the mean normalised differential resistance, when the analyte was presented to the sensor array three times. The dotted line is the standard deviation of sensor response of these three measurements.

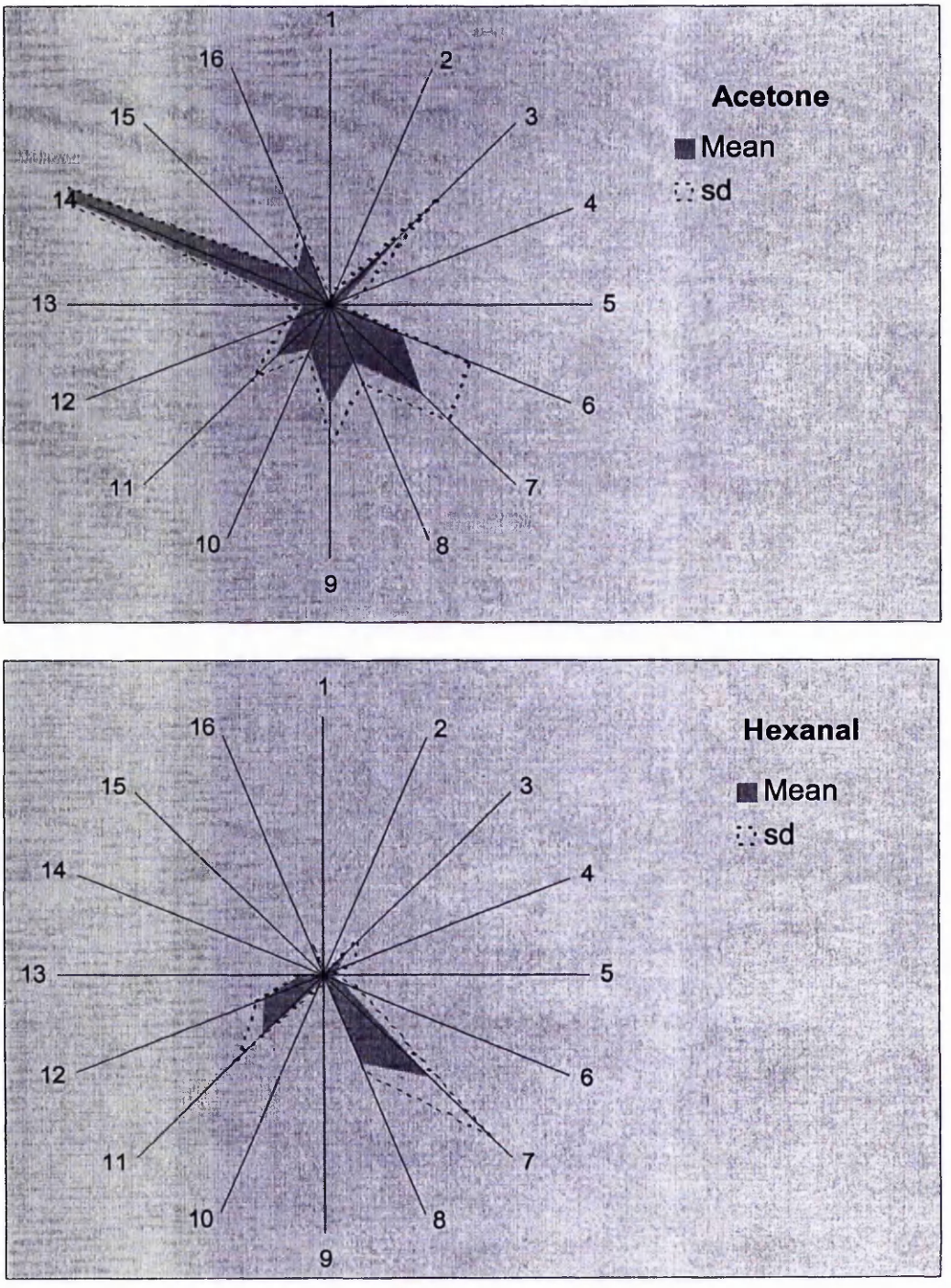

Figure 5.12 (c) Polar plots illustrating characteristic patterns of sensor response for different analytes. The response of each sensor is shown as the mean normalised differential resistance, when the analyte was presented to the sensor array three times. The dotted line is the standard deviation of sensor response of these three measurements.

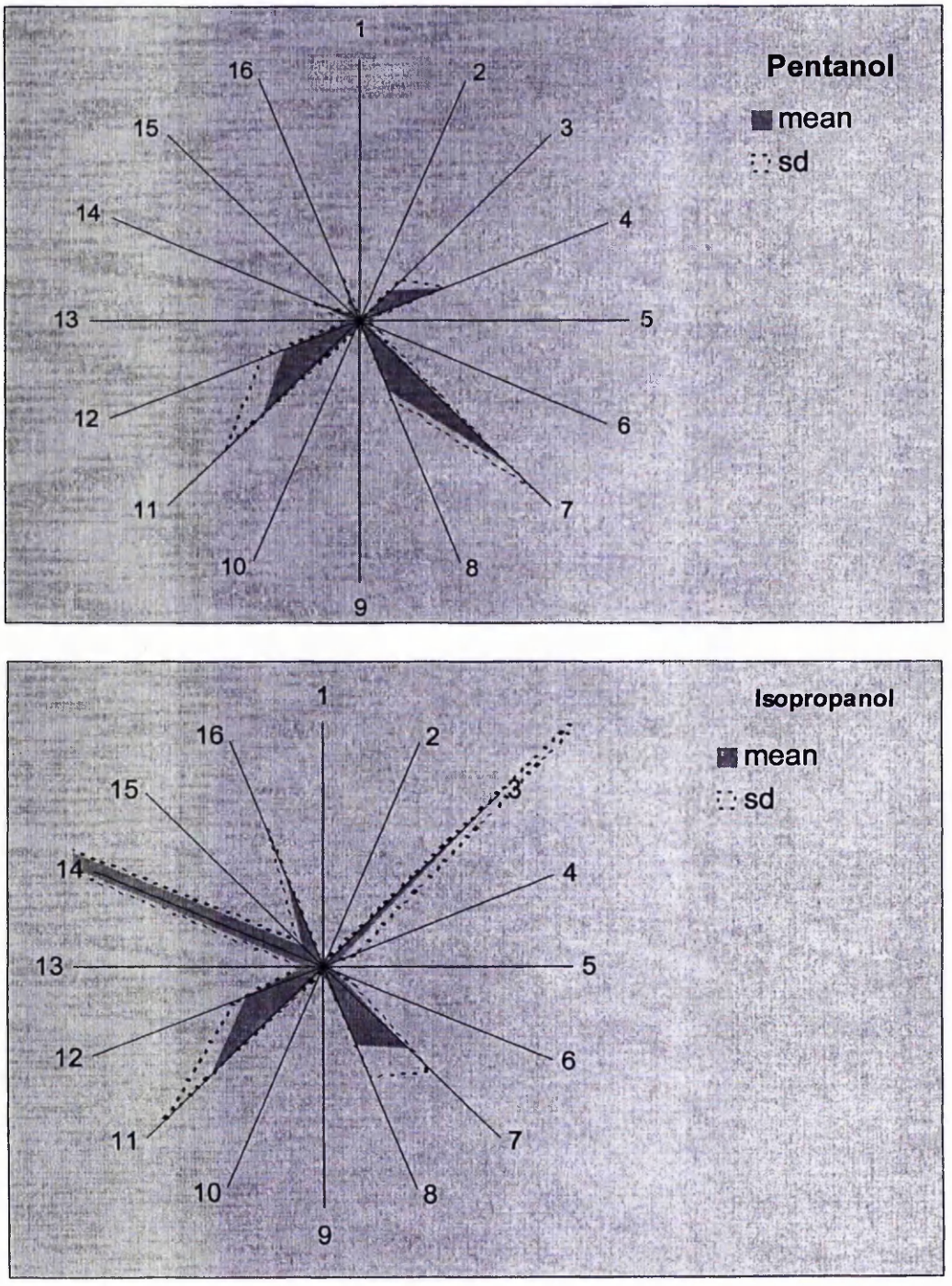

Figure 5.12 (d) Polar plots illustrating characteristic patterns of sensor response for different analytes. The response of each sensor is shown as the mean normalised differential resistance, when the analyte was presented to the sensor array three times. The dotted line is the standard deviation of sensor response of these three measurements.

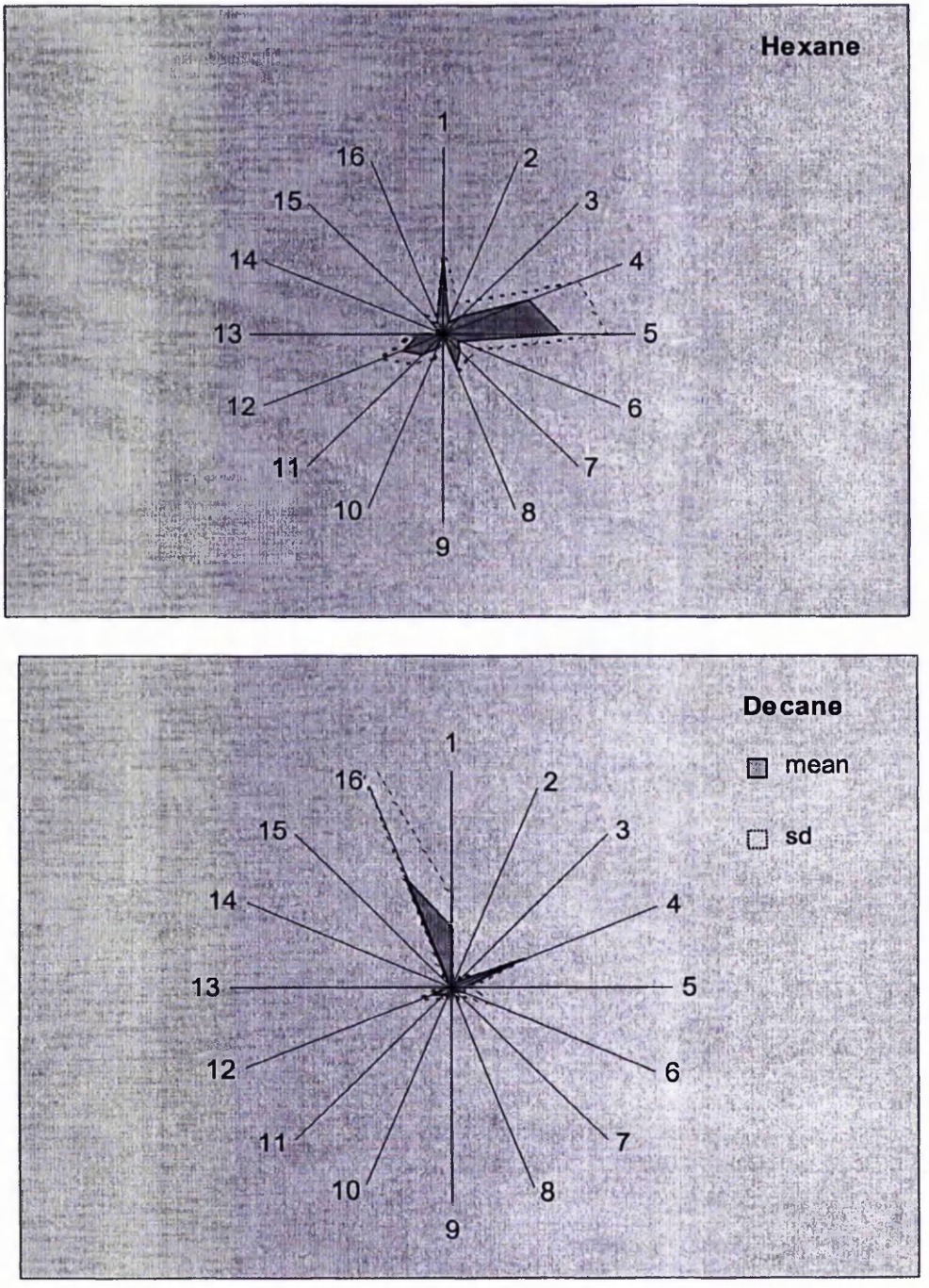

Figure 5.12 (e) Polar plots illustrating characteristic patterns of sensor response for different analytes. The response of each sensor is shown as the mean normalised differential resistance, when the analyte was presented to the sensor array three times. The dotted line is the standard deviation of sensor response of these three measurements.

Further classification of the data was obtained when the first two components of the principal component analysis were plotted, revealing a distinct clustering of data pints for isopropanol, acetone, hexanal, methanol, pentanol and ethanol. However the data clusters for pentane, isoprene and hexane mapped to similar areas on the PCA-plot (Figure 5.13) could not be resolved.

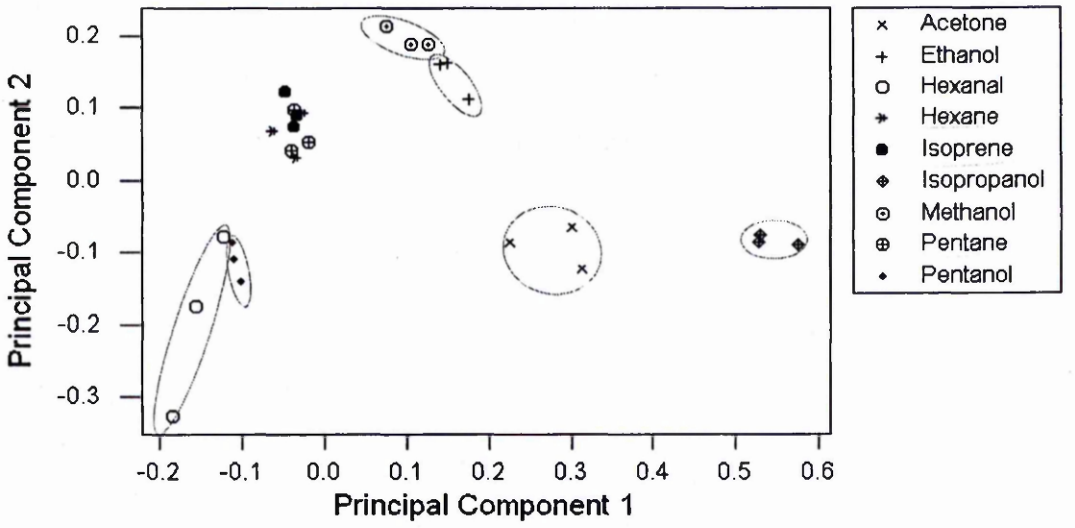

Figure 5.13 Principal component analysis of the responses of 16 sensors to 9 analytes each measured three times.

5.5 DISCUSSION

This study described the construction and application of a 16-sensor microarray, sample presentation system and data analysis protocol that together formed a basic "electronic nose" instrument. The sensors showed sensitivity and specificity for specific

compounds, while the data analysis simplified the complex patterns of sensor response, allowing graphical classification of data. Most of the sensors showed an increase in baseline resistance following exposure to certain analytes. This finding is explained by percolation theory (Section 5.2); the sorption of a gas into the matrix of the polymer causes swelling which increases the distance between the carbon black particles thus increasing the resistance across the electrode (Swann *et al.,* 1998). The response of the sensors to different compounds was reproducible, based on the relatively low variation between the triplicate samples. Small shifts in baseline resistance were noted on repeated exposure to analytes, but these did not preclude discrimination of samples. Similar shifts in baseline resistance are frequently recorded during composite-polymer sensor gas detection, but are not thought to affect sensor performance and could be corrected for electronically (Severin *et al.,* 2000). The multimeters used to measure resistance in these studies were sensitive to large changes (>1Ω) in resistance only, and small changes in resistance could not be detected using these instruments. Thus, the sensitivity and specificity of the gas-sensor array in this study may have been compromised by failure to detect significant alterations in sensor resistance. In this study sensor resistance was recorded after 2 minutes of analyte exposure, and monitoring of alterations in sensor resistance during the period of analyte exposure was not possible. The maximum increase in sensor resistance during the period of analyte exposure (ΔR_{max}) (Lonergan *et al,* 1996), could not be calculated in this study, although this point may be a more accurate measure of resistance change.

There are several issues that must be addressed in the application of an electronic nose for breath analysis. The concentrations of the compounds of interest in breath is very low (ppb) and samples will require concentration to the detection limit of the electronic nose, which for a homologous series of alkanes lies in the region of ppm (Severin *et*

al., 1996). The method of concentration used will affect the potential of the test as a point-of-care device. However portable thermal-desorption units are available and this equipment was previously used to construct a portable electronic nose and gas concentration system (Groves and Zellers, 1996). The gas sensors used in the electronic nose are very sensitive to water vapour (Section 5.2) (Pavlou and Turner, 2000), and since the humidity of exhaled breath is relatively high, the water content would need to be standardised or removed before the sample is presented to the sensors. Many water-removal systems result in unacceptable loss of analyte and studies are underway to develop a water removal system that results in minimal loss of hydrophilic compounds; at present the most commonly employed drying system in electronic nose systems is Naphion® tubing (Miele, 2000).

Breath analysis generally requires highly specific analytical methods that are capable of accurate discrimination between volatile compounds with similar physical and chemical properties. Volatile compounds such as methane and isoprene are present in breath at relatively high concentrations (McKay *et al.*, 1985; Jones *et al.*, 1995), although they are not thought to be associated with any specific pathogenic processes. Therefore, specificity for the compounds of interest in breath must be demonstrated, since cross-reaction with chemically similar gases that are derived from normal metabolic processes would render the test useless for clinical investigation. The electronic nose does not provide such specific identification of volatile compounds, and in this study pentane, isoprene and hexane were poorly discriminated. The response of a composite polymer sensor-array to mixtures of compounds is a linear combination of the responses to the individual analytes (Severin *et al.*, 1996). Since breath analysis requires sharp discrimination between volatile compounds normally present in breath (methane and

isoprene) and compounds associated with disease (ethane and pentane), the electronic nose may lack the specificity necessary for clinical application.

The electronic nose may be of most use for analysis of exhaled breath in conditions that result in high concentrations of specific compounds, for example, exhaled ketones in diabetes. Other conditions such as pulmonary infection and neoplasia may result in evolution of pathognomic series of volatile compounds that are at high enough concentration to permit their use as disease markers (Phillips *et al.,* 1999). The electronic nose may be most successfully applied for analysis of breath where the analytes of interest are the dominant compounds; this instrument is likely to be less successful in detecting very specific analytes at low concentrations, such as pentane and ethane. An example of a pathological condition that may result in the evolution of specific compounds at high concentration in breath is pulmonary haemorrhage in the horse. Exercise induced pulmonary haemorrhage (EIPH) is a common and possibly physiological condition that occurs in most horses exercising at high intensity. It is thought to be one of the most important veterinary problems facing the racing industry (West *et al.,* 1993), yet there is no simple method for the diagnosis of this condition. An electronic nose assay may be capable of detecting a "blood odour" in the exhaled breath of horse with EIPH and could potentially be used as a non-invasive device for diagnosis of this condition.

GC and GC-MS may be the optimum methods for detection of hydrocarbons in exhaled breath, but the electronic nose could have exciting applications in other areas of veterinary clinical investigation. The electronic nose could be an invaluable point-of-care tool, allowing early diagnosis of disease and rapid implementation of appropriate therapeutic measures.

CHAPTER 6 GENERAL DISCUSSION AND CONCLUSIONS

The analysis of exhaled breath is an exciting and rapidly expanding area of medical tecnology. Increasing demands for non-invasive methods for diagnosis of disease and for health screening has led to an upsurge in interest in the analysis of markers of disease in breath. The studies in this report describe the application of advances in breath analysis in veterinary medicine.

6.1 STABLE ISOTOPE BREATH TESTS

The assessment of gastrointestinal transit presents a particular problem to the veterinary clinician. Currently available methods such as radiography and radioscintigraphy are time consuming and in some cases expensive to perform, and generally require that the animal is restrained or sedated. Gastrointestinal transit can be measured in man using a new generation of non-invasive stable isotope breath tests (Swart and van den Berg, 1998). These tests are rapidly gaining popularity as investigative methods in human medicine and a European Concerted Action Plan (BIOMED PL 93-2139) has been established specifically to exploit advances in stable isotope breath test technology for investigation of functional and metabolic gastrointestinal disorders. This study described the use of the ^{13}C-OBT and the ^{13}C-LUBT for the assessment of gastric emptying and OCTT in the dog. The results revealed that collection of exhaled breath could be performed quickly, easily, and with minimal disturbance of the animal. The data produced could be fitted by mathematical models derived for analysis of gastric emptying breath tests, and reproducibility was comparable to previous reports of this test in man. Furthermore, the ^{13}C-OBT parameters were altered by increased test meal

energy density, a condition known to delay the rate of gastric emptying. Simultaneous application of the ^{13}C-OBT and the ^{2}H-octanoic acid saliva test confirmed that post-gastric processing of octanoic acid confers a time delay on the recovery of breath $^{13}CO_2$ in the dog. These results support the further validation of the ^{13}C-OBT and the ^{13}C-LUBT in the dog. Of particular importance is the correlation of the ^{13}C-OBT and the ^{13}C-LUBT against reference methods for assessment of gastrointestinal transit, to validate the tests for application in the dog and to quantify the delay imposed on the test by the absorption and metabolism of the labelled substrate. Following validation of the ^{13}C-OBT and the ^{13}C-LUBT, clinical studies are required to establish the sensitivity and specificity of these tests for detection of disordered gastrointestinal transit in the dog. The possibility that pathological conditions and pharmacological agents may alter the kinetics of substrate absorption and metabolism, must always be considered.

6.2 OXIDATIVE STRESS AND THE HYDROCARBON BREATH TEST

Oxidative stress is a non-specific physiological response to diverse stimuli including drugs, disease, exercise and stress. Oxidative stress is also associated with the ageing process and the ability of an animal to withstand oxidative stress is a direct function of its lifespan (Kapahi *et al.,* 1999). The oxidative stress process carries striking parallels with the concept of whole animal stress and the "general adaptation syndrome" described by Hans Selye in the 1930's (Selye, 1936). The studies that Selye carried out on the responses and resistance of animals to physiological and pharmacological stress were possibly the effects of oxidative stress at a systemic level and whole animal level (Selye, 1950). Selye's description of the "adaptation energy" of the animal encompasses the concept of anti-oxidant status that medicine is striving to find a way of measuring today. Selye defined his adaptation energy as:

"...a finite quantity of which each organism has only a given amount. Presumably, genetic factors determine just how much of it is apportioned to each new-born individual. Yet whatever the total quantity, it may be used up very slowly during a long monotonously restful existence, protected against every kind of exposure, or it may be consumed rapidly to maintain life under ever-changing conditions which require extreme efforts of adaptation." (Selye, 1950).

These conclusions were perhaps the first recognition of oxidative stress, albeit 30 years before the existence of *in vivo* free radicals was reported. Selye also remarked that the ability to isolate, regenerate or transmit the "adaptation energy" would do more for medicine than he could ever hope to accomplish through adaptive hormones. Today, the manipulation of *in vivo* oxidative status is the subject of much research, and the potential for anti-oxidant measures to prevent disease and even prolong life is increasingly recognised. Selye's treatise describing his life's work was called "*The Stress of Life*" (1976), which truly defines oxidative stress, since it is generated by the very process that maintains life (aerobic respiration). The parallels between the original work defining physiological "stress" in animals (Selye, 1950), and oxidative stress have not been examined. This could easily be addressed by repeating the original studies that Selye performed in animals, using modern techniques to monitor what is now termed oxidative stress.

Oxidative stress is not a pathological process in itself, and could never be used to diagnose disease, but rather to monitor health status and assess the effects of pharmacological therapy or lifestyle changes on the pro-oxidant effects of disease. The non-invasive and simple nature of the breath test makes it an attractive method for monitoring of oxidative stress. Many breath tests are available for assessment of breath markers of oxidative stress in the gaseous phase and in the exhaled breath condensate.

Breath ethane, pentane and nitric oxide have been used as gaseous markers of oxidative stress in exhaled breath (Risby and Sehnert, 1999), while hydrogen peroxide, thiobarbituric acid reacting substances (TBARS) and isoprostanes have been detected in the exhaled breath condensate (Montuschi *et al.,* 2000; Antczak *et al.,* 2000). Presently the application of the breath test for assessment of oxidative stress is limited by the complexity and expense of the technology required for breath analysis. The availability of simple and inexpensive methods for measuring markers of oxidative stress in breath would permit more widespread application of these tests, and emergence of the assessment of oxidative status as a valuable clinical tool for monitoring of disease status and efficacy of therapeutic intervention.

The studies in this report detail the preliminary stages of the development of a breath pentane test for assessment of *in vivo* lipid peroxidation in veterinary medicine. The technical difficulties of detecting breath hydrocarbons described in previous studies were also evident in this work. Pentane must be collected and analysed at relatively high temperatures, since its boiling point (36°C) predisposes to condensation on experimental apparatus. The very low boiling point of ethane (-88°C) makes concentration of this compound difficult. Ambient levels of hydrocarbons are high and variable, relative to the levels found in exhaled air, and concentration of breath samples is necessary before analysis. All of these technical difficulties contribute to the complexity of the hydrocarbon breath test and at present preclude the application of this method outside the research laboratory. Further investigation is also necessary into the exact origin of exhaled hydrocarbon. Previous studies have indicated that exhaled hydrocarbons may originate from intestinal fermentation (Hiele *et al.,* 1991), environmental contamination (Phillips, 1997) and other compounds present in breath (Springfield and Levitt, 1994). The true origin of breath hydrocarbons has never been

conclusively shown. More rigorous validation of this method is necessary before it can be applied for clinical investigation. There is currently no ideal method for assessment of lipid peroxidation in the living animal, and despite its disadvantages the hydrocarbon breath test is one of the most widely applied measures of *in vivo* lipid peroxidation. The measurement of serum isoprostanes holds great promise as a sensitive and specific indicator of lipid peroxidation (Morrow *et al.*, 1990). However, the measurement of isoprostanes (by GC-MS or ELISA) involves several cumbersome sample preparation steps, and this method could not be easily applied in the clinical setting. There is an urgent need for development of simple and accurate techniques for investigation of the significance of oxidative stress *in vivo*, and the importance of this process in disease.

Headspace gas-chromatography of volatile oxidation products of ω-3 and ω-6 fatty acids is an interesting method for detection of antioxidant activity, that is worthy of further investigation. This method could be applied to assess oxidative status in liquid or solid biological samples, and even in organ baths (Frankel, 1999). The oxidative susceptibility of isolated hepatocytes (Smith *et al.*, 1982) erythrocyte membranes (Frankel and Tappel, 1991) and lipids (Hans *et al.*, 1996) has been assessed using this method. Headspace GC enabled simultaneous assessment of myocardial function and oxidative stress in an isolated heart organ bath (Salem *et al.*, 1994). This method could be a useful way of assessing lipid peroxidation *in vivo*, that requires no sample preparation and could be valuable for investigation of the efficacy of anti-oxidant measures and for detecting oxidative stress status in biological samples.

6.3 ELECTRONIC NOSE TECHNOLOGY

Application of advances in odour sensing or electronic nose technology for analysis of exhaled breath would be a major progression in the simplification of the breath test.

The electronic nose is sensitive, can be produced relatively cheaply and perhaps most importantly, can be used to make real-time measurements, away from the research laboratory. Therefore, the analysis of exhaled breath using the electronic nose appears to be worthy of further investigation, and could be a major step forward in the development of the next generation of non-invasive breath tests for monitoring of health status. The present studies suggested that the hydrocarbons of interest in breath (pentane and ethane) would not be adequately separated from other compounds present in breath (methane) to permit application of a gas-sensor array for detection of breath hydrocarbons. However, the electronic nose could be a useful tool for detection of breath "odours" that may be produced during specific pathological processes. For example EIPH in horses may be associated with characteristic breath odours. Pulmonary infection and neoplasia have been shown to be associated with specific breath "odour" as detected using the electronic nose in man (Hanson and Steinberger, 1997; D'Amico 2000). The electronic nose could be a valuable investigative tool in other areas of veterinary medicine. An instrument that could detect sepsis in the headspace of body fluids would a very valuable tool, enabling rapid instigation of appropriate anti-microbial or surgical therapy. Several electronic nose assays that could detect the presence of bacteria in culture headspace (Gardner *et al.,* 1998) and in urine (Aathithan *et al.,* 2001) have been described. Other body fluids where rapid detection of sepsis could be a useful diagnostic aid include milk, cerebro-spinal, synovial and peritoneal fluid. A sensor-array that could detect synovial fluid would identify penetration of a synovial structure, and this would be a very valuable instrument in the assessment of wounds. An electronic nose assay that could discriminate between CSF and serum was recently described (Thayler *et al.,* 2000), suggesting that the detection of synovial fluid may be possible.

The evolution of the electronic nose as a clinical tool is still in its infancy and further validation of this method is necessary before routine application is possible. Gas-sensor arrays are subject to several technical problems that must be addressed, including water and temperature sensitivity, sensor drift, baseline variation, sensor poisoning and ageing (Pavlou and Turner, 2000). Realistic clinical application would require an instrument that is stable and that produces reliable results that are independent of ambient conditions. Formal demonstration of assay sensitivity, specificity, repeatability and sample throughput will be necessary, if the electronic nose is to meet industrial standards (Mielle, 2000). Correlation of electronic nose data with reference methods such as GC-MS is rarely carried out, although demonstration that the electronic nose reacts specifically to volatile compounds would greatly support the validation of this method.

Breath microanalysis is an investigative method that is of considerable potential for non-invasive monitoring of health status, and early detection of disease. Advances in analytical technology are producing instruments that are capable of detecting compounds at low concentrations, that may in the future allow realistic application of the breath test as a clinical investigative tool.

REFERENCES

Aathithan A, Plant JC, Chaudry AN, *et al.* Diagnosis of bacteriuria by detection of volatile organic compounds in urine using an automated headspace analyzer with multiple conducting polymer sensors. *J Clin Microbiol* 2001;39:2590-2593

Aeberhard PF, Magnenat LD and Zimmermann WA. Nervous control of migratory myoelectric complex of the small bowel. *Am J Physiol* 1980;238:G102-8.

Aghdassi E and Allard JP. Breath alkanes as a marker of oxidative stress in different clinical conditions. *Free Radic Biol Med* 2000;28:880-6.

Ahluwalia NK and Thompson DG. Ultrasonography. In: Kumar D and Wingate D (eds) *An Illustrated Guide to Gastrointestinal Motility*, 1993, Churchill-Livingston, Edinburgh, pp 242-255.

Aikens J and Dix TA. Perhydroxyl radical (HOO˙) initiated lipid peroxidation. *J Biol Chem* 1991;23:15091-15098.

Ainsworth DM, and Biller DS. Respiratory system. In: Reed SM, and Bayly WM, *Equine Internal Medicine*, 1999, WB Saunders, Pennsylvania, pp289.

Allan FJ, Guilford GW, Robertson ID et al. Gastric emptying of solid radiopaque markers in healthy dogs. Vet Radiol Ultrasound 1996;37:336-344.

Allard JP, Aghdassi E, Chau J, *et al.* Oxidative stress and plasma antioxidant micronutrients in humans with HIV infection. *Am J Clin Nutr* 1998;67:143-7.

Allen KG, Huang CJ and Morin CL. Determination of picomole quantities of hydroperoxides by a coupled glutathione peroxidase and glutathione disulfide specific glutathione reductase assay. *Anal Biochem* 1990;186:108-11.

Allerheiligen SR, Ludden TM and Burk RF. The pharmacokinetics of pentane, a by-product of lipid peroxidation. *Drug Metab Dispos* 1987;15:794-800.

Allescher HD, Tougas G, Vergara P, *et al.* Nitric oxide as a putative nonadrenergic noncholinergic inhibitory transmitter in the canine pylorus in vivo. *Am J Physiol* 1992;G695-G702.

Allescher HD and Daniel EE. Role of NO in pyloric, antral, and duodenal motility and its interaction with other inhibitory mediators. *Dig Dis Sci* 1994;39:73S-75S.

Andreoni KA, Kazui M, Cameron DE, *et al.* Ethane: a marker of lipid peroxidation during cardiopulmonary bypass in humans. *Free Radic Biol Med* 1999;26:439-45.

Antczak A, Kurmanowska Z, Kasielski M, *et al.* Inhaled glucocorticosteroids decrease hydrogen peroxide level in expired air condensate in asthmatic patients. *Respir Med* 2000;94:416-21.

Art T, Kirschvink N, Smith N, *et al.* Indices of oxidative stress in blood and pulmonary epithelium lining fluid in horses suffering from recurrent airway obstruction. *Equine vet J* 1999:31:397-401.

Arterbery VE, Pryor WA, Jiang L, *et al.* Breath ethane generation during clinical total body irradiation as a marker of oxygen-free-radical-mediated lipid peroxidation: A case study. *Free Radic Biol Med* 1994;17:569-576.

Azpiroz F and Malagelada J-R. Pressure activity patterns in the canine proximal stomach: response to distension. *Am J Physiol* 1994;247:G265-G272.

Babbs CF. Oxygen radicals in ulcerative colitis. *Free Radic Biol Med* 1992;13333:169-181.

Babior BM, Kipnes RS and Curnutte JT. Biological defense mechanisms. The production by leukocytes of superoxide, a potential bactericidal agent. *J Clin Invest* 1973;52:741-744.

Babior BM, Curnutte JT and McMurrich BJ. The particulate superoxide-forming system from human neutrophils. Properties of the system and further evidence

Babior BM, Curnutte JT and McMurrich BJ. The particulate superoxide-forming system from human neutrophils. Properties of the system and further evidence supporting its participation in the respiratory burst. *J Clin Invest* 1976;58:989-996.

Balagopalakrishna C, Manoharan PT, Abugo OO, *et al.* Production of superoxide from hemoglobin-bound oxygen under hypoxic conditions. *Biochemistry* 1996;21:6393-6398.

Barker GR, Cochrane GM, Corbett GA, *et al.* Actions of glucose and potassium chloride on osmoreceptors slowing gastric emptying. *J Physiol* 1974;237:183-186.

Basilisco G and Phillips SF. The small intestine and ileo-caecal region. In: Kumar D and Wingate D (eds) *An Illustrated Guide to Gastrointestinal Motility*, 1993, Churchill-Livingston, Edinburgh, pp 410-426.

Bauer AJ and Sanders KM. Gradient in excitation-contraction coupling in canine gastric antral circular muscle. *J Physiol* 1985;369:283-94.

Bayliss WM and Starling EH. The movement and innervation of the large intestine. *J Physiol* 1900a;26:107-118.

Bayliss WM and Starling EH. The movement and innervation of the small intestine. *J Physiol* 1900b;26:125-140.

Becker JM, and Kelly KA. Antral control of canine gastric emptying of solids. *Am J Physiol* 1983; 245: G334 - G338.

Beerda B, Schilder MBH, Janssen NSCRM, *et al.* The use of saliva cortisol, urinary cortisol, and catecholamine measurements for a non-invasive assessment of stress responses in dogs. *Horm Behav* 1996;30:272-279.

Benamouzig R, Mahe S, Tsakiris L, *et al.* Effect of carbonated water on gastric emptying of liquids monitored by ultrasonography and [^{13}C]-glycine breath test. *Annual Meeting of the American Gastroenterological Association*, Florida, 1999;A957.

Benini L, Sembenini C, Heading RC, *et al.* Simultaneous measurement of gastric emptying of a solid meal by ultrasound and by scintigraphy. *Am J Gastroenterol* 1999;94:2861-5.

Bjorkman DJ, Moore JG, Klein PD, *et al.* ^{13}C-bicarbonate breath test as a measure of gastric emptying. *Am J Gastroenterol* 1991;86:821-823.

Bluck LJC, French S, Halliday D, *et al.* Experiments with deuterated octanoic acid to explain the relation between scintigraphy and the ^{13}C breath test for gastric emptying. Proccedings of the Annual BIOMED-SIGN Meeting, Glasgow, June 1999.

Bluck LJC, Harding M, Wright A, *et al.* Measurement of gastric emptying by simultaneous dosing with ^{13}C and ^{2}H octanoic acid. *Gut* 1998;43:S30.

Bolondi L, Bortolotti M, Santi V *et al.* Measurement of gastric emptying time by real-time ultrasonography. *Gastroenterology* 1985;89:752-9.

Bond JH and Levitt MD. Investigation of small bowel transit time in man utilizing pulmonary hydrogen (H_2) measurements. *J Lab Clin Med* 1975;85:546-555.

Braden B, Adams S, Duan LP, *et al.* The [^{13}C]acetate breath test accurately reflects gastric emptying of liquids in both liquid and semisolid test meals. *Gastroenterology* 1995;108:1048-55.

Brener W, Hendrix TR and McHugh PR. Regulation of the gastric emptying of glucose. *Gastroenterology* 1983;85:76-82.

Brogna A, Ferrara R, Bucceri AM, *et al.* Gastric emptying rates of solid food in relation to body mass index: an ultrasonographic and scintigraphic. *Eur J Radiol* 1998;27:258-263.

Bromer MQ, Kantor SB, Wagner DA, *et al.* Measurement of solid phase gastric meptying with a simplified muffin meal using breath testing with either ^{13}C-octanoate or ^{13}C-acetate. *Proceedings of the Annual Meeting of the American Gastroenterological Association*, Georgia, May 2001;2370.

Bromer MQ, Parkman HP. Office-based testing for gastric emptying: a breath away? *J Clin Gastroenterol* 2001;32:374-6.

Brophy CM, Moore JG, Christian PE, *et al.* Variability of gastric emptying measurements in man employing standardized radiolabeled meals *Dig Dis Sci* 1986; 31:799-806.

Brown BP, Ketelaar MA, Schulze-Delrieu K, *et al.* Strenuous exercise decreases motility and cross-sectional area of human gastric antrum. A study using ultrasound. *Dig Dis Sci* 1994;39:940-945.

Bruce SJ, Guilford WG, Hedderley DI, *et al.* Development of reference intervals for the large intestinal transit of radiopaque markers in dogs. *Vet Radiol Ultrasound* 1999;40:472-476.

Bueno L, Rayner V and Ruckebusch Y. Initiation of migrating myoelectric complex in dogs. *J Physiol* 1981;316:309-318.

Bueno L and Ferre J-L. Central regulation of intestinal motility by somatostatin and cholecystokinin octapeptide. *Science* 1982;25:1427-1429.

Bueno L, Fioramonti J, Rayner V, *et al.* Effects of motilin, somatostatin, and pancreatic polypeptide on the migrating myoelectric complex in pig and dog. *Gastroenterology* 1982;82:1395-1402.

Bueno L, Fioramonti J, Fargeas MJ, *et al.* Neurotensin: a central neuromodulator of gastrointestinal motility in the dog. *Am J Physiol* 1985;248:G15-9.

Bueno L, Fergeas MJ, Gue M, *et al.* Effect of corticotrophin-releasing factor on plasma motilin and somatostatin levels and gastrointestinal motility in dogs. *Gastroenterology* 1986;91:884-889.

Bult H, Boeckxstaens GE, Pelckmans PA, *et al.* Nitric oxide as an inhibitory non-adrenergic non-cholinergic neurotransmitter. *Nature* 1990;345:346-347.

Burns J, and Fox SM. The use of a barium meal to evaluate total gastric emptying time in the dog. *Vet Radiol* 1986;27:169-172.

Burrows CF, Bright RM, and Spencer CP. Influence of dietary composition on gastric emptying and motility in dogs: Potential involvement in acute gastric dilatation. *Am J Vet Res* 1985;46:2609-2612.

Calbet JAL and MacLean DA. Role of caloric content on gastric emptying in humans. *J Physiol* 1997;498:553-559.

Cannon WB. The movement of the stomach studied by means of rontgen rays. *Am J Physiol* 1898;1:359-382.

Cannon WB and Leib CW. The receptive relaxation of the stomach. *Am J Physiol* 1910;267-273.

Cappello G, Malatesta MG, Ferri A, *et al.* Gastric emptying of a solid-liquid meal measured with ^{13}C-octanoic acid breath test and real-time ultrasonography: a comparative study. *Am J Gastroenterol* 2000;59:3097-3100.

Caride VJ, Prokop EK, Troncale FJ, *et al.* Scintigraphic determination of small intestinal transit time: comparison with the hydrogen breath technique. *Gastroenterology* 1984;86:714-20.

Chao WH, Askew EW, Roberts DE, *et al.* Oxidative stress in humans during work at moderate altitude. *J Nutr* 1999;129:2009-12.

Chey WD, Shapiro B, Zawadski A, *et al.* Gastric emptying characteristics of a novel (13)C-octanoate-labeled muffin meal. *J Clin Gastroenterol* 2001;32:394-399.

Chiba T, Thomforde GM, Kost LJ, *et al.* Motilides accelerate regional gastrointestinal transit in the dog. *Aliment Pharmacol Ther* 2000;14:955-960.

Chirico S. High-performance liquid chromatography-based thiobarbituric acid tests. *Methods Enzymol* 1994;233:314-8.

Choi MG, Camilleri M, Burton DD, *et al.* Reproducibility and simplification of ^{13}C-octanoic acid breath test for gastric emptying of solids. *Am J Gast* 1998a; 93:92-98.

Choi MG, Camilleri M, Burton DD, *et al.* Dose-related effects of N-demethyl-N-isopropyl-8, 9-anhydroerythromycin A 6,9-hemiacetal on gastric emptying of solids in healthy human volunteers. *J Pharmacol Exp Ther* 1998b;285:37-40.

Christian PE, Datz FL, Sorenson JA, *et al.* Technical factors in gastric emptying studies. *J Nucl Med* 1983;24:264-268.

Clements JA, Heading RC, Nimmo WS, *et al.* Kinetics of acetaminophen absorption and gastric emptying in man. *Clin Pharmacol Ther* 1978;24:420-31.

Code CF and Marlett JA. The interdigestive myo-electric comlex of the stomach and small bowel of dogs. *J Physiol* 1975;246:289-309.

Cominacini L, Garbin U, Davoli A, *et al.* A simple test for predisposition to LDL oxidation based on the fluorescence development during copper-catalyzed oxidative modification. *J Lipid Res* 1991;32:349-58.

Conklin JL. Anatomy of the neuromuscular apparatus of the gastrointestinal tract. In: Anuras SL (ed) *Motility Disorders of the Gastrointestinal Tract.* Raven Press New York, 1992, pp 1-26.

Cornetta AM, Simpson KW, and Strauss-Ayali D. Use of a [13C]urea breath test for detection of gastric infection with *Helicobacter spp.* in dogs. *Am J Vet Res* 1998;59:1364-9.

Corongiu FP, Banni S. Detection of conjugated dienes by second derivative ultraviolet spectrophotometry. *Methods Enzymol* 1994;233:303-10.

Cortot A, Phillips SF and Malagelada J-R. Gastric emptying of lipids after ingestion of a solid-liquid meal in humans. *Gastroenterology* 1981;80:922-927.

D'Amico R. Electronic Nose Applications. *Network of Excellence on Artificial Olfactory Sensing (NOSE)*, Proccedings of Summer School, 2000, Barcelona.

Daugherty MS, Ludden TM and Burk RF. Metabolism of ethane and pentane to carbon dioxide by the rat. *Drug Metab Dispos* 1988;16:666-671.

Davenport HW. The neuromuscular apparatus of the digestive tract. In: Davenport HW, *Physiology of the Digestive Tract*, 1982; pp2-20.

Davis JM, Lamb DR, Burgess WA, *et al.* Accumulation of deuterium oxide in body fluids after ingestion of D_2O-labeled beverages. *J App Physiol* 1987;63:2060-2066.

Davies MJ and Slater TF. Studies on the metal-ion and lipoxygenase-catalysed breakdown of hydroperoxides using electron-spin-resonance spectroscopy. *Biochem J* 1987;245:167-173.

Delbende B, Perri F, Couturier O, *et al.* ^{13}C-octanoic acid breath test for gastric emptying measurement. *Eur J Gastroenterol Hepatol* 2000;12:85-91.

DiNatale C, Macagnano A, Paolesse R, *et al.* Human skin odour analysis by means of an electronic nose. *Sens Actuat* 2000;65:216-219.

DiNatale C, Mantini A, Macagnano A, *et al.* Electronic nose analysis of urine samples containing blood. *Physiol Meas* 1999;20:377-384.

Doleman BJ, Severin EJ and Lewis NS. Trends in odor intensity for human and electronic noses: Relative roles of odorant vapor pressure vs. molecularly specific odorant binding. *Proc Natl Acad Sci* 1998;95:5442-5447.

Donovan DH and Menzel DB. Mechanisms of lipid peroxidation: Iron catalyzed decomposition of fatty acid hydroperoxides as the basis of hydrocarbon evolution *in vivo*. *Experientia* 1978;34:775-776.

Drewe J, Hildebrand P, Descloux L, *et al.* Further validation of the [^{13}C]octanoic acid breath test for gastric emptying of solids. *Gastroenterology* 1998;114:A745.

Duan L-P, Braden B, Caspary WF, *et al.* Influence of cisapride on gastric emptying of solids and liquids monitored by ^{13}C breath tests. *Dig Dis Sci* 1995;40:2200-2206.

Ebert CC, Shah D, Jones MP, *et al.* Reproducibility of solid phase gastric emptying (GE) using ^{13}C-spirulina breath tests. *Proceedings of the Annual Meeting of the American Gastroenterological Association*, Georgia, May 2001;2368.

Edelbroek M, Horowitz M, Maddox A, *et al.* Gastric emptying and intragastric distribution of oil in the prescence of a liquid or a solid meal. *J Nucl Med* 1992;33:1283-1290.

Eeckhout C, De Wever I, Peeters T, *et al.* Role of gastrin and insulin in postprandial disruption of migrating complex in dogs. *Am J Physiol* 1978;235:E666-9.

Ehrlein H-J, Schemann M and Siegle M-L. Motor patterns of small intestine determined by closely spaced extraluminal transducers and videofluoroscopy. *Am J Physiol* 1987;253:G259-G267.

Elliott-Martin RJ, Mottram TT, Gardner JW, *et al.* Preliminary investigation of breath sampling as a monitor of health in dairy cattle. *J agric Engng Res* 1997;67:267-275.

Evans CD, List GR, Dolev A, *et al.* Pentane from thermal decomposition of lipoxidase-derived products. *Lipids* 1967;2:432-434.

Farrugia G, Nitecki S, Harty GJ, *et al.* The effect of flufenamic acid on gastrointestinal myoelectrical activity and transit time in dogs. *Gut* 1998;42:258-265.

Feinle C, Kunz P, Boesiger P, *et al.* Scintigraphic validation of a magnetic resonance imaging method to study gastric emptying of a solid meal in humans. *Gut* 1999;44:106-111.

Fich A, Phillips SF, Neri M, *et al.* Regulation of postprandial motility in the canine ileum. *Am J Physiol* 1989;259:G767-G774.

Flury B and Riedwyl H. *Multivariate Statistics: A Practical Approach.* Chapman and Hall, 1988, London.

Foxthrelkeld JET. Motility and regulatory peptides. In: Kumar D and Wingate D (eds) *An Illustrated Guide to Gastrointestinal Motility*, 1993, Churchill-Livingston, Edinburgh, pp 103-149.

Frank H, Hintze T, Bimboes D, *et al.* Monitoring lipid peroxidation by breath analysis: Endogenous hydrocarbons and their metabolic elimination. *Toxicol Appl Pharmacol* 1980;56:337-344.

Frank H, Thiel D and MacLeod J. Mass spectrometric detection of cross-linked fatty acids formed during radical-induced lesion of lipid membranes. *Biochem J* 1989;260:873-8.

Frankel EM and Tappel AL. Headspace gas chromatography of volatile lipid peroxidation products from human red blood cell membranes. *Lipids* 1991;26:479-484.

Frankel EN. Antioxidant activity by headspace gas chromatography of volatile oxidation products of ω-6 and ω-3 polyunsaturated lipids. *Methods Enzymol* 1999;299:190-201.

Freeman BA and Crapo JD. Biology of disease: free radicals and tissue injury. *Lab Invest* 1982;47:412-26.

Gardner JW, Craven M, Dow C, *et al.* The prediction of bacteria type and culture growth phase by an electronic nose with a multi-layer perception network. *Meas Sci Technol* 1998;9:120-127.

Gardner, J. Conductivity change based sensors and polymer sensors. *Network of Excellence on Artificial Olfactory Sensing (NOSE)*, Proceedings of Summer School, 2000, Barcelona.

Gelmont D, Stein RA and Mead JF. The bacterial origin of rat breath pentane. *Biochem Biophys Res Comm* 1981;102:932-936.

Gerston MD, Kirchgessner AC and Wade PR. Functional anatomy of the enteric nervous system. In: *Physiology of the Gastrointestinal Tract*, Johnson LR (ed), Raven Press, New York, 1994, pp 381-423.

Geypens B, Evenepoel P, Maes B, *et al.* The lactose-(^{13}C)-ureide breath test in combination with the (^{14}C)-octanoate breath test to assess pharmacological

modulation by erythromycin and propantheline of proximal gastro-intestinal transit. *Gastroenterology* 1998b;114:G3117.

Geypens B, Evenpoel P, Peeters M, *et al.* Direct demonstration of the effect of lactulose on colonic bacterial metabolism by application of lactose-(^{15}N)-ureide. *Gastroenterology* 1998c;114:L0196.

Geypens B, Maes B, Ghoos Y, *et al.* Correlation of ileal emptying and gastric emptying calculated from a simultaneous application of two breath tests. *Gastroenterology* 1998d; 114:G3114.

Geypens B, van den Driessche M, Maes B, *et al.* Simultaneous measurement of gastric emptying and oro-cecal transit in children using ^{13}C-breath tests. *Gastroenterology* 1998e;114:A3116.

Geypens B, Ghoos Y, Rutgeerts P, *et al.* Pharmacological modulation of orocecal transit by antidiarrheals monitored by the lactose-[^{13}C]ureide breath test. *Gastroenterology* 1999b;115:G4333.

Geypens B, Maes B, Luypaerts A, *et al.* Double deconvolution of breath tests to assess the pharmacological modulation by cisapride of proximal gastrointestinal transit. *Gastroenterology* 1999c;115:G4332.

Geypens B, Suenaert P, Vos R, *et al.* Breath tests after cecal instillation of lactose-[^{13}C]ureide show immediate yet diverse colonic bacterial metabolism. *Gastroenterology* 2000;118:5396.

Ghoos YF, Maes BD, Geypens BJ, *et al.* Measurement of gastric emptying rate of solids by means of a carbon-labelled octanoic acid breath test. *Gastroenterology* 1993;104:1640-1647.

Goggin JM, Hoskinson JJ, Kirk CA, *et al.* Comparison of gastric emptying times in healthy cats simultaneously evaluated with radiopaque markers and nuclear scintigraphy. *Vet Radiol Ultrasound* 1999;40:89-95.

Granger DN, Rutili G and McCord JM. Superoxide radicals in feline intestinal ischemia. *Gastroenterology* 1981;81:22-29.

Griffith GH, Owen GM, Kirkman S *et al.* Measurement of rate of gastric emptying using chromium-51. *Lancet* 1966;1:1244-5.

Grisham MB and Granger DN. Neutrophil-mediated mucosal injury. Role of reactive oxygen metabolites. *Dig Dis Sci* 1988;33:6S-15S.

Grisham MB and Yamada T. Neutrophils, nitrogen oxides, and inflammatory bowel disease. *Ann N Y Acad Sci* 1992;664:103-115.

Groves WA, Zellers ET. Prototype instrument employing a microsensor array for the analysis of organic vapors in exhaled breath. *Am Ind Hyg Assoc J* 1996;57:1103-8.

Groves WA, Zellers ET and Frye GC. Analyzing organic vapours in exhaled breath using a surface acoustic wave sensor array with preconcentrator: Selection and characterization of the preconcentrator adsorbent. *Anal Chim Acta* 1998;371:131-143.

Gruber P, Rubinstein A, Hon Kin Li V, *et al.* Gastric emptying of nondigestible solids in the fasted dog. *J Pharm Sci* 1987;76:117-121.

Gue M, Honde C, Pascaud X, *et al.* CNS blockade of acoustic stress-induced gastric motor inhibition by kappa-opiate agonists in dogs. *Am J Physiol* 1988;254:G802-G807.

Gue M, Peeters T, Depoortere G, *et al.* Stress-induced changes in gastric emptying, postprandial motility and plasma gut hormone levels in dogs. *Gastroenterology* 1989;97:1101-1107.

Guilford WG, Lawoko D, and Allan FJ. Accuracy of localizing radiopaque markers by abdominal radiography and correlation between their gastric emptying rate and that of a canned food in dogs. *Am J Vet Res* 1997;58:1359-1363.

Gutteridge JM and Quinlan GJ. Malondialdehyde formation from lipid peroxides in the thiobarbituric acid test: the role of lipid radicals, iron salts, and metal chelators. *J Appl Biochem* 1983;5:293-299.

Gutteridge JMC and Halliwell B. The measurement and mechanism of lipid peroxidation in biological systems. *Trends in Biochemical Sciences* 1990;1615:129-135.

Gutteridge JMC. Lipid peroxidation and antioxidants as biomarkers of tissue damage. *Clin Chem* 1995;41:1819-1828.

Haba T and Sarna SK. Regulation of gastroduodenal emptying of solids by gastropyloroduodenal contractions. *Am J Physiol* 1993;G261-G271.

Hall KE, El-Sharkawy TY and Diamant NE. Vagal control of migrating motor complex in the dog. *Am J Physiol* 1982;243:G276-84.

Hall KE, Diamant NE, Sharkawy EL, *et al.* Effect of pancreatic polypeptide on canine migrating motor complex and plasma motilin. *Am J Physiol* 1983;245:G178-185.

Hall JA, Willer RL, Seim HB, *et al.* Gastric emptying of nondigestible radiopaque markers after circumcostal gastropexy in clinically normal dogs and dogs with gastric dilatation-volvulus. *Am J Vet Res* 1992;53:1961-1965 .

Halliwell B and Gutteridge JMC. *Free Radical Biology and Medicine.* Oxford Science, Oxford UK;1999.

Hammer J, Hammer K and Kletter K. Lipids infused into the jejunum accelerate small intestinal transit but delay ileocolonic transit of solids and liquids. *Gut* 1998;43:111-116.

Hans P, Deby C, Deby-Dupont G, *et al.* Effect of propofol on in vitro lipid peroxidation induced by different free radical generating systems: a comparison with vitamin E. *J Neurosurg Anesthesiol* 1996;8:154-8.

Hanson III CW, and Steinberger HA. The use of a novel "electronic nose" to diagnose the presence of intrapulmonary infection. *Anaesthesiology* 1997;87:A269.

Heading RC, Nimmo J, Prescott LF, *et al.* The dependence of paracetamol absorption on the rate of gastric emptying. *Br J Pharmacol* 1973;47:415-21.

Heine WE, Berthold HK and Klein PD. A novel stable isotope breath test: ^{13}C-labeled glycosyl ureides used as noninvasive markers of intestinal transit time. *Am J Gastroenterol* 1995;90:93-98.

Hiele M, Ghoos Y, Rutgeerts P, *et al.* Influence of nutritional substrates on the formation of volatiles by the fecal flora. *Gastroenterology* 1991;100:1597-1602.

Hietanen E, Bartsch H, Bereziat J-C, *et al.* Diet and oxidative stress in breast, colon and prostrate cancer patients: a case-control study. *Eur J Clin Nutr* 1994;48:575-586.

Hinder RA and Kelly KA. Canine gastric emptying of solids and liquids. *Am J Physiol* 1977;233:E335-E340.

Hinder RA. And van Garde S. Individual and combined roles of the pylorus and the antrum in the canine gastric emptying of a liquid and a digestible solid. *Gastroenterology* 1983;84:281-286.

Holzer HH, Turkelson CM, Solomon TE, *et al.* Intestinal lipid inhibits gastric emptying via CCK and a vagal capsaicin-sensitive afferent pathway in rats. *Am J Physiol* 1994;267:G625-9.

Holzer P, Holzer-Petsche U and Leander S. A tachykinin antagonist inhibits gastric emptying and gastrointestinal transit in the rat. *Br J Pharmacol* 1986;89:453-459.

Hornof WJ, Koblik PD, Strombeck DR, *et al.* Scintigraphic evaluation of solid-phase gastric emptying in the dog. *Vet Radiol* 1989;30 242 – 248.

Hotz P, Hoet P, Lauwerys R, *et al.* Development of a method to monitor low molecular mass hydrocarbons in exhaled breath of man: preliminary evaluation of its interest for detecting a lipoperoxidation process in vivo. *Clinica Chemica Acta* 1987;162:303-310.

Houghton LA, Mangnall YF and Read NW. Effect of incorporating fat into a liquid test meal on the relation between intragastric distribution and gastric emptying in human volunteers. *Gut* 1990;31:1226-9.

Humad S, Zarling E, Clapper M, *et al.* Breath pentane excretion as a marker of disease activity in rheumatoid arthritis. *Free Radic Res Commun* 1988;5:101-106.

Hunt JN. Does calcium mediate slowing of gastric emptying by fat in humans? *Am J Physiol* 1983;244:G89-94.

Hunt JN and Stubbs DF. The volume and energy content of meals as determinants of gastric emptying. *J Physiol* 1975;245:209-225.

Hunt JN, Smith JL and Jiang CL. Effect of meal volume and energy density on the gastric emptying of carbohydrates. *Gastroenterology* 1985;89:1326-1330.

Husebye E. The patterns of small bowel motility: physiology and implications in organic disease and functional disorders. *Neurogastroenterol Mot* 1999;11:141-161.

Irvine EJ, Tougas G, Lappalainen R, *et al.* Reliability and interobserver variability of ultrasonographic measurement of gastric emptying rate. *Dig Dis Sci* 1993;38:803-10.

Iwanaga Y, Wen J, Thollander MS, *et al.* Scintigraphic measurement of regional gastrointestinal transit in the dog. *Am J Physiol* 1998;275:G904 - G910.

Jackson AA, Bundy R, Hounslow A, *et al.* Metabolism of lactose-[C-13]ureide and lactose-[N-15,N-15]ureide in normal adults consuming a diet marginally adequate in protein. *Clinical Science* 1999;97:547-555.

Jackson SJ, Bluck LJC and Coward WA. Effects of nutritional manipulation on gastric emptying: a comparison of the ^{13}C-OBT with deuterated octanoic acid. *Stable Isotope Mass Spectrometry Users Group (SIMSUG)* Proccedings of annual meeting, Glasgow 2001.

Jeejeebhoy KN. In vivo breath alkanes as an index of lipid peroxidation. *Free Radic Biol Med* 1991;10:191-193.

Jessup W, Dean RT and Gebicki JM. Iodometric determination of hydroperoxides in lipids and proteins. *Methods Enzymol* 1994;233:284-302.

Jian R, Vigneron N, Najean Y, *et al.* Gastric emptying and intragastric distribution of lipids in man. A new scintigraphic method of study. *Dig Dis Sci* 1982;27:705-711.

Jones AW, Lagesson V and Tagesson C. Origins of breath isoprene. *J Clin Pathol* 1995;48:979-80.

Kapahi P, Boulton ME and Kirkwood TBL. Positive correlation between mammalian life span and cellular resistance to stress. *Free Radic Biol Med* 1999;26:495-500.

Keane FB, DiMagno EP, Dozois RR, *et al.* Relationships among canine interdigestive exocrine pancreatic and biliary flow, duodenal motor activity, plasma pancreatic polypeptide, and motilin. *Gastroenterology* 1980;78:310-6.

Keinke O, Wulschke S and Ehrlein HJ. Neurotensin slows gastric emptying by a transient inhibition of gastric and a prolonged inhibition of duodenal motility. *Digestion* 1986;34:281-8.

Kelly KA, Code CF and Elveback LR. Patterns of canine gastric electrical activity. *Am J Physiol* 1969;217:461-471.

Kirschvink N, Art T, Smith N, *et al.* Effect of exercise and COPD crisis on isoprostane concentration in plasma and bronchoalveolar lavage fluid in horses. *Equine Vet J Suppl* 1999;30:88-91.

Kivits GAA Ganguli-Swarttouw MACR and Christ EJ. The composition of alkanes in exhaled air of rats as a result of lipid peroxidation in vivo. Effects of dietary fatty acids, vitamin E and selenium. *Biochim Biophys Acta* 1981;665:559-570.

Knutson MD and Viteri FE. Concentrating breath samples using liquid nitrogen: a reliable method for the simultaneous determination of ethane and pentane. *Anal Biochem* 1996;242:129-135.

Knutson MD, Handelman GJ and Viteri FE. Methods for measuring ethane and pentane in expired air from rats and humans. *Free Radic Biol Med* 2000;28:514-519.

Knutson MD, Lim AK and Viteri FE. A practical and reliable method for measuring ethane and pentane in expired air from humans. *Free Radic Biol Med* 1999;27:560-571.

Kohlmuller D and Kochen W. Is n-pentane really an index of lipid peroxidation in humans and animals? A methodological reevaluation. *Anal Biochem* 1993;210:268-276.

Kohno Y, Egawa Y, Itoh S, *et al.* Kinetic study of quenching reaction of singlet oxygen and scavenging reaction of free radical by squalene in n-butanol. *Biochim Biophys Acta* 1995;1256:52-56.

Kokoszka J, Nelson RL Swedler WI, *et al.* Determination of inflammatory bowel disease activity by breath pentane analysis. *Dis Colon Rectum* 1993;36:597-601.

Kondo T, Naruse S, Hayakawa T, *et al.* Effect of exercise on gastroduodenal functions in untrained dogs. *Int J Sports Med* 1994;15:186-91.

Kroncke K-D, Fehsel K and Kolb-Bachofen V. Nitric oxide: Cytotoxicity versus cytoprotection. *Nitric Oxide* 1997;1:107-120.

Kruis W, Azpiroz F and Phillips SF. Contractile patterns and transit of fluid in canine terminal ileum. *Am J Physiol* 1985;249:G264-70.

Kunze WAA and Furness JB. The enteric nervous system and regulation of intestinal motility. *Annu Rev Physiol* 1999;61:117-142.

Kuypers FA, van den Berg JJ, Schalkwijk C, *et al.* Parinaric acid as a sensitive fluorescent probe for the determination of lipid peroxidation. *Biochim Biophys Acta* 1987;921:266-74.

Lamb CR. Recent developments in diagnostic imaging of the gastrointestinal tract of the dog and cat. *Vet Clin North Am Small Anim Pract* 1999;29:307-342.

Lane AJ and Wathes DC. An electronic nose to detect changes in perineal odors associated with estrus in the cow. *J Dairy Sci* 1998 Aug;81(8):2145-50.

Langley JN and Anderson HK. On the innervation of the palvic and adjoining viscera. *J Physiol* 1895;18:67-105.

Largilliere C and Melancon SB. Free malondialdehyde determination in human plasma by high-performance liquid chromatography. *Anal Biochem* 1988;170:123-6.

Lavigne ME, Wiley ZD, Meyer JH, *et al.* Gastric emptying rates of solid food in relation to body size. *Gastroenterology* 1978;74:1258-1260.

Lawaetz O, Olesen HP, and Andreasen R. Evaluation of gastric emptying by a simple isotope technique. A Methodological study in the dog. *Scand J Gast* 1981;16:737 - 748.

Lee KY, Kim MS and Chey WY. Effects of a meal and gut hormones on plasma motilin and duodenal motility in dog. *Am J Physiol* 1980;238:G280-3.

Lee JS, Camilleri M, Zinsmeister AR, *et al.* A valid accurate office based non-radioactive test for gastric emptying of solids. *Gut* 2000a;46:768-773.

Lee JS, Camilleri M, Zinsmeister AR, *et al.* Toward office-based measurement of gastric emptying in symptomatic diabetics using [^{13}C]octanoic acid breath test. *Am J Gastroenterol* 2000b;95:2751-2761.

Leese GP, Bowtell J, Mudambo S, *et al.* Post-exercise gastric emptying of carbohydrate solutions determined using the ^{13}C acetate breath test. *Eur J Appl Physiol Occup Physiol* 1995;71:306-310.

Leib MS, Wingfield WE, Twedt DC, *et al.* Gastric emptying of glucose in the dog . *Am J Vet Res* 1986;47:31 – 35.

Lester NV, Roberts GD, Newell SM, *et al.* Assessment of barium impregnated polyethylene spheres (BIPS) as a measure of solid-phase gastric emptying in normal dogs-comparison to scintigraphy. *Vet Radiol Ultrasound* 1999;40:465-71.

Lin HC, Doty JE, Reedy TJ, *et al.* Inhibition of gastric emptying by glucose depends on length of intestine exposed to nutrient. *Am J Physiol* 1989;256:G404-411.

Lin HC, Kim BH, Elashoff JD, *et al.* Gastric emptying of solid food is most potently inhibited by carbohydrate in the canine distal ileum. *Gastroenterology* 1992;102:793-801.

Lin HC, Zhao XT, Wang L, *et al.* Fat-induced ileal brake in the dog depends on peptide YY. *Gastroenterology* 1996;110:1491-1495.

Lonergan MC, Severin EJ, Doleman BJ, *et al.* Array-based vapour sensing using chemically sensitive carbon black-polymer resistors. *Chem Mater* 1996;8:2298-2312.

Lopez Y, Fioramonti J and Bueno L. Central and peripheral control of postprandial pyloric motility by endogenous opiates and cholecystokinin in dogs. *Gastroenterology* 1991;101:1249-55.

Maes BD. *Measurement of Gastric Emptying Using Dynamic Breath Analysis.* PhD Thesis, University of Leuven, 1994a.

Maes BD, Hiele MI, Geypens BJ, *et al.* Pharmacological modulation of gastric emptying rate of solids as measured by the carbon labelled octanoic acid breath test: influence of erythromycin and propantheline. *Gut* 1994c;35:333-337.

Malagelada JR, Carter SE, Brown ML, *et al.* Radiolabeled fiber: a physiologic marker for gastric emptying and intestinal transit of solids. *Dig Dis Sci* 1980;25:81-7.

Malbert CH and Ruckebusch Y. Duodenal bulb control of the flow rate of digesta in the fasted and fed dog. *J Physiol* 1989;409:371-384.

Malbert CH and Ruckebusch Y. Relationships between pressure and flow across the gastroduodenal junction in dogs. *Am J Physiol* 1991;G653-G657.

Magnall YF, Barnish C, Brown BH, *et al.* Comparison of applied potential tomography and impedance epigastrography as methods of measuring gastric emptying. *Clin Phys Physiol Meas* 1988;9:249-54.

Mansi C, Savarino V, Remagnino A, *et al.* Comparison of the gastrokinetic effect of cisapride and levosulpiride on fat induced delayed gastric emptying. *Gastroenterology* 1998;114:A213.

Marshall PJ, Warso MA and Lands WE. Selective microdetermination of lipid hydroperoxides. *Anal Biochem* 1985;145:192-9.

Massias L, Postaire E, Regnault C, *et al.* Thermal desorption-gas chromatographic determination of ethane and pentane in breath as potential markers of lipid peroxidation. *Biomed Chromatogr* 1993;7:200-203.

Mauderly JL. Evaluation of the grade pony as a pulmonary function model. *Am J Vet Res* 1974; 35: 1025-1029.

Maughan RJ and Leiper JB. Methods for the assessment of gastric emptying in humans: an overview. *Diabetes Med* 1996;13:S6-10.

Mayer EA. The physiology of gastric storage and emptying. In: *Physiology of the Gastrointestinal Tract,* Johnson LR (ed), Raven Press, New York, 1994, pp 929-971.

McCord JM and Fridovich I. The reduction of cytochrome c by milk xanthine oxidase. *J Biol Chem* 1968;21:5753-5760.

McEntegart CM, Penrose WR, Strathmann S, *et al.* Detection and discrimination of coliform bacteria with gas sensor arrays. *Sens Actuat* 2000;70:170-176.

McHugh PR and Moran TH. Calories and gastric emptying: a regulatory capacity with implications for feeding. *Am J Physiol* 1979;236:R254-260.

McKay LF, Eastwood MA and Brydon WG. Methane excretion in man--a study of breath, flatus, and faeces. *Gut* 1985;26:69-74.

McKinney, CR McCrea JM, Epstein, S *et al.,* Improvements in MS for Measurementof small differences in isotope abundance ratios. Rev Sci Instrum 1950;21:724-730

Meier-Augenstein, A Kemp, HF and Preston, T. A test meal suitable for measuring gastric emptying of solids by means of a [13C-1]-sodium acetate breath test. Annual Meeting of the European Concerted Action on Stable Isotopes in Gastroenterology and Nutrition, Glasgow, August 1999.

Mendis S, Sobotka PA and Euler DE. Pentane and isoprene in expired air from humans: gas-chromatographic analysis of single breath. *Clin Chem* 1994;40:1485-1488.

Merry RJ, Smith RH and McAllan AB. Glycosyl ureides in ruminant nutrition. *Br J Nutr* 1982;48:275-320.

Meyer JH, Thomson JB, Cohen MB, *et al.* Sieving of solid food by the canine stomach and sieving after gastric surgery. *Gastroenterology* 1979;76:804 – 813.

Meyer JH, Dressman J, Fink A, *et al.* Effect of size and density on canine gastric emptying of nondigestible solids. *Gastroenterology* 1985;89:805 – 813.

Meyer JH, Mayer EA, Jehn D, *et al.* Gastric processing and emptying of fat. *Gastroenterology* 1986b;90:1176-1187.

Meyer JH, Elashoff JD, Domeck M, *et al.* Control of canine gastric emptying of fat by lipolytic products. *Am J Physiol* 1994;266:G1017-G1035.

Meyer JH, Elashoff JD and Lake R. Gastric emptying of indigestible versus digestible oils and solid fats in normal humans. *Dig Dis Sci* 1999;44:1076-1082.

Miele, P. Validity of measurements and sampling methods. *Network of Excellence on Artifical Olfactory Sensing (NOSE)*, Proceedings of Summer School, October 2000, Barcelona.

Miller J, Kauffman G, Elashoff H, *et al.* Search for resistances controlling canine gastric emptying of liquid meals. *Am J Physiol* 1981a;241:G403-G415.

Miller LJ, Malagelada J-R, Taylor WF, *et al.* Intestinal control of human postprandial gastric function: the role of components of jejunoileal chyme in regulating gastric secretion and gastric emptying. *Gastroenterology* 1981b;80:763-769.

Miller MA, Parkman HP, Urbain J-LC, *et al.* Comparison of scintigraphy and lactulose breath hydrogen test for assessment of orocecal transit. *Dig Dis Sci* 1997;42:10-18.

Miller ER, Appel LJ and Risby TH. Effect of dietary patterns on measures of lipid peroxidation: results from a randomized clinical trial. *Circulation* 1998;98:2390-5.

Minami H and McCallum RW. The physiology and pathophysiology of gastric empying in humans. *Gastroenterology* 1984;86:1592-1610.

Mitsui T, Naitoh K, Tsuda T, *et al.* Is endogenous isoprene the only coeluting compound in the measurement of breath pentane? *Clin Chim Acta* 2000;299:193-198.

Miyabayashi T, and Morgan JP. Gastric emptying in the normal dog. *Vet Radiol* 1984;25:187-191.

Mizuta H, Kawazoe Y, Haga K, *et al.* Effects of meals on gastric-emptying and small intestinal transit times of a suspension in the beagle dog assessed using acetaminophen and salicylazosulfapyridine as markers. *Chem Pharm Bull* 1990;38:2224-2227.

Mochiki E, Satoh M, Tamura T, *et al.* Exogenous motilin stimulates endogenous release of motilin through cholinergic muscarinic pathways in the dog. *Gastroenterology* 1996;111:1456-1464.

Mohler ER, Reaven P, Stegner JE, *et al.* Gas chromatographic method using photoionization detection for the determination of breath pentane. *J Chromatogr B Biomed Appl* 1996;685:201-9.

Mohler ER and Hathaway DR. Clinical use of photoionization gas chromatography for detection of lipid peroxidation. *Methods Enzymol* 1999;300:456-462.

Mohr C, HeineW, and Wutzke K. *Clostridium innocuum*: a glucoseureide-splitting inhabitant of the human intestinal tract. *Biochim Biophys Acta* 1999;1472:550-554.

Montuschi P, Kharitonov SA, Ciabattoni G, *et al.* Exhaled 8-isoprostane as a new non-invasive biomarker of oxidative stress in cystic fibrosis. *Thorax* 2000;55:205-9.

Moore JG, Christian PE, Brown JA, *et al.* Influence of meal weight and caloric content on gastric emptying of meals in man. *Dig Dis Sci* 1984;29:513-519.

Morgan KG, Schmatz PF and Szurszewski JH. The inhibitory effects of vasoactive intestinal polypeptide on the mechanical and electrical activity of canine antral smooth muscle. *J Physiol* 1978;282:437-450.

Morgan KG, Muir TC and Szurszewski JH. The electrical basis for contraction and relaxation in canine fundal smooth muscle. *J Physiol* 1981;311:475-488

Mori TA, Croft KD, Puddey IB, *et al.* An improved method for the measurement of urinary and plasma F2-isoprostanes using gas chromatography-mass spectrometry. *Anal Biochem* 1999;268:117-25.

Morrison DJ, Dodson B and Preston T. Measurement of urinary total ^{13}C and ^{13}C-urea by isotope ratio mass spectrometry after administration of lactose[^{13}C]-ureide. *Rapid Commun Mass Spectrom* 1999;13:1252-1256.

Morrow JD and Roberts LJ 2nd. Mass spectrometric quantification of F2-isoprostanes in biological fluids and tissues as measure of oxidant stress. *Methods Enzymol* 1999;300:3-12.

Morrow JD, Hill KE, Burk RF *et al.* A series of prostaglandin F2-like compounds are produced in vivo in humans by a non-cyclooxygenase, free radical-catalyzed mechanism. *Proc Natl Acad Sci* 1990;87:9383-7.

Mossi S, Meyer-Wyss B, Beglinger C, *et al.* Gastric emptying of liquid meals measured noninvasively in humans with [^{13}C]acetate breath test. *Dig Dis Sci* 1994;39:107S-109S.

Mudambo KS, Leese GP and Rennie MJ. Gastric emptying in soldiers during and after field exercise in the heat measured with the [13C]acetate breath test method. *Eur J Appl Physiol Occup Physiol* 1997;75:109-114.

Muelas MS, Ramirez P, Parrilla P, *et al.* Vagal system involvement in changes in small bowel motility during restraint stress: an experimental study in the dog. *Br J Surg* 1993;80:479-483.

Muir P, Papasouliotis K, Gruffydd-Jones TJ, *et al.* Evaluation of carbohydrate malassimilation and intestinal transit time in cats by measurement of breath hydrogen excretion. *Am J Vet Res* 1991;52:1104-1109.

Mukhopadhyay AK, Johnson LR, Copeland EM, *et al.* Effect of secretin on electrical activity of small intestine. *Am J Physiol* 1975;229:484-8.

Muller-Lissner SA, Sonnenberg A, Schattenmann G, *et al.* Gastric emptying and postprandial duodenogastric reflux in pylorectomized dogs. *Am J Physiol* 1982;242:G9-14.

Murphy D, Reid SW, Love S. Breath hydrogen measurement in ponies: a preliminary study. *Res Vet Sci* 1998;65:47-51.

Musial F and Enck P. Stress and gastrointestinal motility. In: Kumar D and Wingate S. *An Illustrated Guide to Gastrointestinal Motility.* Churchill-Livingstone, UK, 1993;pp104-117.

Nair V, Cooper CS, Vietti DE, Turner GA. The chemistry of lipid peroxidation metabolites: crosslinking reactions of malondialdehyde. *Lipids* 1986;21:6-10.

Nakano M, Ito T, Arimoto T, *et al.* A simple luminescence method for detecting lipid peroxidation and antioxidant activity in vitro. *Biochem Biophys Res Comm* 1994;202:940-947.

Nieuwenhuijs VB, Verheem A, van Duijvenbode-Beumer H, *et al.* The role of interdigestive small bowel motility in the regulation of gut microflora, bacterial overgrowth, and bacterial translocation in rats. *Ann Surg* 1998;228:188-193.

Nourooz-Zadeh J, Tajaddini-Sarmadi J and Wolff SP. Measurement of plasma hydroperoxide concentrations by the ferrous oxidation-xylenol orange assay in conjunction with triphenylphosphine. *Anal Biochem* 1994 220:403-9.

Nourooz-Zadeh J. Gas chromatography-mass spectrometry assay for measurement of plasma isoprostanes. *Methods Enzymol* 1999;300:13-7.

Nusynowitz ML and Benedetto AR. The lag phase of gastric emptying: clinical, mathematical and in vitro studies. *J Nucl Med* 1994;35:1022-1023.

Nycyk JA, Drury JA and Cooke RWI. Breath pentane as a marker for lipid peroxidation and adverse outcome in preterm infants. *Arch Dis Child Fetal Neonatal Ed* 1998;79:F67-69.

O'Sullivan CK, and Guilbault GG. Commercial quartz crystal microbalances – theory and applications. *Biosens Bioelectron* 1999;14:663-670.

Oberle RL and Amidon GL. The influence of variable gastric emptying and intestinal transit rates on the plasma level curve of cimetidine; An explanation for the double peak phenomenon. *J Pharmacokinet Biopharm* 1987;15:529-544.

Olopade CO, Zakkar M, Swedler WI, *et al.* Exhaled pentane levels in acute asthma. *Chest* 1997;111:862-5.

Ondrula D, Nelson RL, Andrianopoulos G, *et al.* Quantitative determination of pentane in exhaled air correlates with colonic inflammation in the rat colitis model. *Dis Colon Rectum* 1993;36:457-462.

Orihata M and Sarna SK. Nitric oxide mediates mechano- and chemoreceptor-activated intestinal feedback control of gastric emptying. *Dig Dis Sci* 1996;41:1303-1309.

Ozaki H, Gerthoffer WT, Hori M, *et al.* Ca^{2+} regulation of the contractile apparatus in canine gastric smooth muscle. *J Physiol* 1993;460:33-50.

Pagani F, Sagrada A, Brambilla A, *et al.* A model for studying saliva secretion in the conscious dog. *Arch Int Pharmacodyn Ther* 1988;291:253-262.

Page ES. Continuous inspection schemes. *Biometrika* 1954;41:100-115.

Pallikarakis N, Sphiris N and Lefebvre P. Influence of the bicarbonate pool and on the occurrence of $^{13}CO_2$ in exhaled air. *Eur J Appl Physiol Occup Physiol* 1991;63:179-83.

Papasouliotis K, Gruffydd-Jones TJ, Sparkes AH, *et al.* A comparison of orocaecal transit times assessed by the breath hydrogen test and the sulphasalazine/sulphapyridine method in healthy beagle dogs. *Res Vet Sci* 1995;58:263 - 267.\

Pappas TN, Debas HT, Chang AM, *et al.* Peptide YY release by fatty acids is sufficient to inhibit gastric emptying in dogs. *Gastroenterology* 1986;91:1386-1389.

Paredi P, Kharitonov SA and Barnes PJ. Elevation of exhaled ethane concentration in asthma. *Am J Respir Crit Care Med* 2000a;162:1450-1454.

Paredi P, Kharitonov SA, Leak D, *et al.* Exhaled ethane is elevated in cystic fibrosis and correlates with carbon monoxide levels and airway obstruction. *Am J Respir Crit Care Med* 2000b;161:1247-1251.

Paredi P, Kharitonov SA, Leak D, *et al.* Exhaled ethane, a marker of lipid peroxidation, is elevated in chronic obstructive pulmonary disease. *Am J Respir Crit Care Med* 2000c;162:369-373.

Parkman HP, Harris AD, Krevsky B, *et al.* Gastroduodenal motility and dysmotility: An update on techniques available for evaluation. *Am J Gastroenterol* 1995;90:869-892.

Parry AD, Chadwick PR, Simon D, *et al.* Leg ulcer odour detection identifies β-haemolytic streptococcal infection. *J Wound Care* 1995;4:403-406.

Pastorino AM, Zamburlini A, Zennaro L, *et al.* Measurement of lipid hydroperoxides in human plasma and lipoproteins by kinetic analysis of photon emission. *Methods Enzymol* 1999;300:33-43.

Paulsson NJP and Winquist F. Analysis of breath alcohol with a multisensor array: instrumental setup, characterization and evaluation. *Forensic Sci Int* 1999;105:95-114.

Pavlou AK and Turner APF. Sniffing out the truth: Clinical diagnosis using the electronic nose. *Clin Chem Lab Med* 2000;38:99-112.

Pavlou AK, Magan N, Sharp D, *et al.* An intelligent rapid odour recognition model in discrimination of *Helicobacter pylori* and other gastroesophageal isolates *in vitro*. *Biosens Bioelec* 2000;15:333-342.

Peachey SE, Dawson JM and Harper EJ. Gastrointestinal transit times in young and old cats. *Comp Biochem Physiol A Mol Integr Physiol* 2000;126:85-90.

Peeters TL, Vantrappen G, Janssens J. Fasting plasma motilin levels are related to the interdigestive motility complex. *Gastroenterology* 1980;79:716-9.

Pelli MA, Trovarelli G, Capodicasa E, *et al.* Breath alkanes determination in ulcerative colitis and Crohn's disease. *Dis Colon Rectum* 1999;42:71-76.

Peracchi M, Gebbia C, Ogliari C, *et al.* Influence of caloric intake on gastric emptying of solids assessed by ^{13}C-octanoic acid breath test. *Scand J Gastroenterol* 2000;35:814-818.

Perri F, Clemente R, Festa V, *et al.* ^{13}C-octanoic acid breath test: Valueless test for gastric emptying? *Gastroenterology* 1998;114: 856-857.

Phillips M, Greenberg J and Sabas M. Alveolar gradient of pentane in normal human breath. *Free Radic Res* 1994;20:333-7.

Phillips M, Erickson GA, Sabas M, *et al.* Volatile organic compounds in the breath of patients with schizophrenia. *J Clin Pathol* 1995;48:466-9.

Phillips M. Method for the collection and assay of volatile organic compounds in breath. *Anal Biochem* 1997;247:272-8.

Phillips M, Gleeson K, Hughes JM, *et al.* Volatile organic compounds in breath as markers of lung cancer: a cross-sectional study. *Lancet* 1999;353:1930-1933.

Pincemail J, Deby C, Dethier A, *et al.* Pentane measurement in man as an index of lipoperoxidation. *Bioelectrochem Bioenerg* 1987;18:117-125.

Ping W, Yi T, Haibao X, *et al.* A novel method for diabetes diagnosis based on electronic nose. *Biosens Bioelec* 1997;12:1031-1036.

Piretti MV, Pagliuca G and Vasina M. Proposal of an analytical method for the study of the oxidation products of membrane lipids. *Anal Biochem* 1987;167:358-361.

Pitkanen OM, Hallman M and Andersson SM. Determination of ethane and pentane in free oxygen radical-induced lipid peroxidation. *Lipids* 1989;24:157-159.

Poitras P. Motilin is a digestive hormone in the dog. *Gastroenterology* 1984;87:909-13.

Porter SN, Howarth GS and Butler RN. An orally administered growth factor extract derived from bovine whey suppresses breath ethane in colitic rats. *Scand J Gastroenterology* 1998;33:967-974.

Pouteau E, Dumon H, Biourge V *et al.* Hydrogen production in dogs adapts to addition of lactulose and to a meat and rice diet. *J Nutr* 1998;128:2666-2668.

Preston, T. and MacMillan, D.D. Rapid sample throughput for biomedical stable isotope tracer studies. *Biomed Environ Mass Spectrom* 1988;16:229-35.

Prosser SJ, and Scrimgeour CM. High-precision determination of $^{2}H/^{1}H$ in H_2 and H_2O by continuous-flow isotope ratio mass spectrometry. *Anal Chem* 1995;67:1992-1997.

Quigley EMM. Distinctive patterns of interdigestive motility at the canine ileocolonic junction. *Gastroenterology* 1984;87:836-844.

Radosevich PM, Nash JA, Lacy DB, *et al.* Effects of low- and high-intensity exercise on plasma and cerebrospinal fluid levels of ir-beta-endorphin, ACTH, cortisol, norepinephrine and glucose in the conscious dog. *Brain Res* 1989;498:89-98.

Read NW and Houghton LA. Physiology of gastric emptying and pathophysiology of gastroparesis. *Gastroenterology Clinics of North America* 1989;18:359-373.

Read NW, Al-Janabi MN, Edwards CA, *et al.* Relationship between postprandial motor activity in the human small intestine and the gastrointestinal transit of food. *Gastroenterology* 1984;86:721-7.

Read NW, AL-Janabi MN, Bates TE, *et al.* Interpretation of the breath hydrogen profile obtained after ingesting a solid meal containing unabsorbable carbohydrate. *Gut* 1985;26:834-842.

Riely CA, Cohen G and Lieberman M. Ethane evolution: A new index of lipid peroxidation. *Science* 1974;183:208-210.

Risby TH and Sehnert SS. Clinical application of breath biomarkers of oxidative stress status. *Free Radic Biol Med* 1999;27:1182-1192.

Risby TH, Jiang L, Stoll S, *et al.* Breath ethane as a marker of reactive oxygen species during manipulation of diet and oxygen tension in rats. *J Appl Physiol* 1999;86:617-622.

Robertson MD and Mathers JC. Gastric emptying rate of solids is reduced in a group of ileostomy patients. *Dig Dis Sci* 2000;45:1285-1292.

Ruemmele FM, Heine WE, Keller KM, *et al.* Metabolism of glycosyl ureides by human intestinal brush border enzymes. *Biochim Biophys Acta* 1997;1336:275-280.

Salem YH, Dulchavsky SA, Dutta S, *et al.* Effect of inhibition of lipid peroxidation on myocardial oxidant damage. *J Surg Res* 1994;56:606-10.

Samson M, Vermeijden R, Van Dam S, *et al.* Prevalence of abnormal gastric emptying is about thirty percent in well-regulated diabetic patients not selected on the basis of upper gastrointestinal symptoms. *Proceedings of the Annual Meeting of the American Gastroenterological Association*, Georgia, May 2001;2363.

Sarna SK. Cyclic motor activity; Migrating motor complex: 1985. *Gastroenterology* 1985;89:894-913.

Sarr MG, Kelly KA and Go VL. Motilin regulation of canine interdigestive intestinal motility. *Dig Dis Sci* 1983;28:249-56.

Schemann M and Ehrlein HJ. Effect of neurohumoural agents on jejunal contraction spread and transit in the fed dog. *Gastroenterology* 1986a;90:1950-1955.

Schemann M and Ehrlein H-J. Postprandial patterns of canine jejunal motility and transit of luminal content. *Gastroenterology* 1986b;90:991-1000.

Schlang JC, Kelly KA and Go VLW. Postprandial hormone inhibition of canine interdigestive motility. *Am J Physiol* 1986;240:G221-224.

Schmid HR, Ehrlein HJ. Effects of enteral infusion of hypertonic saline and nutrients on canine jejunal motor patterns. *Dig Dis Sci* 1993;38:1062-72.

Schoeller DA, Schneider JF, Solomons NW, *et al.* Clinical diagnosis with the stable isotope for ^{13}C in CO_2 breath tests: methodology and fundamental considerations. *J Lab Clin Med* 1977;90:413-421.

Schoeller DA, Klein PD, Watkins JB, *et al.* ^{13}C abundances of nutrients and the effect of variations in ^{13}C isotopic abundances of test meals formulated for $^{13}CO_2$ breath tests. *Am J Clin Nutr* 1980;33:2375-2385.

Schulze-Delrieu K and Shirazi SS. Pressure and length adaptations in isolated cat stomach. *Am J Physiol* 1987;G92-G99.

Segall HJ, Wilson DW, Dallas JL, *et al.* trans-4-Hydroxy-2-hexenal: a reactive metabolite from the macrocyclic pyrrolizidine alkaloid senecionine. *Science* 1985;229:472-475.

Selye H. A syndrome produced by diverse nocuous agents. *Nature* 1936;265:32.

Selye H. *The Physiology and Pathology of Exposure to Stress : A Treatise Based on the Concepts of the General-Adaptation Syndrome and the Diseases of Adaptation.* Acta, Montreal, 1950.

Selye H. *The Stress of Life.* McGraw-Hill, New York,1976.

Sethi RS. Transducer aspects of biosensors. *GEC J Res* 1991;9:81-96.

Severin EJ, Sanner RD, Doleman BJ, *et al.* Differential detection of enantiomeric gaseous analytes using carbon black-chiral polymer composite, chemically sensitive resistors. Anal Chem 1998;70:1440-1443

Severin EJ, Doleman BJ and Lewis NS. An investigation of the concentration dependence and response to analyte mixtures of carbon black/insulating organic polymer composite vapor detectors. *Anal Chem* 2000;72:658-668.

Shimasaki H. Assay of fluorescent lipid peroxidation products. *Methods Enzymol* 1994;233:338-46.

Siegel JA, Urbain J-L, Adler LP, *et al.* Biphasic nature of gastric emptying. *Gut* 1988;29:85-89.

Siegle M-L and Ehrlein H-J. Digestive motor patterns and transit of luminal contents in canine ileum. *Am J Physiol* 1988;254:G552-G559.

Smith MT, Thor H, Hartizell P, *et al.* The measurement of lipid peroxidation in isolated hepatocytes. *Biochem Pharmacol* 1982;31:19-26.

Sobotka PA, Brottman MD, Weitz Z, *et al.* Elevated breath pentane in heart failure reduced by free radical scavenger. *Free Radic Biol Med* 1993;14:643-647.

Soll AH. Peptic ulcer and its complications. In: *Diseases of the Gastrointestinal Tract and Liver*; Shearman DJC (ed), Churchill Livingstone, Edinburgh,1997.

Sonnenberg A, Muller-Lissner A, Schattenmann G, *et al.* Duodenogastric reflux in the dog. *Am J Physiol* 1982;242:G603-G607.

Speakman JR, Perez-Camargo G, McCappin T, *et al.* Validation of the doubly-labelled water technique in the domestic dog (*Canis familiaris*). *Br J Nutr* 2001;85:75-87.

Spiller RC, Trotman IF, Higgins BE, *et al.* The ileal brake--inhibition of jejunal motility after ileal fat perfusion in man. *Gut* 1984;25:365-74.

Spiller RC. Chemical detection of transit. In: Kumar D and Wingate D. *An Illustrated Guide to Gastrointestinal Motility.* Churchill-Livingstone, 1993, pp308-318.

Springfield JR and Levitt MD. Pitfalls in the use of breath pentane measurements to assess lipid peroxidation. *J Lipid Res* 1994;35:1497-1504.

Spyrou NM and Castillo FD. Electrical impedence measurement. In: Kumar D and Wingate D (eds) *An Illustrated Guide to Gastrointestinal Motility*, 1993, Churchill-Livingston, Edinburgh, pp 276-278.

Stanghellini V, Borovicka J and Read NW. Feedback regulation and sensation. Frontiers in gastric emptying. *Dig Dis Sci* 1994;39:124S-127S.

Stanghellini V, Malagelada JR, Zinsmeister AR, *et al.* Stress-induced gastroduodenal motor disturbances in humans: possible humoral mechanisms. *Gastroenterology* 1983;85:83-91.

Strike, PW. *Statistical Methods in Laboratory Medicine.* Butterworth-Heinemann Ltd., UK, 1991;pp288-300.

Strunz UT, Code CF and Grossman MI. Effect of gastrin on electrical activity of antrum and duodenum in dogs. *Proc Soc Exp Biol Med* 1979;161:25-27.

Sutton JA, Thompson S and Sobnack R. Measurement of gastric emptying rates by radioactive isotope scanning and epigastric impedance. *Lancet* 1985;1(8434):898-900.

Sutton DGM, Bahr A, Preston T *et al.* Equine gastric emptying: validation of the ^{13}C-octanoic acid breath test for solid phase measurement using radioscintigraphy. *Biomed-SIGN-Meeting* 1999, June 28-29, Glasgow.

Suzuki T, Nakaya M, Itoh Z *et al.* Inhibition of interdigestive contractile activity in the stomach by peptide YY in Heideihain pouch dogs. *Gastroenterology* 1983;85:114-121.

Swann MJ, Glidle A, Cui L, *et al.* The determination of gaseous molecular density using a hybrid vapour sensor. *Chem Comm* 1998;2753-2754.

Swart GR, and van der Berg JWO. ^{13}C-Breath tests in gastroenterological practice. *Scand J Gastroenterol* 1998; (Supplement 225):13-18.

Symonds EL, Butler RN and Omari TI. Assessment of gastric emptying in the mouse using the [^{13}C]-octanoic acid breath test. *Clin Exp Pharmacol Physiol* 2000;27:671-675.

Szurszewski JH. A migrating electric complex of the canine small intestine. *Am J Physiol* 1969;217:1468-1473.

Szurszewski JH. Electrical basis for gastrointestinal motility. In: Johnson LR (ed) *Physiology of the Gastrointestinal Tract*, 1987; Raven Press, New York, pp383-422.

Szurszewski JH. A 100-year perspective on gastrointestinal motility. *Am J Physiol* 1998;274:G447-G453.

Tappel AC and Zalkin H. Inhibition of lipid peroxidation in mitochrondria by vitamin E. *Arch Biochem Biophys* 1959;80:333-336.

Thayler ER, Bruney FC, Kennedy FC *et al.* Use of an electronic nose to distinguish cerebrospinal fluid from serum. *Arch Otolaryngol Head Neck Surg* 2000;126:71-74.

Theodorakis MC. External scintigraphy in measuring rate of gastric emptying in beagles. *Am J Physiol* 1980;239:G39 - G43.

Thomas PA, Schlang JC, Kelly KA, *et al.* Can endogenous gastrin inhibit canine interdigestive gastric motility. *Gastroenterology* 1980;78:716-721.

Thomas SM, Jessup W, Gebicki JM, *et al.* A continuous-flow automated assay for iodometric estimation of hydroperoxides. *Anal Biochem* 1989;176:353-9.

Thomas, D. (1911) *Arch Anat Physiol* Physiol. Abt, pg 9.

Thomsen L, Robinson TL, Lee JCF, *et al.* Interstitial cells of Cajal generate a rhythmic pacemaker current. *Nature Medicine* 1998;4:848-851.

Thor P, laskiewiez J, Konturek JW, *et al.* Role of gastrointestinal peptide and insulin in glucose induced changes in intestinal motility patterns. *Am J Physiol* 1987;252:G8-12.

Thor P, Laskleuriez J, Konturek P, *et al.* Cholecystokinin in the regulation of intestinal motility and pancreatic secretion in dogs. *Am J Physiol* 1988;255:G498-504.

Toshniwal PK, and Zarling EJ. Evidence for increased lipid peroxidation in multiple sclerosis. *Neurochem Res* 1992;17:205-207.

Valenzuela JE. Effect of intestinal hormones and peptides on intragastric pressure in dogs. *Gastroenterology* 1976;71:766-9.

van den Brom WE, and Happé RP. Gastric emptying of a radionuclide-labeled test meal in healthy dogs: A new mathematical analysis and reference values. *Am J Vet Res* 1985;47:2170 – 2174.

van den Driessche ML, van Limbergen J, Hoffman I, *et al.* ^{13}C breath tests suggest supra-colonic motility disorders in constipated children. *Gastroenterology* 1999;115:G0435.

van den Driessche M, Van Malderen N, Geypens B *et al.* Lactose-[^{13}C]Ureide breath test: A new noninvasive technique to determine orocecal transit time in children. *J Pediatr Gastroenterol Nutr* 2000;31:433-438.

Vincent IC and Michell AR. Comparison of cortisol concentrations in saliva and plasma of dogs. *Res Vet Sci* 1992;53:342-345.

Viramontes BE, Kim D-Y, Lee JS, *et al.* Validation of a stable isotope gastric emptying breath test for normal, accelerated or delayed gastric emptying. *Proceedings of the Annual Meeting of the American Gastroenterological Association*, Georgia, May 2001;2366.

Vollhardt, KPC. *Organic Chemistry.* WH Freeman and Co., 1987, New York.

Wade CR and van Rij AM. *In vivo* lipid peroxidation in man as measured by the respiratory excretion of ethane, pentane, and other low-molecular weight hydrocarbons. *Anal Biochem* 1985;150:1-7.

Wagner BA, Buettner GR and Burns CP. Free radical-mediated lipid peroxidation in cells: Oxidizability is a function of cell lipld bis-allylic hydrogen content. *Biochemistry* 1994;33:4449-4453.

Walsh JH. Gastrointestinal hormones. In: In: *Physiology of the Gastrointestinal Tract*, Johnson LR (ed), Raven Press, New York, 1994, pp 1-127.

Weber J and Kohatsu S. Pacemaker localization and electrical conduction patterns in the canine stomach. *Gastroenterology* 1970;59:717-727.

Weisbrodt NW, Wiley JN, Overholt BF, *et al.* A relation between gastroduodenal muscle contractions and gastric emptying. *Gut* 1969;10:543-548.

Weisbrodt NW, Copeland EM, Thor PJ, *et al.* The myoelectric activity of the small intestine of the dog during total parenteral nutrition. *Proc Soc Exp Biol Med* 1976;153:121-4.

Wendland BE, Aghdassi E, Tam C, *et al.* Lipid peroxidation and plasma antioxidant micronutrients in Crohn disease. *Am J Clin Nutr* 2001;74:259-64.

West JB, Mathieu-Costello O, Jones JH, *et al.* Stress failure of pulmonary capillaries in racehorses with exercise-induced pulmonary haemorrhage. *J Appl Physiol* 1993;75:1097-109.

Wilbur BG, and Kelly KA. Effect of proximal gastric complete gastric and truncal vagotomy on canine gastric electric activity, motility and emptying. *Annal Surg* 1973;178:295-303.

Williams NS, Meyer JH, Jehn D, *et al.* Canine intestinal transit and digestion of radiolabeled liver particles. *Gastroenterology* 1984;86:1451-1459.

Wingate DL, Pearce EA, Hutton M, *et al.* Quantitative comparison of the effects of cholecystokinin, secretin, and pentagastrin on gastrointestinal myoelectric activity in the conscious fasted dog. *Gut* 1978;19:593-601.

Wood JD. Physiology of the enteric nervous system. In: Johnson LR (ed) *Physiology of the Gastrointestinal Tract*, Raven Press, New York, 1994; pp423-482.

Wutzke K, Heine W, Plath C, *et al.* Evaluation of orocaecal transit time: a comparison of the lactose (^{13}C, ^{15}N) ureide $^{13}CO_2$ and the lactulose H_2 breath test in humans. *Eur J Clin Nutr* 1997;51:11-19.

Wyse CA, Murphy DM, Preston T, *et al.* Assessment of the rate of solid-phase gastric emptying in ponies by means of the ^{13}C-octanoic acid breath test: a preliminary study. *Equine Vet J* 2001;33:197-203.

Zentek J. Influence of diet composition on the microbial activity in the gastrointestinal-tract of dogs. *In-vitro* studies on the metabolic-activities of the small-intestinal microflora. *J Anim Physiol Anim Nutr* 1995;74:62-73.

Ziegler D, Schadewaldt P, Pour Mirza A, *et al.* [^{13}C] Octanoic acid breath test for non-invasive assessment of gastric emptying in diabetic patients: Validation and relationship of gastric symptoms and cardiovascular autonomic function *Diabetologia* 1996;39: 823-830.

Zontine WJ. Effect of chemical restraint drugs on the passage of barium sulfate through the stomach and duodenum of dogs. *J Am Vet Med Assoc* 1973;15:878-84.

Analar, BOH Laboratory Supplies, Poole, BH15 1TD

Becton Dickinson, UK Limited, Between Towns Road, Cowley, Oxford, UK

Burke Electronics, 4 Park Gardens, Glasgow, UK

Cabot Co., Billerica, MA, USA.

Cambridge Isotope Laboratories, Andover, MA 01810, USA.

Cambridge Isotope Labortories, Andover, MA 010, USA

Cenvet, Veterinary Instrumentation, 5 Beete Road, Welshpool, Australia.

Chrompack, PO Box 8033, 4330 EA Middleburg, The Netherlands.

CK Gas Products Limited, 1 Marino Way, Finchampstead, Wokingham, Berkshire, UK.

Cole-Palmer, Unit 3, River Brent Business Park, Trumpers Way, Hanwell, London, UK.

Europa Scientific, Crewe, UK

Glasgow Valve and Fitting Company, 11 Macadam Place, South Newmoor, Irvine UK

Goodfellow Cambridge Limited, Huntingdon UK

Goodfellow Limited, Huntingdon, UK

GMI Medical Limited, Renfrew, Scotland

Hamiliton Bonaduz AG, PO Box 26, CH-7402 Bonaduz, Switzerland.

Isotec Inc., CK Gas Products Ltd., UK

Jones Chromatography Limited, New Road, Hangoed, Mid Glamorgan, UK

KAD-Detection Systems, Unit 4, Barmill Road, Galston, Ayrshire, UK.

Labco Ltd., Cressex Business Park, High Wycombe, Buckinghamshire,UK

Labtech International Ltd., Uckfield, UK.

Microsoft Corporation, One Microsoft Way, Redmond, WA 98052-

Minitab Inc, Minitab Headquarters, 3081 Enterprise Drive, State College, PA 16801-3008, USA

Nalgene, 75 Panorama Creek Drive, PO Box 20365, Rochester, NY 14602-0365

Omnifit, 2 College Park, Coldhams Lane, Cambridge UK.

Pedigree Petfoods, Melton Mowbray, Leicestershire LE13 1BB

PhaseSep, Phase Seperations Limited, Deeside, Clwyd, UK.

QuinTron Instrument Company, 3712 West Pierce Street, Milwaukee, Wisconsin, USA 53215.

Rocket of London, Watford, UK

Shipley Limited, Heraldway, Coventry, CV3 2RQ

Sigma-Aldrich, Fancy Road, Poole, Dorset, UK.

SKC Limited, Blandford Forum, Dorset, UK

Sloan Technology, California, USA

Supelco, Supelco Park, Bellefonte, PA 16823, USA.

Valco Instruments Co. Inc., PO Box 55603, Houston, TX 77255, USA.

Varian Ltd, 28 Manor Road, Walton-on-Thames, Surrey, UK

Young Scientific Glassware, 11 Colville Road, Acton, London, UK

APPENDIX TWO - LIST OF ABBREVIATIONS

^{13}C-OA	^{13}C-octanoic acid
^{13}C-OBT	^{13}C-octanoic acid breath test
4-HNE	4-hydroxy-2-*trans*-nonenal
AP	Action potential
APE	Atomic percent excess
APT	Applied potential tomography
BIP	Barium impregnated polyethylene bead
BSA	Body surface area
CCK	Cholecystokinin
CD	Crohn's disease
CF	Cystic fibrosis
COPD	Chronic obstructive pulmonary disease
COX	Cyclooxygenase
CV	Coefficient of variation
ENS	Enteric nervous system
FID	Flame ionisation detection
FOX	Ferrous oxidation xylenol orange
GC	Gas chromatography
GC-FID	Gas chromatography-flame ionization detection
GC-PID	Gas chromatography-photo ionization detection
GEC	Gastric emptying coefficient
GSH	Reduced glutathione
GSSG	Oxidised glutathione
HCBT	Hydrocarbon breath test
HCFA	Hydrocarbon free air
HIV	Human immunodeficiency virus
HPLC	High performance liquid chromatography
IPAN	Intrinsic primary afferent neuron
IRMS	Isotope ratio mass spectrometry
MDA	Malondialdehyde
MMC	Migrating motor complex

MRI	Magnetic resonance imaging
MS	Multiple sclerosis
NA	Not applicable
NM	Not measured
NS	Not significant
NO	Nitric oxide
$ONOO^-$	Peroxynitrite
p	Probability
P2VPS	Poly(2-vinylpyridine-co-styrene)
P4VP	Poly(4-vinylphenol)
PABS	Poly(acrylonitrile-co-butadiene-co-styrenetoluene)
PCL	Poly(caprolactone)
PDR	Percent dose recovery
PEG	Poly(ethylene glycol)
PEGPEG	Poly(ethelene-block-polyethyleneglycol)
PEMA	Poly(ethylene-co-methylacrylate)
PEVA	Poly(ethylenecovinylacetate)
PIB	Poly(isobutylene)
PID	Photoionisation detection
PMMA	Poly(methylmethacrylate)
PP	Pancreatic polypeptide
ppb	Parts per billion
ppm	Parts per million
ppt	Parts per thousand
PS	Poly(styrene)
PSF	Polysulfone
PUFA	Polyunsaturated fatty acid
PVA	Poly(vinylacetate)
PVPK	Poly(vinylmethylketone)
PVPr	Poly(vinylpyrrolidone)
PVVA	Poly(vinylchloride-co-vinylacetate)
RA	Rheumatoid arthritis
RAO	Recurrent airway obstruction
RO	Reverse osmosis
SAW	Surface acoustic wave

sd	Standard deviation
se	Standard error of the mean
SIBT	Stable isotope breath test
TBA	Thiobarbituric acid
TBARS	Thiobarbituric acid reactive substance
TPP	Triphennylphosphine
UC	Ulcerative colitis
VIP	Vasoactive intestinal peptide
VOC	Volatile organic compound

APPENDIX THREE – SUMMARY OF THE EFFECT OF GASTROINTESTINAL PEPTIDES ON GASTROINTESTINAL MOTILITY IN THE DOG

Hormone	Released	Physiological Stimulus	Action on Gastric Motility	Action on SI Motility	Reference
Secretin	Enterochromaffin cells	Duodenal pH < 4.5 Fatty acids in small intestine	Decreased intra-gastric pressure; Inhibits gastric emptying	Increased duodenal and jejunal myoelectrical activity	Valenzuela, 1976 Walsh, 1994 Wingate *et al,*1978
Gastrin	G-cells of small intestinal mucosa	Gastric distension Amino acids	Inhibited MMC; Increased incidence of antral AP and slow wave frequency; Abolished MMC in antrum	Increased frequency of gastric and duodenal slow wave; Increased incidence of duodenal AP and slow wave frequency; Suppression of MMC and increased AP frequency	Wingate *et al.,* 1978 Thomas *et al.,* 1980 Strunz *et al.,* 1979 Thor *et al.,* 1987 Suzuki *et al.,* 1983
Cholecystokinin	Endocrine cells and nerves	Fatty acids or amino acid in duodenum	Increased intra-gastric pressure Inhibited MMC	Increased duodenal AP activity Postprandial CCK antagonism reduced AP frequency in SI but	Valenzuela *et al.,* 1976 Wingate *et al.,* 1978 Thor *et al.,* 1987

Candidate Hormones Affecting Gastrointestinal Motility in the Dog

Hormone	Released	Physiological Stimulus	Action on Gastric Motility	Action on SI Motility	Reference
Pancreatic Polypeptide (PP)	Pancreatic islets	Protein fat and glucose in duodenum	Administration of non-physiological dose inhibits Phase III activity in antrum	Administration of non-physiological dose inhibits Phase III activity in jejunum. Endogenous PP probably has little effect on intestinal motility	Hall *et al.*, 1983
Peptide YY	L- type endocrine cells of distal small intestine	Nutrients in duodenum	Inhibits gastric emptying Inhibits contractile activity of MMC	Inhibits intestinal transit. Responsible for fat-induced ileal brake.	Pappas *et al.*, 1986 Suzuki *et al.*, 1983 Lin *et al.*, 1996

Paracrine Peptides thought to affect Gastrointestinal Motility in the Dog

Paracrine	Released	Gastric Motility	Small Intestinal Motility	Reference
Somatostatin	D-cells and nerves	Cyclic variation with antral motility	May facilitate progression of Phase III activity to duodenum Intra-arterial somatostatin stimulated ileal motility	Bueno *et al.*, 1986 Foxthrelkeld, 1993

Table A2 Candidate hormones and paracrine peptides affecting gastrointestinal motility in the dog.

Neuroendocrine	Released	Gastric Motility	Small Intestinal Motility	Reference
Vasoactive Intestinal Peptide	Enterochromaffin cells	Increased intra-gastric pressure		Valenzuela *et al,* 1976
Gastrin Releasing Peptide	Central, peripheral and enteric nerves			Foxthrelkeld, 1993
Enkephalins	Mucosal cells	Morphine delayed gastric emptying; Naloxone opioid antagonism had no effect on gastrointestinal motility	Pharmacological dose administered systemically reduced small intestine contractile activity in the fed state	Foxthrelkeld, 1993 Schemann and Ehrlein,1986a
Neurotensin	Mucosal cells of jejunum and ileum	Pharmacological dose decreased rate of gastric emptying	Central administration shortens MMC, no effects after systemic administration => probably no physiological effect on intestinal motility; decreased force & frequency of duodenal contractions	Bueno *et al.,* 1985 Keinke *et al.,* 1986

APPENDIX FOUR - DETAILS OF ANIMALS

Details of Dogs

Dog No.	Age (years)	Sex	Breed	Body Weight (kg)	Body Surface Area (m^2)
1	9	Male	Greyhound	31.25	1.00
2	9	Male	Greyhound	33.75	1.05
3	9	Male	Greyhound	30	0.98
4	9	Female	Greyhound	27.5	0.92
5	9	Female	Greyhound	30.25	0.98
6	10	Male	Greyhound	33	1.04
7	3	Female	Terrier	10	0.47
8	9	Female	Labrador	29.5	0.96
9	3	Female	Terrier	7.5	0.39
10	3	Male	Lurcher	27	0.91
11	2.5	Female	Terrier	11.5	0.51
12	4	Male	Collie X	20	0.74
13	2	Female	Alsation X	23	0.82
14	4	Male	Spaniel	19.5	0.73
15	1.5	Male	Terrier	6	0.33
16	8	Male	Beagle	29	0.95
17	5	Male	Terrier	9.5	0.45
18	2.5	Male	Collie X	22	0.79
19	8	Female	Alsation X	25	0.86
20	8	Female	Labrador X	21.5	0.78
21	4	Female	Labrador	37	1.12
22	2	Male	Labrador	31	1.00
23	9	Female	Labrador	25	0.86
24	0.7	Female	Labrador X	15	0.61
25	8	Female	Spinone	39	1.61
26	4	Female	Spaniel	20	0.74
27	5	Male	Pointer	28.5	0.94

Details of Horses

Horse No.	Age (Years)	Sex	Weight. (kg)	Breed	Clinical History
1	12	Female	539	Thoroughbred	Recurrent airway obstruction
2	18	Female	469	Thoroughbred	Lameness
3	9	Female	680	Irish Draught	Healthy
4	26	Female	445	New Forest	Recurrent airway obstruction
5	15	Female	326	Pony	Allergic dermatitis

APPENDIX FIVE - VALIDATION OF BREATH COLLECTION TECHNIQUE

Objective

To assess the reliability of the breath collection method, by assessing the correlation and repeatibility between replicate breath samples taken at each time point.

Study Design

Replicate breath samples taken during the studies to estimate optimum substrate dose (Chapter 3) and the reproducibility studies (Chapter 3), were analysed in this study. The correlation coefficient describing the relationship between replicate A and replicate B was calculated. The repeatibility of the breath sampling technique was assessed using the method described by Altman and Bland (1986).*

There was a good correlation between the ^{13}C-enrichment of replicate A and B in this study ($r = 0.98$), indicating a strong relationship between the replicate samples. The repeatibility of the breath sampling method was demonstrated by plotting the mean ^{13}C concentration of each pair of breath samples against their difference, as shown in Figure 6A, below. The mean difference between the replicate samples was 0.03 ppm and was considered unlikely to affect clinical interpretation of the ^{13}C-breath tests in these studies. Most of the data points ($n = 436$) fell within 2 standard deviations of the mean. The results of this study suggest that the breath sampling method is sufficiently accurate for the purposes of this study, and in Chapter 3, Section 3.2, single breath samples were taken.

*Bland, JM and Altman, DG. Statistical methods for assessing agreement between two methods of clinical measurement. Lancet 1986;1:307-310

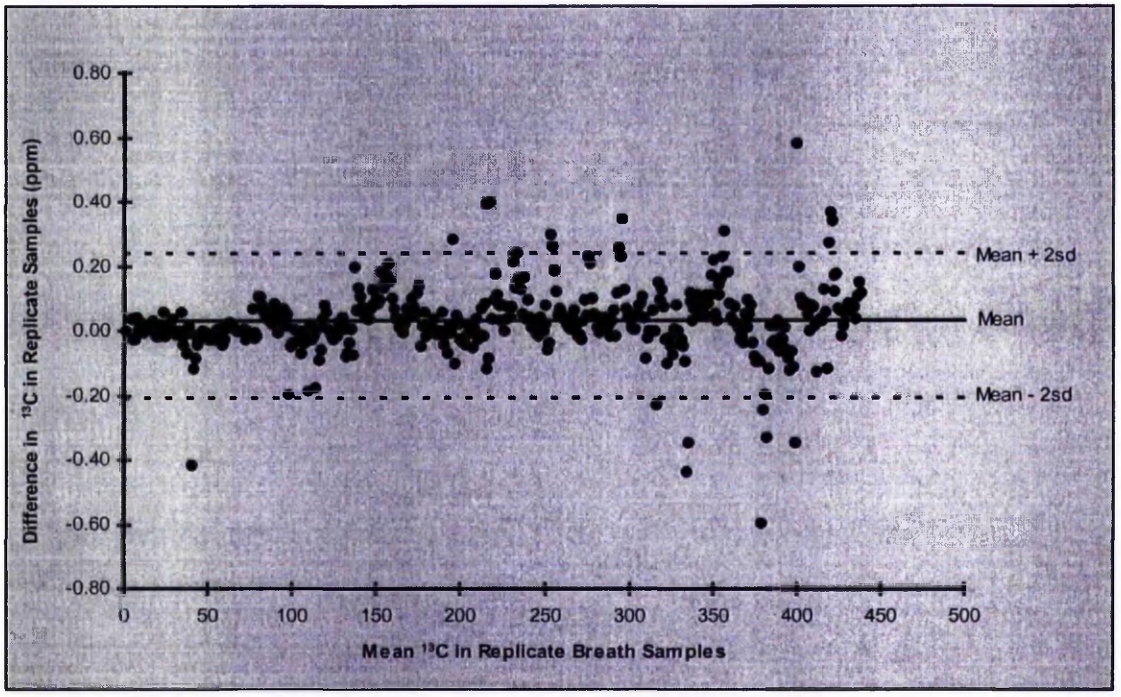

Figure 6A: Altman-Bland plot illustrating the repeatibility of the breath sampling method used in this study. A line illustrating the mean difference (0.03ppm) between the replicate breath samples is shown and the mean±2sd.

APPENDIX SIX - ORDER OF INGESTION OF TEST MEAL IN ENERGY DENSITY STUDY

To assess the effect of test meal energy density on the rate of gastric emptying as measured using the ^{13}C-octanoic acid breath test, a test meal of high energy density (Meals 1) and a test meal of low energy density (Meal 2) were ingested in random order on 3 occasions by each dog.

Dog Number	Day 1	Day 2	Day 3	Day 4	Day 5	Day 6
1	1	1	2	1	2	2
2	2	1	2	1	2	1
3	1	1	1	2	2	2
4	1	2	1	1	2	2

Meal 1 (High Energy Density) = 1 slice bread
1 egg yolk
30g margarine
175ml skimmed milk

Meal 2 (Low Energy Density) = 1 slice bread
1 egg yolk
5g margarine
200ml skimmed milk

Oro-caecal transit time was defined as the point of detection of a significant and sustained rise of $^{13}CO_2$ or H_2 in the exhaled breath (Wutzke *et al.,* 1997). The cumulative sum (CUSUM) procedure was used to detect the point at which a significant increase in $^{13}CO_2$ and H_2 occurred (Papasouliotis *et al.,* 1995). The CUSUM procedure is based on examination of the cumulative sum of the deviation between a reference value and the observed values; this technique was developed for use in manufacturing control (Page, 1954) and allows accurate determination of significant deviation from a baseline value. CUSUM values were defined as:

$$CUSUM = \sum (X_i - \mu_c) \qquad \text{(Eq.A1)}$$

where μ_c is a control value estimated from the baseline (Strike, 1991), and in this case the mean of $H_2/^{13}C$ measurements taken at timepoints –30, 0 and 30 minutes. The CUSUM values were presented on a CUSUM plot, and deviations from the control value were detected as a change in slope of the CUSUM trace, see Appendix Five. The scaling of the CUSUM-plot is by convention, presented such that the unit distance between the points on the X-axis maps to $W.\sigma_T$ on the Y-axis (CUSUM), where σ_T is the deviation of the baseline (sd of $H_2/^{13}C$ measurements taken at timepoints –30,0 and 30 mins) and W is a scaling factor, ideally set to W = 2 (Strike, 1991). Scaling of the axes in this way means that a CUSUM value that is at slope 1 relative to the X-axis deviates from the control value (μ_c) by $\pm 2\sigma_T$, and significant deviations from the control value can be detected graphically. A V-mask control mechanism can be used to detect the point at which the CUSUM values deviate outside a defined range, i.e. when the assay becomes "out of control". The point of the V-mask is placed a defined

distance (d) in front of the last CUSUM value; if any of the previous CUSUM values fall outside the angle of the V-mask, this indicates that the assay is out of control (Figure 6.A). The sensitivity of this method to detection of changes in the assay is determined by the values of the angle of the V-mask (2θ), and the distance from the last CUSUM point (d). The angle of the V-mask is defined as:

$$\theta = \tan^{-1}\left(\frac{U}{2W}\right)$$ Strike, 1991, (Eq. A2)

where U is the magnitude of the change in the control value that is to be detected; in physiological systems this is generally two standard deviations, ($2\sigma_T$). W is the scaling factor of the CUSUM-plot conventionally set to 2. The distance of the V-mask from the last CUSUM value, d is defined as:

$$d = \frac{(h.W)}{U}$$ Strike, 1991, (Eq. A3)

where h is taken to be 2.7, a value suggested for detection of a bias of ±2sd from the mean, in biological systems (Strike, 1991).

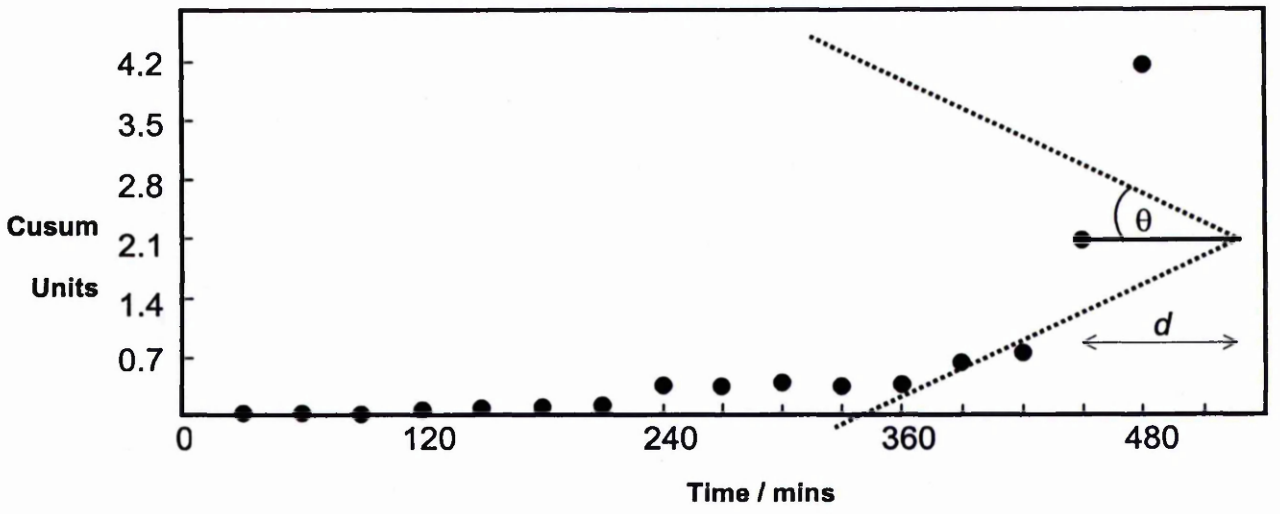

Figure 6.A: CUSUM-plot illustrating use of V-mask rule to estimate the point of significant increase above baseline. The total deviation (of the baseline (σ_T) was 0.35; Y-axis is scaled in units of $2\sigma_T$, i.e. 0.7. The half-angle of the v-mask (θ) was 26.56° and the distance (d) from the last CUSUM point was 2.6 time units. One CUSUM point is located outside the arms of the V-mask indicating that a significant change has occurred at time = 450.

The V-mask is by definition, a graphical method for detection of a divergent CUSUM-plot, but this method can be computerised using the decision-interval rule (Strike, 1991). A command sequence was established in an Excel spreadsheet to use the decision-interval rule to determine the point of divergence of the CUSUM plot of the breath test data, and hence calculate the OCTT. A reference interval (K_L - K_U) was set up such that:

$$K_U = \mu_c + K$$
$$K_L = \mu_c - K$$

where $K = 2\sigma_T . \tan\theta$ (Eq. A4)

Each data point (X_i) was analysed: if X_i fell within the reference interval (K_L - K_U), no action was taken. If X_i fell outside the reference interval, then the basic CUSUM procedure was followed such that:

If $X_i > K_L$ then CUSUM = X_i - K_L

If $X_i < K_U$ then CUSUM = X_i - K_U (Eq. A5)

A decision interval (A_U - A_L) was defined to identify when a divergent CUSUM value was detected, such that:

$A_U = +A$

$A_L = -A$

where $A = 2\sigma_T.d.\tan\theta$ (Eq. A6)

If the CUSUM value fell between the decision interval (A_U - A_L), the calculation was terminated as a significant deviation had been detected. In the present study, this identified the point of OCTT, and no further calculations were performed.

Detection limit	analyte concentration corresponding to an assay signal falling 3.3 standard deviations above baseline.
Biosensor	chemical sensor detecting biological parameter or analytical information obtained using a biological detector that is converted to an electrical signal using a transducer.
Drift	change in the parameters of an analytical system that is non-systematic, possibly caused by external factors such as temperature or intrinsic factors such as aging.
Accuracy	the closeness of agreement between the value which is accepted either as a conventional true value or an accepted reference value, and the value found using the analytical procedure.
Precision	the closeness of agreement between a series of measurements obtained from multiple sampling of the same homogenous sample under the assay conditions.
Reproducibility	reproducibility is an expression of the precision between laboratories
Range	the range of an analytical procedure is the interval between the upper and lower concentration of analyte in the sample, for which it has been demonstrated that the analytical procedure has a suitable level of precision, accuracy and linearity
Assay validation	assessment of the standard parameters of assay performance
Assay robustness	the ability of an assay to give consistent results regardless of the external conditions, this is an index of the reliability of the assay under normal usage
Specificity	the ability to assess unequivocally the analyte in the presence of other components that might be expected to be present, such as impurities and degradants.
Linearity	the ability of an analytical procedure to obtain test results that are directly proportional to the concentration of analyte in the

sample. For assays that are not linear, another mathematical relationship should be demonstrated.

All definitions from: ICH Harmonised Tripartite Guideline "Validation of Analytical Procedures" recommended for adoption to the regulatory bodies of the European Union in 1994 by the ICH Steering Committee (International Conference on Harmonisation of Technical Requirements for Registration of Pharmaceuticals for Human Use)

APPENDIX NINE - LIST OF PUBLICATIONS AND PRESENTATIONS

Yam PS and Wyse CA. The ^{13}C-octanoic acid breath test for assessment of solid phase gastric emptying in dogs. *World Veterinary Congress*, Lyon, September 1999.

Wyse CA, Preston T, Morrison DJ and Yam PS. The ^{13}C-octanoic acid breath test for assessment of solid phase gastric emptying in dogs: preliminary studies. *British Small Animal Veterinary Congress*, Birmingham, April 2000.

Yam PS, Wyse CA, and Preston T. The ^{13}C-octanoic acid breath test for assessment of solid phase gastric emptying in dogs. *Annual Meeting of the European Concerted Action on Stable Isotopes in Gastroenterology and Nutrition*, Glasgow, August 1999.

Wyse CA, Preston T, Morrison DJ and Yam PS. The ^{13}C-octanoic acid breath test for assessment of solid phase gastric emptying in dogs. *American Journal of Veterinary Research.* In Press.

Yam PS, Wyse CA and Preston T. The ^{13}C-lactose-ureide breath test for assessment of oro-caecal transit time in dogs: a preliminary study. *British Small Animal Veterinary Congress*, Birmingham, April 2001.

Wyse CA, Preston T, Slater C and Yam PS. A comparison of the ^{13}C-octanoate breath test and the ^{2}H-octanoate saliva test for assessment of solid-phase gastric emptying in the dog. *Meeting of European Society of Veterinary Internal Medicine*, Dublin, September 2001.

Wyse CA, Yam PS, Slater C, Cooper JM and Preston T. A comparison of recovery of $^{13}CO_2$ in exhaled breath with ^{2}H in body water following ingestion of ^{2}H/^{13}C-octanoic acid in a dog. In preparation for submission to the *American Journal of Veterinary Research.*